University of Strathclyde
Department of Naval Architecture, Ocean and Marine Engineering

Investigating the Performance and Emission Characteristics of Diesel-LPG Engine Operation

By

Anye Ngang Emmanuel

A thesis presented in fulfilment of the requirements for the degree of Doctor of Philosophy

March 2019

Acknowledgements

The completion of this thesis has been possible thanks to the help from a variety of people. Firstly, I thank my supervisors, Professor Peilin Zhou and Dr Gerasimos Theotokatos for their counsel, support, and guidance throughout this work.

I also thank Charles Keay and Sokratis Stoumpos for the help they provided during the setting up of the experimental systems including data acquisition devices. Appreciation also goes to Prof. Slobodan J. Popovic, Maciej Mikulski, and Dr Ngayihi Valery Abbe, who provided advice on how to go about developing and implementing the zero-dimensional mathematical code used in this work. Also, enormous gratitude goes to the various people at AVL – Advanced simulation technologies in Graz (Austria) and Maribor (Slovenia) who provided me with sound advice and training.

Financial support throughout this PhD came from a variety of sources and without these funds; this work would not have been possible. Consequently, recognitions go to the commonwealth scholarship commission in the UK for the prestigious scholarship they provided. Acknowledgements also go to John Blackburn Main and the Institute of Marine Engineering, Science & Technology (IMarEST) for the postgraduate award granted me to attend conferences and gain relevant experience to support and complement my PhD research studies.

I want to thank Dr Ngwantung Akamangwa, Dr Elif Oguz, and Dr John Ngwa-Ndifor for proof-reading and reviewing the initial draft and then providing me with invaluable feedback.

I equally thank my wife, kids and family for their tolerance and endurance throughout my studies. Last but not least, I am forever grateful to God Almighty for granting me this opportunity as I am persuaded that He orders my steps according to His plan and purpose for my life.

Abstract

In the last couple of decades, attention has been placed on reducing atmospheric emissions globally, including the enforcement of stricter requirements which target emissions from internal combustion engines. This is not surprising considering the spate of public attention about the health impacts of atmospheric pollution. Then again there are concerns about their environmental impact. Consequently, engine developers, end-users, and researchers, increasingly are reconsidering the century-long idea of dual fuel engines. While there have been successful attempts to develop viable, sustainable alternatives to power diesel engines, the extent to which engine performance and emissions may be affected remains unknown. Therefore, this study evaluates the performance and emission characteristics of a diesel engine modified to run simultaneously with diesel and liquefied petroleum gas (LPG). The aim of this research is to numerically investigate the performance and emission characteristics associated with dual fuel engine operation (wherein LPG and diesel fuels are simultaneously used) with regards to the diesel engine operation at various operating regimes, taking into consideration different fuel mass ratios. With this in mind, this study presents a one-dimensional model developed using AVL BOOST to simulate the diesel and diesel-LPG engine operational modes. The model is calibrated using the peak cylinder pressure, the timing of the peak cylinder pressure, power and torque. For the maximum LPG scenario (70% diesel and 30% LPG) investigated at 2435 rpm, compared to the diesel engine operation, the maximum cylinder pressure was shown to increase from 77.16 bar to 93.42 bar representing an increase of 21.07%. Additionally, at 2435 rpm, the results from the study suggest a fairly linear increment in power when LPG mass ratio in the diesel-LPG fuel mixture is increased from 10 to 30%. It is remarkable that the highest mass ratio of LPG used in the diesel-LPG fuel mixture produces the highest brake thermal efficiency at 2435 rpm. Regardless of the speed, increasing the LPG fuel mass ratio in the diesel-LPG fuel mixture leads to a reduction in the nitrogen oxide (NO_x) emissions because the formation of NO_x depends on the oxygen concentration and the presence of LPG, leads to reduction of the oxygen concentration at the onset of NO_x formation which consequently causes the NO_x emissions to reduce.

Table of Contents

List of Figures

List of Tables

Nomenclature

List of Abbreviations

A/F	Air/Fuel
ABDC	After Bottom Dead Centre
ATDC	After Top Dead Centre
BDC	Bottom Dead Centre
BTDC	Before Top Dead Centre
CA	Crank Angle
CED	Cambridge Electronic Design
CFD	Computational Fluid Dynamics
CI	Compression Ignition
CNG	Compressed Natural Gas
DAQ	Data Acquisition
DI	Direct Injection
ECU	Electronic Control Unit
EGR	Exhaust Gas Recirculation
Eqn.	Equation
EU	European Union
EVO	Exhaust Valve Open
FPSO	Floating Production Storage and Offloading
FSL	Flame Speed Limit
GUI	Graphical User Interface
HCCI	Homogenous Charge Compression Ignition
ICE	Internal Combustion Engine
IDI	Indirect Injection
IMO	International Maritime Organisation
IVC	Inlet Valve Close
LED	Light-Emitting Diode
LHV	Lower Heating Value
LNG	Liquefied Natural Gas
LPG	Liquefied Petroleum Gas

MARPOL	Marine Pollution
MATLAB	Matrix Laboratory
NAOME	Naval Architecture Ocean and Marine Engineering
NG	Natural Gas
NGVC	Natural Gas Vehicle
OEM	Original Equipment Manufacturer
rpm	Revolutions per Minute
SI	Spark Ignition
TDC	Top Dead Centre
UNECE	United Nations Economic Commission for Europe
UK	United Kingdom

List of Chemical Symbols

CO	Carbon monoxide
CO_2	Carbon dioxide
CH_4	Methane
C_2H_6	Ethane
C_3H_8	Propane
HC	Hydrocarbon
NO	Nitrogen monoxide
NO_2	Nitrogen dioxide
NO_x	Oxides of Nitrogen
SO_2	Sulphur dioxide

1 Introduction

1.1 Prelude

Internal Combustion Engines (ICEs) are probably going to remain dominant for the foreseeable future. With this perceived dominance of ICEs, comes enormous pressure for them to be more efficient, reliable and yet much more environmentally friendly. There is a further insistence on keeping their design, manufacture and operation as cost-effective as practically possible. In an attempt to satisfy these expectations placed on ICEs, there has been a great deal of research and development put out.

Gaining prominence among several of the research themes is the concept of operating traditional ICEs with a second fuel – one which is more environmentally friendly. Several terminologies have been used to capture this method of operating traditional ICEs. The most common phrase in use has been "dual fuel". About a century ago, the concept of dual fuel operation for the internal combustion engine was being discussed, but it faded away because of the unrivalled thermal efficiency of the diesel-only engine. Nevertheless, this idea later resurfaced, drawing greater focus and attention from academics, scientists, manufacturers and policymakers. These interests have developed especially because there have been encouraging results following breakthrough research on the use of gaseous fuels to power internal combustion engines (Mbarawa and Milton, 2005). Global research on engine performance and alternative fuels has been driven by stricter emission regulations in many countries, but market dynamics, such as oil prices and the availability of cleaner fuels, have also been contributing factors.

There is evidence to suggest that replacing some of the diesel with a gaseous fuel while retaining efficiency identical to that of a diesel-only engine currently appears to be the ideal option (Carlucci et al., 2008, Christen and Brand, 2013, Karim, 2003b, Sahoo et al., 2009). Considering the spate of public attention about the health impacts of atmospheric pollution and the concerns about their environmental impact,

it is worthwhile investigating the performance and emissions characteristics of diesel engines operating simultaneously with gaseous fuels. While there have been successful attempts to develop viable, sustainable alternatives to power diesel engines, the extent to which engine performance and emissions may be affected provides avenues to be further explored. Consequently, this study uses a one-dimensional (1-D)/zero-dimensional (0-D) code for the development of diesel and dual-fuel engine model. The model is then used to parametrically investigate, analyse and subsequently discuss the effects of various mass ratios of gas-to-diesel on the performance of a diesel engine which has been retrofitted to also operate in dual fuel mode (using liquefied petroleum gas and diesel).

1.2 Problem Statement

There is the need to reduce the emissions emanating from internal combustion engines while making them (ICE) more fuel-efficient, cost-efficient and improving their performance characteristics. One way of achieving this is to make use of a more environmentally friendly fuel option such as liquefied petroleum gas (LPG). However, because using only LPG to power ICEs compromises the efficiency gains and stronger performance of the diesel engine, it is prudent to combine the two fuel types. Achieving this requires knowledge of what quantity of gas can be used to substitute for diesel while allowing for optimum engine performance. Additionally, understanding the complex nature of combustion for an engine that uses a combination of diesel and LPG is primordial to the success of the engine design and operation. Consequently, while using a one-dimensional model, this thesis provides insight into the performance and emission characteristics of a retrofitted diesel-LPG engine operation.

1.3 Background and Contextualization of Study

In the last couple of decades, attention has been placed on reducing emissions from engines. This is not surprising considering the spate of public awareness around the health impacts of atmospheric pollution. The enforcement of stricter requirements to limit emissions from engines, along with the depletion of traditional petroleum resources contribute in part to the sustained quest for finding viable alternative methods of powering ICEs. Several solutions are being researched and investigated worldwide, and one that is gaining remarkable attention is the use of gaseous fuels along with liquid diesel in compression ignition engines – like the diesel engine. According to Selim et al. (2009), utilising alternative gaseous fuels like liquefied petroleum gas; natural gas etc. has great potential to simultaneously reduce dependence on conventional liquid petroleum fuels and some pollutant emissions from diesel engines.

Additionally, liquefied petroleum gas (LPG) which primarily consists of propane, butane as well as other hydrocarbons, is reported to be a viable alternative gaseous fuel (Raslavičius et al., 2014, Leermakers et al., 2011, Goldsworthy, 2012). LPG is advantageous when compared to other gaseous fuels in the sense that, it is relatively easier to store and transport it. This is primarily because, at atmospheric pressure, it can readily be liquefied between the pressures 0.7–0.8 MPa.

Furthermore, LPG has a high octane number (this is a figure that indicates the anti-knocking properties of a fuel, based on a comparison with a mixture of iso-octane and heptane), thus making it suitable for usage in spark ignition engines. On the other hand, the cetane number (this is a measure of the ignition quality of fuel) for LPG is low. As a result of high cyclic variations due to LPG's low cetane number, it makes it quite tricky for LPG to be utilised in a large proportion of compression ignition engines (Negurescu et al., 2013, Oguma et al., 2003, Tira et al., 2012). However, one ideal way of ensuring its practical usage in CI engines is to use it along with conventional liquid fuel. CI engines that simultaneously burn two entirely different fuels (one is gaseous and the other liquid), in varying proportions are referred to as 'dual-fuel engines (Karim, 2015). This study focuses on investigating the performance of a conventional four-stroke diesel engine which was retrofitted to

operate in dual-fuel (diesel-LPG) mode. The limitations of LPG to auto-ignite along with the desire to retain or surpass efficiencies identical to that of the diesel-only engine contextualise this study even more. Additionally, the fact that retrofitting of diesel engines to operate in dual-fuel mode requires minimum modification supports the practicality and applicability of this work.

1.4 The motivation for Choosing LPG as Fuel in ICEs

Apart from the environmentally friendly nature of gaseous fuels, a few other economic factors can be made to support the usage of LPG. Some of these are discussed in the sub-sections that follow.

1.4.1 Cost Considerations

The cost of energy is a significant driver that influences the decision of switching from traditional petroleum usage to alternative fuels (such as LPG and LNG). In the shipping industry, for example, the fuel cost has tremendous (about 75%) effect on the overall operation cost of ships as shown in Figure 1.1.

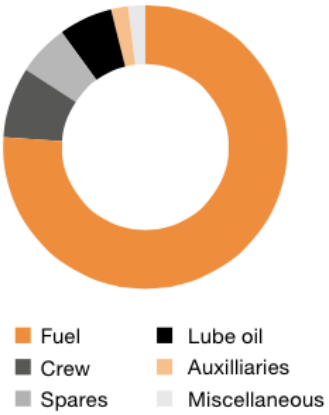

Figure 1.1 Share of fuel Cost on the overall operating cost of a ship (Wärtsilä, 2013)

In several other sectors and industries, fuel/energy costs also constitute a substantial portion of the total operating costs of running engines. Thus it is paramount for

owners and operators of ICEs to find cost-saving incentives (alongside the environmental benefits) to justify the reason for using alternative fuels such as LPG and LNG to power their engines. In this regard, a review of fuel prices for various fuels suggests that LPG would offer cost-saving incentives. Figure 1.2 and Figure 1.3 reveal that compared to diesel and unleaded (Petrol/Gasoline), LPG prices would provide substantial financial savings, thus offering another benefit that further serves as motivation to consider the usage of LPG or LNG which tends to be more environmentally friendly.

Last prices from 26.9.2018

LPG	Unleaded	Diesel	Heat Oil
N/A	N/A	N/A	N/A

Record prices

	Minimum price	Maximum price
LPG	0.538 €/L	1.066 €/L
Unleaded	1.239 €/L	1.773 €/L
Diesel	1.256 €/L	1.827 €/L
Heat oil	0.787 €/L	0.927 €/L

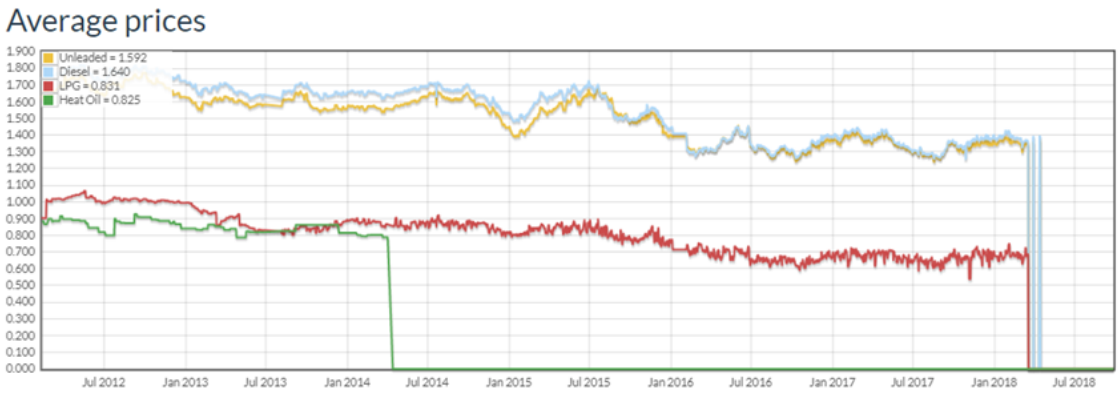

Figure 1.2 Average Fuel Prices in the United Kingdom (Matvoz, 2018)

As shown in Figure 1.2, Matvoz (2018) demonstrates that using LPG is more economical than petrol, diesel and other sources of power. Based on fuel prices in the United Kingdom, his statistical analysis concludes that the cost of filling a tank of LPG is half the cost of filling a tank of petrol or diesel. The purpose of Figure 1.2 is to illustrate that apart from the obvious environmental benefits, the usage of LPG also offers cost-saving incentives which is a good motivation for the choice of LPG to power dual fuel engine. The study by Matvoz has been chosen to support my argument on the basis of the fact that my research is carried out in the United Kingdom and the sample size for Matvoz's statistics perfectly suit my context.

Despite his updated statistics about fuel prices in the United Kingdom market, I am of the opinion that this a vivid reflection of the behaviour of the fuel prices globally. Hence, the motivation for the choice of LPG based on the above could be valid globally.

Matvoz (2018) fuel price statistics is fully justified and endorses that provided by Eurostat (2017) and portrayed in Figure 1.3. The statistical approach adopted by Eurostat (2017) compares fuel prices across the European Union. They also illustrate the comparatively cheaper nature of LPG. Their findings are, therefore, relevant in the current context of energy efficiency and the support they lend to my argument of the cost-saving potential associated with the usage of LPG to power engines.

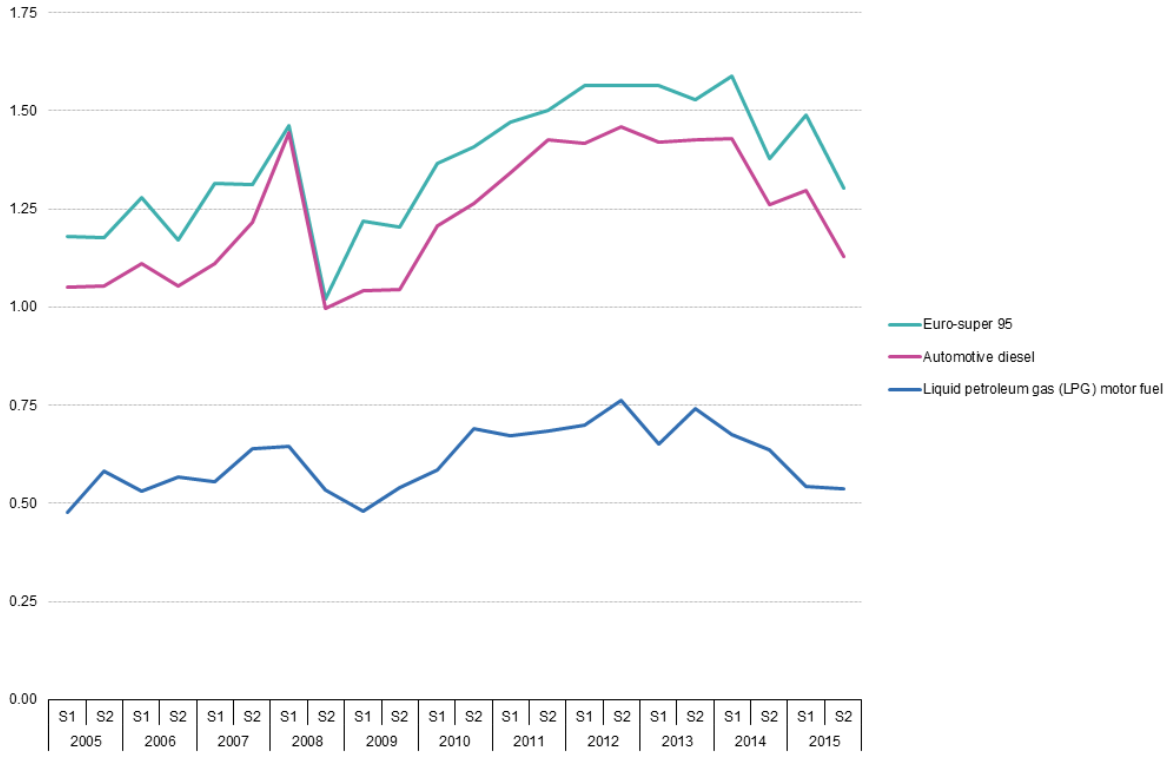

(') Weighted average. Inclusive of taxes and duties. Reference periods refer to the end of each half year.

Figure 1.3 Consumer prices of petroleum products across the EU from 2005-2015 (Eurostat, 2017)

1.4.2 Demand and Supply of LPG

For the last decade, the increasing demand for LPG has led to an average rise of about 4.1% in its production across several regions. It is believed that the LPG production would further increase in the coming years (Gist et al., 2006, Holmes, 2008, Esther, 2016, Viola, 2018) due to several reasons – stringent environmental legislation, cost benefits, etc. Figure 1.4 reveals that over 284 million tons of LPG were produced in 2014. The increase in LPG production coincides with an increase in its production growth from Russia and the Middle East (Esther, 2016)

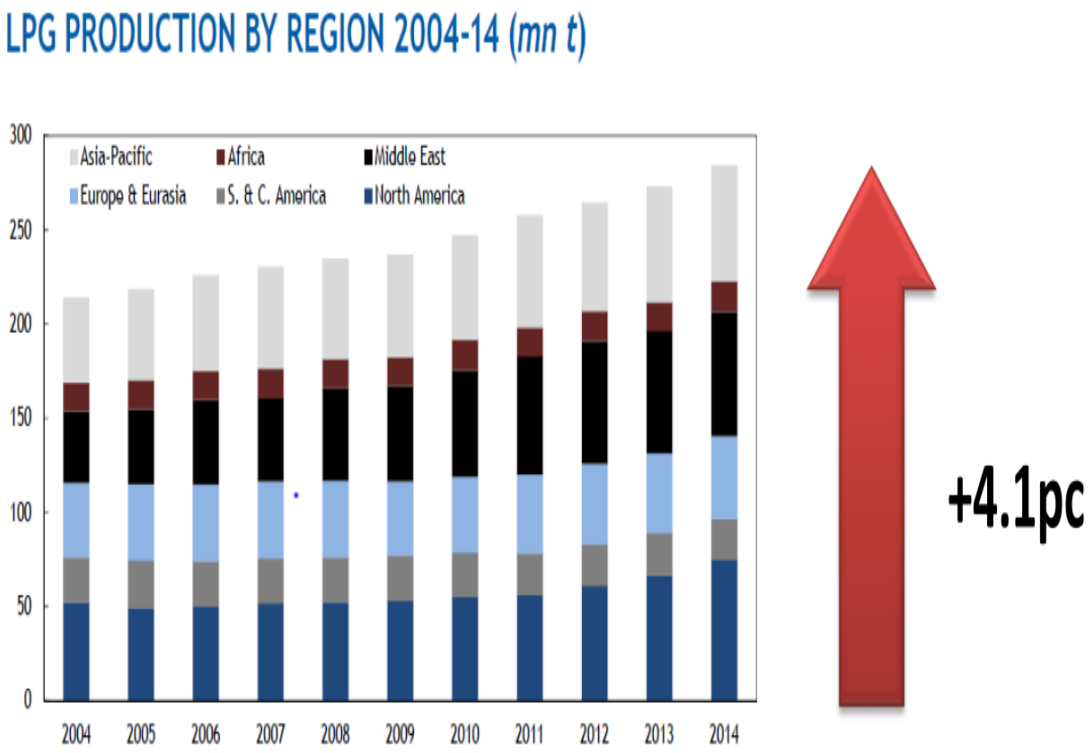

Figure 1.4 LPG Production by region from 2004 to 2014 (Esther, 2016)

On average, the consumption of LPG has been steady across many areas for the past decade. But between the years 2013 and 2014, 4% increase in consumption suggests that the world is embracing more and more the need to switch to more environmentally friendly fuels (Esther, 2016). While 284 million tons were produced, 275 million tons were consumed during the same period. Therefore LPG production has been sufficient to cater for the consumption needs of customers. This

trend is likely to continue for the foreseeable future. Figure 1.5 reveals Asia-pacific as a key LPG consuming region. This is not surprising given that there is a direct link between a region's population size and its consumption of LPG as shown in Figure 1.6. Overall, the balance in demand and supply of LPG promotes the case for its usage on the evidence of its availability.

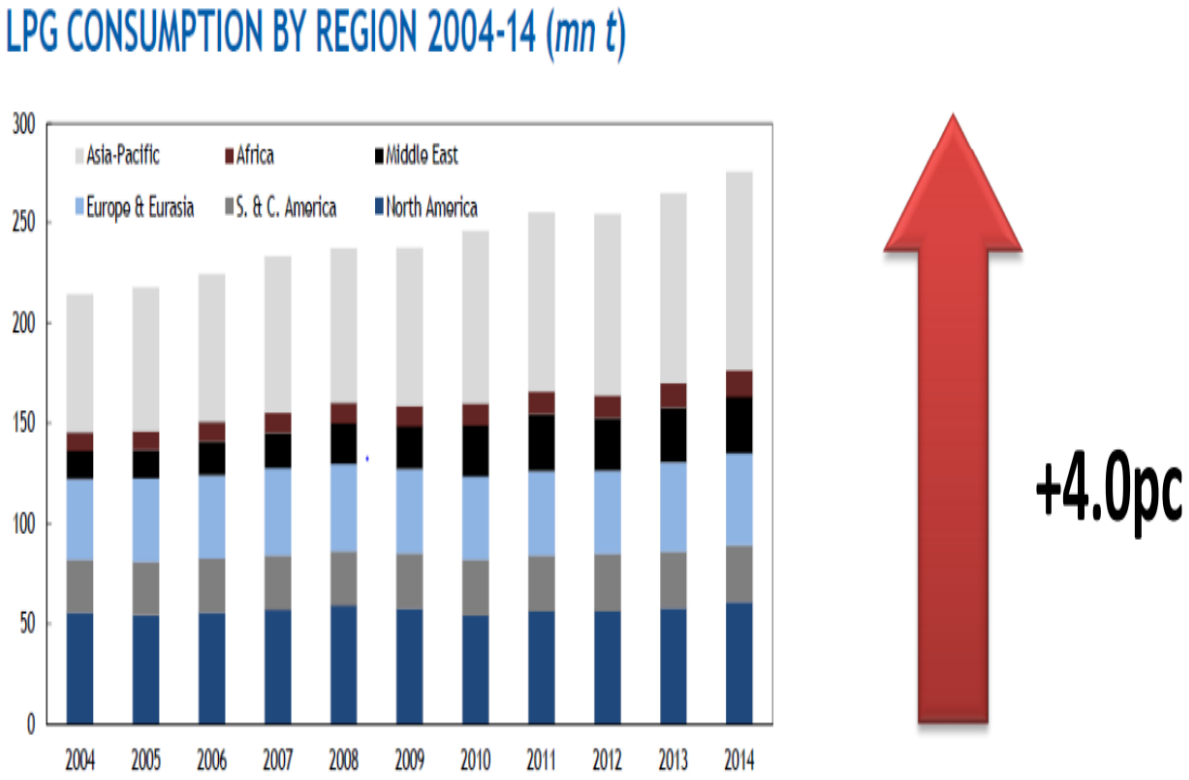

Figure 1.5 LPG Consumption by region from 2004 to 2014 (Esther, 2016)

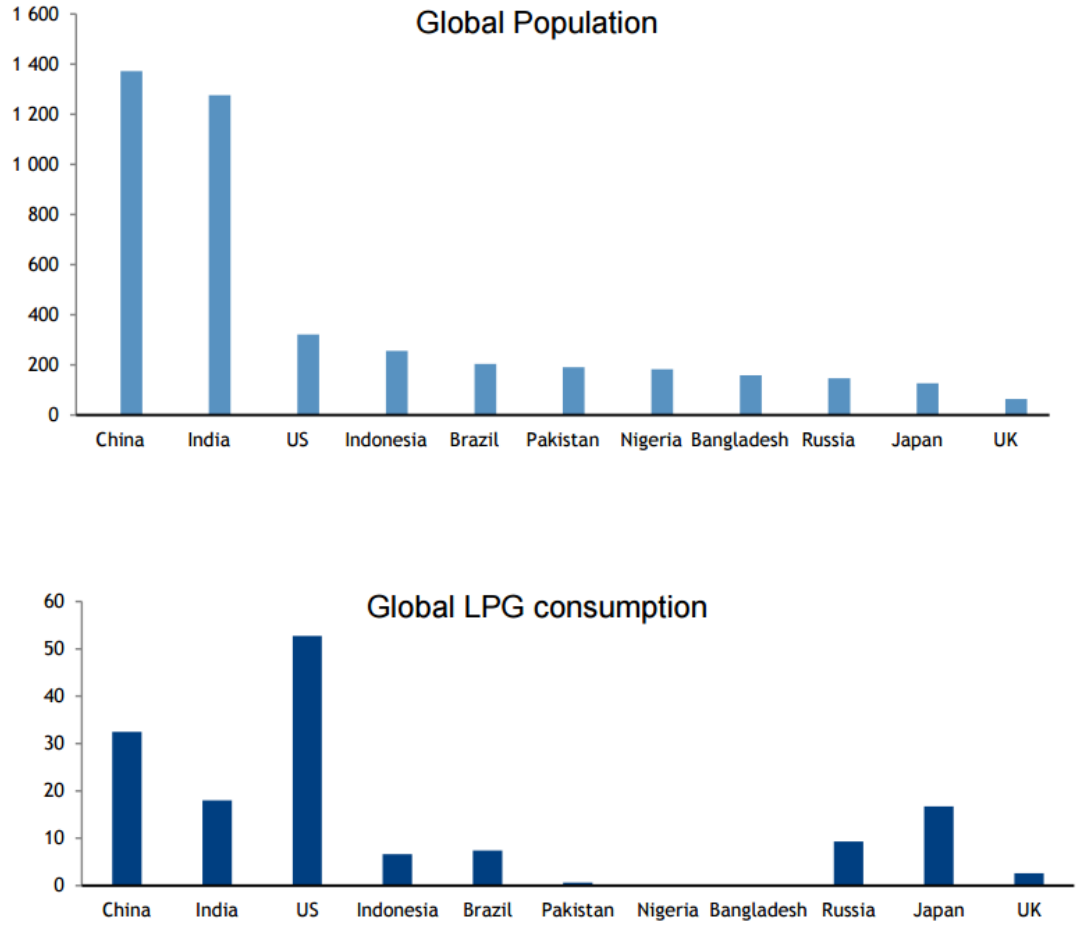

Figure 1.6 Influence of Global Population on LPG consumption (Esther, 2016**)**

Figure 1.7 and Figure 1.8 forecast that, until the year 2020, while demand for LPG will stay robust, its production will not be running out. Indeed, production is said to rise by up to about 30 million tons per year between now and 2020. It is forecasted that this increase in production vis-à-vis the demand would be driven by Russia and the Asia-Pacific region. Gas processing is predicted to dominate production in the coming years more than the production from the refinery. Although some growth in LPG demand and production is uncertain in some regions/countries, the LPG export capacity of the United States of America could reach 40 million tons per year by 2020. The future market dynamics strongly suggest that LPG would be readily available in most parts of the world by 2020.

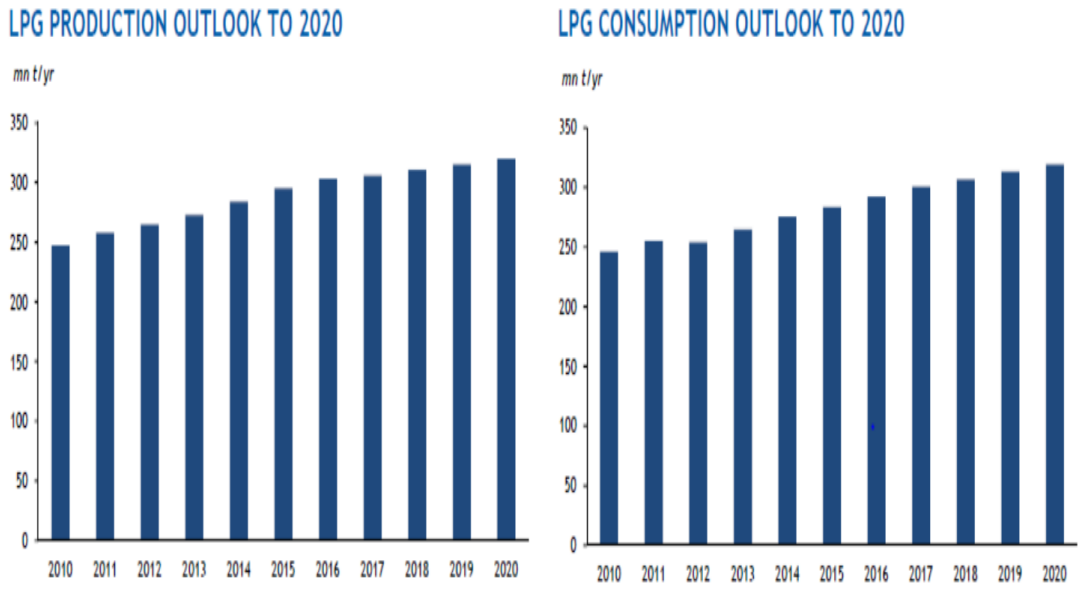

Figure 1.7 Forecast of LPG supply and demand till the year 2020 (Esther, 2016)

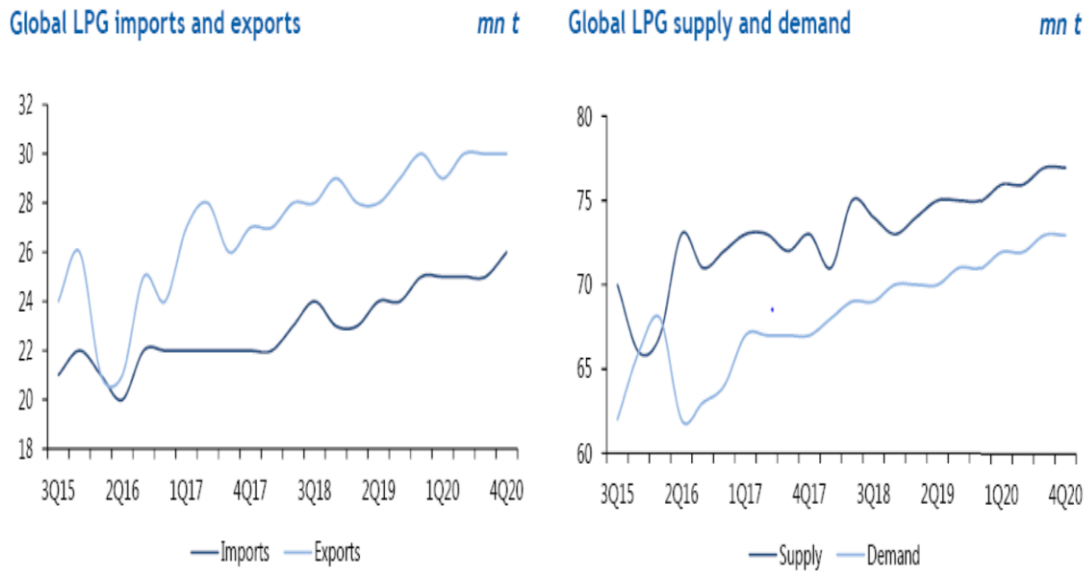

Figure 1.8 Global Outlook of LPG imports, exports, supply and demand for certain quarters of certain years (Esther, 2016)

1.5 Dual-Fuel Engine Application across Some Sectors

Internal combustion engines that operate using liquefied petroleum gas (LPG) and natural gas (NG) along with either diesel or petrol are said to be using technologies described as "well-proven" especially as these work in a similar fashion to the gasoline-powered spark-ignition engines (Robert Bosch GMBH, 1996)

They have been used in spark-ignition engines as well as in compression-ignition engines. LPG and NG can be used alongside a secondary fuel – diesel in compression ignition engines because of their inability to self-ignite. The secondary liquid fuel provides the source of ignition for the gaseous fuel thereby enabling the gaseous fuel to function admirably. Two examples of gaseous fuel used in engines for vehicles are discussed in the sub-sections below.

1.5.1 Liquefied Petroleum Gas Vehicles

Figure 1.9 reveals the LPG consumption for several sectors. While it shows that the domestic sector accounts for most of the LPG usage, this study is predominantly interested in the way LPG is used in the transport sector.

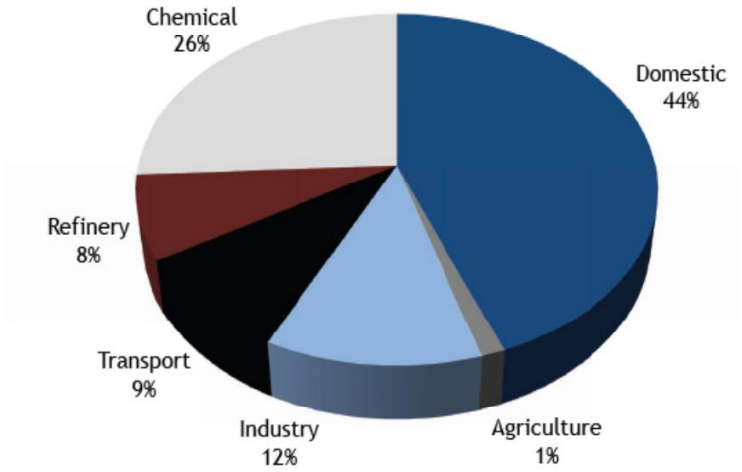

Figure 1.9 LPG Consumption by Sector (Argusmedia, 2016)

In vehicle applications, LPG is kept as a liquid in a distinct vessel at a pressure of about 10 bars despite the possibility of it withstanding pressures of between 20 to 30 bars. The supply of LPG to the engine in such an application is controlled by a regulator or a vaporiser which then converts the LPG to a vapour. Prior to being drawn into the combustion space (where the LPG is burnt to produce power), the vapour is taken to a mixer situated close to the intake manifold. In the intake manifold, this vapour is metered and mixed with filtered air. It is accepted that LPG systems have demonstrated that they are reliable as far as power, engine durability and cold starting are concerned. LPG technology is thought to be most popular in Armenia with an estimated 20-30% of vehicles being run on LPG given that it is cheaper than diesel and petrol. However, other places where LPG technology is quite popular include the European Union, Australia, Turkey, Serbia, South Korea, Philippines, Hong Kong and India. Furthermore, cold start problems are said to be minimal as LPG has a high energy content per unit of mass, but unfortunately, its energy content per unit of volume is low (Norris, 2009).

LPG is readily available in most parts of the world with several LPG filling stations operational. Figure 1.10 and Figure 1.11 show the LPG re-fuelling locations in the UK and Glasgow respectively. Looking at the maps in both figures, it is evident that almost the entire territory in each case has access to an LPG filling station.

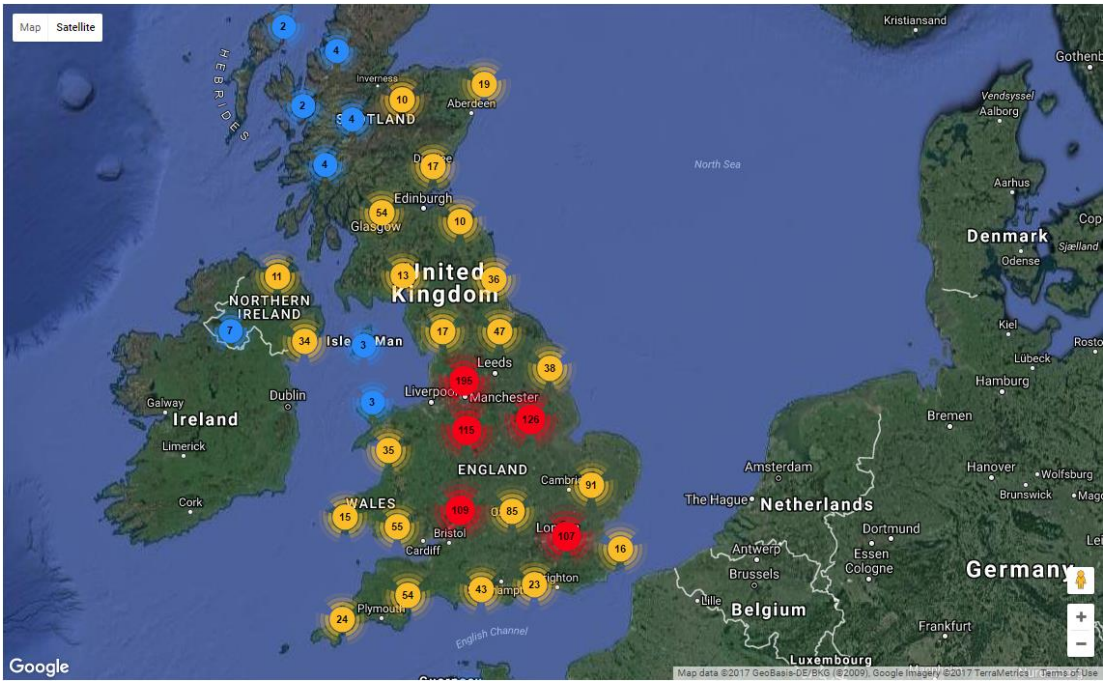

Figure 1.10 Map of LPG filling stations across the United Kingdom (Matvoz, 2017)

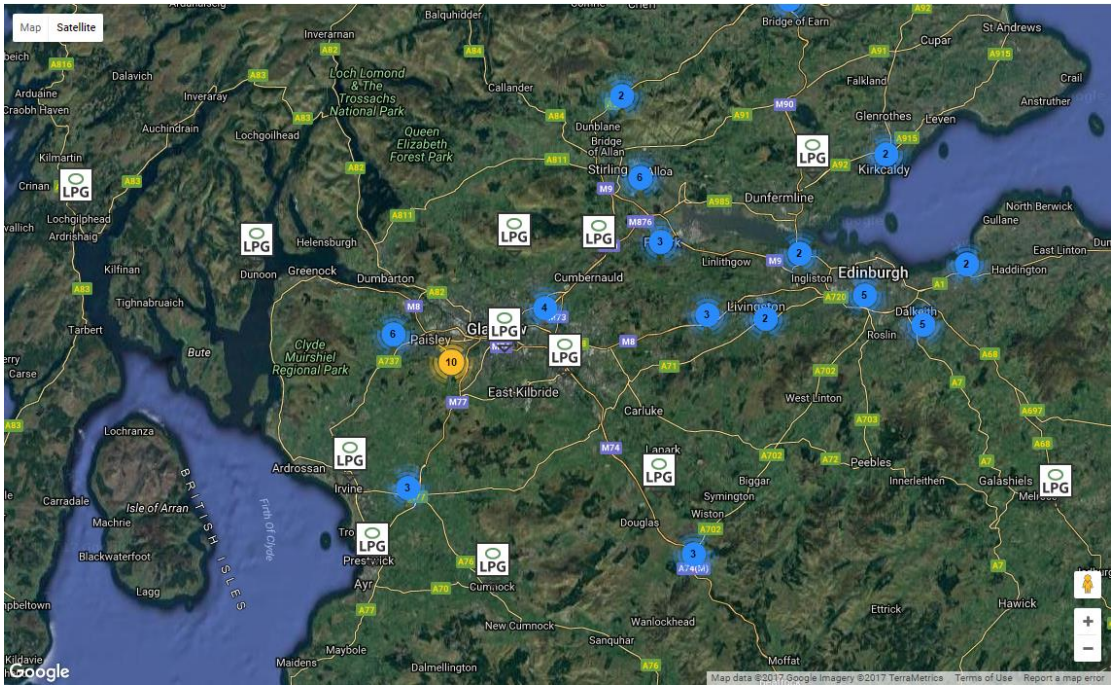

Figure 1.11 Zoom-in showing the location of the LPG stations in Glasgow, UK (Matvoz, 2017)

1.5.2 Natural Gas Vehicles

Diverse engine technologies that operate using natural gas include the following: stoichiometric combustion, lean burn, single point injection; and multi-point injection. For such applications, natural gas is stored onboard in either compressed (CNG) or liquefied (LNG) form. South America is documented to have the leading market share accounting for about 48% of around 7 million NGVC that were running on the world's roads in 2008. The USA has approximately 130,000 vehicles, mostly buses. Italy leads the European market with its long-standing tradition of utilising CNG vehicles. In 2008, about 500,000 were reported to be running in Italy. Figure 1.12 shows the growth of NGVCs by regions, from 1991 to 2008. South America and Asia demonstrated the highest growth.

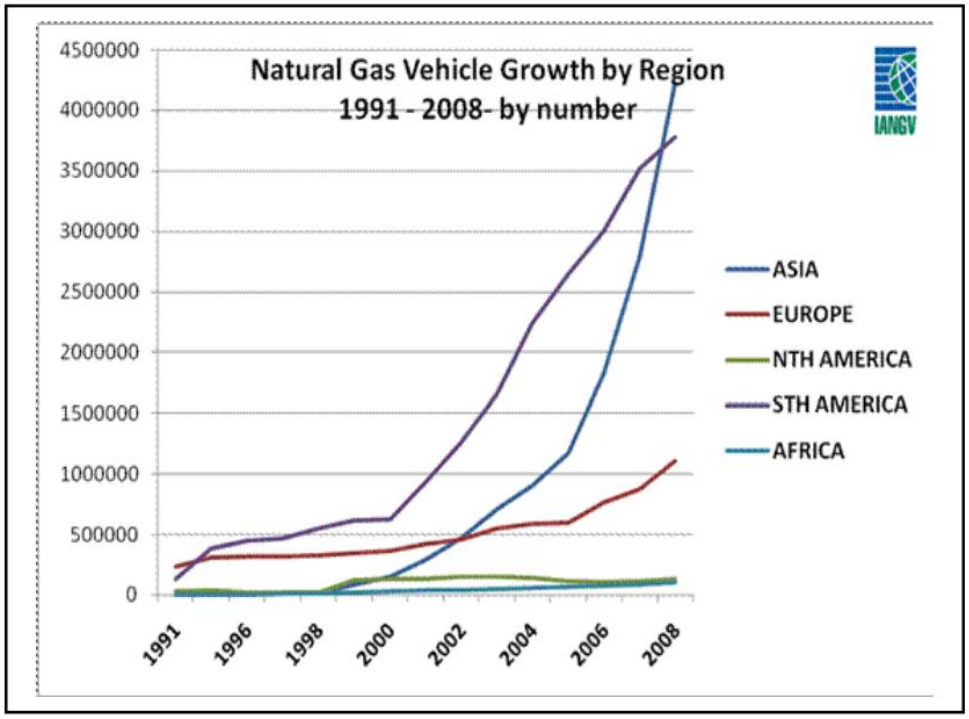

Figure 1.12 Natural gas vehicles by regions 1991 – 2008 (EPA, 2007)

1.5.3 Marine and Offshore Applications

Forecasts indicate that there is going to be an increase in the need for seaborne means of transportation in the near future. This forecasted growth in demand for seaborne transportation will coexist with the stricter emissions requirements (IMO, 2014) already put in place since the public has become quite concerned about the environmental footprint of shipping. Consequently, the shipping industry has investigated the utilisation of alternative fuels for running engines that propel ships. With the abundance of marine carriers in the world nowadays, there is the utmost need for them to be more cost efficient while simultaneously complying with stringent emissions legislation. In a sense, there is interest for these carriers to be cost-efficient and reliable. In view of this, utilising natural gas rather than diesel or heavy fuel oil has demonstrated tremendous potential in reducing fuel cost, while simultaneously offering a decrease in emissions. Therefore, this permits the many carriers to comply with the current strict environmental legislation.

It is therefore not uncommon to assert that the application of dual fuel engines in the maritime industry has been predominant on ships where there is a readily available source of gas, e.g. Liquefied Natural Gas (LNG) carriers (Richards, 1999). Gas-diesel and typical dual fuel low speed, two-stroke engines for propulsion have been developed. Companies such as Wärtsilä, MAN B&W, Cummins, and Caterpillar have all significantly contributed to establishing dual fuel engine practice (Wärtsilä, 2015, MAN, 2012, Cummins, 2018, CAT, 2018). One main advantage that dual fuel engines bring to the shipping industry is their fuel flexibility. It is documented that the engine efficiency in gas mode sometimes equals or surpasses the efficiency in oil mode.

With regards to the offshore industry, it is believed that oil platforms are an ideal environment in which the application of dual-fuel engines should thrive (Richards, 1999). It is argued that this is because there is ready availability of gas at very minimal (if not zero) cost. Despite this suggestion of ready availability of gas, caution is required as there cannot be a total reliance on the supply. Looking at the traditionally fixed oil platform, and comparing with the floating, production, storage and offloading (FPSO) vessel, it is believed that the dual fuel engine applications are more beneficial to the latter rather than the former. To support the argument above, the Wärtsilä 46DF engine has been specifically designed for high output segments like offshore vessels, Floating storage and regasification units (FSRU) and FPSO (Wärtsilä, 2014).

1.5.4 Power Generation

There has been growing pressure on several industries to reduce the number of emissions produced. The power generation sector has not been left out. In this regard, the prevalent institution of emission regulations to power generation units as well as stationary plants provides a reasonable avenue in which dual fuel engine applications can thrive. In addition, several parts of the world use gas pipelines. This offers a readily available (and in most instances cheaper) source of natural gas, thus enhancing the ease of application of dual engines.

1.6 Project Outline, Organization, and Structure

The current research presented in this thesis is organised and presented in eight chapters as shown in **Error! Reference source not found.**. Chapter one introduces the entire study. It states the research problem and also provides the rationale and background for the study. Interestingly, taking into account various studies, this chapter offers evidence to support and make a case for the choice of gaseous fuel usage in internal combustion engines. The chapter then closes by giving an outline of the thesis and a summary of its contribution to knowledge.

The second chapter is relatively shorter and more concise. It specifies the central aim and enumerates some specific objectives of the study.

Chapter three reviews the literature relevant to the study. Given the nature of the research carried out, this chapter additionally reviews information on modelling and simulation of combustion in ICEs. The chapter concludes by presenting some of the author's views in a critical appraisal of the literature.

The overall methodology is organised and described across the next three chapters (four, five and six). Hence, Chapter four begins by outlining the experimental study carried out. It illustrates the set-up of the engine within the laboratory. Additionally, it describes the process of modifying diesel engines to operate as dual fuel engines.

Then, Chapter five discusses the engine model development of the diesel and diesel-LPG engine implemented using AVL BOOST. It also presents and provides a brief overview of the theoretical framework of several sub-models used to build the overall one-dimensional engine model.

Chapter six provides insight into the calibration and validation of the various models based on the cylinder pressure data and several performance parameters, notably the maximum cylinder pressure, the timing of the peak cylinder pressure, power and torque.

Chapters seven and eight bring the study to a close, with the former, providing discussion and analyses of the results obtained. The latter concludes the study by giving a brief overview of the entire study, assumptions, limitations, significant contribution and recommendations for future studies. Figure 1.13 presents a

flowchart summarising the outline and organisation of the thesis into the eight chapters written and presented.

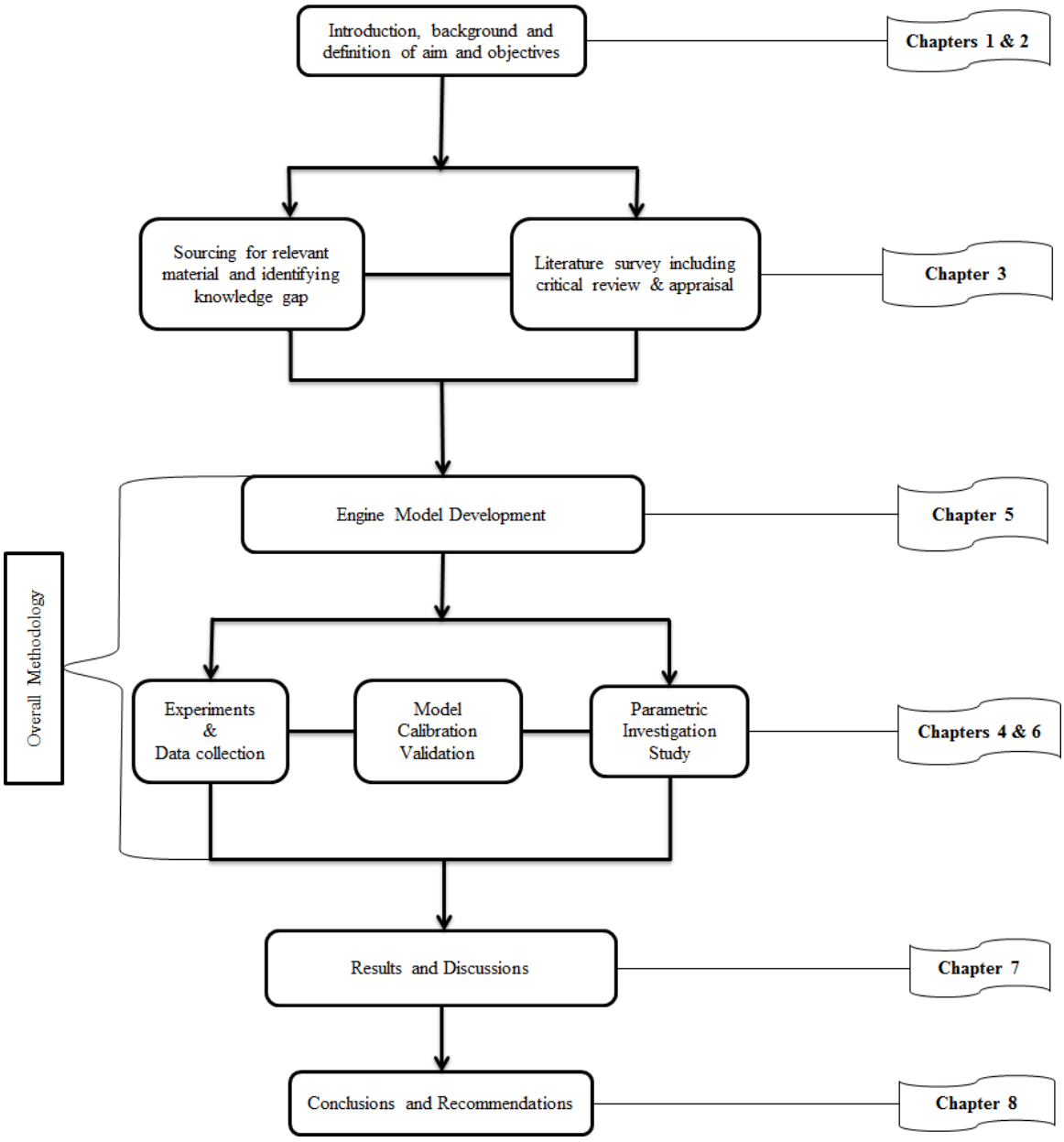

Figure 1.13 Outline of Thesis

2 Aim and Objectives

2.1 Aim

The main aim of this research is to numerically investigate the performance and emission characteristics associated with dual fuel engine operation (wherein LPG and diesel fuels are simultaneously used) with regard to the diesel engine operation at various operating regimes. In this context, using a case study diesel engine, the study seeks to develop a one-dimensional model to evaluate various performance and emission characteristics of a diesel engine that has been adapted to operate simultaneously on LPG and diesel. Within this framework, the study also intends to calibrate and validate the developed model. Subsequently, this study proposes and presents the results of a parametric study computed and executed using the developed one-dimensional model and taking into account the following engine operating parameters:

- Various mass ratios of diesel to LPG
- Engine speed
- Engine load

Using the developed model, the study also targets to shed light on the behaviour of diesel-LPG pollutants particularly nitrogen oxide (NO_x), carbon monoxide (CO) and soot.

2.2 Specific Objectives

Throughout this work, some specific objectives, tasks or goals have been set to ensure the achievement of the overall aim stipulated in section 2.1. A discussion of how these objectives are achieved is presented throughout the various chapters of this thesis. The goals are enumerated as follows:

- Provide a survey of the literature (including a critical review and appraisal) about the dual-fuel engine concept

- Carry out experiments to obtain engine measurements
- Appropriately process the engine measurements obtained, so they are used for development and calibration of the one-dimensional model
- Use AVL BOOST to develop a one-dimensional computational model for the LPG-diesel engine operation:
  - ❖ Wherein the effect of various engine operating regimes are investigated
- Calibrate the developed model using relevant parameters such as maximum cylinder pressure, maximum power and torque for each scenario studied.
- Investigate the effects of various LPG-to-diesel fuel ratios on the engine torque, power, etc.

2.3 Hypothesis

Usage of a gaseous fuel along with conventional diesel as an alternative internal combustion engine fuelling option is thought to be very promising. This study sets out to further investigate this thought and the hypothesis that, the higher the amount of gaseous fuel used to substitute diesel, the more environmentally friendly the internal combustion engine (in this case diesel/LPG engine) will be.

2.4 Synopsis of Chapter Two

In summary, this chapter provided the overall aim of the research and also specified the objectives that put in place to enable the main objective of the thesis to be achieved. To reiterate, the aim is to investigate the diesel-LPG engine performance and emission characteristics through the development, calibration, and validation of a one-dimensional computational model. The next chapter reviews relevant literature and provides a critical appraisal of the dual-fuel engine concept.

3 Literature Review

3.1 Working Principle of Dual-Fuel Engines

A dual-fuel engine is an internal combustion engine that has a gaseous fuel as its primary fuel and yet requires an amount of diesel for purposes of ignition of the gas/air mixture. Figure 3.1 illustrates the dual fuel engine working principle.

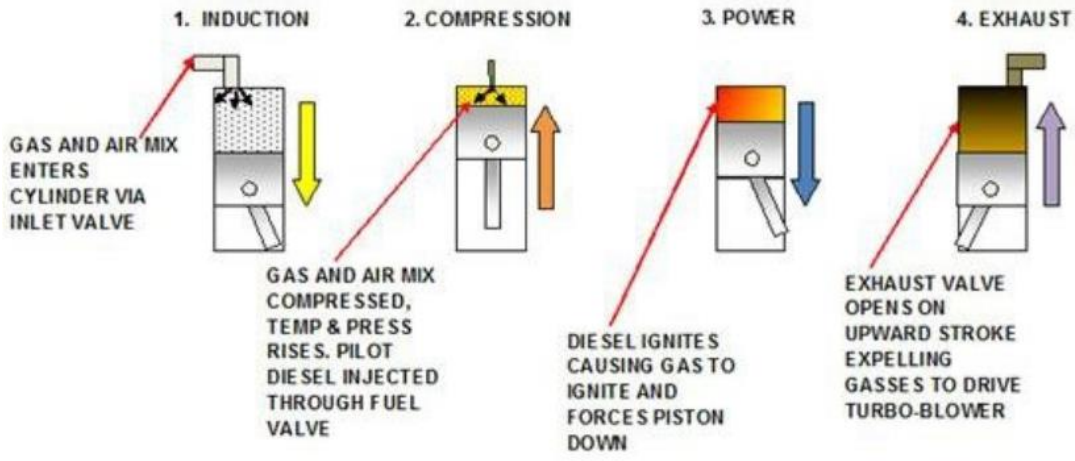

Figure 3.1 Overview of dual fuel engine working principle (Scot, 2011)

By modifying (i.e. adding dual-fuel specific hardware too) the traditional diesel engine, the dual-fuel engine is achieved. This engine can operate in a dual-fuel mode as well as in a diesel-only mode. However, it cannot run in gas-only mode. In the dual-fuel mode, there is the introduction of gas into the intake system. Since gaseous fuel has been introduced into the system, the air/gas mixture is then drawn into the cylinder via the intake valve.

Nonetheless, this mixture would not auto-ignite on its own. There must, therefore, be a deliberate source of ignition. To this effect, when the piston is approaching the end of the compression stroke, a small amount of diesel is injected into the cylinder. This diesel fuel ignites and its combustion causes burning of the gas/air mixture.

This study focuses on the internal combustion engines of the reciprocating type. Reciprocating ICEs could be further classified either as a spark-ignition (SI) or a compression-ignition (CI) type (Heywood, 1988). From the explanation in the previous paragraph, it is appropriate to state that dual fuel engines borrow and combine the combustion concepts of both the SI and CI, i.e. the air/gas mixture is carburetted first and then it is compressed like in a conventional diesel-only engine. Comparatively, the dual-fuel engine is advantageous in the sense that, it employs the difference of flammability of two fuels. Furthermore, in most cases, the engine can be made to switch from dual-fuel mode to diesel-only mode. It is this particular advantage that has been successfully utilised to combat the poor performance associated with operating the dual-fuel engine at light load. Given that the case study engine used for this research is originally a diesel engine that has been modified, it is evident that this engine can be operated in pure diesel operation at low load. Hence, overcoming poor performance at low load is not the focus in this present contribution.

3.2 Dual-Fuel Engine Characteristics

It is primordial to understand some of the fundamental things that characterise the dual fuel engine. For the sake of emphasis and precision, dual-fuel engine here refers to one that uses gas and still requires an amount of diesel to ignite. This engine thus retains the features of a traditional diesel-only engine.

3.2.1 Combustion

It is well documented that for burning (combustion) to occur in a conventional dual-fuel engine; there is going to be some amount of liquid fuel being injected into pre-mixed air and gas (Richards, 1999). With this in mind, as well as with the fact that the dual-fuel engine primarily emanates from the diesel-only engine, it is prudent to have a look into what the combustion process of both engine types involves. The slight difference between their combustion processes is that; in the case of the dual-

fuel engine, the process takes place in five stages; whereas, for the diesel-only engine, the process takes place in four stages (Sahoo et al., 2009).

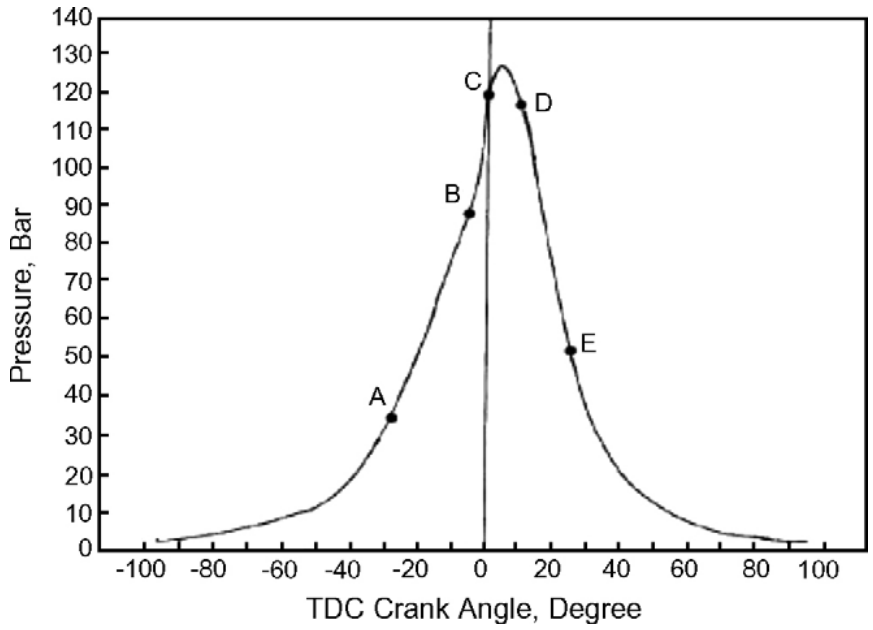

Figure 3.2 Stages of the combustion process in a diesel-only engine (Nwafor, 2003)

Figure 3.2 graphically represents the changes in pressure with regard to the Top Dead Centre crank angle for a diesel-only combustion process. The vertical axis represents cylinder pressure in bar while the horizontal axis tracks the crank angle in degrees. The negative crank angles are used to depict angles of the crank prior to the piston reaching Top Dead Centre. It is evident from the above graph that for a diesel-only engine, four stages are involved in its combustion process. These stages are;

- A – B: Period of delay in ignition
- B – C: Premixed combustion
- C – D: Controlled combustion
- D – E: Late combustion

For the dual-fuel engine operation, there are five stages involved in the combustion process. Figure 3.3 graphically represents the cylinder pressure and crank angle for the combustion process in a dual-fuel engine. The five stages involved in the dual fuel engine combustion as revealed in Figure 3.3 are:

- A – B: Ignition delay of pilot liquid fuel
- B – C: Premixed combustion of pilot liquid fuel
- C – D: Ignition delay of primary fuel (gas)
- D – E: Rapid combustion of primary fuel (gas)
- E – F: Diffusion combustion

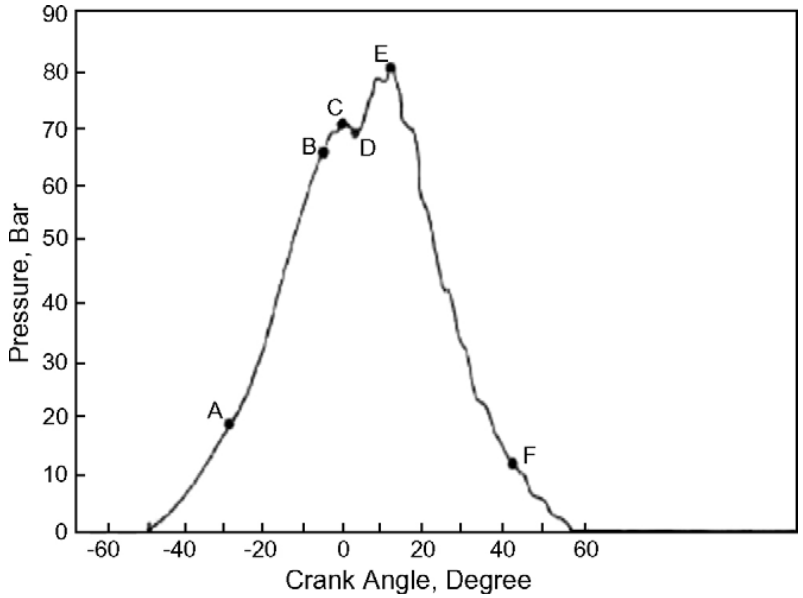

Figure 3.3 Pressure versus crank angle analysis of dual fuel pilot injection (Nwafor, 2003)

Comparing and contrasting the combustion process of both the diesel-only and dual-fuel engine operations will further enhance the argument being made earlier in this work, that the dual-fuel engine takes its inspiration from the diesel-only engine. Much more than just the fact that there are five stages involved in the dual-fuel operation, some other significant differences can be spotted (even by visual inspection of the graphs in Figure 3.2 and Figure 3.3).

Firstly, Figure 3.3 reveals that there is a much longer period (when compared to that for diesel-only operation) for which the injected fuel delays before igniting. Several reasons could be advanced for this. One of such reasons would be the fact that, in a dual-fuel engine, there is the addition of gas to air. The implication of this gas substitution for air is a consequent reduction in the concentration of oxygen. This reduced concentration of oxygen then accounts for the increased ignition delay period (Sahoo et al., 2009)

A second difference between the combustion processes is that there is a relatively low-pressure rise in the dual-fuel operation when compared to that of the diesel-only operation. This low-pressure rise could be attributed to only a small quantity of diesel fuel being ignited.

Thirdly, owing to the auto-ignition temperature of the gas/air mixture, there is a longer ignition delay. This results in a time lag emanating between the development of the first and second pressure rise. Though there is an ignition delay, it is short in comparison with the delay period by the diesel fuel injected.

3.2.2 Fuel injection and ignition

This is a very vital characteristic not just for diesel-only engines but also for dual-fuel engines. Fuel is usually injected into the combustion chamber prior to the piston approaching top-dead-centre. This happens at very high pressures. Presently the consensus is that the dual-fuel engine still uses the standard diesel-only fuel injection system (Sahoo et al., 2009, Rogers, 1999). Despite this existing consensus, it is believed that there is an avenue for future research to explore this area further.

Although the dual-fuel engine relies on the conventional diesel fuel injection system to provide a pilot amount of liquid diesel fuel, the engine induces a compressed premixed (gas/air) fuel into the combustion chamber. This compressed mixture is subsequently made to ignite due to the energy that emanates from the burning (combustion) of the diesel spray produced from the standard diesel-only injection system.

The analysis of literature reveals that there are some discrepancies in the amount of pilot fuel required to ignite the compressed mixture of gas and air. Sahoo et al. (2009) document that between 10 to 20% of the pilot fuel is required whereas Rogers (1999) argues that between 5 to 8% is needed. Another study reveals that a minimum liquid fuel quantity of 5 to 10 % of the maximum full load fuel is essential to achieve good spray penetration and atomization. In the same study, the authors go on to emphasise that for a dual-fuel engine that does not need to revert to a 100% diesel-

only operation, the minimum pilot fuel quantity can be reduced to less than 1% while employing a much smaller fuel-injection system (Weaver and Turner, 1994).

From exploring the research carried out over the years, there is significant evidence to argue that, there is no specific amount that can be expected to satisfy the purpose of all the existing engines in the world. Thus each engine would have a quantity range that best suits its operations. The required amount of pilot fuel would differ for engines due to reasons involving design parameters as well as the point of operation of the engines.

"Ideally, there is a need for optimum variation in the liquid pilot fuel quantity used any time in relation to the gaseous fuel supply to provide for any specific engine the best performance over the whole load range desired" (Mansour et al., 2001).

3.2.3 Dual-fuel engine performance and emissions

It is useful at this stage to reiterate that the focus of this work is centred on the gas-to-diesel fuel ratio of dual-fuel engines. This aspect of the dual-fuel engine is very vital when it comes to examining the dual-fuel engine performance and emission characteristics. It is however quite essential to also establish the fact that, the gas-to-diesel fuel ratio is not the only factor that affects the performance and emissions of dual-fuel engines. Some other factors (engine design and operation parameters) include diesel fuel injection timing, the conditions surrounding the intake manifold, the type of gaseous fuel utilised, load, the speed and compression ratio.

3.2.3.1 Effect of diesel fuel mass on performance and emissions

Given the focus of this thesis, it is entirely necessary to explore the impact that the mass of diesel fuel injected has on the performance and emission characteristics of the dual-fuel engine. It is argued that the mass of diesel fuel injected is one of the most critical factors (Sahoo et al., 2009). This argument supports particularly the extensive work done about the operation of the dual-fuel engine at light load (Karim, 1983).

Despite the agreement of the importance of the diesel mass, there is evidence to suggest that in the past, several diesel engines have witnessed poor combustion and atomization within their injection systems. This is reported to be caused by the quantity of diesel fuel injected per cycle being well under 5–10 % of the optimum design level.

Previous research (see, for example, Badr et al., 1999) reveals that the quantity of diesel fuel would no longer affect carbon monoxide emissions as well as the unburned methane gas when the engine operates way beyond a certain limiting equivalence ratio.

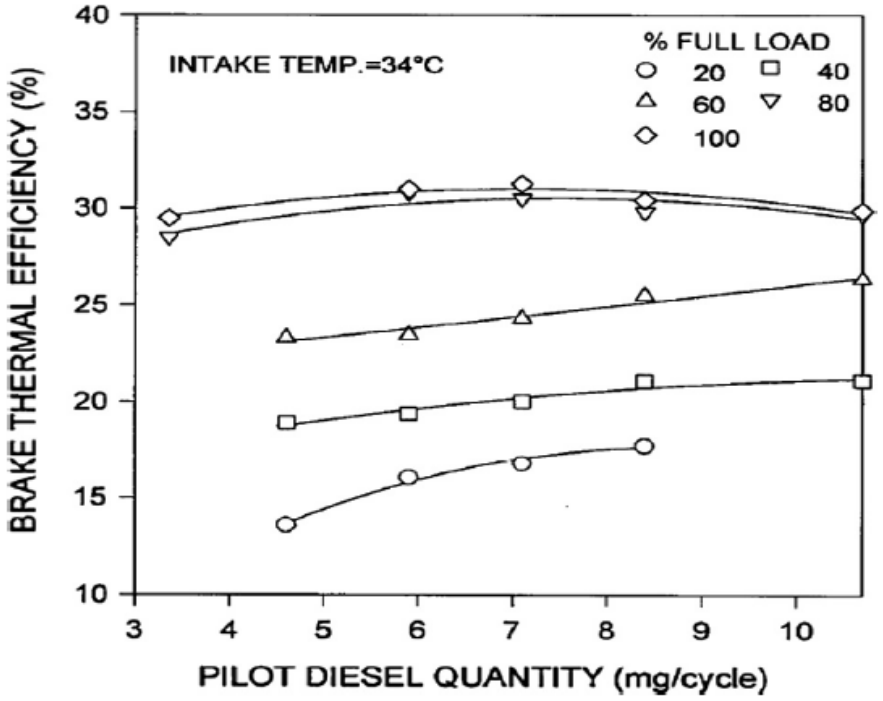

Figure 3.4 Impact of diesel quantity on brake thermal efficiency (Poonia et al., 1998)

Figure 3.4 shows the impact that the quantity of pilot fuel has on the brake thermal efficiency for single cylinder constant speed engine and 34 °C intake temperature. For engine loads ranging from 20 to 60%, the brake thermal efficiency was shown to increase with a corresponding increase in pilot fuel quantity. However, for higher loads (80 and 100%), higher quantities of pilot fuel instead led to a decrease in brake thermal efficiency (Poonia et al., 1998). Therefore, this implies that higher combustion rates can be expected for large pilot fuel quantities and high engine

outputs. Should this scenario occur, there is a tendency to witness a drop in the efficiency of the engine by virtue of the pilot fuel quantity being increased beyond the optimal amount.

A much more detailed study that explored the issue of knock has been carried out and documented (Nwafor, 2002, Nwafor and Rice, 1994). The central theme addressed in the study is the impact/effect of the pilot fuel/gas ratio on the knock characteristics of a dual fuel engine. A typical comparison between the knock characteristics of pure diesel and those of dual fuel operations are provided.

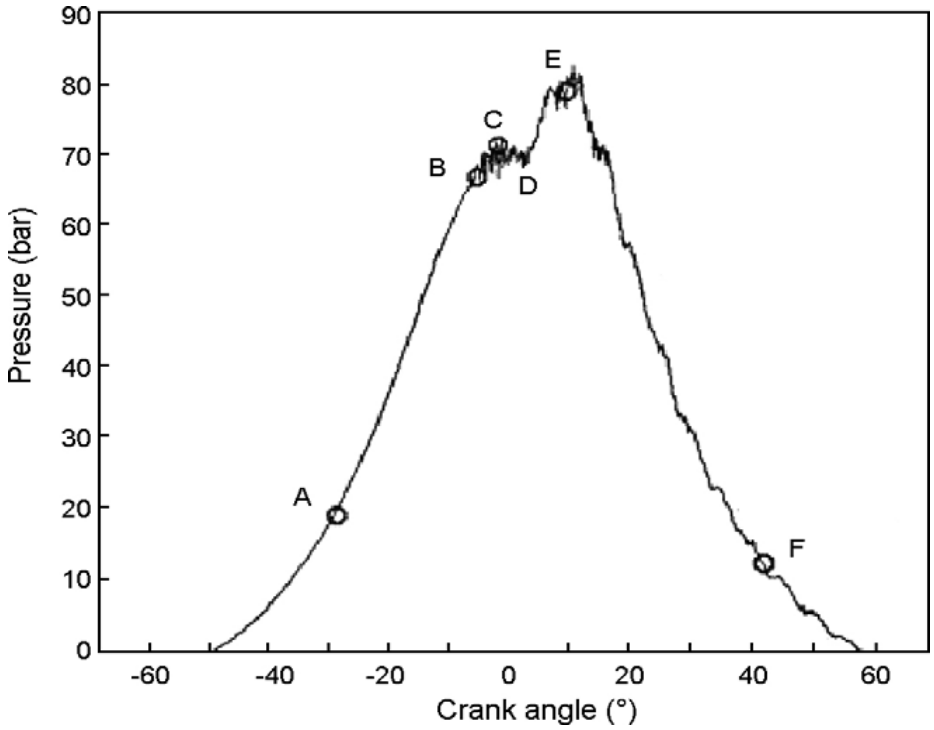

Figure 3.5 Pressure vs crank angle for pilot injection of a dual fuel engine (Nwafor, 2002)

From Figure 3.5, ripples can be seen between points *B*-*C*-*D*-*E* and even slightly after *E*. The appearance of these ripples is indicative of the occurrence of combustion knock. It is argued that the extent of knock during longer ignition delay depends very much on the ratio of the primary fuel (natural gas) to the pilot fuel (diesel), and thus on the load and speed of operation for the dual fuel engine (Table 3.11)

Table 3.1 Effect of pilot fuel/gas ratio on knock characteristics of a dual-fuel engine operating at 3000 rpm (Nwafor, 2002)

Load (N)	Pilot fuel (kg/h)	Gas supply (kg/h)	Total fuel (kg/h)	% pilot fuel	% gas supply	Mixture strength
6.61	0.305	0.626	0.931	32.76	67.24	0.557
13.18	0.292	0.720	1.012	28.85	71.15	0.620
17.72	0.271	0.792	1.063	25.49	74.51	0.667
23.78	0.295	0.846	1.141	25.85	74.15	0.730
28.82	0.313	0.882	1.195	26.19	73.81	0.779
33.87	0.331	0.907	1.238	26.74	73.26	0.823
38.92	0.343	0.936	1.279	26.82	73.18	0.866
44.47	0.307	1.008	1.315	23.35	76.65	0.922

In dual fuel engines, increasing the pilot fuel and reducing the primary fuel is believed to lead to a reduction of the knocking occurrence. It is worth stating, that, while this is beneficial to combatting knock, it is not the ideal solution as it defeats the environmental and cost-effective purposes behind using a lot more natural gas as primary fuel. This further enhances the necessity for further research into the gas/liquid fuel ratio and its effects on dual fuel engine performance and emissions.

Keeping constant the engine speed, pilot fuel injection timing and compression ratio, the effect of pilot fuel quantity on a dual fuel engine investigated using a Ricardo E6, single cylinder, variable compression, IDI diesel engine (Selim, 2004). The investigations show that when the quantity of pilot diesel fuel is increased, there is a corresponding increase in torque output of the engine. Using three different primary fuels (Methane, Compressed Natural Gas, and Liquefied Petroleum Gas) it is shown that when the diesel fuel quantity is increased, the results achieved include: greater energy being released on ignition; improved pilot fuel injection characteristics: larger size of pilot mixture envelope with greater entrainment of the gaseous fuel; a larger number of ignition centres requiring shorter flame travels and a higher rate of heat transfer to unburned gaseous fuel-air mixture (Badr et al., 1999). All these factors (achieved results) enumerated above tend to increase both the thermal efficiency and power output of the dual fuel engine (Abd-Alla et al., 2000).

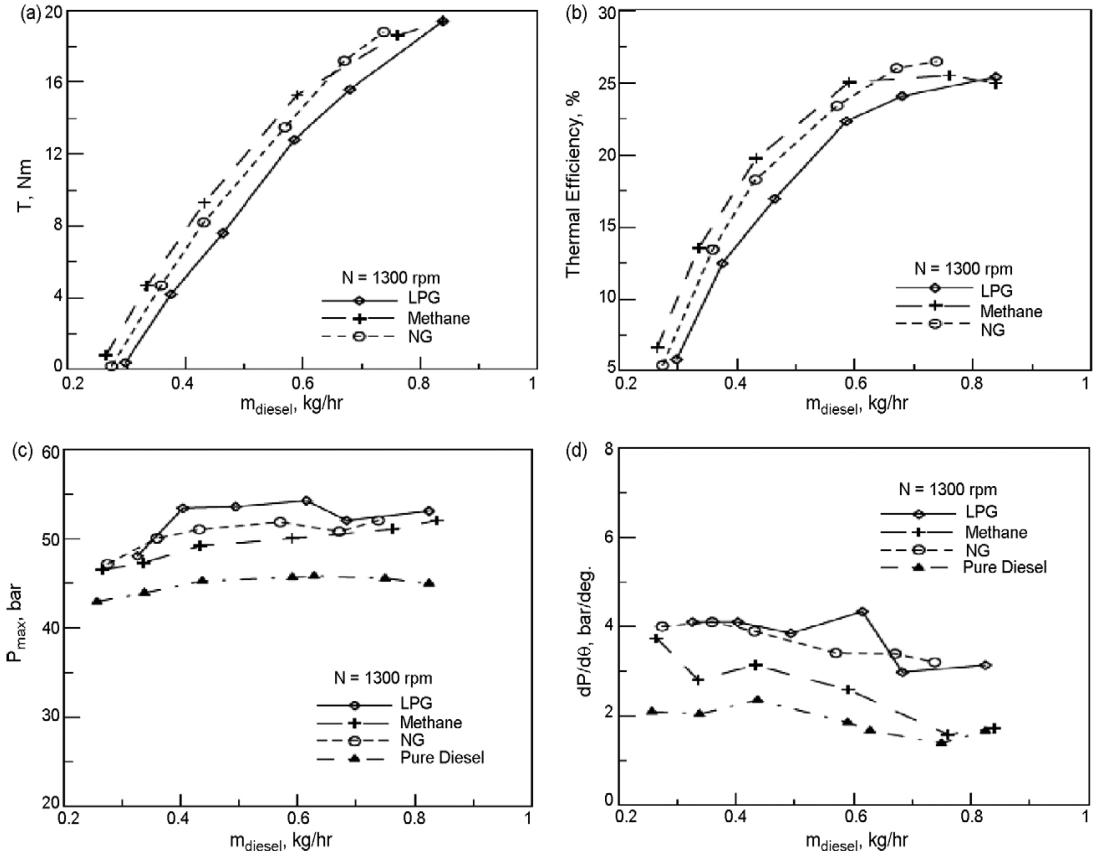

Figure 3.6 Effects of pilot fuel mass on engine performance and noise (Selim, 2004)

The Figure 3.6(a-d) reveals the impact of pilot fuel mass on the performance and noise of a dual fuel engine operating at 1300 rpm, with an injection timing of 35° BTDC (Before Top-Dead-Centre) and a compression ratio of 22.

There is a much higher maximum combustion pressure being attained by increasing the pilot diesel fuel mass (Figure 3.6c). In Figure 3.6d, the rate of maximum pressure rise is generally reduced when there is an increase in pilot fuel quantity. The combustion noise is measured through the intermediary of the change in pressure with respect to the crank angle ($dP/d\theta$), and this is seen to decrease when the pilot diesel fuel quantity is first increased. The reason to support this observation is the increase in flame volume that emanates from an increase in pilot fuel quantity which burns the primary gaseous fuel smoothly and at a low combustion rate (Sahoo et al., 2009). However, increasing the quantity of pilot diesel fuel beyond a certain threshold, the period of ignition delay of the pilot diesel is being increased and thus the pressure rise rate ($dP/d\theta$) for the gas-air mixture increases (Selim, 2001).

3.2.3.2 Effects of other parameters on dual-fuel engine performance

Some other parameters would impact on the performance and emissions of the dual-fuel engine. The previous section (3.2.3.1) focused solely on the effect that the quantity/mass of pilot fuel has on the engine performance. In this section, by way of comparison, the impact of some other parameters are being discussed.

Regarding the effect of the engine load, there is one school of thought that advocates that, as the engine load is being increased, there is a corresponding increase in the combustion noise. Emphasis by this same school of thought is made to clarify that, the combustion noise in the case of a dual-fuel engine is always higher than that for a pure diesel engine (Selim, 2001). In another study, it is shown that, at part load conditions (for both dual-fuel mode and diesel-only mode), there is a decrease in the performance of the engine. While acknowledging that NO_x and SO_2 emissions are reduced (without increasing particulate emissions) in the dual fuel mode, it is argued that CO emissions are substantially higher at all operating conditions for a dual-fuel engine when compared against its diesel engine counterpart. The same study also suggests that HC emissions are slightly higher in a dual-fuel engine (Uma et al., 2004). Another study observed a 1-2% reduction in the engine output – they called this a minor decrease in comparison to the diesel case. In the case of this study that used producer gas and rice bran oil on a CI engine, it is demonstrated that while HC and exhaust gas temperatures rise, the CO, CO_2, NO and NO_2 emissions are seen to drop (Singh et al., 2007). In yet another study, lower levels of NO_x as well as drastic decreases in soot emission, alongside higher CO and HC emissions are reported. The study goes on to highlight the fact that there is a longer combustion duration for a dual-fuel engine than for a diesel only engine at their respective low load operations. However, at higher loads, the combustion duration is shorter in the former when compared to the later (Hountalas and Papagiannakis, 2000). There is agreement that both CO and HC emissions are higher for dual fuel than for diesel (Hountalas and Papagiannakis, 2000, Uma et al., 2004)

While Signh et al., (2007) agree with the above two about an increase in HC for dual fuel operation, they contrast the above as far as emissions of CO are concerned.

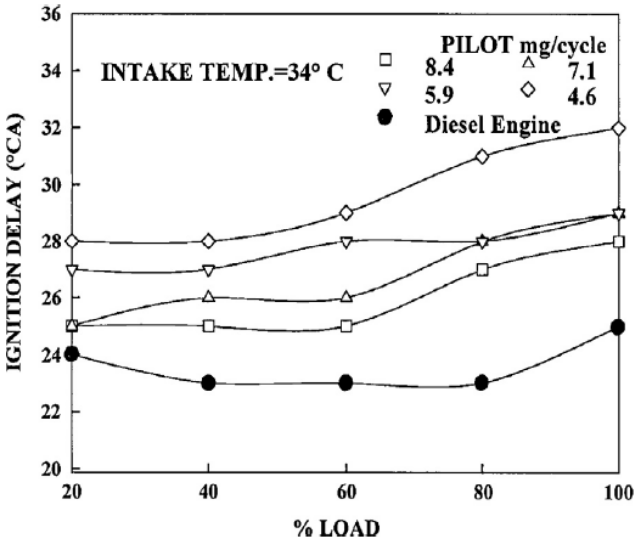

Figure 3.7 Comparing ignition delay at various loads for both diesel and dual-fuel engine operation (Poonia et al., 1998)

Figure 3.7 shows that generally, for all load conditions, the ignition delay in the dual-fuel mode of operation is higher than for the corresponding diesel-only operation. In dual-fuel operation and, regardless of the pilot fuel quantity, the ignition delay was shown to generally increase with an increase in load condition. However, the lower the pilot fuel quantity, the higher the ignition delay was (Poonia et. al., 1998).

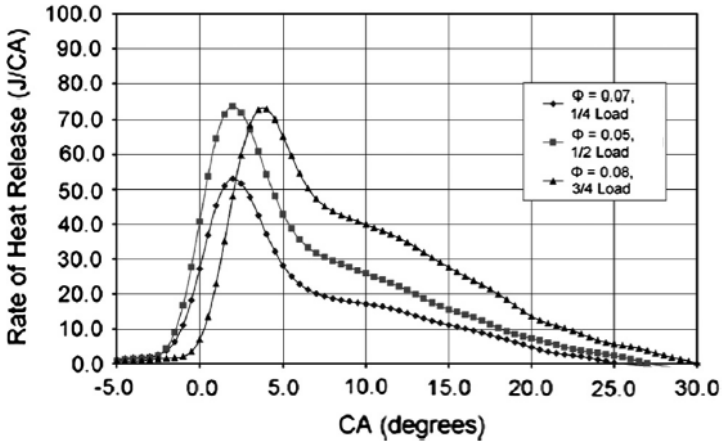

Figure 3.8 Effect of engine load on the rate of heat release for propane-diesel at 1500 rpm (Stewart et al., 2007)

Figure 3.8 reveals that at low load, a lower rate of heat release was observed for the 4-cylinder engine used in the study by Stewart et al. (2007). They argue that, for low

loads, due to pre-ignition chemical reactions, the more reactive primary fuel will cause a delay in the combustion process hence lowering the rate of heat release. From their study, they also demonstrate that, as the load increases, the primary fuel illustrates the significance of the second stage of the combustion process to the entire energy conversion process. Consequently, as load increases, a larger proportion of the energy is released during the diffusion combustion phase. The ¾ load condition suggests a higher amount of energy being released than the ½ load condition. For both the half and three-quarter load conditions, it was observed that using propane as the primary fuel, led to a 20% reduction in energy consumption (Stewart et. al., 2007).

Another parameter which studies have focused on in the past is the effect of engine speed on performance and emissions of the dual-fuel engine. As concerns this parameter, maximum combustion pressure is marginally higher for all engine speeds in the case of dual-fuel. At a given speed condition, the dual-fuel possesses a slightly higher equivalence ratio (Mansour et al., 2001). According to Selim (2001, 2004), the rate of pressure rise is shown to decrease with an increase in the speed of the engine. When compared to the diesel case, it is observed that the rate of pressure rise is higher for the dual-fuel case.

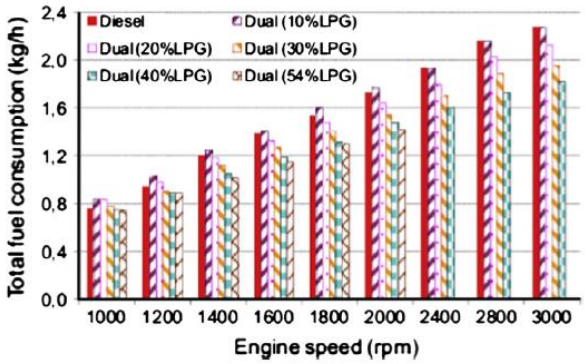

Figure 3.9 Effect of engine speed on total fuel consumption for diesel operation as well as various LPG quantities in dual-fuel mode (Le, 2011)

As shown in Figure 3.9, generally, the higher the speed, the more fuel is consumed for both diesel and dual-fuel engine operation modes. However, for several speeds, the study reveals that increasing the LPG percentage reduces the total fuel consumed by the engine. They further suggest that at higher engine speeds, the quality of fuel

injection and evaporation are better, thereby leading to the improved fuel economy of the dual fuel engine (Le, 2011).

Concerning the effect of the pilot fuel injection timing, there is an increase in the efficiency of fuel conversion between an injection timing of 15-45° before top dead centre (BTDC). After this injection timing range, it is believed that the fuel conversion efficiency decreases. At a timing of 45° BTDC, the NO_x emissions are higher than those observed at 15° BTDC (retarded timing) or 60° BTDC – advanced timing (Krishnan et al., 2004). Selim (2001) notes that as injection timing increases from 25-40° BTDC), the pressure rise rate of a dual fuel engine is higher than for a 100% diesel engine. In a separate study, the same author (Selim, 2004) suggests that there is a reduction in torque output as well as in engine thermal efficiency as a consequence of advancing the timing of the pilot fuel injection. In yet another study, it was evident that the result of advancing the injection timing was an improvement in thermal efficiency. However, when this advancement of injection timing was done at medium and high load operating conditions, knocking occurred early. Also, with the advance in injection timing, there was an increase in NO_x, reduction in CO and unburned hydrocarbon emissions (Abd-Alla et al., 2002). Another investigation on the effect of pilot fuel injection timing reveals that with advanced injection timing, there are higher Hydrocarbon emissions as well the exhaust temperatures being high. Furthermore, the study highlights the fact that standard dual timing shows a longer period of delay at high loads than the advanced injection timing operation (Nwafor, 2000).

Concerning the effect of engine compression ratio on dual fuel engine performance and emissions, Selim (2004) explains that by using a high compression ratio in a dual fuel engine, knocking commences earlier – this is more pronounced when the fuel utilised is liquefied petroleum gas (LPG). Generally, combustion noise is thought to increase when the compression ratio is increased.

The engine intake manifold conditions have also been studied and the following observation pertaining to its impacts and effects on the performance and emissions of dual fuel engine made. A combination of intake heating and exhaust gas recirculation (EGR) is shown to improve thermal efficiency. The practice of EGR controls the rate of pressure rise, and when the EGR ratio exceeds 50%, it leads to the deterioration of

engine combustion characteristics. In addition, EGR alongside intake heating will lead to a reduction of NO_x emissions as well as total hydrocarbons (THC) (Kusaka et al., 2000).

Turning attention to the effect of the type of gaseous fuel on engine performance and emissions, the deterioration in engine performance when 40% CO_2 in biogas was used, was observed to be much more in comparison to an engine in which 96% methane was used as primary fuel. However, 30% CO_2 in biogas is depicted to improve engine performance as compared to the same, running on methane as primary fuel (Bari, 1996). It is also suggested that the overall efficiency drops with gas substitution and adding CO_2 affects this more at elevated speeds. In addition, the exhaust temperature is affected more by natural gas substitution than by CO_2 addition with exception to this being observed when there is a maximum natural gas substitution. Furthermore, CO is affected mainly by natural gas substitution and not very much by gas quality (Henham and Makkar, 1998)

3.3 Computational Modelling and Simulation

To be able to analyse the critical features of a process in detail, there is the need to develop and utilise a practical and acceptable combination of assumptions and equations – a process known as modelling. In this section, various models used in engine simulation are presented. Over the years, there has been an increase in the use of various models to understand, predict or improve engine performance. Given the wide range of engine configurations that are possible, as well as the numerous sub-models that can be applied in overall engine models, engine simulation is, therefore, a very broad and large subject. Engine simulation and modelling have also gained prominence as a vital and fruitful research tool. This has caused numerous engine research centres to come up with their engine models – each with varying degrees of complexity, scope, and ease of use. Several reasons can be advanced for the growth in engine modelling. Some of these include;

- For any research that focuses on engines, the utilisation of engine modelling is very relevant. It is almost impossible nowadays to do any research on engines without the use of a model of some sort.
- Using computer models for engine simulation provides substantial savings that would otherwise not be made when experimental work is used to investigate engine modifications

While models can never replace real engines, they have proven to provide good and practically acceptable estimates of engine performance taking into consideration possible engine modifications. Focusing on compression ignition engines and depending on the level of detail required, engine models could be multi-dimensional (3D or 2D) or zero-dimensional.

3.3.1 Multi-dimensional models

These types of models are predominantly referred to as computational fluid dynamics (CFD) models. They have the inherent ability to provide detailed geometric information on the flow based on the solution of the governing flow equations (Heywood, 1988). In CFD models, concerning numerical calculations of reactive flows, constraints of computational time and storage severely limit the complexity of the reaction mechanisms that can be incorporated. CFD models are based generally on the resolution of Navier Stokes equations – with the entire process habitually split into a number of parts to be solved. After the application of appropriate physical models, the governing equations that such models rely on are solved using numerical methods (Shi et al., 2011, Blazek, 2015).

Multi-dimensional models require a lot more computational time compared to zero-dimensional models. This causes their utilisation to be used mostly for research and development that focuses on new prototypes or for the simulation of concrete physical phenomena taking place during an engine cycle (Wang et al., 2012, Wilcox, 1998).

As far back as the 1970s, the first attempt to use CFD for in-cylinder engine modelling was made. Lack of powerful computers and general CFD codes for engine

applications hindered the extensive use of CFD in the1970s. However, with advancements in technology and capability of computers, CFD modelling tools with detailed fuel chemistry allow researchers and designers to achieve simulation results that are somewhat reliable. Several commercial codes using CFD have been developed, some of which are KIVA, Open Foam, AVL FIRE, ANSYS FLUENT etc. In the published literature as well as in peer-reviewed journals, several studies have used multi-dimensional (CFD) models of some sort (Ghomashi, 2015, Mattarelli et al., 2014, Liu and Karim, 2007).

The models described in this section are not the main focus of this study. In the next section, zero-dimensional models (which constitute the core of this work/study) are being discussed in relation to internal combustion engines with a focus on diesel and dual-fuel engine applications.

3.3.2 Zero/One-dimensional models

These types of models are based essentially on the laws of thermodynamics and on semi-empirical relationships that describe the rate of combustion of the injected fuel mass. They are based on the equations for conservation of energy and mass according to the first law of thermodynamics. 0-D models are found to be attractive due to the relative simplicity with which they are implemented. In addition, they require less computational time while providing analyses of reasonable accuracy taking into account the assumptions that such models are usually based on. With the powerful computing tools available nowadays, these types of models can provide real-time simulation of the combustion in diesel as well as in dual-fuel engine applications. In 0-D models, the gas composition within the cylinder is assumed to be homogenous throughout the entire engine cycle (Rakowski, 2012). Among the leading pioneers in the field of thermodynamic 0-D simulation applied to combustion in compression ignition engines, the works of the following can be cited; (Heywood, 1988, Krieger and Borman, 1966, Watson et al., 1980).

While the authors mentioned above focused on application to diesel engines, other authors developed models for dual fuel applications. Another author (Raine, 1990)

developed a model that was limited to computing the efficiency parameters of a dual-fuel engine. Making use of the fundamental laws of conservation of mass, energy and momentum, (Hountalas and Papagiannakis, 2000, Hountalas and Papagiannakis, 2001, Hountalas and Papagiannakis, 2002, Papagiannakis et al., 2005, Papagiannakis et al., 2007) developed a dual fuel model that used diesel as pilot fuel and natural gas as primary fuel. They published several papers to which the reader is referred.
(Mikulski et al., 2015) developed a Zero-dimensional model which was implemented using the MATLAB environment.
For the development of zero-dimensional thermodynamic models to investigate combustion in internal combustion engines, several sub-models are required. Two such submodels (of prime importance) are discussed in the subsequent section.

3.3.2.1 Heat release models

To model combustion, heat release characteristic is fundamental. Heat release defines the amount of heat energy produced during fuel combustion in an engine. The amount of heat released is linked to the mass fraction of fuel burned as the crankshaft rotates. Without taking into account losses, heat release is defined by the following equation:

$$Q_{in} = m_f LHV \qquad \textit{Eqn. 3.1}$$

Where, m_f is the mass fraction of fuel burned and LHV is the lower heating value of the fuel. Thermodynamically, heat is not released during combustion; the temperature rise is due to the change in the composition of the initial reactants to the products of combustion in an exothermic reaction (Benson and Whitehouse, 1979).
Theoretically, the mass fraction burned ranges from 0 to 100%, but this is very much far from reality. Consequently, there is the necessity to adequately define the evolution of the mass fraction of fuel burned in the cylinder. The most widely used approach to do this is that of Vibe. This approach consists of writing a function describing the evolution of the mass fraction of burned fuel. The derivative of this

function is then written as a function of the crank angle using an exponential type of function (Vibe, 1970). The original Vibe function is:

$$x = 1 - \exp\left(-6.908\left(\frac{\phi}{\phi_d}\right)^{m+1}\right) \qquad \textit{Eqn. 3.2}$$

Its derivative is:

$$\frac{dx}{d\phi} = \frac{6.908(m+1)}{\phi_d}\left(\frac{\phi}{\phi_d}\right)^{m} \exp\left[-6.908\left(\frac{\phi}{\phi_d}\right)^{m+1}\right] \qquad \textit{Eqn. 3.3}$$

Where; φ is a measure of the crankshaft rotation angle taken from the start of combustion, φ_d is the total combustion duration. The parameter m is a shape parameter that needs to be adjusted with respect to the experimental data for each given engine.

For a very long time, the zero-dimensional model as proposed by Vibe has been used for engine simulation. However, it has been shown that this model has some limitations as it does not take into account the pre-mix condition within the combustion cycle. In addition, the shape parameter and the exponential coefficient require a lot of adjusting to match experimental data (Galindo et al., 2011, Borg and Alkidas, 2008).

Because of the limitations associated with the Vibe approach as enumerated above, to use the 0-D Vibe model in the simulation of compression ignition engines requires modification. This modification would enable a more accurate description of the combustion taking place in compression ignition engines. Some of these modifications involve using double, triple or multiple Vibe functions (Watson et al., 1980, Miyamoto et al., 1985, Yasar et al., 2008).

In the case of using the double Vibe functions, this entails the superposition of two individual Vibe functions. Thus the double Vibe function (like the other modified forms of the single Vibe function) is used to approximate the heat release of a compression ignition engine more correctly. In the case of double Vibe function, the first one is used to model the premixed combustion peak while the second one models diffusion controlled combustion as shown in Figure 3.10.

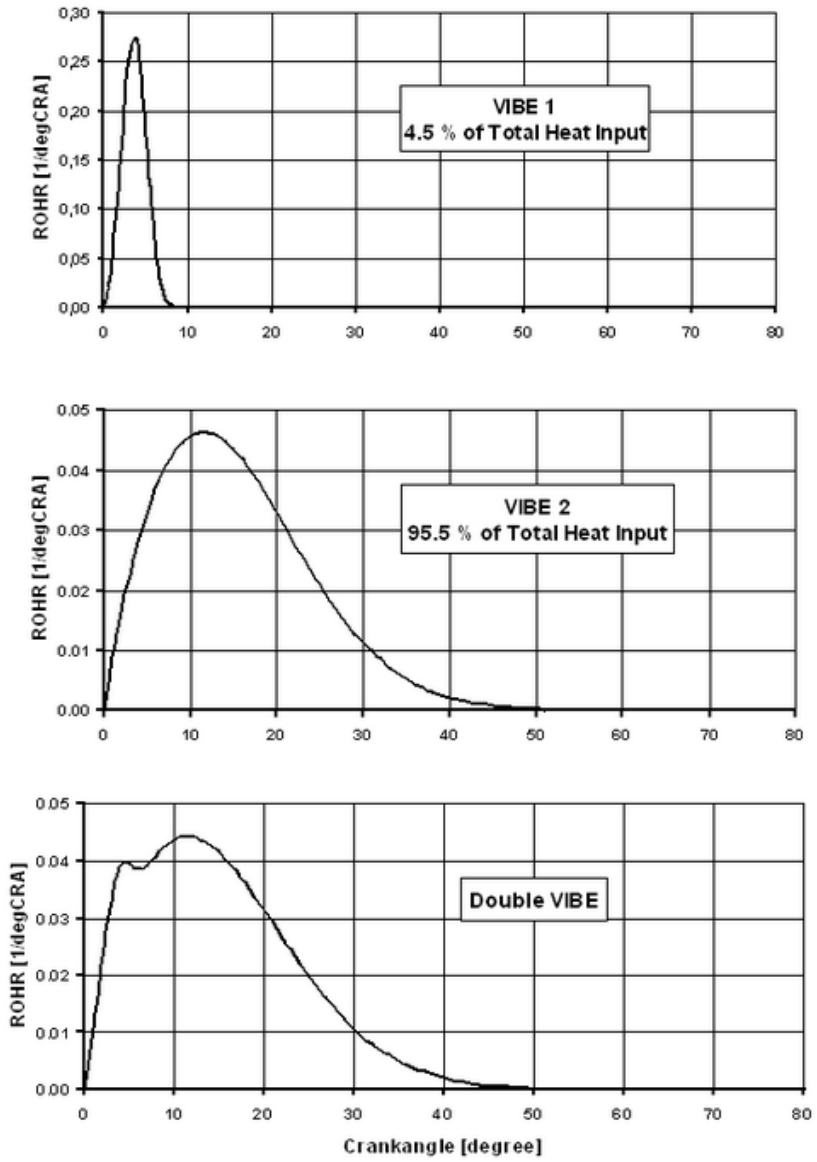

Figure 3.10 Superposition of two vibe functions to more correctly approximate heat release (AVL, 2014).

To free themselves from the cumbersome task of adjusting the multiple smoothing coefficients associated with using the Vibe model, Chmela et al. (1998) proposed an innovative model that bases its assumption on fuel/air mixture. Consequently, they suggest that combustion is proportional to the average turbulent kinetic energy associated with the rate of fuel injection. In addition, according to the authors, the decrease over time in the turbulent energy is proportional to the total kinetic energy of the injected fuel. Although this proposal by (Chmela et al., 1998, Dimitrov and Pirker, 2006) can be seen to more accurately predict heat release; it would be

possible only on the assumption that there is no impact of the fuel jet on the piston head.

Another approach to model heat release is to consider the combustion space as a single zone and base calculations on the first law of thermodynamics as well as the ideal gas equations (Krieger and Borman, 1966, Ferguson and Kirkpatrick, 2015). The algorithm proposed by Borman and Krieger (1966) is based on the use of polynomial constants to calculate the adiabatic index (specific heat ratio) as a function of the crankshaft angle to determine the internal energy within the cylinder at each instant of the cycle. The difficulty associated with the use of this model is the number of constants to be found and smoothed to calibrate such models for each given type of engine and fuel.

Another approach to model the combustion characteristics is the Mixing Controlled Combustion (MCC) (Chmela et al., 1998, Chmela and Orthaber, 1999). The MCC considers the effects of the premixed (PMC), and diffusion (MCC) controlled combustion processes according to:

$$\frac{dQ_{MCC}}{d\alpha} = \frac{dQ_{MCC}}{d\alpha} + \frac{dQ_{PMC}}{d\alpha} \qquad \textit{Eqn. 3.4}$$

In the mixing controlled combustion regime, the heat release is a function of the fuel quantity available (f_1) and the turbulent kinetic energy density (f_2)

$$\frac{dQ_{MCC}}{d\alpha} = C_{comb}\, f_1\left(m_{F,} Q_{MCC}\right) f_2\left(k,V\right) \qquad \textit{Eqn. 3.5}$$

With

$$f_1(m_F, Q) = \left(m_F - \frac{Q_{MCC}}{LCV} \right) \left(W_{oxygen,available} \right)^{C_{EGR}} \qquad \textit{Eqn. 3.6}$$

$$f_2\left(k,V\right) = C_{Rate} \frac{\sqrt{k}}{\sqrt[3]{V}} \qquad \textit{Eqn. 3.7}$$

Where:

Q_{MCC} is the cumulative heat release for the mixture controlled combustion [kJ]

C_{comb} is the combustion constant [kJ/kg/deg CA]

C_{Rate} is the mixing rate constant [s]

k is the local density of turbulent kinetic energy [m^2/s^2]

m_F is the vaporised fuel mass [kg]

LCV is the lower heating value [kJ/kg]

V is the cylinder volume [m^3]

α is the crank angle [degCA]

$W_{oxygen,available}$ is the mass fraction of available Oxygen at the start of injection [-]

C_{EGR} is the EGR influence constant [-]

It is worth noting that the MCC model is advantageous over the vibe model because it has the ability to predict combustion characteristics in direct injection compression ignition engines.

3.3.2.2 Heat transfer models

The heat released by the injected fuel mass experiences some losses due to convective, conductive and radiative heat transfers towards the cylinder walls. Given these losses, the actual quantity of heat released within the cylinder of an engine is given by:

$$Q_{total} = Q_{in} - Q_{loss} \qquad \textit{Eqn. 3.8}$$

Where Q_{loss} accounts for the heat loss. These losses have been the subject of several investigations over the years and have led to different expressions to account for them. Generally, they can be expressed by an expression of the type:

$$Q_{loss} = Ah_c\left(T_{cyl} - T_{wall}\right) \qquad \textit{Eqn. 3.9}$$

Where, A is the surface area, T_{cyl} is the gas temperature in the cylinder, T_{wall} is the wall temperature in cylinder liner and h_c is the heat transfer coefficient. Several models for determining the heat transfer coefficient have been proposed. Among some of the commonly used ones is that of (Woschni, 1967). This model was developed for a high pressure cycle and can be summarized as follows:

$$h_c = 130 D^{-0.2} p_c^{0.8} T_c^{-0.53} \left[(C_1 C_m) + \left(C_2 \frac{V_D T_{c,1}}{p_{c,1} V_{c,1}} \right) (p_c - p_{c,0}) \right]^{0.8} \qquad \textit{Eqn. 3.10}$$

Where:

$C_1 \quad = 2.28 + 0.308 \frac{c_u}{c_m}$

$C_2 \quad = 0.00324$ for DI engines

D Cylinder bore

c_m Mean piston speed

c_u Circumferential velocity

V_D Displacement per cylinder

$p_{c,0}$ Cylinder pressure without combustion (motoring conditions)

$T_{c,1}$ Temperature in the cylinder at intake valve closing (IVC)

$p_{c,1}$ Pressure in the cylinder at intake valve closing (IVC)

Woschni (1991) published another formula aimed at a more accurate prediction of heat transfer at part load. This modified formula took into account the volume of the cylinder when the piston is at top dead centre as well as the indicated mean effective pressure (IMEP).

Other heat transfer models include those proposed by (Hohenberg, 1979, Chiodi and Bargende, 2001), who published an improved correlation for the working cycle of a spark ignition engine. Hohenberg's model tried to simplify that of Woschni but failed to take into account the different cycle times. AVL also carried out experiments and measurements which led to the modification of the Woschni heat transfer model. According to the authors, the heat transfer during gas exchange strongly influences the volumetric efficiency of the engine (Wimmer et al., 2000). For more studies with an emphasis on heat transfer models, see (Jennings and Morel, 1991, Imaboppu et al., 1993, Zeng and Assanis, 2004).

3.3.3 Phenomenological models

With these types of models, details of different phenomena occurring during the combustion are added to the basic equation for energy conservation. They are useful for describing combustion in internal combustion engines. Phenomenological models, therefore, are perceived to be an essential tool used in studying the various processes that take place during the entire combustion process within the cylinder of an internal combustion engine. Over the years, certain phenomenological models have been developed successfully for applications of spark-ignition and diesel engines. Generally, these models consist of several zero-dimensional sub-models that are coupled to one another. Some of the main sub-models include; injection and spraying, evaporation, ignition delay, emission submodels (NOx. PM, etc.).

For the studies that focus on dual fuel engine applications, a number of phenomenological models have been developed (Krishnan et al., 2007, Liu and Karim, 1997, Mansour et al., 2001, Papagiannakis et al., 2005, Pirouzpanah and Saray, 2006). In these developed models, a few methods were used to describe the heat release of the gaseous as well as the pilot fuel. One of such methods used to picture the heat release of the premixed gaseous charge is chemical kinetic modelling while heat release for the pilot has been described by mass burning rates as well as a quasi-dimensional description of the pilot (Liu and Karim, 1997, Mansour et al., 2001).

3.3.3.1 Fuel injection and spray modelling

Fuel injection and spraying have been and continue to be the subject of several studies. It has been shown that the finesse of spraying and mixing affects the quality of combustion within the cylinder. Thus the finer the droplets of the fuel mixture, the more homogenous the distribution of droplets inside the cylinder; the more the air/fuel mixture within the cylinder is likely to burn completely (Lakshminarayanan and Aghav, 2010, Challen and Baranescu, 1999). Several different models have been

proposed for the modelling of fuel injection and spraying. In general, the fuel injection can be characterised by;

- Liquid jet penetration and break-up length within the combustion chamber
- Penetration of the liquid-vapour mixture
- The spray cone angle and the equivalent spray angle

In their study, the authors (Dos Santos and Le Moyne, 2011) present a review of the different correlations that characterise fuel injection and spray atomization. Most empirical correlations describing the fuel jet penetration have similarities. These similarities focus on the factors that influence fuel jet penetration, some of which include: fuel density, injection pressure, the diameter of injector holes and air pressure inside the cylinder. Some of the existing empirical correlations for evaluating fuel jet penetration can be seen in (Kuleshov, 2009, Dent, 1971, Elkotb, 1982, Hiroyasu and Arai, 1990, Naber and Siebers, 1996, Siebers, 1999).

Given that the combustion process occurring in a dual fuel engine is more complicated than that taking place in a diesel engine, modelling fuel injection and spraying is a bit tricky. The dual fuel combustion process is complex because it combines features of both traditional spark ignition and diesel combustion. Other studies (Anant et al., 2012, Johnson et al., 2012) developed phenomenological models to capture the complex nature of dual fuel combustion.

In dual fuel combustion, the ignition of a homogeneous lean pre-mixed charge admitted into the cylinder during the intake stroke is controlled by the fuel spray of the pilot diesel, with atomization of this pilot fuel leading to several ignition points from which individual flamelets emanate (Karim, 2003a).

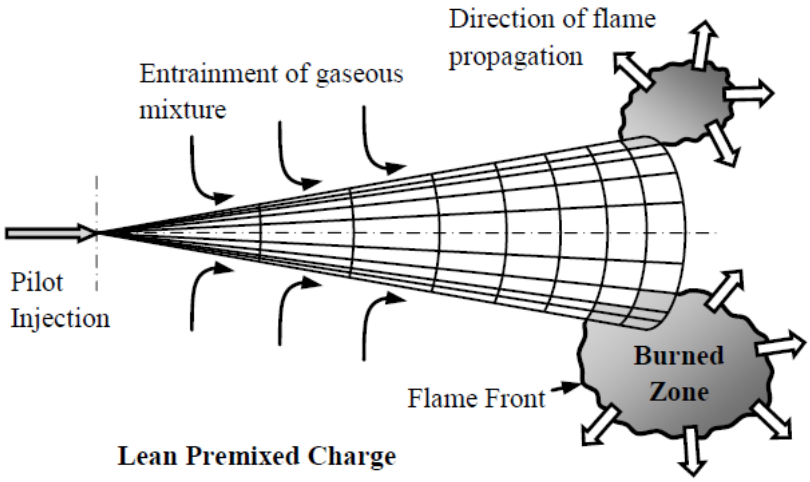

Figure 3.11 Visualization of dual fuel combustion concept (Johnson et al., 2012)

In the dual fuel model described in Figure 3.11, a multi-zone approach wherein spray discretisation is realised by breaking, separating it in three dimensions is used. Detailed mathematical treatment of phenomenological dual fuel model is provided in (Anant et al., 2012, Johnson et al., 2012).

3.3.3.2 Modelling evaporation

The concentration of vapours inside the combustion chamber as a result of fuel injection and spraying is proportional to its rate of evaporation. This influences engine performance. Fuel evaporation on its part is influenced by, the fuel jet distribution, ambient temperature as well as gas mixture composition within the combustion space. Because of the significant influence of fuel evaporation on engine performance, several works (Wu et al., 2003, Murty, 1975, Clift et al., 2005) included it in their models

Generally, models aimed at studying or describing evaporation of fuel sprayed within compression ignition engines are based on the following hypothesis

- Fuel droplets possess homogenous physical properties
- The equations of state used to describe the thermodynamic parameters of the fuel droplets are based on the ideal gas theory
- The effects of radiation and gravitation are said to be negligible

Some of the earliest theoretical approaches to modelling fuel droplet evaporation in compression ignition engines were proposed by (Godsave, 1953, Spalding, 1953). Their approach, known as the "The d^2- law" defines the variation of the square of the fuel droplet diameter in relation to time. For a compression ignition engine, this variation of the square of fuel droplet diameter is given by:

$$d_k^{\,2} = d_0^{\,2} - K\tau_i \qquad \textit{Eqn. 3.11}$$

Where, d_0 and d_k are the initial diameter of the fuel droplet and the fuel droplet diameter at the time of observation respectively. K is the evaporation constant and τ_i is the time elapsed from the beginning of evaporation of a given fuel droplet till the time of observation.

According to Kuleshov (2009), the evaporation constant K is given by:

$$K = \frac{4\exp(6)\left[N_{UD} D_p p_s\right]}{\rho l} \qquad \textit{Eqn. 3.12}$$

Where, N_{UD} is the Nusselt diffusion number, D_p is the diffusion coefficient for fuel vapours within the combustion space and p_s is the saturated fuel vapour pressure.

The constant K characterises the rate of decrease of the fuel droplet sizes initially formed after spraying. From the equation above, it is evident that the evaporation constant is inversely proportional to the fuel density. Thus the higher the density of fuel, the slower its droplets will evaporate after spraying. During the period of fuel injection into the combustion space of a compression ignition engine, the speed of combustion is defined essentially by the speed of evaporation of the fuel droplets.

3.3.3.3 Ignition delay models

Ignition delay is one of the most important criteria impacting on the combustion process of internal combustion engines. Its timing is believed to exert a great deal of influence on the combustion process in diesel and dual fuel engines. Thus, ignition

delay affects the efficiency of the engine as well as the tail-pipe emissions that emanate from it. Additionally, it also influences the noise generated in the engine.

Ignition delay is defined as the time interval between the start of injection and the start of combustion. This delay, consist of a physical delay – during which atomization, evaporation, and mixing of the injected fuel with cylinder contents (diesel and air for a pure diesel engine; diesel, air and gaseous fuel for a dual fuel engine) occur. It also consists of a chemical delay that is attributed to the pre-mixed combustion reactions. Generally, these two constituents (physical and chemical) of ignition delay are considered to occur simultaneously and have thus been the subject of several research works. Consequently, some empirical equations have been developed to determine this ignition delay period. The current trend in research is to reduce the ignition delay time in a bid to allow for a reduction in the emissions of nitrogen oxides (Lakshminarayanan and Aghav, 2010).

Under different experimental conditions, several correlations have been suggested for modelling ignition delay of diesel fuels. Some of the various experimental set-ups include using constant volume bombs (Hiroyasu et. al., 1983), steady flow burners (Reuter and Scheie, 1988, Spadaccini, 1977) and combustion engines (Watson et. al., 1980). Several of the suggested correlations use an Arrhenius-type equation in an attempt to forecast the influence of in-cylinder pressure and temperature on the ignition delay period. These correlations are similar to the one proposed by Wolfer that is:

$$\tau_{id} = Ap^{-n} \exp\left(\frac{E_a}{RT}\right) \qquad \textit{Eqn. 3.13}$$

Where:

E_a is the activation energy

T and p are the cylinder temperature and pressure respectively

A and n are adjustable coefficients.

R is the gas constant

Table 3.2 Empirical constants used in various ignition delay correlations similar to Arrhenius form adapted from (Assanis et al., 2003)

Author of Ignition delay Correlation	Experimental Apparatus Used	A	n	$\frac{E_a}{R}$
Wolfer	Constant volume bomb	0.44	1.19	8360
Kadota	Single droplet	6.58	0.52	4400
Watson	Diesel Engine	3.45	1.02	2100
Ikegami	Free Piston engine	0.44	1.19	4650
Spadaccini	Steady flow	4.00 E-10	1.00	20080
Hiroyasu	Constant volume bomb	$0.1\varphi - 1.04$	2.50	6000
Pischinger	Steady flow	0.008	1.14	7813

Table 3.2 enumerates the various empirical constants used in various ignition delay correlations similar to the Arrhenius form of correlation while in Table 3.33, a summary of the different correlations from previous research as well as the experimental conditions under which these correlations were obtained is presented.

As seen in Table 3.2 and Table 3.3, various approaches have been proposed for the estimation of ignition delay. These approaches were based on experiments carried out using various different test facilities such as constant volume bombs, compression machines and engines and steady-state reactors. The correlations by (Kadota et al., 1976, Lahiri et al., 1997, Wolfer, 1938, Fujimoto et al., 1980) were based on experiments carried out in a constant volume bomb. As such, these correlations fall short when it comes to predicting ignition delay under unsteady diesel and dual fuel engine conditions. Then again, (Hardenberg and Hase, 1979) and (Watson et al., 1980) developed their correlations taking into consideration engine data. Their correlations were not entirely successful in yielding suitable predictions under extensively different operating situations given that they overlooked the influence of mixture quality.

On the other hand, (Assanis et al., 2003) compared various correlations and discovered much better predictability using the Watson (1980) correlation. They provided an improvement to the correlations by introducing the equivalence ratio and also fine-tuning the empirical constants. In that way, they suggested that, by making their correlations depend on the equivalence ratio, it renders them more dynamic.

Turning attention to the advantages and disadvantages of some of the correlations developed by the above-referenced studies, it is my view that, the correlation proposed by Watson (1980) is disadvantageous given that it requires the use of mean values of temperature and pressure which would necessitate the use of an iterative solution to assess the mean properties of the ignition delay period. The correlation by Hardenberg and Hase (1979) appears to be plausible on account of several advantages. Remarkably, their correlation recognises that the ignition delay depends on engine speed and the auto-ignition quality of the fuel. Additionally, the temperature and pressure were determined at a single operating condition. Therefore, if this correlation is not being applied within a computer simulation of an engine paradigm, then the temperature and pressure can be evaluated by assuming the compression can be modelled as a polytropic process. However, due caution must be exercised when treating the dependence of the ignition delay on the cetane number as purported by their correlation. Their evaluation of the cetane number by ignition delay measurements made in a CFR engine with an indirect injection combustion system appears to be something of a pitfall.

Table 3.3 Ignition delay correlations and experimental conditions under which they were achieved

Author	Ignition delay correlation	Reference
Ikura et al.	$DI = AP^B\varphi^C \exp\left(\frac{D}{T}\right)$ DI in ms, P in atm, T in K For diesel: $A = 2.76\exp(-2),\ B = -1.23, C = -1.60,\ D = 7280$ Experimental conditions: Constant volume chamber and injector with one hole $660 \leq T \leq 900K$ $6 \leq P \leq 31atm$ $0.5 \leq \varphi \leq 1.0$	(Ikura et al., 1975)
Hardenberg & Hase	$DI = \left[0.36 + 0.22\overline{S_p}\right]\exp\left[\frac{618840}{CN+25}\left(\frac{1}{RT_{im}\varepsilon^{n_c-1}} - \frac{1}{17190}\right) + \left(\frac{21.2}{P_{im}\varepsilon^{n_c} - 12.4}\right)^{0.63}\right]$ CN is the cetane number of fuel T_{im} and P_{im} are Temperature (in K) and Pressure (in bar). $\overline{S_p}$ is the mean piston speed (in m/s)	(Hardenberg and Hase, 1979)
Fujimoto et al.	$\boldsymbol{DI = AP^n\varphi^{-1.9}\exp\left(\frac{5130}{T}\right)}$ $\boldsymbol{DI}$ in ms, $\boldsymbol{P}$ in atm, $\boldsymbol{T}$ in K For heavy fuel oil: $\boldsymbol{P \leq 40atm, A = 1.37\exp(-1), n = -1.06}$ $\boldsymbol{P \geq 40atm, A = 2.97\exp(-3), n = 0}$ Experimental Conditions: In a constant volume chamber and injector with 9 holes $\boldsymbol{710 \leq T \leq 810K}$ $\boldsymbol{11 \leq P \leq 73atm}$ $\boldsymbol{0.71 \leq \varphi \leq 1.0}$	(Fujimoto et al., 1980)

In the case of dual-fuel engines, the cylinder consists of the air-gas mixture to which diesel is injected. The air-gas mixture is ignited by the energy released from the burning diesel fuel. In studies comparing dual fuel engine operation to that of spark-ignition engines, it was observed that when the pilot dose in a dual fuel engine is as little as less than 1% of the overall energy, it can still provide ignition energy of around 35J more than that produced in the spark ignition engine (Saito et al., 1999, Saito et al., 2000). Since the air-gas mixture in a dual fuel engine is ignited by the energy from diesel fuel, it can be assumed that the commencement of combustion of both the gaseous and liquid fuel fractions coincides. Therefore, to determine the time of ignition in dual fuel engines comprises of accurately modelling ignition delay of the diesel fuel (Piętak and Mikulski, 2011). By the characteristic nature of the dual fuel engine operation, it is evident that the conditions under which ignition delay is taking place are fundamentally different from those is a traditional diesel engine. Consequently, ignition delay tends to increase with an increase in gas concentration.

Despite the numerous experimental and theoretical studies to examine correlations for ignition delay, only a few have been validated for dual fuel engine systems. For example, using the Hardenberg & Hase correlation, auto-ignition was described in a zero-dimensional combustion model for dual fuel operation (Stelmasiak, 2003). Meanwhile, an equation similar in form to that proposed by (Wolfer, 1959) but having the added advantage of taking into account the chemical composition of the cylinder load was suggested (Zeng and Assanis, 2004). The correlation postulated by Zeng and Assanis has been shown to describe ignition delay in a dual fuel engine better than other correlations (Mikulski et al., 2015, Piętak and Mikulski, 2011) and is determined using the following equation:

$$\tau_{id} = A\varphi^{-k} p^{-n} \exp\left(\frac{E_a}{RT}\right) \qquad \textit{Eqn. 3.14}$$

Where:

φ is the equivalence ratio, T and p are the cylinder temperature and pressure respectively, E_a is the activation energy, A, k and n are adjustable coefficients. R is the gas constant.

Another approach (Andree and Pachernegg, 1969) estimates the ignition delay by solving the following differential equation 3.15.

$$\frac{dI_{id}}{d\alpha} = \frac{T_{UB} - T_{ref}}{Q_{ref}} \qquad \textit{Eqn. 3.15}$$

Once the ignition delay integral (I_{id}) reaches a value of 1 at a particular crank angle (α_{id}), the ignition delay is therefore calculated from

$$\tau_{id} = \alpha_{id} - \alpha_{SOI} \qquad \textit{Eqn. 3.16}$$

Where:

I_{id} is the ignition delay integral [-]

T_{ref} is the reference temperature [K]

T_{UB} is the unburned zone temperature [K]

Q_{ref} is the reference activation energy [K]

τ_{id} is the ignition delay [s]

α_{SOI} is the start of injection timing [degCA]

α_{id} is the ignition delay timing [degCA]

3.4 Critical Review and Appraisal

There is a vast amount of literature that focuses on how to reduce emissions from direct injection diesel engines. Various approaches have been proposed towards achieving this, including the use of gaseous fuels as a supplement for liquid diesel fuel (Papagiannakis and Hountalas, 2003). This approach in which gaseous fuel is used to supplement liquid diesel is advantageous in the sense that it offers flexibility. As others have highlighted (Badr et al., 1999, Papagiannakis et al., 2010), when a diesel engine is modified to allow it use a gaseous fuel, it can still revert to operating only on diesel. A growing body of literature, has investigated this approach using

different types of gaseous fuels, for example, producer gas (Uma et al., 2004), methane (Mansour et al., 2001), hydrogen (Saravanan and Nagarajan, 2009), LPG (Badr et al., 1999) etc. The comprehensive use of all these various gaseous fuel types is plausible and provides a wide array of options for practical applicability at the discretion of the engine operator.

In their paper of 2015, Demir et al. used experimental results obtained from a homogeneous charge compression ignition (HCCI) engine fuelled with 85% iso-octane and 15% n-heptane to compare the performances of two combustion codes for zero-dimensional (0-D) analyses. The two codes compared were the Chemkin-Pro and Stochastic Reactor Model (SRM) suite. In their analyses, they showed that both codes have their advantages and disadvantages with the SRM suite providing better convergence of results. While the focus of their comparative study was the performance of the two codes, they concluded that using detailed mechanisms to model combustion was more stable and closer to certain experimentally-obtained data (inlet temperature and exhaust emissions). One major drawback to using detailed mechanisms was the increase in computer run time by factors of 10 and 100 for Chemkin-Pro and SRM suite respectively (Demir et al., 2015). Their study is significant and relevant because researchers in this field of study and constantly faced with a choice of what framework, software or code to use when carrying out various studies and obviously the trade-off between runtime and accuracy of results vis-à-vis the task is an important factor in choosing one software, code or methodology over another.

In recent years, there has been growing interest in investigating dual-fuelling options in spark-ignition (SI) engines (Ceviz et al., 2015, Erkuş et al., 2015, Çinar et al., 2016, Ravi and Porpatham, 2017, Pradeep et al., 2015, Prashant et al., 2016). The variations in LPG temperature were investigated to verify how it affects the performance and emission characteristics of an SI engine. Controlling the temperature of LPG before it is injected into the manifold of the engine has been identified to improve performance while simultaneously reducing NO emission (Ceviz et al., 2015). For SI engine fuelled with LPG, the variation in ignition timing for certain excess air ratios and its effect on engine operating parameters and emissions have been widely studied. Improved engine performance was shown for

advanced injection timing and excess air ratios higher than 0.8 (Erkuş et al., 2015). After carrying out modifications to a single cylinder, 4-stroke SI engine that allowed it to run on LPG also, the classical spline method for various valve lifts was used to re-design the camshaft and improve the engine volumetric efficiency. The engine performance and emissions were then examined for different valve lifts, and it was demonstrated that increasing the valve lift led to the improved volumetric efficiency of the engine when LPG was used as fuel. LPG usage produced lower CO and HC emissions in comparison to gasoline (Çinar et al., 2016). A single cylinder diesel engine modified to operate as an LPG fuelled lean burn SI engine was examined to ascertain the influence of the piston squish area in relation to the overall piston area. For all the operating conditions investigated, it was reported that improved performance was observed for when the piston squish area was 30% of the total piston area. However, unstable combustion was associated with areas higher than 30% of the entire piston area (Ravi and Porpatham, 2017). Modification to a two-stroke SI engine that allowed direct injection of LPG in gaseous form from the cylinder head has been investigated. Improvements in engine thermal efficiency along with significant reductions in HC emissions were reported (Pradeep et al., 2015). Another study which examined the effects of ethanol blend on combustion parameters of a 4-cylinder, turbocharged dual-fuel engine found that ethanol addition initially led to an increase in ignition delay but also caused a reduction in the ignition delay. The rate of pressure rise, net heat release, and peak pressures were also analysed (Prashant et al., 2016).

In my opinion, all the above studies reviewed, accurately portray the potential that exists when a gaseous fuel is used to substitute the liquid fuel in an SI engine. The study presented by Çinar et al. (2016) is intriguing in its usage of a classical spline method applied to valve lifts to improve engine efficiency. In their conclusion, Prashant et al., (2016) provided findings that appear to be contradictory as far as the influence of a gaseous fuel on ignition delay is concerned. However, the authors presented an innovative concept by using ethanol blend as the gaseous fuel to investigate combustion parameters in a dual fuel engine. The arguments provided by Erkuş et al. (2015) adequately support their demonstration of improved engine performance as a consequence of advanced injection timing. It appears to me that

Ravi and Porpatham (2017) provided a new and intriguing direction by examining the influence of piston squish area for dual fuel operation of an SI engine.

An increasing number of studies have focused on the use of natural gas as the primary fuel to investigate the multi-fuelling (gas and liquid fuels used simultaneously) concept applied to Internal Combustion Engines (Fu and Xiao, 2017, Jung et al., 2017, Wang et al., 2016, Cameretti et al., 2016, Yang et al., 2016). For a natural gas-diesel dual fuel engine, the importance of precisely controlling the diesel substitution rate (DSR) is highlighted, and a closed-loop control algorithm has been proposed which uses an estimated DSR from a support vector regression-based model. Using their closed-loop algorithm, the authors reported a deviation of 1.32% when controlling the DSR in actual operation. Their proposed model provided a desirable estimation with a root mean square error of 0.46% and a maximum absolute error of 1.89% (Fu and Xiao, 2017).

Using a commercially available one-dimensional engine simulation tool (GT-Power), a numerical study has been carried out to investigate the effect of intake valve closure on the air/fuel ratio for diesel-natural gas, dual-fuel engine. Thermal efficiency and NOx emission were also optimised using a Latin hypercube sampling and multi-objective Pareto optimisation. The optimal Pareto solutions for varying engine operating loads of 50%, 75%, and 100% revealed that the average brake power increased by 1.1%, 2.9%, and 2.8% and the NOx concentration decreased by 31.1%, 22.2% and 20.3% respectively (Jung et al., 2017).

The impact of pilot diesel ignition has also been studied for a 6-cylinder turbocharged diesel-natural gas, dual-fuel engine under light load operating conditions. It was shown that, in a two-stage auto-ignition mode, when the diesel injection timing is 42.5° crank angle (CA) Before-Top-Dead-Centre (BTDC), the brake thermal efficiency was 35%, with NOx emissions of 60 ppm and total unburned hydrocarbon of 0.4% (Wang et al., 2016).

Using a common rail diesel engine supplied with natural gas, the effect of injection timing on engine performance and emission were examined using CFD modelling with the results validated by experimental investigations. The study concluded that the start of injection timing considerably influenced combustion development NOx emissions as well as the total Hydrocarbon emissions. For injection timings ranging

from 17°CA to 32.5°CA BTDC, the study further revealed lower CO_2 emissions for a dual fuel case with 80% NG substitution when compared to diesel operation (Cameretti et al., 2016).

In a different study, while stating the effects that pilot injection timing have on combustion noise and particle emission, after experimental investigation using a diesel-natural gas engine at low load, it has been suggested that advanced pilot injection timing increases combustion noise. The conclusion of the study suggests that to reduce combustion noise and particle emissions, the optimal range of injection timing is from 17°CA BTDC to 20°CA BTDC (Before-Top-Dead-Centre) (Yang et al., 2016).

Combustion duration and ignition delay of a dual-fuel diesel engine that uses different proportions of hydrogen, producer gas and a mixture of both as secondary fuel have been examined. The study illustrated that for a mixture of producer gas and hydrogen in the ratio of 60–40 respectively, combustion duration and ignition delay are shorter than when producer gas alone was used. At 80% engine operating load condition for 50% hydrogen substitution, reduction in combustion duration was 4°CA whereas, for the same load condition and 50% producer gas, the maximum rise in combustion duration was 9°CA while the maximum rise in ignition delay was 7°CA. The study reports that the combustion duration and ignition delay when producer gas and hydrogen are used as a dual fuel in the ratio of 60:40 respectively, is lower than when producer gas alone is used (Dhole et al., 2016).

A mathematical model to predict thermodynamic properties and brake thermal efficiency (BTE) for a dual-fuel diesel engine using a variety of secondary fuels was developed. Using the developed model, the BTE was predicted to be 3–4% less than the experimentally measured BTE while the predicted maximum pressure rise and net heat release rate are 6–7% less than the experimental results (Lata and Misra, 2010). In another study which utilised a zero-dimensional, multiphase mathematical model of a dual-fuel engine, the impact of enhancing natural gas with other gases during the combustion process was simulated, and the results revealed that there is a significant impact on the combustion process when the gas composition is changed (Mikulski and Wierzbicki, 2016). By adding higher hydrocarbons to methane, the engine performance could be improved by as much as 6% with the additions of

higher carbon amounting to 20% of total fuel volume (Mikulski and Wierzbicki, 2016).

A novel technique constituting the application of an original model of liquid fraction injection based on normal distribution, as well as using a new correlation for computing ignition delay of diesel fuel in the presence of a gaseous fuel contributed to the authors developing a zero-dimensional, 2-phase combustion model for a dual-fuel compression ignition engine (Mikulski et al., 2015). Meanwhile, by varying proportions of methane-hydrogen mixture and equivalence ratio, the performance of a dual-fuel engine was examined, and it was concluded that by introducing some hydrogen with the methane, the performance characteristics of the methane-fuelled spark-ignition engine could be improved while allowing operations with overall leaner mixtures (Karim et al., 1996).

Applying the fundamental laws of conservation of energy, mass, and momentum to the combustion process in a dual-fuel engine using natural gas and diesel, a model was developed and used in another research. Lower peak combustion pressures were observed following the simultaneous use of diesel and natural gas for a normal injection timing and pilot fuel quantity. Dual fuel operation led to higher values of brake specific fuel consumption compared to the respective ones under diesel operation. In addition, dual fuel operation also led to a reduction of nitric oxide and soot emissions while contributing to an increase in carbon monoxide emissions compared to the corresponding pure diesel operation (Papagiannakis et al., 2007).

Several studies, for instance (Papagiannakis et al., 2005, Papagiannakis et al., 2010, Saraf et al., 2009, Aslam et al., 2006) have been carried out using different techniques, frameworks or methodologies to investigate the performance and emission characteristics of dual-fuel engines. Using experiments conducted on a single-cylinder, naturally aspirated four-stroke, air-cooled direct injection high-speed Lister LV1 diesel engine and developed mathematical models, Papagiannakis and Hountalas (2003) examined the effect of liquid fuel percentage replaced by gaseous fuel on performance, soot and nitric oxides. Their analysis of experimental data revealed that dual fuel operation causes higher ignition delays compared to conventional normal diesel operation. Furthermore, they reach the conclusion that the deployment of natural gas to substitute for diesel fuel has a positive effect on

Nitrogen Oxide (NO) emissions but leads to high Carbon monoxide (CO) and Hydrocarbon (HC) emissions. Although I find their methodology and results very interesting and consistent, it appears to me that statistical analysis consistent with the design of experiments is missing.

A very comprehensive review examining the technology, performance, and emission in dual-fuel engines has also been compiled. In their review, the authors point out that many existing diesel-only engines can be converted to dual-fuel operation with the conversions justified by fuel cost savings (Weaver and Turner, 1994).

Experimental investigation of the effect of variation of the LPG composition on the performance and emission characteristics of a two-cylinder, naturally aspirated, four-stroke DI diesel engine converted to run as a pilot-injected dual fuel engine was done (Saleh, 2008). Despite not providing any combustion history, the study (Saleh, 2008) reported that for the 70% Propane blend, NOx and SO_2 emissions decreased by 27–69% whereas the CO emissions increased by 15.7% compared to the conventional diesel engine. A recent review of the literature on the subject matter of engines which use conventional diesel and LPG has found that LPG-diesel dual fuel engines demonstrate a good thermal efficiency at high outputs. Despite the good thermal efficiency, at high outputs, further examination of the literature suggests that owing to the poor utilisation of the fuel charges at low loads, LPG-diesel dual fuel engines perform poorly at low loads (Ashok et al., 2015).

In my opinion, the recent review by Ashok et al. (2015) provides an accurate account of the progress made in the area of LPG-diesel dual-fuel engines. The authors trace the development of research in this subject area and draw our attention to several factors that can be varied to overcome the poor performance of LPG-diesel dual-fuel engines. Some of these factors constitute a neglected area in the field of dual fuel engine performance, combustion and emissions studies indicating gaps in knowledge that need to be filled.

Few researchers have addressed the problem of gaseous fuel-to-diesel fuel ratio in relation to LPG-diesel dual fuel engine operation and its effect on engine performance and emissions. Previous work conducted on a Cummins Model5/9, 4-stroke diesel engine by Mbarawa and Milton (2005) showed that 86% of natural gas could be substituted for diesel at low speeds. Unfortunately, this figure is

inconsistent with that of the few other researchers that have attempted to study this, for instance, Weaver and Turner (1994) suggest 5 to 10% of diesel fuel whereas Sahoo et al. (2009) who claim 10 to 20% of diesel fuel is required. In my opinion, this is a crucial and major issue of discussion as far as the operation, performance and emissions of LPG-diesel dual-fuel engines are concerned and necessitates further research studies. The characteristics of the effect of mass ratios of LPG to diesel deployed for LPG-diesel dual fuel engine operation have not been dealt with in depth. Furthermore, one of the main issues in our knowledge of LPG-diesel dual fuel engine operation, performance and emissions raises questions pertaining to the influence of the injection timing given that the content of the cylinder charge differs from that of a diesel or gasoline engine.

For the light load issues that continue to plague the smooth operation of dual-fuel engines, there could be several potential solutions. The current solution employed in most dual-fuel engines nowadays is to ensure that the engines operate exclusively on diesel at the light load operation. While this is the current status quo, it is not necessarily satisfactory as it raises a major drawback in the sense that the dual fuel engine concept is attempting to reduce pollutant emissions associated with the diesel engine. There is still some considerable controversy surrounding allowing dual-fuel engines to revert to diesel operation at light load as the international community wants to get to a time where the tail-pipe emissions from engines are at their barest minimum. Another undesired effect of reverting from dual fuel operation to 100% diesel is the fact that, end users seek to cut down fuel cost associated with running their engines. Given the fact that diesel fuel prices have traditionally been on the increase, operating an engine on 100% diesel would be more costly than the dual fuel operation of the same engine.

Despite its shortcomings, the current practice still contents itself with reverting from dual fuel operation to diesel-only operation at light load. An explanation for this is that the alternative solutions currently proposed are not offering better results. Some of these alternative solutions include reducing the quantity of air admitted in the intake charge at light-load conditions. The benefit of this solution is the possibility of getting the total amount of fuel entering the engine to be reduced without making the mixture too lean to burn. In my opinion, there is still some more research that needs

to be done in which the gaseous fuel could be mixed with a portion of the incoming flow of air through stratification of the air/gas charge. In the light of the recent events in the world, it is vital that researchers keep investigating means and ways of improving the LPG-diesel dual fuel engine operation at light-load operating conditions.

In essence, the investigation of dual-fuel engine performance using computational simulation and mathematical modelling is still very innovative. The innovative nature of mathematical models is evident by the insufficient availability of comprehensive models that can accurately predict thermodynamic changes within the working medium of the dual fuel engine. Despite the extensive application of computationally demanding techniques to investigate diesel and gasoline engine operation, there is still a big need for equally established computer models specific to investigating dual fuel engines particularly when LPG is the gaseous fuel used. Given the identified gaps in knowledge, this study aims to use computational simulation and mathematical modelling to numerically investigate the effect of various LPG to diesel fuel mass ratios, injection timing and engine operating conditions (speed and load) on the performance and emissions of LPG-diesel dual-fuel engines. Therefore, the present study is relevant as it aims to precisely examine the use of LPG along with diesel in a 1.9L, four-stroke, four cylinders, and naturally aspirated, high-speed diesel engine seeking to address the effects of various gaseous fuel mass ratios on the engine performance and emission characteristics. This study is also vital, because of the recent rising interest in dual fuel engines owing to:

- Global concerns about the depleting liquid fuel resources,
- Stringent environmental legislation that ICEs are expected to meet,
- The public perception of gaseous fuels as more environment-friendly,

The high octane number of gaseous fuels which means they can be used in conventional diesel engines with little modification while providing efficiencies comparable to their diesel engine counterparts.

In this context, this research has been initiated to examine ways in which tailpipe emissions from existing diesel engines can be reduced while providing opportunities for cost-saving associated with the usage of a cheaper and more environmentally fuel option. Table 3.4 presents various types of test engines and fuels with which the

growing body of literature has carried out experiments about dual fuel engine performance and emissions.

3.5 Synopsis of Chapter Three

In summary, the chapter presented a survey of literature about dual-fuel engine operation. The focus is then turned to review literature pertaining to the various types of models that can be used to model and simulate combustion in ICE generally. With the various models reviewed, the chapter highlights that a zero/one-dimensional model will be used for this study. Following the surveyed literature, a critical review and appraisal of the reviewed literature are then presented from which an indication of the knowledge gap emanates.

Table 3.4 Some test engines and their respective fuel types used by researchers to examine dual fuel engine performance and emissions, adapted from Sahoo et al., (2009)

RESEARCHER(S)	TEST ENGINE USED	PILOT FUEL	PRIMARY FUEL
Abd, Soliman, Badr, Abd (2000,2002)	Single cylinder, 4-Stroke, water cooled engine (Ricardo E6)	Diesel	Methane, Propane
Badr, Karim, Liu (1999)	Two single cylinder, 4-Stroke, Water cooled, DI, normally aspirated laboratory dual fuel engines	Diesel	Methane
Bari (1996)	Two cylinder, 4-stroke cycle diesel engine (16.8 KW at 1500 rpm, Model-2105 Nang Chang Company, China), water cooled, naturally aspirated with double swirl combustion chamber	Diesel	Biogas
Henham, Makkar (1998)	Two-cylinder, 4-stroke, water-cooled, IDI Lister Petter LPWS2 diesel engine	Gasoil	Biogas
Krishnan et al. (2004)	Single-cylinder DI, CI engine	Diesel	Natural Gas
Kusaka , Okamato, Daisho, Kihara, Saito (2000)	Water-cooled, 4-Stroke-cycle, and 4- cylinder conventional DI diesel engine	Diesel	Natural Gas
Mansour, Bounif, Aris, Gaillard (2001)	Naturally aspirated, V-8 Deutz FL8 412F 4-cycle diesel engine	Diesel	Natural Gas
Nwafor (2000, 2002, 2003)	Petter model AC1 single cylinder, air-cooled, high speed, IDI, 4-stroke diesel engine	Diesel	Natural Gas
Nwafor and Rice (1994)	Petter model AC1 single cylinder, air-cooled, high speed, IDI, 4-stroke diesel engine	Diesel	Natural Gas
Papagiannakis and Hountalas (2004)	Single cylinder, naturally aspirated, 4-stroke, air cooled, direct injection, high speed, Lister LV1 DI diesel engine with bowl in piston combustion chamber	Diesel	Natural Gas
Selim (2004)	Ricardo E6 single cylinder variable compression IDI diesel engine	Diesel	CH_4, CNG, LPG
Selim (2001)	Ricardo E6 single cylinder variable compression IDI diesel engine	Diesel	CNG
Singh, Singh, Pathak (2007)	Naturally aspirated multi cylinder DG with matching alternator	FD	Producer Gas
Uma, Kandpal, Kishore	Direct injected 6-cylinder, vertical, 4-stroke engine with mechanical injector	Diesel	Producer Gas

4 Experimental Setup and Methodology

4.1 Introduction to Chapter Four

This chapter presents the experimental, methodological approach, analysis of variance and the various statistical metrics used to analyse the measured data. It also provides an overview of the experimental facility and the procedure for modifying diesel engines to allow them to operate simultaneously with diesel and LPG. In this study cylinder pressure data for the 1.9L naturally aspirated diesel engine was obtained from operating the engine test rig at various speeds and load conditions. In a similar manner, the engine performance data was obtained as shown in Appendix 1, Table A.1 and displayed in Figure A.1. The effort was made to capture the engine behaviour across the low, medium and high engine operating load conditions. These experimentally-acquired data are subsequently used during engine model calibration. This chapter informs the audience of the experimental procedures used and also provides insight into the layout of the facility used in carrying out the study. Furthermore, the experimental approach including error and uncertainty analyses are also presented in this chapter. Table 4.1 provides the specifications of the naturally aspirated diesel engine test rig used for the experimental study.

Table 4.1 Technical specifications of diesel engine test rig

Parameter	Value/Specification
Engine Model	Volkswagen SDI
Identification Code	ARD
Number of Cylinders	4
Displacement	1896cc
Bore	79.5 mm
Stroke	95.5 mm
Nominal power	44 kW @ 3600 rpm
Nominal torque	130 Nm @ 2200 rpm
Dynamometer type	Eddy current
Cooling	Air cooled
Dyna. Max. Power	55 kW for 20 Min

4.2 Diesel Engine Test Rig

Mounted and housed within the engine laboratory of the Department of Naval Architecture, Ocean and Marine Engineering (NAOME) at the University of Strathclyde, is a self-contained diesel engine test rig that allows for investigation of standard engine performance parameters. The test rig is a four-cylinder, water-cooled, 1.9-litre diesel engine supported on a strong steel framework via flexible mounts. The frame also houses the fuel tank, battery, and electrical enclosures. Additionally, the test rig has a variable load eddy current dynamometer, which acts as a brake, enabling direct measurement of engine torque. Furthermore, safety interlocks and emergency stops are provided for the engine, along with protection guards around moving parts. Software for data logging and control alongside the engine manufacturer's diagnostic software are installed on a computer from which the starter and dynamometer can be controlled. Standard instrumentation which includes sensors for engine speed, torque, air flow, cooling water temperature (inlet and outlet of the heat exchanger), cooling water flow, etc. Figure 4.1 provides a

drawing of the diesel engine. Table 4.2 presents the names for each of the numbered parts in Figure 4.1.

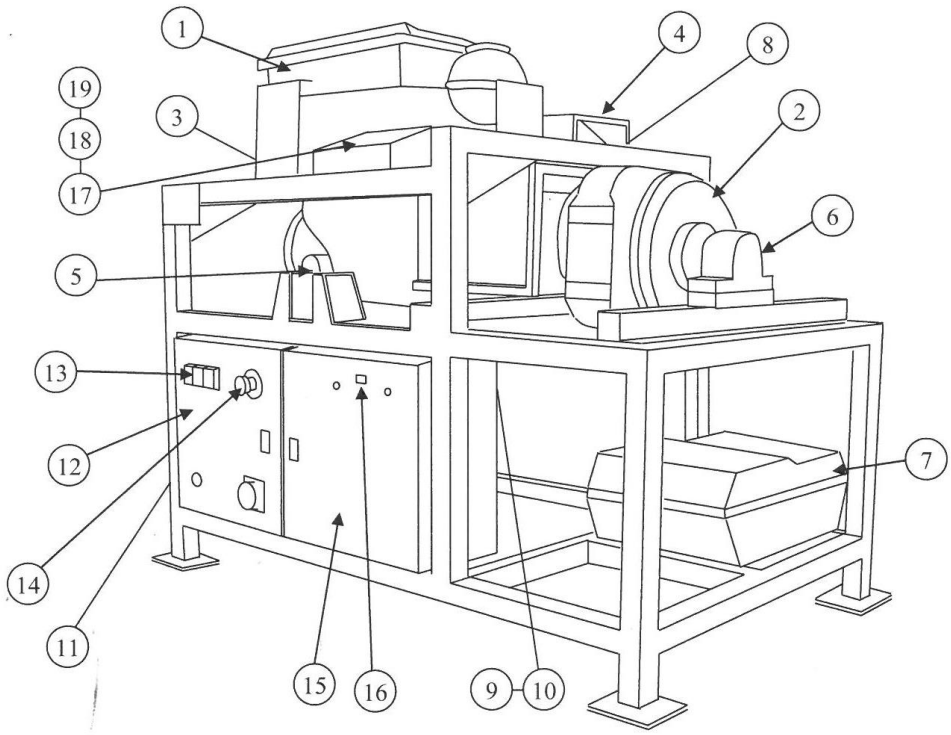

Figure 4.1 Armfield CM12 diesel engine test rig

Table 4.2 Specification of parts of the CM12 diesel engine

Part No	Part Name	Part No	Part Name	Part No	Part Name
1	Engine	8	Heat exchanger	15	Enclosure
2	Dynamometer break	9	Exhaust Silencer	16	USB Interface
3	Front Mount	10	Exhaust Silencer	17	Programmable Logic Circuit
4	Rear Mount	11	Battery	18	Potentiometer
5	Stabiliser bars	12	Enclosure	19	Potentiometer
6	Ball bearing units	13	Circuit breakers		
7	Fuel tank	14	Emergency stop button		

Figure 4.2 presents a pictorial view of the diesel engine test rig as installed in the engine laboratory. It also shows the computers used for data acquisition.

Figure 4.2 Pictorial view of the CM12 engine (diesel-only mode)

4.3 Modification of Diesel Engines for Dual-Fuel Operation

The rapid depletion of traditional fossil fuels and the need to promote the use of environmentally friendly fuels are among some of the factors that have brought dual-fuel engine operation to the limelight in modern times. The combustion characteristics of the dual-fuel engine have been shown to bear characteristics similar to both the diesel engine and the spark-ignition engine. Consequently, it can be argued that the dual-fuel engine concept is a modification of the diesel engine concept more so because it allows for the simultaneous use of both a gaseous fuel and a liquid fuel. There is the need for the dual-fuel engine to be able to retain some of the attractive features of the diesel engine while accommodating the use of several gaseous fuels alongside the liquid diesel.

Several manufacturers all over the world have developed and introduced dual-fuel engine systems in parallel with their diesel engine lines. Other manufacturers (notably in the transport sector) have designed and introduced dual-fuel engines. It is therefore evident that dual-fuel engines have been in operation already and have been reported to be doing so satisfactorily. In some cases, they have also been seen to provide substantial economic and environmental benefits when used. Despite their success-story so far, avenues for their improvement still abound especially as their performance is concerned. For example, attempts can be made to improve the dual-fuel engine efficiency, power production, as well as maximising the diesel fuel substitution.

Depending on the gaseous fuel used, dual-fuel engines could have different names. For example, diesel/Methane or diesel/liquefied petroleum gas (LPG) engines with Methane and LPG deployed as the respective gaseous fuels. This study focuses on a diesel engine that has been retrofitted (using a commercially-available conversion kit) to use diesel and liquefied petroleum gas.

It is widely accepted that diesel engines can be modified to allow them to operate in a dual-fuel mode. This modification can be done to accommodate several types of gaseous fuels. Regarding this study, the emphasis is on modifying the diesel engine to run using LPG and diesel. Given that there are not many engines designed solely for dual-fuel operation, the modification/conversion of conventional diesel engines to their dual-fuel counterpart which does not require significant modification to the engine is of great importance. Details of diesel to dual-fuel engine conversion and the potential benefits have been outlined (Karim, 2015).

Modification of the diesel engine involves adding an LPG line to the intake manifold together with an evaporator (Sproat et al., 2006). In some applications, LPG is kept as a liquid in a distinct vessel at a pressure of about 10 bars despite it being able to withstand the pressure of between 20 to 30 bars. The supply of LPG to the engine is controlled by a regulator or a vaporiser which then converts the LPG to a vapour. Before being drawn into the combustion space (where the LPG is burned to produce power), the vapour is taken through a regulating valve to a mixer situated close to the intake manifold. In the intake manifold, this vapour is metered and mixed with filtered air. Added to the combustion space containing the mixture of LPG and air, is

an amount of liquid diesel. In most cases, this addition takes place through the conventional diesel injection systems (Ergenç and Koca, 2014, Goldsworthy, 2012, Karim, 2015, Paykani et al., 2011, Rao et al., 2010, Bora et al., 2013).

LPG systems have demonstrated that they are reliable as far as power; engine durability and cold starting are concerned. LPG technology is thought to be most popular in Armenia with an estimated 20-30% of vehicles being run on LPG given that it is cheaper than diesel and petrol. However, other places where LPG technology is quite popular include the European Union, Australia, Turkey, Serbia, South Korea, Philippines, Hong Kong and India. LPG has high energy content per unit of mass, but unfortunately, its energy content per unit of volume is low (Norris, 2009, Norris et al., 2010).

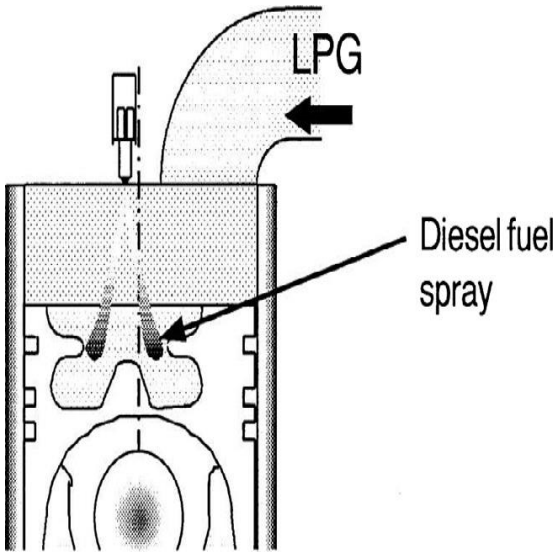

Figure 4.3 Diesel-LPG Combustion (Ogawa et al., 2001)

The diesel engine test rig described in section 4.2 was modified to run as a dual-fuel engine, simultaneously using diesel and liquefied petroleum gas to produce power.

Figure 4.8 provides a pictorial view of the engine after the modifications. By comparing Figure 4.2 and Figure 4.8, the presence of the LPG cylinder in the latter is evidence of the modification that was performed to the original engine. This modification then allows the engine to be operated in dual-fuel mode. The adaptation carried out on the diesel engine was done using a commercially available kit – AC STAG DIESEL. However, when required, the engine was still able to operate in

diesel-only mode. The subsequent paragraphs shed more light on the conversion process and the kit used.

The AC STAG DIESEL system was used to modify the diesel engine for it to operate in dual-fuel (LPG-diesel) mode. The system's conversion kit consists of several components – LPG cylinder and its auxiliaries, piping for LPG, LPG injectors, an LED switch, gas pressure sensor and a vaporiser. An electronic control unit (ECU) is also installed to monitor and control several parameters (such as speed, pressure, temperature, and knock) to ensure the safe operation of the engine in dual-fuel mode.

The AC STAG DIESEL system controls the supply of LPG to the diesel engine. Initially, it pre-heats the gaseous fuel upstream of the intake collector, through evaporation. It also stabilises the pressure according to the requirements of the vaporiser. Pressurised LPG in the vapour phase is then supplied to the LPG injectors mounted on the engine and subsequently injected into the intake manifold. Electronic signals from the LPG controller command the operation of the injectors.

Figure 4.4 AC STAG DIESEL LPG Conversion Kit

For the injection of LPG into the diesel engine, each component of the conversion kit (shown in Figure 4.4) was appropriately mounted or installed. Firstly, the LPG cylinder was placed next to the engine as seen in Figure 4.8. The flat nature of the surface helped to ensure that the cylinder was stable. The cylinder was also placed away from the hot surfaces of the engine for safety reasons.

The vaporiser (reducer) was mounted on the support frame of the engine test rig as shown in Figure 4.5. It was placed close to the engine to optimise the length of

piping between the injectors and vaporiser. By mounting the vaporiser as shown in Figure 4.5, care was taken to ensure that it was not exposed to high temperatures from the engine.

LPG injectors were installed on the intake manifold of the engine. The nozzles for gas injection were placed such that they had access to the inlet ducts that deliver air into the individual cylinders.

The LED switch was mounted where it could be quite visible to the operator. The switch has an AC stag button at the centre which enables switching-over of fuel from diesel to LPG and vice versa. It also indicates the mode of operation, and four LEDs in the form of a circle indicate the LPG level in the tank

For detection of LPG pressure, a pressure sensor was fitted on the gas tube between the vapour phase filter and the LPG injectors. Also for safe operation, a knock sensor positioned as close to the engine width and height centre-line crossing is used. Output readings from all sensors can be observed from the AC STAG diagnostic software on a computer.

Upon installation of all the components of the conversion kit, a computer with AC STAG diagnostic software was connected using a USB interface to the STAG DIESEL. This allowed for calibration of the system. For operation purposes, the diagnostic software also allowed the control of the quantity of LPG injected.

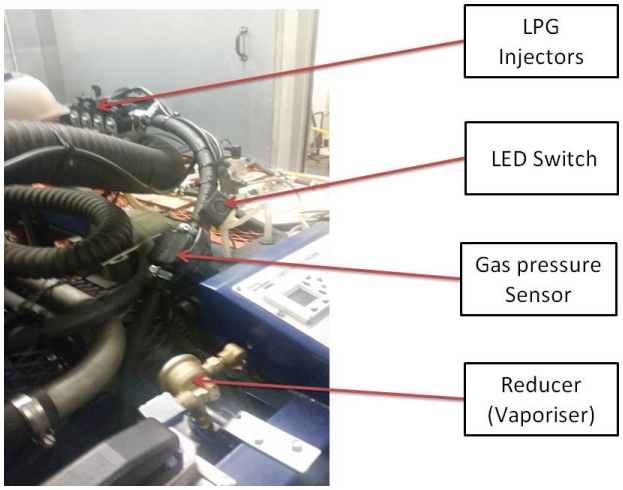

Figure 4.5 Elements of conversion kit mounted on the engine

4.4 Design of Experiments and Data Acquisition

Regarding internal combustion engines, experiments are sometimes conducted to explore, estimate or confirm the effects of various parameters. Using the design of experiments methodology, the experiments in this study were conducted to collect and understand the data from the combustion process. This data would subsequently be used to verify and validate the predicted results of the combustion process (obtained using computational simulation). The process of designing, planning, conducting, analysing and interpreting the results of the experiments involved the use of statistical methods and thinking, which would permit the study to draw objective conclusions. Experiments included the following sequence of activities:

4.4.1 Defining the experiment objectives

The objective of the experiment was to identify and obtain data of the significant thermodynamic parameters affecting the combustion process and to use this data to validate a developed zero/one-dimensional model. In addition, the experiments also sought to explore and estimate the performance of the test facility.

4.4.2 Defining the hypothesis

The main assumption that motivates the experiment is the idea that, the in-cylinder pressure is the most significant thermodynamic parameter characterising the combustion in internal combustion engines. It is assumed that as the engine operating load increases, the cylinder pressure also increases leading to higher maximum cylinder pressures being attained during combustion.

4.4.3 Experiments and measurements

The experiments were carried out using the retrofitted naturally aspirated, 4-cylinder, 4-stroke diesel-LPG engine described in previous sections in this chapter. As shown in the schematic diagram in Figure 4.7, the engine under investigation was coupled to an air-cooled eddy current dynamometer (See Appendix 3, Table A.2 for dynamometer specifications). Both the engine and dynamometer are controlled with software supplied that allows both 'manual' and 'automatic' control. During each experiment and operation, control of the brake setting was done automatically using the Armfield CM12 integrated engine software installed on a computer. The 'manual' mode warrants the operator to specify the brake percentage which is the power to the dynamometer from which the engine is loaded. In contrast, the 'automatic' mode requires that the operator specifies a set point rpm and then a proportional-integral-derivative (PID) controller will adjust the brake percentage setting from the specified rpm. All the experiments and data presented in this study were obtained by operating the engine test rig in 'automatic' mode.

Table 4.3 Specifications of flow meters used to determine the diesel flow rate

	VZS-005-ALU	VZS-003-ALU
Manufacturer	BIOTECH	BIOTECH
Flow range	0.005-1.5 L/min	0.005-0.3 L/min
Pulse output/litre	3600 Pulses/L	7000 Pulses/L
Accuracy	+/- 1%	+/- 1%
Repeatability	+/- 0.5%	+/- 0.5%
Operating pressure	0.8-30 bar	0.8-30 bar
Running temperature	-20…+100 °C	-20…+100 °C
Voltage	5 – 24 VDC_{max}	5 – 24 VDC_{max}
Output current	25 mA_{max}	25 mA_{max}
Weight	circa 80g	circa 70g

To measure diesel flow rates, two *BIOTECH* oval gear flow meters (Table 4.3) were installed – one on the diesel supply-line and the other on the return line. The output from each of the flow meters was then used as input for the National Instrument DAQ device. This device was connected via a USB port to a laptop, and with the help of LabVIEW, a programme (Shown in Figure 4.6) was set up to facilitate determination of the diesel fuel flow rate. For the block diagram shown in Figure 4.6, a visual display provided the volumetric flow rates determined and used in the simulation.

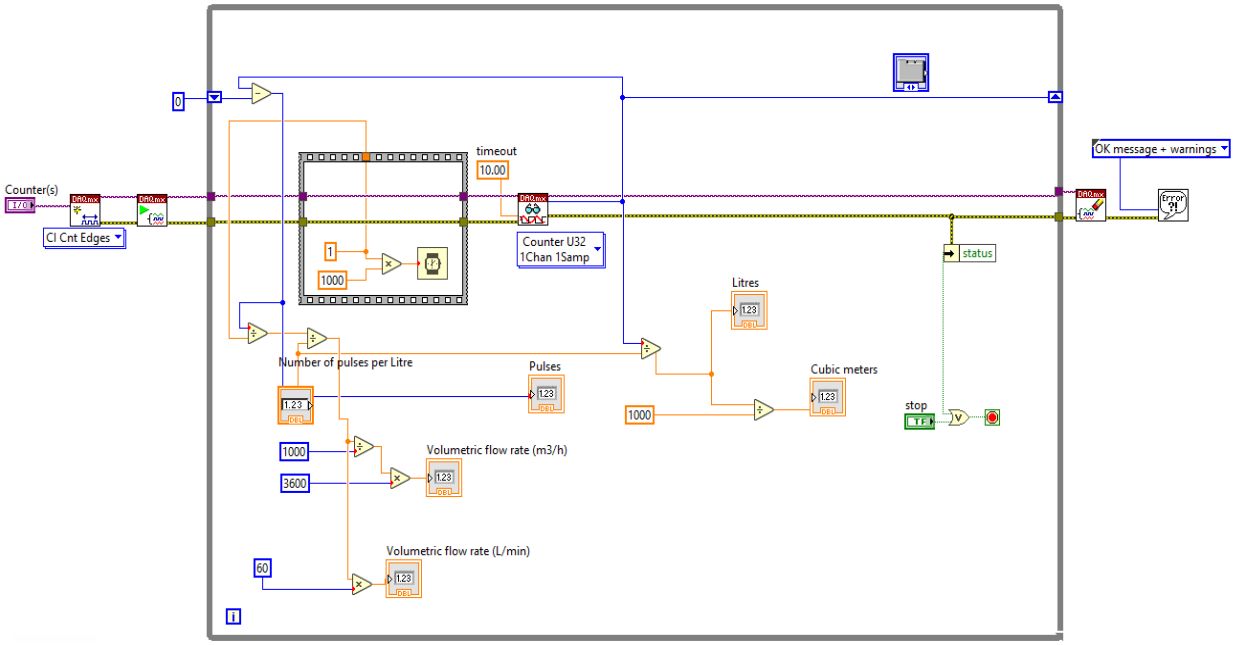

Figure 4.6 Block diagram designed to measure diesel fuel flow rate

Following the modification carried out as described in the previous section, during experiments, LPG was drawn from a cylinder and admitted into the intake manifold of the engine in vapour form after passing through a vaporiser. The admission of LPG to the engine was controlled using the ECU of the LPG system connected to a laptop via USB. Excess air (lambda) sensors installed on the engine and monitored through the ECU during LPG injection helped to avoid engine knocking. A load cell mounted on a support frame was attached to the LPG storage cylinder. This load cell was used to measure the weight of the LPG cylinder throughout the entire duration of

each experiment while LPG was injected into the engine. With the load cell connected to a Cambridge Electronic Design (CED) transducer amplifier, its analogue signal was then processed and using software called SPIKE, digital waveforms were recorded and stored. This enabled the weight of the bottle to be taken over time, and hence the amount of LPG injected by way of mass was determined.

The engine was cooled using an Armfield CM12 -26 heat exchanger system that was connected to the main water supply of the building in which the engine was housed. The temperature of the cooling water into and out of the engine was observed and recorded. Also, the flow rate of the cooling water was measured.

Additionally, air inlet pressure and temperature were measured using sensors mounted on the intake manifold of the engine. The exhaust temperature was equally monitored. The power, torque, and speed of the engine were measured and recorded at regular intervals.

4.4.4 Obtaining engine performance data

The internal combustion engine produces varying torque and power in relation to the operating speed and load conditions. Therefore, in the case of the diesel engine, by measuring the torque and power at different operating speeds, the author produced the characteristic curves shown in Appendix 1, Figure A.1.

To obtain the above-mentioned characteristic curves, the author followed the following procedure. Firstly, load the Armfield CM12 programme installed on a computer in the engine laboratory. Following the manufacturers' prescribed procedure, start the engine ensuring that it is running under computer-controlled load. The engine test rig contains Volkswagen (VW) diagnostic software. This software is then loaded. With the software loaded, the appropriate measuring blocks are selected.

Subsequently, adjust the set-point of the controller to the desired operating speed in intervals and allow the engine speed to stabilise at each new speed before proceeding to the next. Once the engine speed is steady, input the fuel injection data on the

simulator diagram screen. Then proceed to record a sample by clicking on the 'GO' button of the VW diagnostic software program. Repeat these steps for various other engine speeds and record the data. The data is then extracted and plotted using Microsoft Excel as shown in Appendix 1 Figure A.1. This Figure can then be compared to that of the engine Manufacturer shown in Appendix 2, Figure A.2.

Some other performance parameters that are measured through the various measuring blocks of the VW diagnostic software are presented in Appendix 1, Table A.1.

The volumetric efficiency of the engine is given by:

$$\eta_v = \frac{q_{air}}{2V_s n/60} \qquad \textit{Eqn. 4.1}$$

In Eqn. 4.1, q_{air} is the volume flow rate of air through the system, V_s is the swept volume and n is the engine speed in rpm.

The thermal efficiency is then defined by:

$$\eta_T = \frac{P_b}{\dot{m}_f LHV} \qquad \textit{Eqn. 4.2}$$

Where LHV is the energy content of the fuel and $\dot{m}_f$ is the fuel mass flow rate.

$$\dot{m}_f = 2\dot{m}_{injected_{cycle}} \frac{n}{60} \qquad \textit{Eqn. 4.3}$$

Where $\dot{m}_{injected_{cycle}}$ is the mass of fuel injected per cycle.

4.4.5 Obtaining the cylinder pressure measurements

To carry out this experiment and measure the pressure in the cylinder, the author made use of the CM12-12 Engine Indicator Set that was supplied by the manufacturer. Load the Armfield CM12 program and specify the type of experiment

to be carried out. In this case, I chose ‘cylinder pressure’ experiment. I then started the engine and made sure it was running under computer controlled load. I proceeded to specify the engine speed in a similar manner to the previous experiment described in section 4.4.4. When the engine speed was stable, I proceeded to collect data by clicking the ‘Go’ button on the VW diagnostic software of the simulator diagram on the computer. The software recorded cylinder pressure data from the engine at regular intervals for 1000 samples. This was repeated for other engine operating speeds and the results stored.

As shown in the schematic diagram in Figure 4.7, the engine under investigation was coupled to an air-cooled eddy current dynamometer. The eddy current dynamometer manufactured by Zelu is air-cooled, with a maximum power of 55 kW for 20 minutes and a maximum torque of 145 NM. Both the engine and dynamometer are controlled with software supplied by Armfield that allows both ‘manual’ and ‘automatic’ control. During each experiment and operation, control of the brake setting was done automatically using the Armfield CM12 integrated engine software installed on a computer. The ‘manual’ mode warrants the operator to specify the brake percentage which is the power to the dynamometer from which the engine is loaded. In contrast, the ‘automatic’ mode requires that the operator specifies a set point rpm and then a proportional-integral-derivative (PID) controller will adjust the brake percentage setting the specified rpm. All the experiments and data presented in this study were obtained by operating the engine test rig in ‘automatic’ mode. The CM12 engine also contains an engine indicator set. The engine indicator set comprises a high-temperature pressure sensor installed into one of the cylinders. A separate charge amplifier (Kistler type 5011) provides signal conditioning for generating a voltage which can be logged on the computer. A special routine in the Armfield software allows for the high-speed data acquisition of this signal. The special routine in the Armfield software allowed cylinder pressure and volume data to be logged at the count of pulses that represent time in seconds. Therefore the cylinder pressure history is generated over time. The time data is then converted to crank angles using the following equation:

$$Crankangle = 6(Time)(rpm) \qquad \textit{Eqn. 4.4}$$

4.4.6 Analysing and interpreting experimental data/results

The measured values of various physical quantities have some degree of uncertainty. This uncertainty could emanate from several factors such as the type of instrument used, the calibration of the instrument, the experimental procedure, errors in observation etc. It is therefore vital to assess the reliability and repeatability of the measured data. One way to assess the measured data is to repeat the measurements a number of times and then examine the various values obtained for errors and uncertainty. In this study, uncertainties are classified into two categories namely the random uncertainty and the systematic uncertainty. To evaluate the random uncertainties in this study, descriptive statistical metrics as shown in Table 4.4 are used while the systematic uncertainties are accounted for based on the accuracy of the pressure transducer as provided by the manufacturer (See Appendix 3, Table A.2). The random uncertainty component (∂P_{random}) in the cylinder pressure measurement is given by the standard error ($\sigma_{\bar{p}}$) shown in Table 4.4. Assuming that the systematic error in the pressure transducer is given by the accuracy of +/- 0.4 specified by the manufacturer as shown in Appendix 3, Table A.2; let this value constitute the systematic uncertainty component ($\partial P_{systematic}$) in the cylinder pressure data. Therefore the total uncertainty in each cylinder pressure data is computed using the root mean square and given by:

$$\partial P_{total} = \sqrt{\left(\partial P_{random}\right)^2 + \left(\partial P_{systematic}\right)^2} \qquad \textit{Eqn. 4.5}$$

The analyses presented in Table 4.4 highlight the statistical metrics used to analyse the measured cylinder pressure data for each engine operating speed. The various statistical metrics used to provide valuable information about the average cylinder pressure observed for each engine operating speed; the maximum cylinder pressure attained the range of pressure within the cylinder, etc.

In instances where the ambient pressure is higher than the system pressure, the term vacuum pressure is applied. It is, therefore, possible for gauge pressures to be

negative and this explains why in Table 4.4, for the 2435 rpm, the minimum, median and modal pressure values are negative.

Tests are performed on a 5% - level of significance using an analysis of variance (ANOVA) with the results presented in Table 4.5. This is done to determine the relevance of the cylinder pressure data as well as the impact of the predicted results. The first part of Table 4.5 is a summary of the cylinder pressure data that is subjected to the one-way ANOVA. The data is grouped according to the experimental runs carried out. For each of the engine operating speed, 1000 samples were collected as shown by the 'count' column. For each operating speed, the data are summed up with the average and variance calculated. The second part of Table 4.5 presents the results of the one-way ANOVA. From the ANOVA results, the following are true:

- The average cylinder pressure for each run is not the same, and this is to be expected given the nature of the combustion process with cycle to cycle (or cylinder to cylinder) variations
- The figures of the variance are quite large which implies there is some widespread from the average cylinder pressure. Again this is justified because of the nature of the diesel engine combustion process

- The interaction between the groups of the experimentally-measured cylinder pressures is statistically significant since the *P-Value* is less than 5% and the *F value* is higher than the *F critical* value.
- With 1000 samples for each engine operating speed taken at a sampling rate corresponding to every 0.255 milliseconds; it is believed that this reflects the behaviour of the cylinder pressure with acceptable accuracy.

Also, the percentage error between the measured and simulated parameters is computed using equation 4.6, and the results reveal errors which are believed to be within the acceptable limits as will be shown later in Chapter six.

$$Error = \left(\frac{Experimentvalue - Simulationvalue}{Experimentvalue} \right) 100 \qquad \textit{Eqn. 4.6}$$

Table 4.4 Statistical Analysis of the random uncertainties associated with cylinder pressure data

Descriptive Statistic Item	**Statistical Values for the Cylinder Pressure Data at Different Speeds**		
	3050 rpm	**2470 rpm**	**2435 rpm**
Mean Pressure [bar]	6.58	5.18	4.34
Standard Error [bar]	0.44	0.37	0.39
Median Pressure [bar]	0.92	0.67	-0.31
Mode Pressure [bar]	0.67	0.37	-0.55
Standard Deviation [bar]	14.08	11.56	12.47
Sample Variance	198.29	133.56	155.6
Kurtosis	8.60	7.88	9.64
Skewness	3.03	2.96	3.20
Range [bar]	72.94	54.50	66.89
Minimum Pressure [bar]	0.43	0.12	-0.98
Maximum Pressure [bar]	66.37	70.36	77.70
Sum [bar]	6584.05	5176.15	4338.38
Count	1000.00	1000.00	1000.00
Confidence Level (95.0%)	0.87	0.72	0.77

Table 4.5 One-way analysis of variance (ANOVA) of cylinder pressure data

SUMMARY

Groups	Count	Sum	Average	Variance
3050 rpm	1000	4338.379	4.338379	155.6108
2470 rpm	1000	6584.045	6.584045	198.2996
2435 rpm	1000	7176.941	7.176941	233.6736

ANOVA

Source of Variation	*SS*	*df*	*MS*	*F*	*P-value*	*F crit*[1]
Between Groups	5990.493	4	1497.623	8.950582	3.36E-07	2.373711
Within Groups	835770	4995	167.3213			
Total	841760.5	4999				

[1] *SS* is the sum of squares, *df* is the degrees of freedom, *MS* is the mean square, *F* is the *F*-static, *P*-value is the value in relation to the 5% level of significance and *F crit* is the critical value

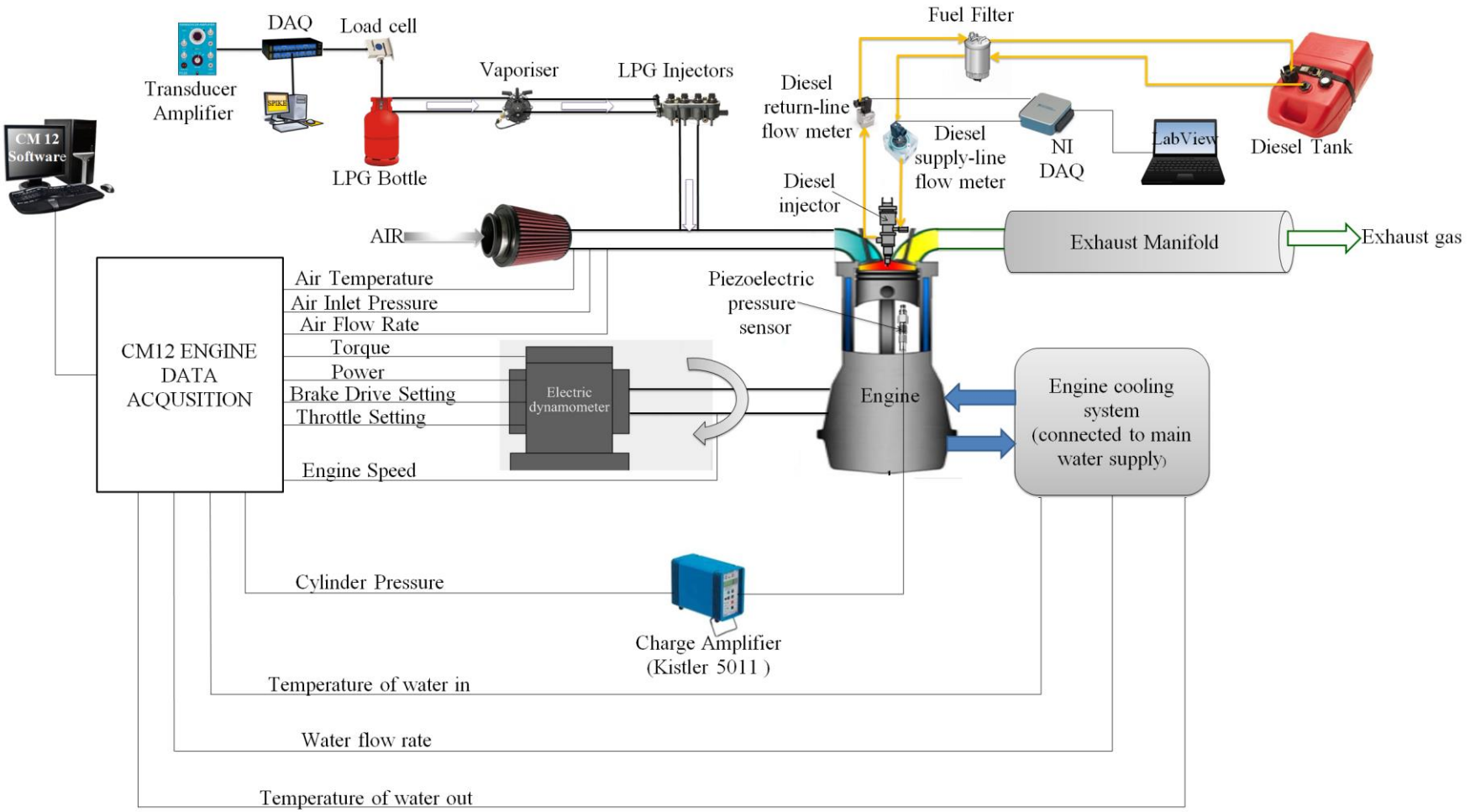

Figure 4.7 Schematic illustration of the experimental set-up

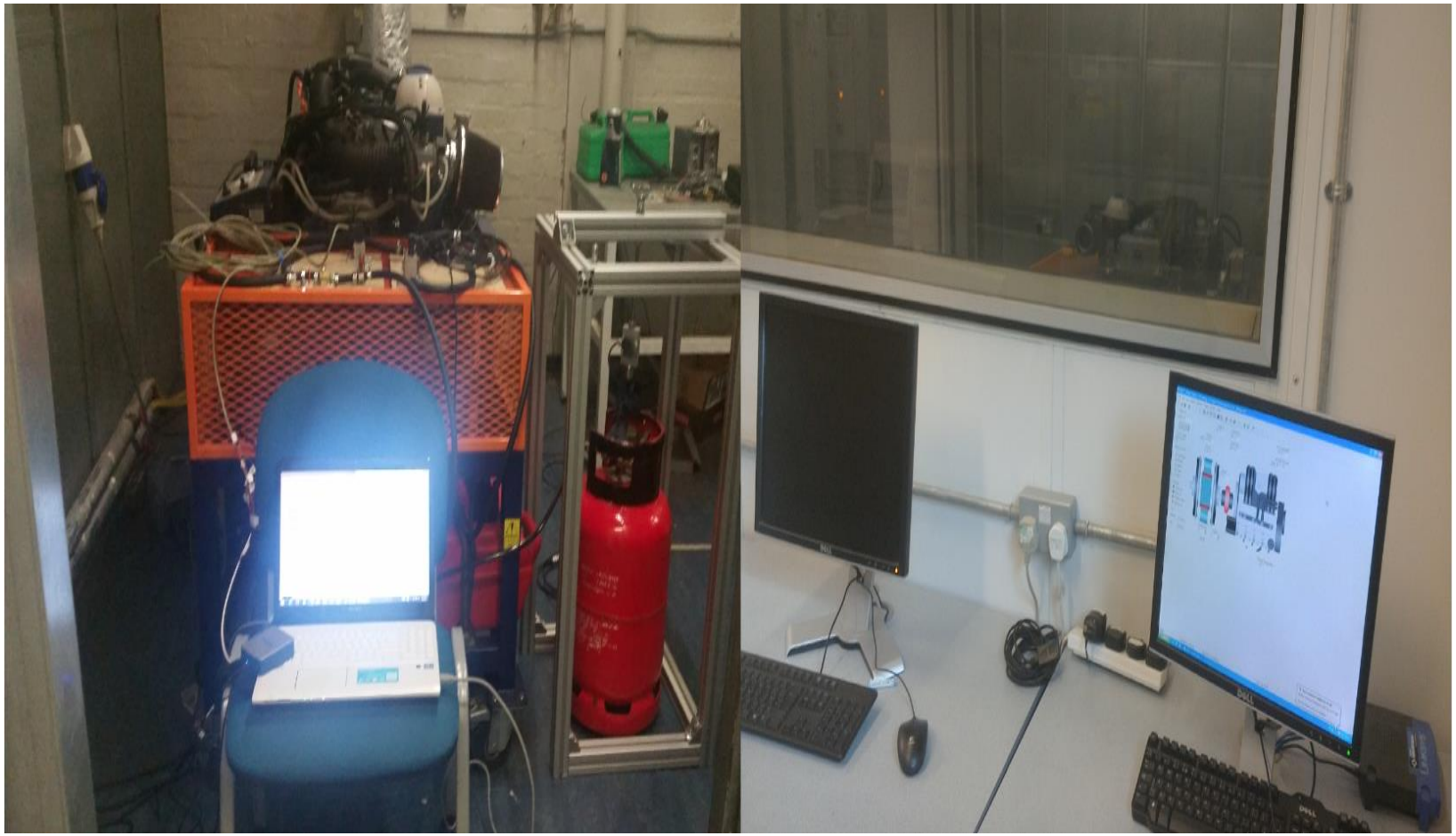

Figure 4.8 Pictorial view of the experimental set-up

4.5 Synopsis of Chapter Four

Summarily, in this chapter, following the design of experiments framework, the experimental setup and procedure used in this study have been presented. Also, error and uncertainty analysis based on statistical methods and thinking have been presented. Additionally, the chapter highlights the modifications done to the diesel engine to allow it to operate in dual-fuel mode. However, following the modification to the diesel test engine, there was a breakdown in the facility which persisted for more than two years of this study and prevented the author from obtaining cylinder pressure measurements for the LPG-diesel dual fuel engine operation. The experimental study concludes that the interaction between the groups of the experimentally-measured cylinder pressures is statistically significant since the P-Value is less than 5 per cent and the F value is higher than the F critical value. The subsequent chapter focuses on the computational simulation methodology.

5 Engine Model Development

5.1 Introduction to Chapter Five

This chapter aims to describe the computational simulation and present the relevant mathematical formulation underlining the various submodels used to develop the overall engine model. In other words, this chapter presents the computational research method and tool used to carry out the study and derive the results shown in the subsequent chapters. Predominantly, in this study computer simulation is used. According to Harper and Selvin (1973), "*Simulation is the act of creating a working model or a symbolic model of some real-life process; the scientist studies the model rather than the real-life process and thereby hopes to learn something about the real-life process. One type of symbolic model is computer simulation. Scientists have represented the real-life process in the language of the computer and have let the computer generate data which describes the process being studied"(Harper and Selvin, 1973).*

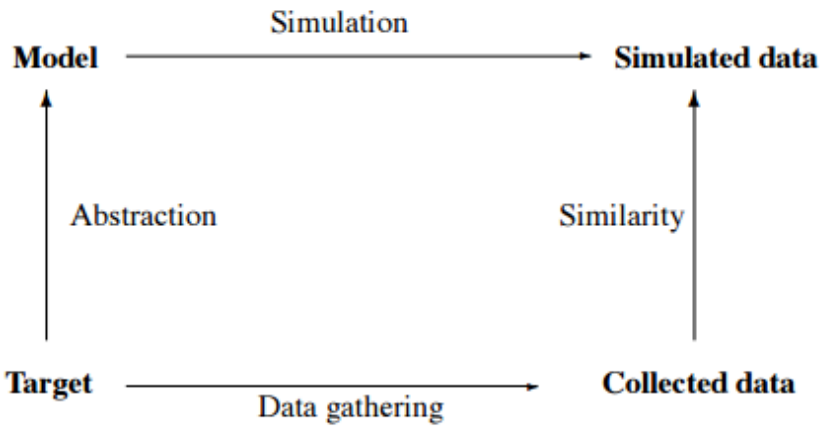

Figure 5.1 Simulation as a research method

Highlighting the logic of simulation as a research method (Figure 5.1), a model is developed based on several assumptions. In this study, a computer program is

utilised to carry out simulation and produce simulated data. The simulated data is then compared in relation to the collected experimental data.

In engineering, the term simulation insinuates the development and utilisation of adequate formulations that would permit critical processes, which are happening within the object of interest to be analysed. In this study, the object of interest is a diesel engine retrofitted to operate as a dual fuel (diesel-LPG) engine. Early application of simulation to the operating cycle of the internal combustion engine contributed in one way or the other to improving engine performance. These early applications of simulations contributed to the development of internal combustion engines, leading to an increase in their performances by estimating potentialities, limitations, and practicability of different concepts (Chiodi, 2011). Over the years, the capabilities of computers have tremendously increased, and as a result, numerical simulation of very complex scientific and engineering processes is now possible. For internal combustion engines, a numerical simulation can be done using commercially available simulation software. Most commercial software is developed using one programming language or the other and would require that the user provides input information to use them. The amount of input information required would depend on the complexity of the simulation task required. Alternatively, engineers and researchers can write their mathematical codes and use several computer software packages to implement their written codes. Either of these approaches would rest on mathematical formalism and would, therefore, require a fundamental understanding of mathematical equations used to describe various processes occurring in the internal combustion engine. For this current research, a commercially available software package – AVL BOOST was used to build the models, and section 5.2 explains why this particular methodological tool was chosen.

5.2 AVL BOOST Simulation Tool

The processes that occur within an engine are quite complex. Several tools for engine simulation exist. These tools rely on one approach or the other to carry out simulations. Some approaches (models) utilised for effective engine simulation

include transfer function models, mean value models, 3-dimensional models and 0-D/1-D models. The latter is the predominant approach used in this study. The purpose of the commercially available simulation software package described below is developed to approach engine simulations from a one-dimensional perspective. Consequently, this software package was chosen on account of the following reasons described below.

AVL BOOST™ is a fully integrated internal combustion engine simulation tool. Developed within AVL's applied thermodynamic department, it is capable of providing advanced models that allow for accurate prediction of the engine performance, tailpipe emissions, and acoustics. As an engine cycle and gas exchange simulation software, able to also simulate combustion, AVL BOOST permits users to construct a model of the complete engine. With a plethora of elements made available to the user, creating the engine model involves selecting elements from a toolbox and then connecting using pipe elements. Inside the pipes, one-dimensional gas dynamics that rely on an adjusted Godunov scheme are applied to produce a great degree of correctness for the result. The software, which is powerful and user-friendly, can simulate steady-state operational points along with engine transients.

Additionally, it can be applied to a range of tasks, some of which include:

- Optimising component geometry, e.g. inlet system, exhaust system, valve sizes etc. with respect to power output, torque and fuel consumption,
- Optimisation of valve timing and cam profiles,
- The layout of supercharging systems,
- Orifice noise optimisation,
- Evaluation of transient engine performance (acceleration/load pick up, deceleration/load drop) taking into account the entire powertrain and vehicle dynamics.

As a vital element in the simulation-driven design and development procedures of IC Engines at AVL and many successful OEM's all around the world, it is used for several industries. Accordingly, BOOST has been used for the simulation and modelling of a wide range of engine speeds, sizes, and configurations, including two-stroke and four-stroke engines.

Mindful of other one-dimensional software packages available for the simulation of engines, the software (BOOST) was chosen over its competitors as it offers the following for the effective realisation of this study:

- The graphical user interface (GUI) based on Windows technology,
- Interactive pre-processor including a model editor for guided input of the required data,
- Interactive post-processor for fast analysis of results and comparison with testbed data,
- Extensive interactive context orientated help facility,
- Efficient simulation based on the one-dimensional treatment of pipe flow and advanced models of other engine components,
- Provision to link user-defined sub-routines to the BOOST – code (FORTRAN compiler required),
- Animated display of pressure waves.

In engine models constructed using BOOST, numerical outputs can provide values such as pressure, temperature, air/fuel ratio, and many more, at measuring points in the simulation model.

5.3 Simulation of Diesel and Diesel-LPG Engine Operation

The first part of the simulation procedure focused on the diesel mode of operation for the diesel engine. This approach was chosen to verify where peak cylinder pressures lie and to serve as guidelines for the assumptions to be used in the modelling of the dual fuel engine. Having a model of the diesel engine operation would allow the author to carry out calibration based on the peak cylinder pressure, the timing of peak cylinder pressure, maximum power and torque since the dual fuel cylinder pressure measurements could not be obtained experimentally due to a breakdown of the experimental facility. The simulation of the diesel model of engine operation was done using AVL BOOST. The task of simulating the entire diesel engine was approached in several stages. Initially, a single cylinder model was developed for the

diesel-only mode. This model was then calibrated to ensure that the modelled parameters match as close as practically possible, the collected experimental data in terms of peak cylinder pressure, the timing of peak cylinder pressure, torque and power. Subsequently, the entire diesel-LPG engine model was set up.

5.3.1 Single-cylinder configuration

As mentioned above, a single cylinder model is first built as shown in Figure 5.2. The simplicity of such an initial model allows for easy calibration of cylinder geometry as well as combustion parameters. This model consists of two system boundaries (SB1 and SB2) which simulate the ambient conditions at the intake and exhaust respectively. Additionally, there is a cylinder (C1) to which the system boundaries are connected using pipes (1 & 2). In defining the cylinder characteristics, both the intake and exhaust valve geometries are specified as well as the fuel mass injected directly into the cylinder. The engine element (E1) is placed to reflect the fact that this model is for an engine. This model is then run and the results obtained are calibrated to match as much as practically possible, the results obtained experimentally from the engine test rig.

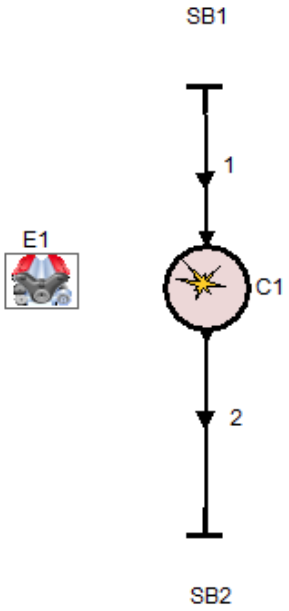

Figure 5.2 Single cylinder diesel-only model

5.3.2 Complete engine configuration

After calibrating the 1-cylinder model, the entire engine is then set up. The pre-processing (setup) stage in AVL BOOST consists of selecting the relevant elements required to build the model. The selected components are then placed in the working area. Using the appropriate connections in the working area, the elements are then connected as desired to represent the engine working cycle. Figure 5.3 shows the schematic of the entire 4-cylinder diesel engine model.

The engine configuration in Figure 5.3 is set up assuming that the four cylinders exhibit identical behaviour. In the model, two system boundaries – SB1 and SB2 are used to model the ambient conditions for intake and exhaust respectively. SB1 is connected to a plenum (PL1) which models the intake manifold of the engine. The connection of SB1 to PL1 is through the intermediary of an air cleaner. Each connection of one element to another is made through pipes. In the model, each of the black lines with arrows is used to represent pipes. The numbers by each pipe denote the pipe number and are used for purposes of pipe identification.

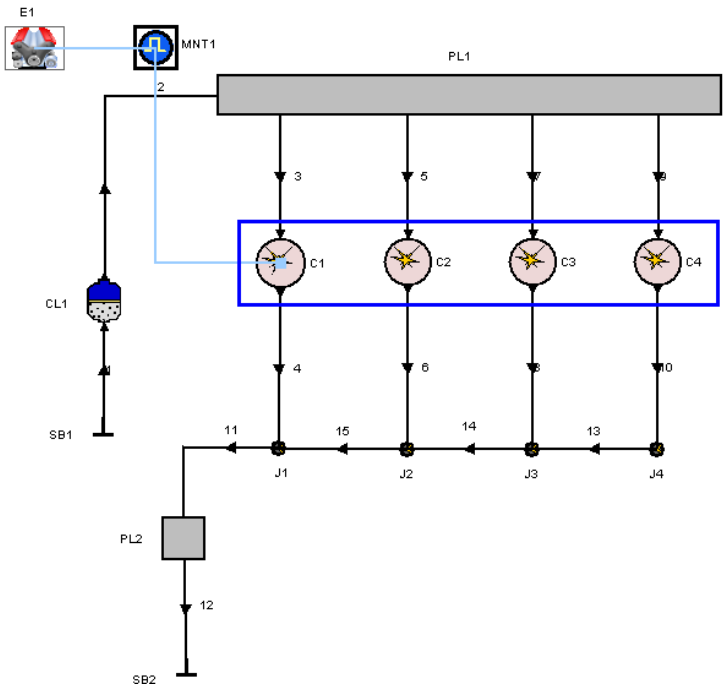

Figure 5.3 Engine setup to simulate diesel and diesel-LPG operational modes using AVL BOOST

Air is drawn through an air-cleaner into the engine manifold (PL1) and eventually distributed to each of the cylinders (C1 –C4). AVL BOOST is configured in such a way that intake and exhaust valves are modelled as part of the cylinder arrangement. Consequently, while providing input data for each cylinder, information about each of the valves – valve lift and valve timing as well as flow coefficients – is also provided. Also, the heat transfer sub-model is specified when setting up the cylinder configuration. The sub model used in this simulation is that of Woschni (1978).

With air in the cylinder, diesel fuel is then injected into the cylinder. Diesel injection is achieved by providing the fuel mass per cycle, which is admitted into each cylinder. Combustion then takes place and the heat released is modelled using a double-Vibe function. After combustion, exhaust gases are expelled through the exhaust manifold. In the model, the exhaust manifold is represented by a second plenum (PL2). The exhaust manifold collects exhaust gases from each cylinder via each of the junctions (J1 – J4) and then channels them to the atmosphere (SB2).

In AVL BOOST, to simulate an engine cycle, an engine element (E1) must be placed in the working area where the model is being built. This engine element provides the opportunity to specify the type of cycle being simulated – in this case, a 4-stroke cycle as depicted in Figure 5.4. It also allows for the specification of the engine's firing order as well as the sub-model used to simulate engine fraction. A monitor (MNT1) is placed to observe and provide results from the actuator and sensor channels specified when building the model. In the case of this simulation, the sensor channel specified is the indicated mean effective pressure (IMEP). A summary of the relevant simulation input data is shown in Appendix 4, Table A.3.

The second part of the simulation procedure focused on the diesel-LPG engine operation. As illustrated in Figure 5.3, the AVL BOOST commercially available software package was used to simulate the LPG-diesel engine operation. The same configuration was used to simulate the pure diesel and LPG-diesel engine operations respectively. The fundamental difference (not visible by merely looking at the engine elements and pipes illustrated above) in the configuration of the engine for both scenarios simulated involved the manner in which the composition of the respective fuels was configured and described. This difference is highlighted in section 5.4.1.

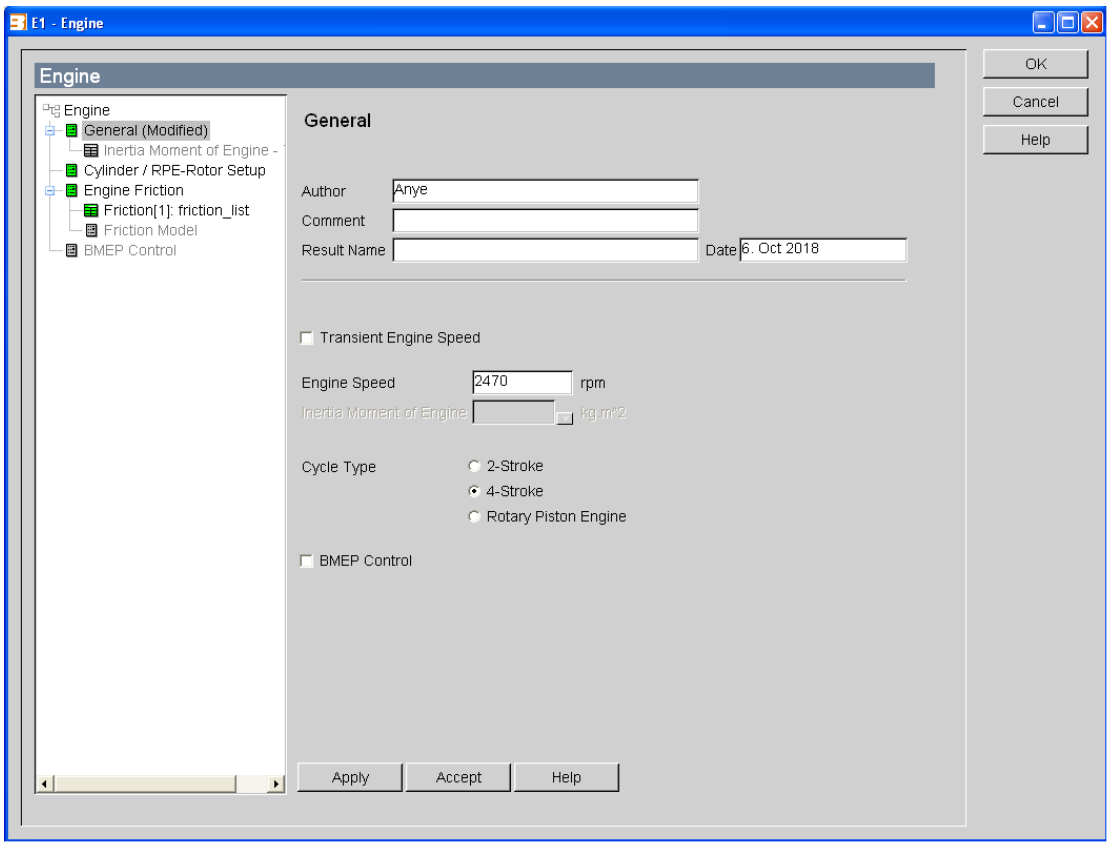

Figure 5.4 Specifications of the cycle type and engine speed defined for the engine element

5.3.3 Fuel (species) setup

The purpose of this sub-section is to inform the reader of the way that the fuel is set up during the various engine simulations in AVL BOOST. To enable users to define and structure the fuel (alternatively referred to as species transport according to the software terminology) or describe its composition, two different approaches exists as shown in Figure 5.5 and Figure 5.7. Upon choosing either of the approaches provided, the software calculates the fuel properties, for example, the heat capacity in each cell at each time step bearing in mind that several fuel properties depend on their composition.

5.3.3.1 Classic species transport

To set up and investigate the diesel engine operation, it was decided that the best method for the simulation and investigation of the diesel engine operational mode in this study was the classic species approach. I opted for this approach (as shown in Figure 5.5) on the basis of the fact that it allows for calculations involving only a single fuel. For the case of diesel engine operation, to enable me to compute the conservation equations for the combustion products and the fuel vapour, the classic species transport approach was used. Accordingly, the mass fraction of air is calculated from

$$W_{air} = 1 - W_{FV} - W_{CP} \qquad \textit{Eqn. 5.1}$$

Where:

W_{air} is the mass fraction of air

W_{FV} is the mass fraction of fuel vapour

W_{CP} is the mass fraction of the combustion products

To determine the air-fuel ratio characteristic for the combustion products, the following equation is applied

$$AF_{CP} = \frac{W_{CP} - W_{FB}}{W_{FB}} \qquad \textit{Eqn. 5.2}$$

Where:

AF_{CP} is the air-fuel ratio of the combustion products

W_{FB} is the mass fraction of burned fuel

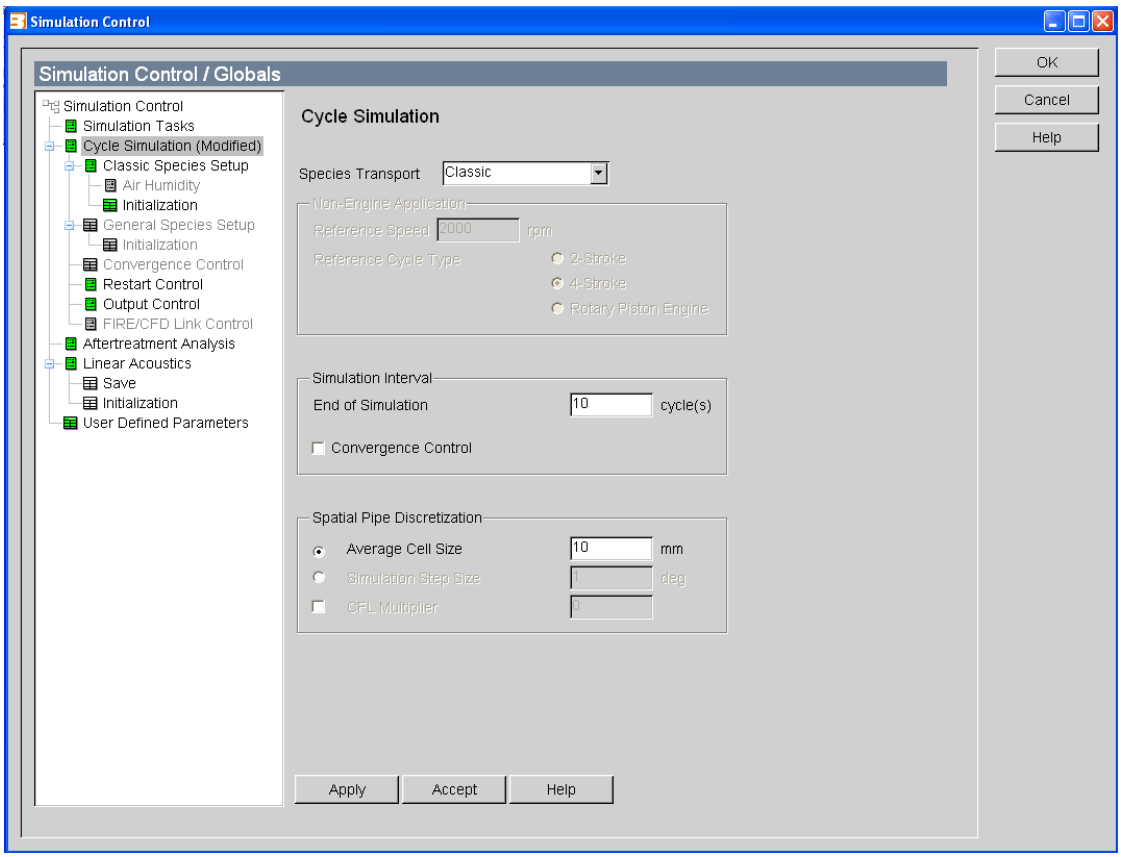

Figure 5.5 Specification of classic species transport used to simulate pure diesel operation

For the diesel engine operation and according to the diesel fuel option stipulated by the classic species transport, the air-fuel ratio is used as a measure of the gas composition to calculate the gas properties of the exhaust gases. In this context, the air-fuel ratio refers to that at which the combustion took place from whence the exhaust gases under consideration in this study are perceived to emanate. According to AVL BOOST, the composition of the combustion gases is obtained from the chemical equilibrium considering dissociation at high temperatures in the cylinder.

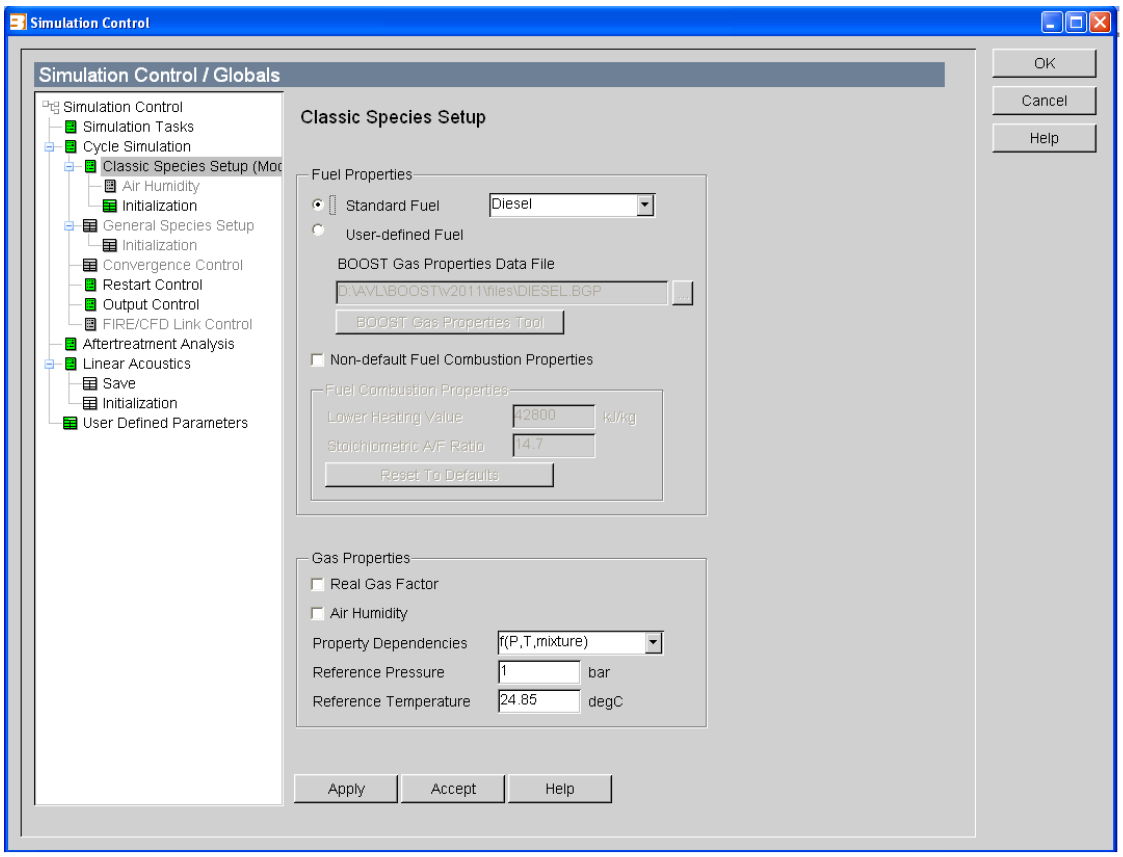

Figure 5.6 Setup of classic species used to define diesel fuel for simulation

Figure 5.6 illustrates that the classic species set up in which the fuel option defined is diesel along with its thermodynamic properties as provided by the software user guide.

5.3.3.2 General species transport

So that the dual fuelling option comprising the simultaneous use of diesel and LPG could be defined, the approach employed was the general species approach as shown in Figure 5.7. This approach consists describing the gas composition based on an arbitrary number of species that is defined by the user as shown in Figure 5.8. Given that LPG mainly consists of propane and butane in different ratios, I specified them as constituents of LPG. The ratio of propane to butane in LPG varies depending on seasons. For this study, 60% propane and 40% butane was used.

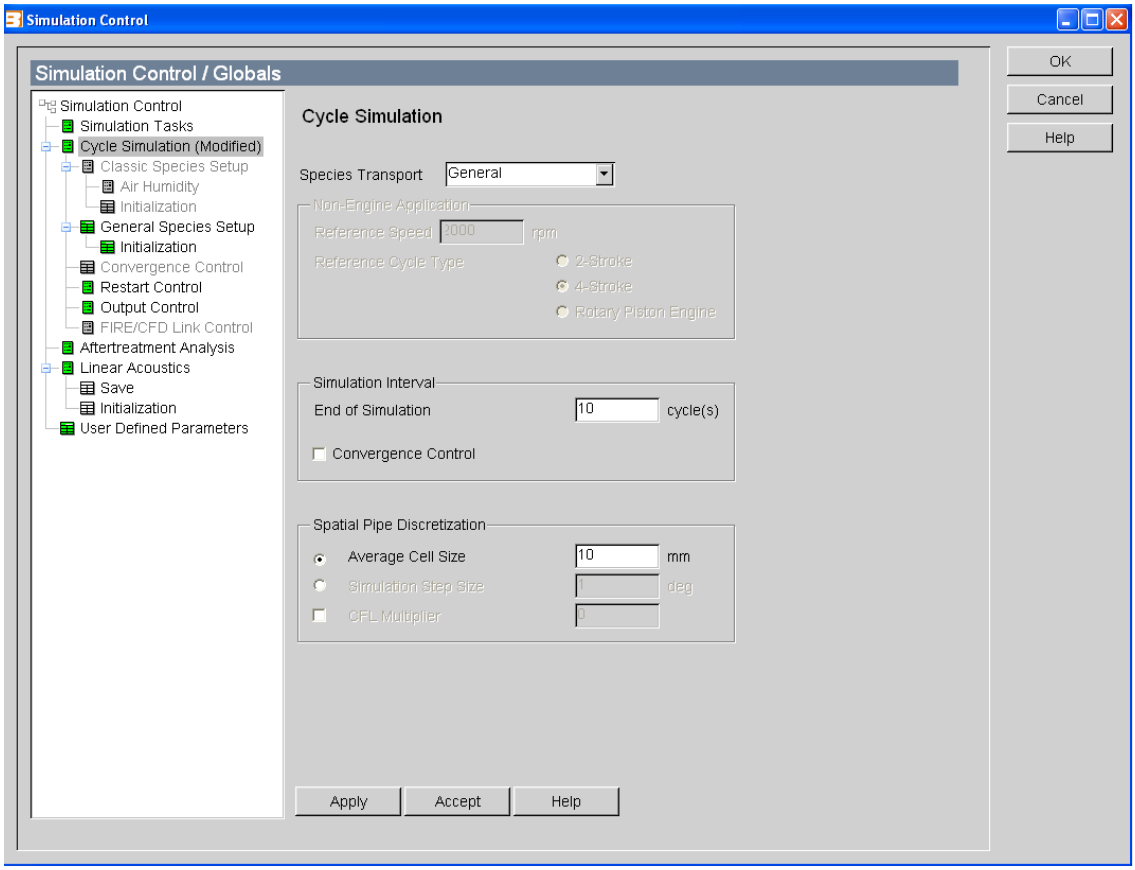

Figure 5.7 Specification of general transport species used to simulate LPG and diesel fuels

In the calculations for the general species approach adopted to simulate the dual fuelling option, the treatment of the fuel defined was generalised. This implies that that BOOST considered the fuel to comprise of a mixture of the various constituents specified by the user. For each of the fuel components, I specified the ratio that defined the mass of each component relative to the total fuel mass for the overall simulation. For this study, I created several simulations to reflect the scenarios to be investigated. Consequently, I had scenarios for fuel mass ratios as follows; 95% diesel and 5% LPG, 90% diesel and 10% LPG, 80 diesel and 20% LPG, 70% diesel and 30% LPG. For each of this scenarios, to represent the LPG, I maintained the ratio of propane to butane as 60% to 40% respectively.

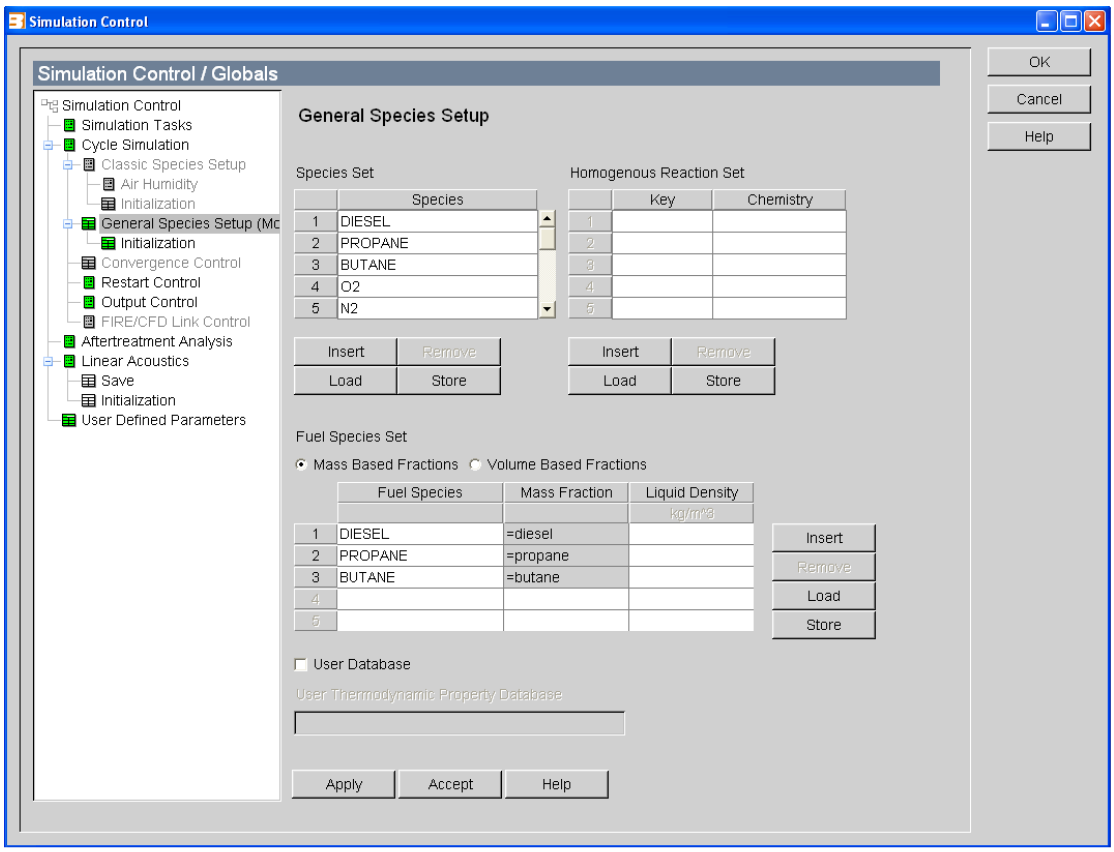

Figure 5.8 Setup of general species used to define the various fuel mass ratios

For the cylinder element as shown in Figure 5.3, the definition of fuel composition as shown in Figure 5.8 affects the Cylinder (injection and evaporation). This implies that the injected/evaporated mass is distributed to all species defined as the fuel components using the specified ratio in each scenario simulated.

5.3.4 Combustion model

In this study, the AVL Mixing Controlled Combustion (MCC) model (Chmela et al., 1998, Chmela and Orthaber, 1999) was utilised to model the combustion in this study as shown in Figure 5.9. The purpose of the AVL MCC model is to predict combustion characteristics in direct injection compression ignition engines. After reviewing the options at my disposal, it was decided that the best possible way offered by AVL BOOST to simulate dual fuel combustion in a direct injection engine

was the AVL MCC model. As a result, it was chosen because it is one of the most practical and feasible ways within the remits of the AVL BOOST software to capture the combustion characteristics with the ability to predict, unlike the Vibe models that predominantly predefine the combustion characteristics.

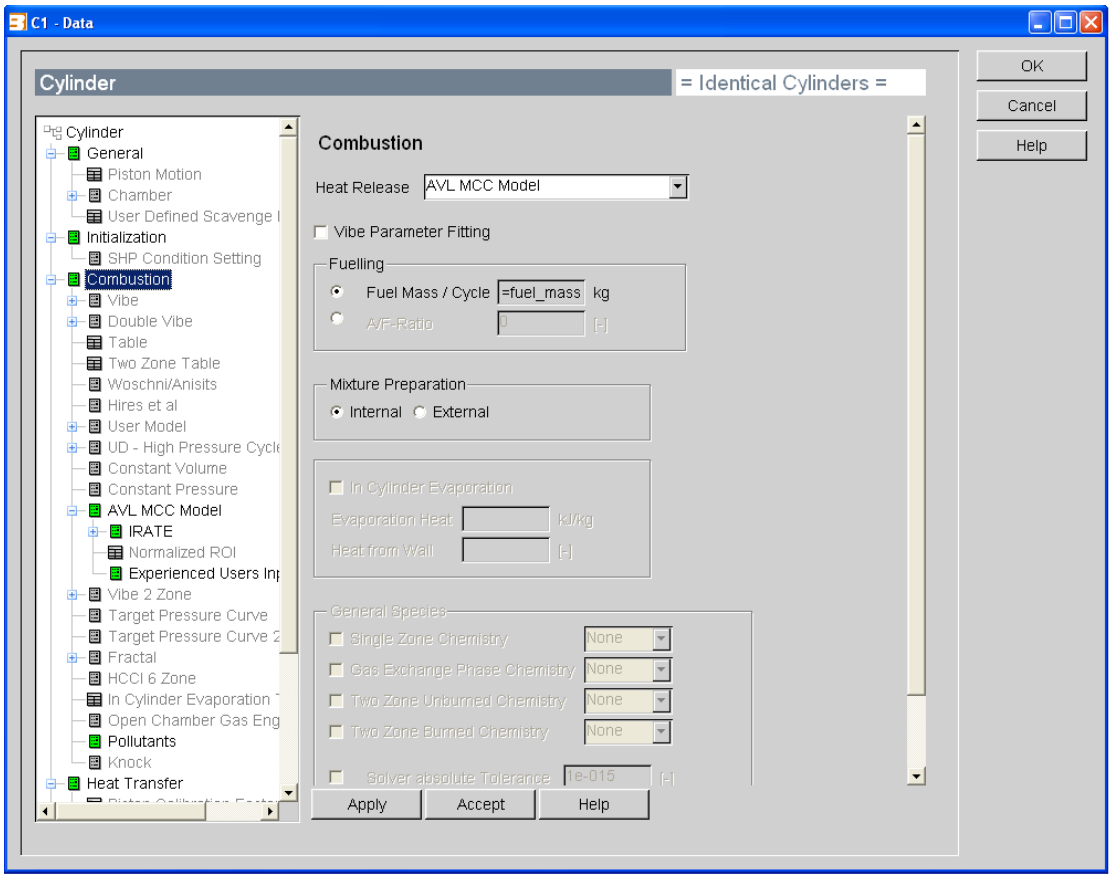

Figure 5.9 Specifying AVL MCC as the combustion submodel

The AVL MCC model predicts the rate of heat release and NO_x production in direct injection engines by the amount of fuel in the cylinder and on the turbulent kinetic energy introduced by the fuel injection. With regards to this sub-model, the computation considers the effects of the premixed (PMC), and diffusion (MCC) controlled combustion processes according to:

$$\frac{dQ_{MCC}}{d\alpha} = \frac{dQ_{MCC}}{d\alpha} + \frac{dQ_{PMC}}{d\alpha} \qquad \textit{Eqn. 5.3}$$

In the mixing controlled combustion regime, the heat release is a function of the fuel quantity available (f_1) and the turbulent kinetic energy density (f_2)

$$\frac{dQ_{MCC}}{d\alpha} = C_{comb} f_1(m_{F,} Q_{MCC}) f_2(k,V) \qquad \textit{Eqn. 5.4}$$

With

$$f_1(m_F, Q) = \left(m_F - \frac{Q_{MCC}}{LCV} \right) \left(W_{oxygen,available} \right)^{C_{EGR}} \qquad \textit{Eqn. 5.5}$$

$$f_2(k,V) = C_{Rate} \frac{\sqrt{k}}{\sqrt[3]{V}} \qquad \textit{Eqn. 5.6}$$

Where:

Q_{MCC} is the cumulative heat release for the mixture controlled combustion [kJ]

C_{comb} is the combustion constant [kJ/kg/deg CA]

C_{Rate} is the mixing rate constant [s]

k is the local density of turbulent kinetic energy [m^2/s^2]

m_F is the vaporised fuel mass [kg]

LCV is the lower heating value [kJ/kg]

V is the cylinder volume [m^3]

α is the crank angle [degCA]

$W_{oxygen,available}$ is the mass fraction of available Oxygen at the start of injection [-]

C_{EGR} is the EGR influence constant [-]

Since the AVL MCC method chosen represents a viable and innovative method used to determine the heat release, this approach incorporates the Andree and Pacherneeg model (Andree and Pachernegg, 1969) to calculate the ignition delay by solving the following differential equation 5.7. The ignition delay calibration factor and other

relevant parameters associated with the usage of the AVL MCC model in this simulation are shown in Figure 5.10.

$$\frac{dI_{id}}{d\alpha} = \frac{T_{UB} - T_{ref}}{Q_{ref}} \qquad \textit{Eqn. 5.7}$$

Once the ignition delay integral (I_{id}) reaches a value of 1 at a particular crank angle (α_{id}), the ignition delay is therefore calculated from

$$\tau_{id} = \alpha_{id} - \alpha_{SOI} \qquad \textit{Eqn. 5.8}$$

Where:

I_{id} is the ignition delay integral [-]

T_{ref} is the reference temperature [K]

T_{UB} is the unburned zone temperature [K]

Q_{ref} is the reference activation energy [K]

τ_{id} is the ignition delay [s]

α_{SOI} is the start of injection timing [degCA]

α_{id} is the ignition delay timing [degCA]

The AVL MCC methodology used here has many interesting and valuable applications given that for the premixed combustion regime, a Vibe function is used to describe the actual heat release owing to just the premixed combustion according to the following equation:

$$\frac{\left(\frac{dQ_{PMC}}{Q_{PMC}}\right)}{d\alpha} = \frac{a}{\Delta\alpha_c}(m+1)y^m e^{-ay(m+1)} \qquad \textit{Eqn. 5.9}$$

$$y = \frac{\alpha - \alpha_{id}}{\Delta\alpha_c} \qquad \textit{Eqn. 5.10}$$

Where:

Q_{PMC} is the total fuel heat input for the premixed combustion = $m_{fuel,id} C_{PMC}$

$m_{fuel,id}$ is the total amount of fuel injected during the ignition delay phase

C_{PMC} is the premixed combustion parameter [-]

$\Delta\alpha_c$ is the premixed combustion duration = $\tau_{id} C_{PMC-Dur}$

$C_{PMC-Dur}$ is the premixed combustion duration factor

m is the shape parameter, m =2

a is the Vibe parameter, a= 6.9

One benefit of the AVL MCC combustion model is that the model is fully integrated with a droplet heat-up and evaporation model. The equilibrium temperature for the droplet evaporation can be calculated iteratively (Sitkei, 1964) from:

$$\lambda_C (T_c - T_d) = \frac{30.93E4\left(\frac{T_d}{P_c}\right)}{e^{\left(\frac{4150}{T_d}\right)}}\left(20 + 0.26(T_d - 273.15) + 0.3(T_c - 273.15)\right) \qquad \textit{Eqn. 5.11}$$

Utilising the equilibrium temperature, the velocity of the evaporation results from computing the following equation:

$$v_e = 0.70353\left(\frac{T_d}{P_c e^{\left(\frac{4159}{T_d}\right)}}\right) \qquad \textit{Eqn. 5.12}$$

Furthermore, the change in droplet diameter along with the corresponding change in droplet mass over time can be deduced from:

$$d_d = \sqrt{d^2{}_{d,o} - v_e t} \qquad \textit{Eqn. 5.13}$$

Where:

λ_c is the thermal conductivity of the cylinder [W/ms]

T_c is the temperature in the cylinder

T_d is the equilibrium temperature of the isothermal droplet evaporation [K]

P_c is the pressure in the cylinder [Pa]

v_e is the evaporation velocity [m^2/s]

d_d is the actual droplet diameter [m]

$d_{d,o}$ is the initial droplet diameter [m]

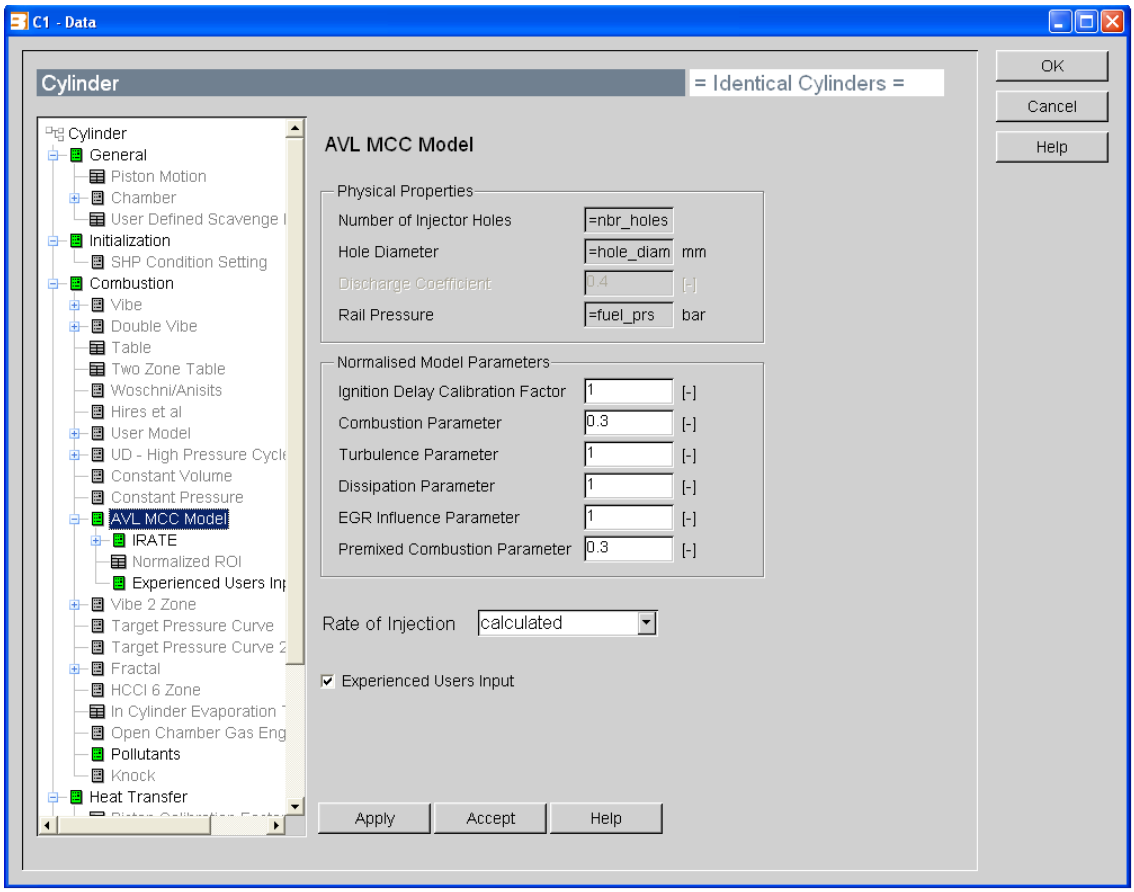

Figure 5.10 Illustration of AVL MCC model parameters

5.3.5 Heat transfer model

To take into account the effect of heat transfer in the simulation, the Woschni model was utilised as shown in Figure 5.11. The heat transfer to the walls of the combustion chamber, i.e. the cylinder head, the piston and the cylinder liner was calculated with the help of the following equation:

$$Q_W = A_i \alpha_w \left(T_c - T_{wi}\right) \qquad \textit{Eqn. 5.14}$$

Where:

Q_{wi} is the wall heat flow

A_i is the surface area

α_w is the heat transfer coefficient

T_c is the gas temperature in the cylinder

T_{wi} is the wall temperature

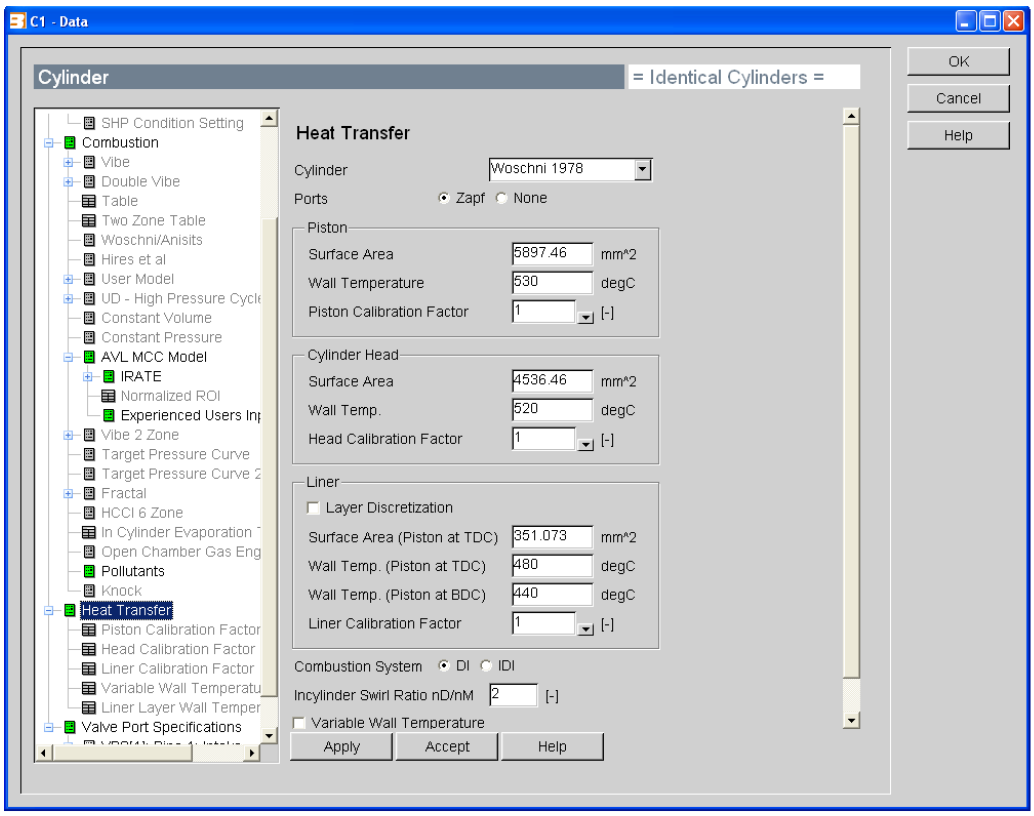

Figure 5.11 Specifying Woschni 1978 as heat transfer submodel

As concerns the liner wall temperature, the axial temperature variation between the piston at TDC and BDC positions is taken into consideration using the following equation:

$$T_L = T_{L,TDC}\left(\frac{1-e^{cx}}{xc}\right) \qquad \textit{Eqn. 5.15}$$

With

$$c = \ln\left(\frac{T_{L,TDC}}{T_{L,BDC}}\right) \qquad \textit{Eqn. 5.16}$$

Where:

T_L is the liner temperature

$T_{L,TDC}$ is the liner temperature at TDC position

$T_{L,BDC}$ is the liner temperature at BDC position

x is the relative stroke

To enable the determination of the heat transfer coefficient mentioned in Equation 5.14, this study makes use of the Woschni model (Woschni, 1967) which is summarised as follows for the high-pressure cycle:

$$\alpha_w = 130 D^{-0.2} P_c^{\,0.8} T_c^{\,-0.53} \left[C_1 c_m + C_2 \left(\frac{V_D T_{c,1}}{P_{c,1} V_{c,1}} \right) \left(P_c - P_{c,0} \right) \right]^{0.8} \qquad \textit{Eqn. 5.17}$$

Where:

$C_1 = 2.28 + 0.308 \frac{c_u}{c_m}$

$C_2 = 0.00324$ for DI engines

D is the cylinder bore

c_m is the mean piston speed

c_u is the circumferential velocity

V_D is the displacement per cylinder

$P_{c,0}$ is the cylinder pressure of the motored engine

$T_{c,1}$ is the temperature in the cylinder at the intake valve closing

$P_{c,1}$ is the pressure in the cylinder at the inlet valve closing

5.3.6 Emission models

To investigate the emission characteristics in this study, oxides of nitrogen (NO_x), carbon monoxide (CO) and soot were considered as illustrated in Figure 5.12. Given that the experimental facility at the disposal of this author could not measure emissions, the various emission models in this study could not be calibrated nor validated. Hence, the findings from this study are based strictly on computational simulation and the ability of the chosen AVL MCC combustion model to predict these emissions. That said, the various constants and multipliers for the emission models shown in Figure 5.12 were used based on the AVL Software user guidelines for naturally aspirated direct injection engines.

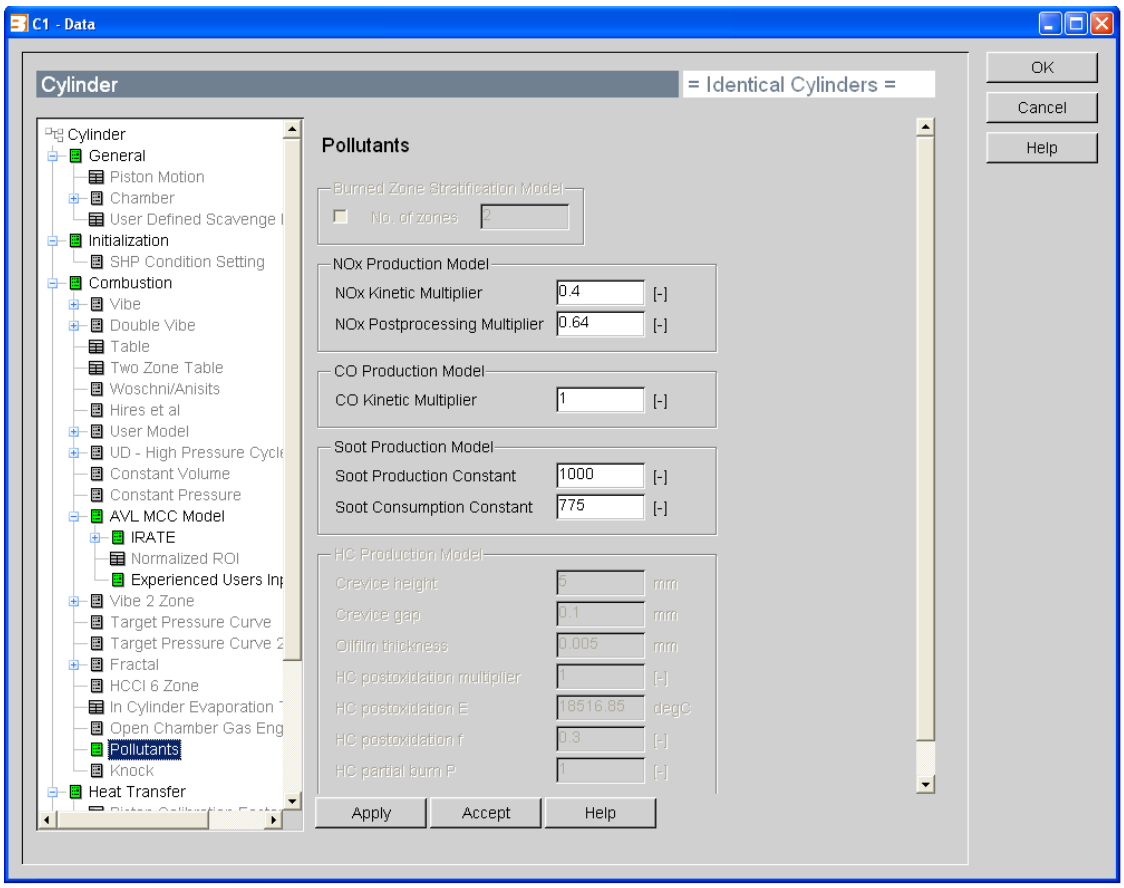

Figure 5.12 Illustration of emission models simulated

5.3.6.1 Nitrogen oxides (NOx)

Exhaust gases of an engine can contain oxides of nitrogen. A majority of this will be nitrogen oxide (NO), with a little amount of nitrogen dioxide (NO_2) and traces of various nitrogen-oxygen combinations. Collectively, these are all grouped as NO_x with x representing some suitable number. When NO_x is emitted from engines into the atmosphere, it reacts to form ozone, and this is one of the major causes of photochemical smog. Consequently, NO_x emissions are very undesirable hence, legislation and regulations that restrict the permitted amount of NO_x emissions continue to become more and more stringent. In view of this, this study has been designed to investigate NOx emissions. In AVL BOOST, the NO_x formation model

implemented is based on that of (Pattas and Häfner, 1973). In addition, the following six reactions based on the well-known Zeldovich mechanism are taken into account and incorporated. The reactions and their respective constants used are provided in Table 5.1.

Table 5.1 NO_x reaction rates and their various constants (AVL BOOST, 2014)

	Stoichiometry	Rate [mole/cm^{3}s] $k_1 = k_{0,i} T^a e^{\left(\frac{-TA}{T}\right)}$	k_0 [cm^3,mol,s]	a [-]	T_A [K]
R1	$N_2 + O = NO + N$	$r_1 = k_1 c_{N_2} c_O$	4.93*E*13	0.0472	38048.01
R2	$O_2 + N = NO + 0$	$r_2 = k_2 c_{O_2} c_N$	1.48*E*08	1.5	2859.01
R3	$N + OH = NO + H$	$r_3 = k_3 c_{OH} c_N$	4.22*E*13	0.0	0.0
R4	$N_2 + O = NO + NO$	$r_4 = k_4 c_{N_2O} c_O$	4.58*E*13	0.0	121306
R5	$O_2 + N_2 = N_2O + O$	$r_5 = k_5 c_{O_2} c_{N_2}$	2.25*E*10	0.825	50569.7
R6	$OH + N_2 = N_2O + H$	$r_6 = k_6 c_{OH} c_{N_2}$	9.14*E*07	1.148	36190.66

All the reaction rates (r_i) in Table 5.1 have units of mole/cm^{3}s while the concentrations (c_i) are molar concentrations under equilibrium conditions with units of mole/cm^3. The N_2O concentration is then calculated according to:

$$c_{N_2O} = 1.1802E-6\left(T^{0.6125}\right)e^{\left(\frac{9471.6}{T}\right)} c_{N_2}\sqrt{P_{O_2}} \qquad \textit{Eqn. 5.18}$$

The final rate of NO production/destruction in mole/cm^{3}s is calculated according to:

$$r_{NO} = 2C_{PostProcMult} C_{KineticMult}\left(1-\alpha^2\right)\left(\frac{r_1}{1+\alpha AK_2}\right)\left(\frac{r_4}{1+AK_4}\right) \qquad \textit{Eqn. 5.19}$$

Where:

$$\alpha = \left(\frac{c_{NO,act}}{c_{NO,equ}}\right)\left(\frac{1}{C_{PostProcMult}}\right) \qquad \textit{Eqn. 5.20}$$

$$AK = \frac{r_1}{r_2 + r_3} \qquad \textit{Eqn. 5.21}$$

$$AK = \frac{r_4}{r_5 + r_6} \qquad \textit{Eqn. 5.22}$$

5.3.6.2 Carbon monoxide (CO)

Carbon monoxide is a colourless, odourless, poisonous gas that can arise due to incomplete combustion. When there is not enough oxygen to convert all carbon to carbon dioxide, some fuel does not get burned, and some carbon would end up as CO. CO is thought to be an undesirable emission and also signifies lost chemical energy that was not fully used in the engine. To investigate the CO emissions, the CO formation model implemented in BOOST is based on (Onorati et al., 2001). The CO formation model is developed to take into account the following two reactions shown in Table 5.2.

Table 5.2 Stoichiometric reactions for CO formation (AVL BOST, 2014)

	Stoichiometry	Rate
R1	$CO + OH = CO_2 + H$	$r_1 = 6.76E10\left(e^{\left(\frac{T}{1102}\right)}\right)c_{CO}c_{OH}$
R2	$CO + O_2 = CO_2 + O$	$r_2 = 2.51E12\left(e^{\left(\frac{-24055}{T}\right)}\right)c_{CO}c_{O_2}$

According to the CO emission model, the final rate of CO production/destruction in mole/cm^{3}s is evaluated from the following equation:

$$r_{CO} = C_{Const}(r_1 + r_2)(1-\alpha) \qquad \textit{Eqn. 5.23}$$

Where:

$$\alpha = \frac{c_{CO,act}}{c_{CO,equ}} \qquad \textit{Eqn. 5.24}$$

5.3.6.3 Soot

The exhaust emanating from compression ignition engines contains solid carbon soot particles. Soot comprises mainly of carbon. However, other elements like oxygen and hydrogen are commonly present in minute amounts. Soot is produced during the high-temperature combustion of the fuel. The AVL BOST software used incorporates models for soot formation. To investigate soot, the soot formation model is based on (Schubiger et al., 2002).

5.4 Synopsis of chapter five

In summary, this chapter has presented the methodological approach adopted in the computational simulation of the diesel and diesel-LPG engine operational modes. While justifying the choice of the simulation tool, this chapter has also outlined the various sub-models used in the simulation. This simulation of both the diesel and diesel-LPG operations was done using a commercially available software – AVL BOOST. The next chapter presents the calibration and validation of the computational models.

6 Calibration and Validation of Computed Models

6.1 Introduction to Chapter Six

Following the computational simulation methodology presented in the previous chapter, turning now to the developed models, this chapter describes the calibration and validation of the AVL BOOST models. The chapter opens with a brief introduction and illustration of the overall calibration and validation process as illustrated in Figure 6.1. It then proceeds to describe the calibration procedure and show the various calibration constants and parameters. Subsequently, this chapter discusses the percentage error analysis that was performed on the peak cylinder pressure, the timing of the peak cylinder pressure, the power and the torque.

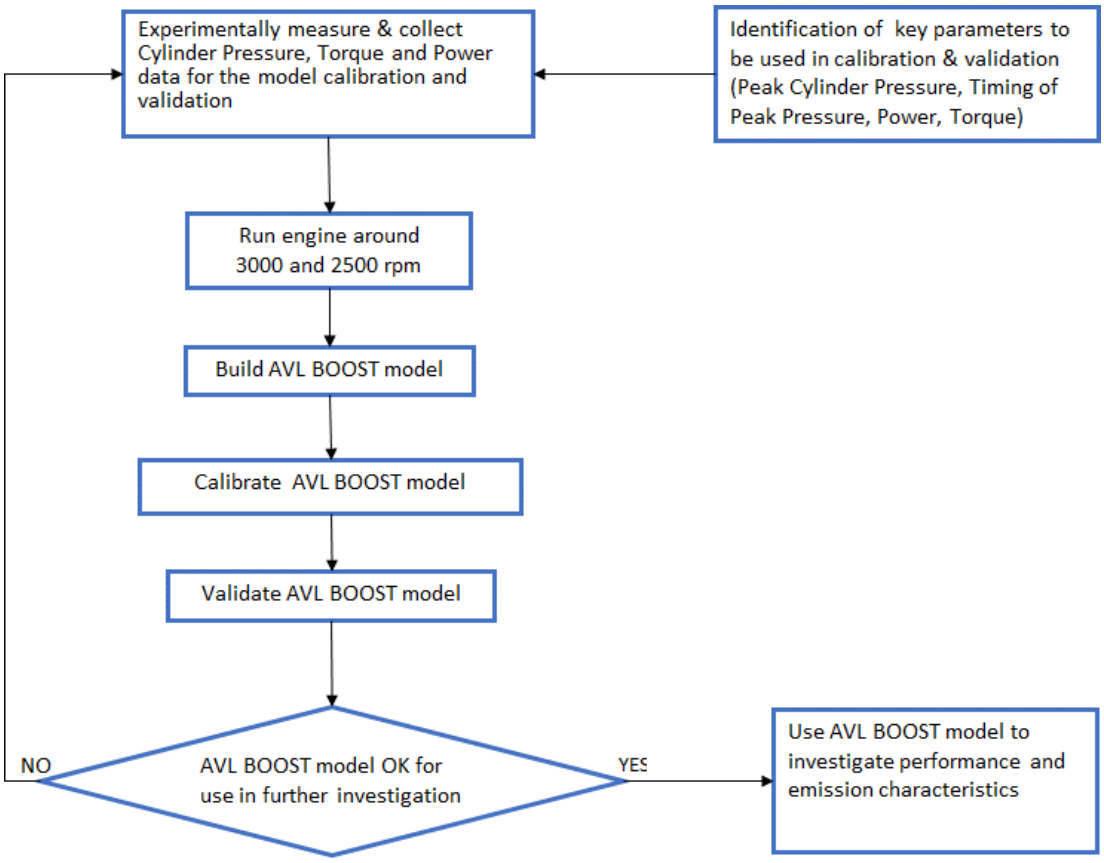

Figure 6.1 Overall modelling, calibration and validation process flow

6.2 Description of Calibration Procedure

To calibrate the models developed, firstly, as illustrated in Figure 6.1, key parameters to be used for the calibration and validation were identified. They include; the peak cylinder pressure, the timing of the peak cylinder pressure, the power and the torque. Following on from this, experimental testing was executed targeting steady state engine operating regimes around 2500 and 300 rpm. Once these target speeds were identified, the set-point of the controller was adjusted to the desired operating speed in intervals and the engine speed allowed to stabilise at each interval before proceeding to the next. This was repeated until the engine stabilised around the target operating speeds. Eventually, the measurements that were obtained corresponded to the engine speeds and torque as reported in Figure 6.3, Figure 6.4 and Figure 6.5 also shown in Table 6.2.

At each of these speeds and loads, the cylinder pressure measurements were obtained. The software on the diesel engine test rig is designed to record the pressure in intervals of time. From the time, I calculated the crank angles using Equation 4.4 as earlier mentioned in Chapter Four. Following analysis of the measured cylinder pressures obtained, the peak cylinder pressures were identified in each case, and the corresponding timing (crank angle) at which these peak cylinder pressures occurred were observed and recorded.

Attention was then turned to building the model in AVL BOOST. As earlier mentioned in chapter five, firstly, a single-cylinder model was developed. This 1-cylinder model was then calibrated with the focus being on the combustion sub-model as illustrated in Figure 6.2. Following the choice of combustion model used, it is essential to calibrate the combustion parameters and constants at a specific operating regime before utilising them in engine simulation. The calibration was made for each of the models and after the constants were found, they retained their values for the various operating regimes examined in this study. As shown in Figure 6.2, while focusing on the combustion model, the goal was to match computed with the experimental cylinder pressure diagram ensuring that the corresponding values of peak pressure and the timing at which it occurs match as well as the performance parameters of torque and power.

Table 6.1 Combustion model calibration parameters

Parameter	Diesel	Diesel-LPG
Ignition Delay Calibration Factor [-]	1	1
Combustion Parameter [-]	0.3	0.3
Turbulence Parameter [-]	1	1
Dissipation Parameter [-]	1	1
EGR Influence Parameter [-]	1	1
Premixed Combustion Parameter [-]	0.3	0.53

In an effort calibrate the combustion sub-model of the 1-cylinder diesel engine model, it was decided to modify the combustion parameters shown in Table 6.1. Using guidelines provided by BOOST for the combustion parameters of a naturally aspirated direct injection engine, the modification was done to enable the simulated pressure trace match as close as practically possible that obtained from measured data.

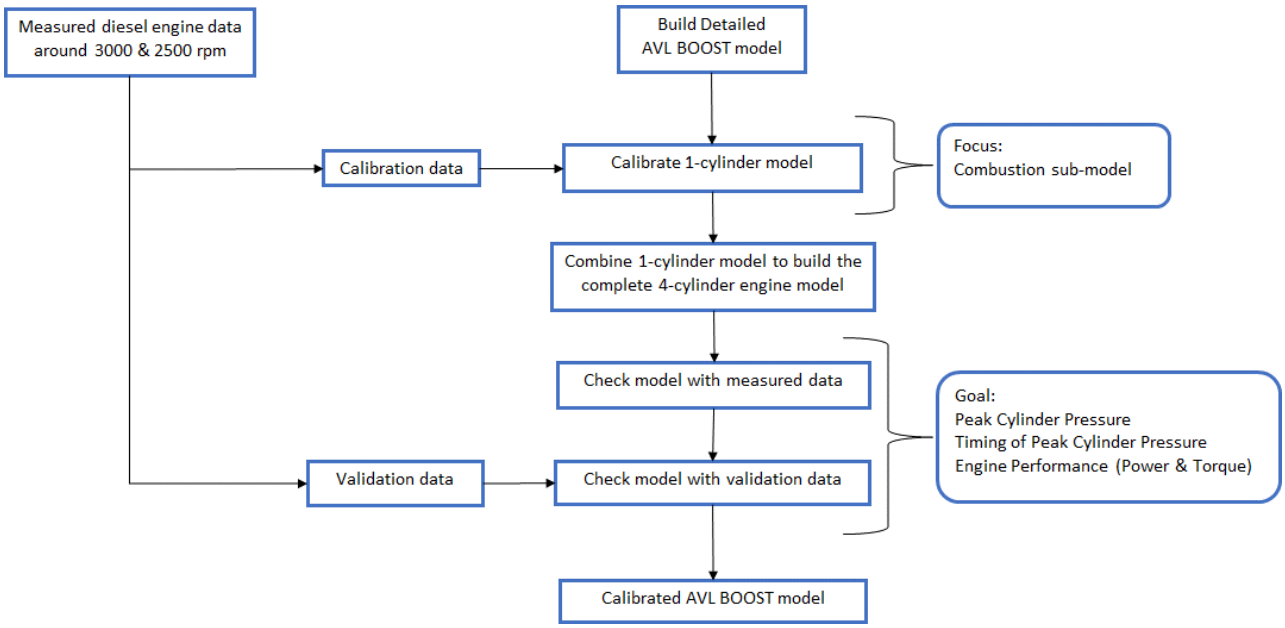

Figure 6.2 Calibration procedure

To validate the model, the predicted cylinder traces from the computational simulation are compared with the experimental ones at 3050 rpm engine speed with 38 Nm, 2470 rpm engine speed with 100 Nm and 2435 rpm engine speed with 133 Nm. The effectiveness of the calibration procedure is illustrated by the various cylinder pressure diagrams for each scenario examined as shown in Figure 6.3, Figure 6.4 and Figure 6.5. As shown in these Figures, at all the operating regimes investigated, the pressure diagrams involving the variation of the cylinder pressure with respect to crank angle, depict acceptable agreement following on from the calibration procedure enumerated above. The curve in blue line signifies the measured pressure while that in red line signifies the computed pressure simulated with the help of AVL BOOST using the AVL MCC combustion model described in chapter five.

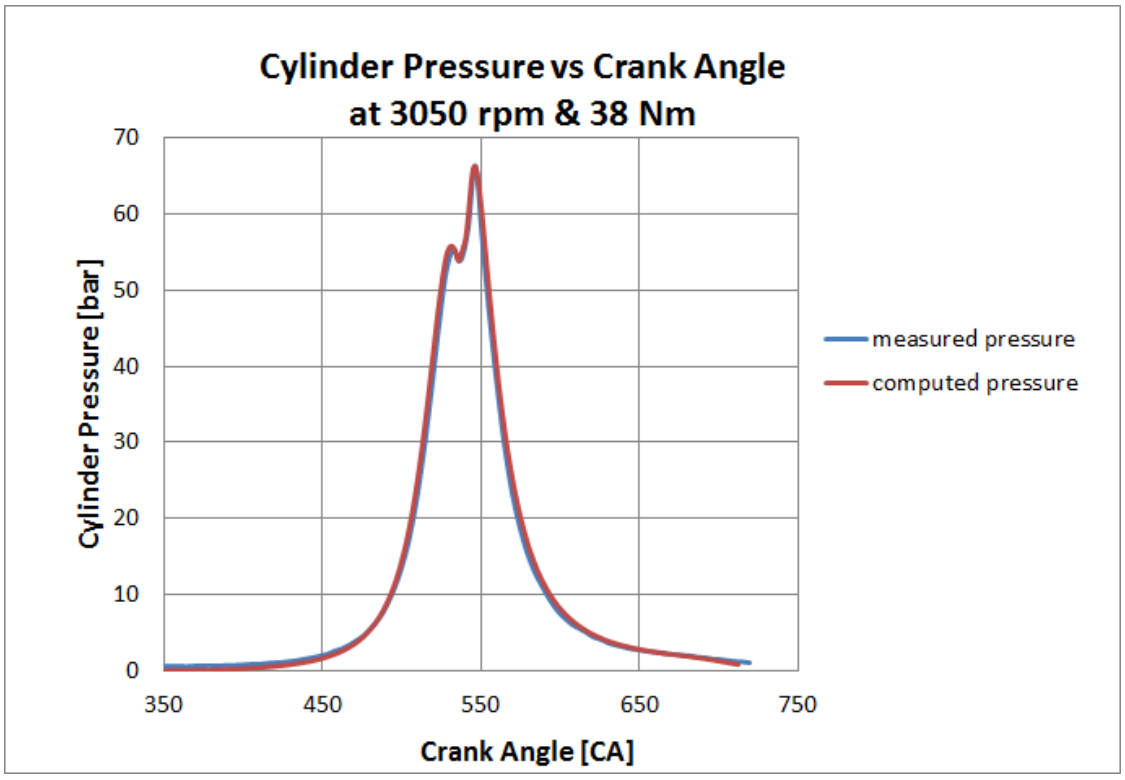

Figure 6.3 Model validation based on cylinder pressure at 3050 rpm & 38 Nm

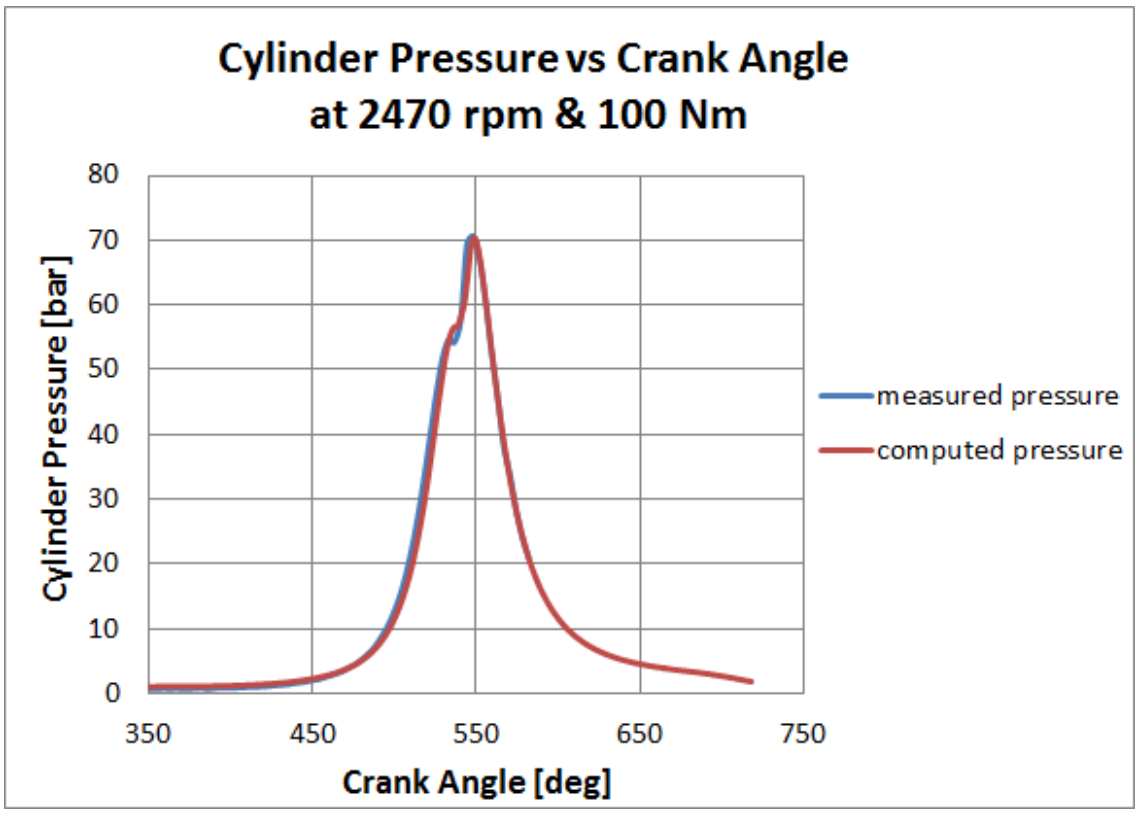

Figure 6.4 Model validation based on cylinder pressure at 2470 rpm & 100 Nm

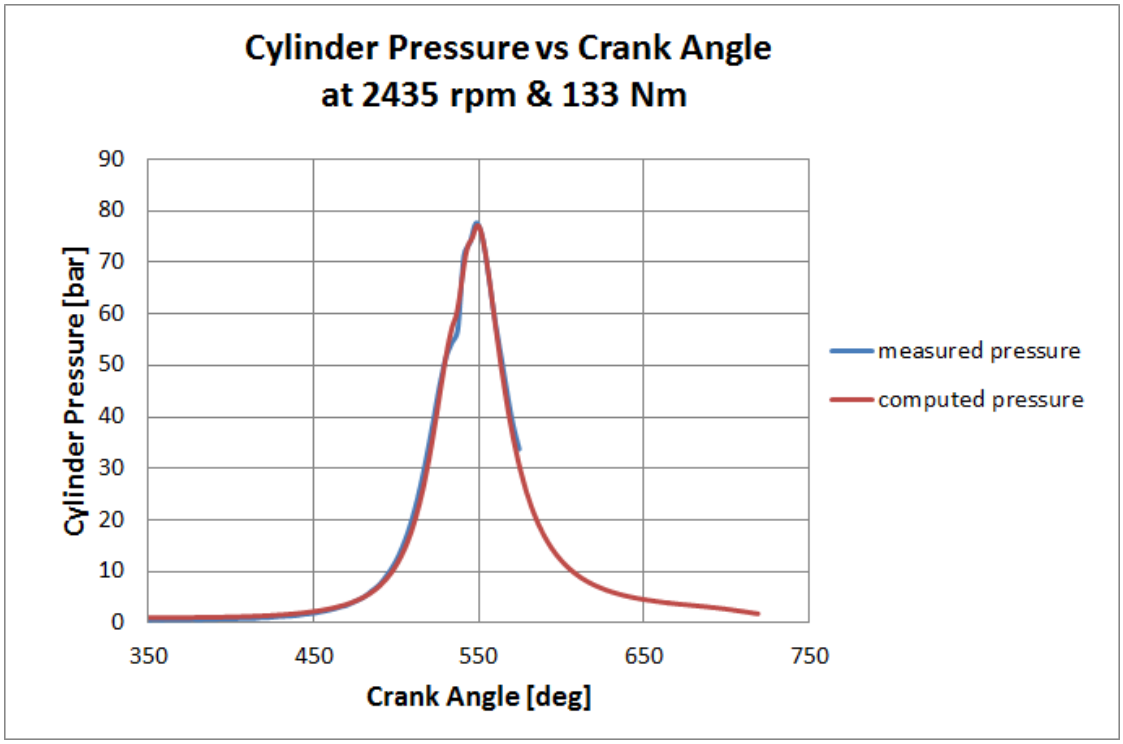

Figure 6.5 Model validation based on cylinder pressure at 2435 rpm & 133 Nm

Given that the cylinder pressure measurements obtained as shown in Figure 6.3, Figure 6.4 and Figure 6.5 were for the diesel engine operating scenarios, it is essential for the sake of clarity to emphasise that calibration and validation in this study were therefore based on the diesel cylinder pressure measurements. In this regard, to validate the models, the percentage error between the measured and calculated peak cylinder pressure, power and torque were evaluated at three different operating regimes as shown in Table 6.2. The difference between the measured and computed peak pressure, power and torque for all the cases investigated range from -0.45% to 3.85%. However, a difference in timing at which the peak pressure occurs of just 1-degree After-Top-Dead-Centre corresponds to a percentage error of -12.5%.

Table 6.2 Validation of models based on the percentage error between the simulated and measured peak cylinder pressure

Speed [rpm]	Designation	Pmax [bar]	Timing of Pmax [degCA ATDC]	Torque [Nm]	Power [kW]
3050	Simulated	66.32	6	36.70	11.72
	Measured	66.37	6	38.17	12.19
	% Error	0.08	0	3.85	3.85
2470	Simulated	70.68	9	100.00	25.50
	Measured	70.36	8	100.30	25.58
	% Error	-0.45	-12.5	0.30	0.30
2435	Simulated	77.16	9	132.50	33.79
	Measured	77.70	8	133.00	33.91
	% Error	0.70	-12.5	0.38	0.38

The calibration procedure described above, in my opinion, is evident for the diesel engine operation. As far as the calibration of the diesel-LPG operational model is concerned, this work has some limitations owing particular to an extended break down in the research facility that hindered the author from obtaining cylinder pressure measurements when running the engine on diesel and LPG. Nevertheless, despite this limitation and checking with some expert opinions, it is my view that the diesel-LPG model developed with AVL BOOST behaves as expected. To model the

diesel-LPG engine operation, I modified the fuel (species) as described in chapter five. As seen in Table 6.1, I also increased the premixed combustion parameter (based on recommendations provided by BOOST) to account for the presence of LPG in the combustion chamber.

Besides, although there are also limitations because, the experimental facility at the disposal of the author could not allow for measurements of emissions, the various emission models could not be calibrated. However, following the choice of the AVL MCC combustion model used and following on from its calibration with appreciable accuracy along with the ability of the model to predict emissions, it is my opinion that the emission models provide an adequate indication of the behaviour of the different emissions in the various modes of operation investigated. That said, Table 6.3 presents constants and multipliers of the different emission sub-models used to carry out this study. The constants were used based on guidelines for a naturally aspirated direct injection engine, provided to users of AVL BOOST.

Table 6.3 NOx, CO and Soot emission model constants

Parameter	**Diesel**	**Dual Fuel**
NOx Kinetic Multiplier [-]	0.4	0.4
NOx Post processing Multiplier [-]	0.64	0.64
CO Kinetic Multiplier [-]	1	1
Soot Production Constant [-]	1000	1000
Soot Consumption Constant [-]	775	775

These pollutant emission constants were assumed constant for all the cases examined to investigate the impact of various LPG fuel mass ratios.

6.3 Synopsis of Chapter Six

In summary, chapter six has described the calibration procedure based on the cylinder pressure measurements obtained for the engine operating regimes presented when the fuel used was diesel fuel. The chapter also highlights the analysis of the percentage error used in validating the models based on the peak cylinder pressure, the timing of the peak cylinder pressure, the power and the torque. This study shows satisfactory performance of the adopted calibration procedure with the comprehensive error analysis demonstrating errors considered to be within acceptable limits.

7 Results and Discussions

7.1 Introduction to Chapter Seven

Several factors affect the operation, performance, and emissions of dual-fuel engine applications. In particular, the nature and extent of emissions emanating from the exhaust in dual-fuel engine applications are controlled by changes in a number of factors. Some of the main factors include:

- The composition and type of gaseous fuel utilised
- The amount and properties of the diesel fuel
- The injection timing
- The engine speed and its range
- The engine size and type, cylinder geometry, compression ratio etc.

Since the main of this study was, as mentioned in Chapter two, to numerically investigate the performance and emission characteristics associated with dual fuel engine operation wherein LPG and diesel fuels are simultaneously used, this Chapter presents the results obtained and proceeds to discuss them. In view of all the factors enumerated above, before presenting and discussing the results, the reader's attention is drawn to the operational factors that the study proposed to consider in this study as mentioned in section 2.1 In this regard, this study examined the performance and emission characteristics of the diesel-LPG operation for 3 case studies as illustrated in Table 7.1. The fuel composition for each scenario including their various energy contents are shown in Appendix 4, Table A.3**.**

Table 7.1 Diesel-LPG engine operating regimes simulated

	Case 1	**Case 2**	**Case 3**
Speed [rpm]	3050	2470	2435
Fuel Mass Ratio [%]	95%Diesel 5%LPG 90%Diesel 10%LPG 80%Diesel 20%LPG 70%Diesel 30%LPG	95%Diesel 5%LPG 90%Diesel 10%LPG 80%Diesel 20%LPG 70%Diesel 30%LPG	95%Diesel 5%LPG 90%Diesel 10%LPG 80%Diesel 20%LPG 70%Diesel 30%LPG

Consequently, the results presented in the subsequent sections of this Chapter follow on from these examined case studies and are in keeping with the stipulated aim of research.

7.2 Diesel-LPG Combustion Parameters

In this section of the study, to evaluate the combustion characteristics of the diesel-LPG engine operation in relation to the diesel engine operation, the cylinder pressure, the maximum cylinder pressure, the maximum rate of pressure rise and the rate of heat release are investigated with the findings presented

7.2.1 Pressure and Maximum Rate of Pressure Rise

To assess the effect of various fuel mass ratios, the first set of analysis focused on the cylinder pressure and the maximum rate of pressure rise. For the case studies enumerated in Table 7.1, this first set of analyses examined, highlighted the effect of various fuel mass ratios on the cylinder pressure. Generally speaking, compared to the pure diesel operation, it was observed that the cylinder pressure when LPG was introduced was relatively higher as shown in Figure 7.1, Figure 7.2 and Figure 7.3. However, by decreasing the mass ratio of diesel fuel while increasing that of LPG, this provides evidence that the cylinder pressure increases with an increase in the LPG fuel mass ratio. The addition of LPG to the combustion chamber causes the burning process to intensify and the burning rate of pre-formed mixtures increases. This explains why the cylinder pressure is shown to increase with every increase in the LPG fuel mass ratio introduced.

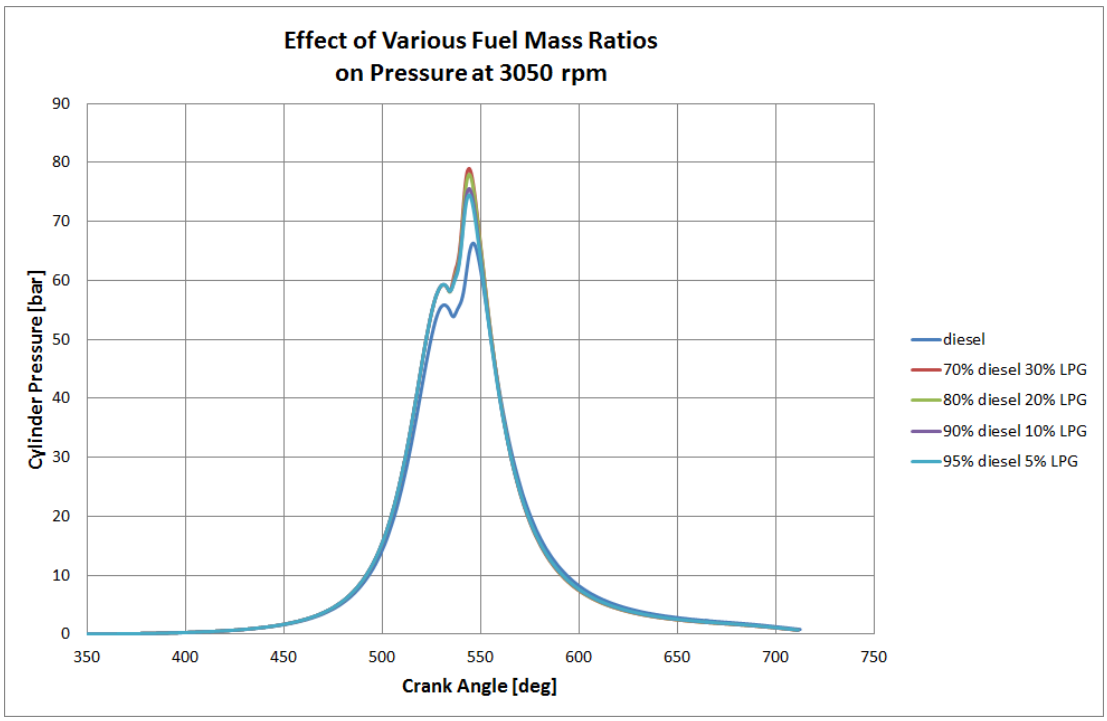

Figure 7.1 Effect of variation in fuel mass ratios on cylinder pressure at 3050 rpm

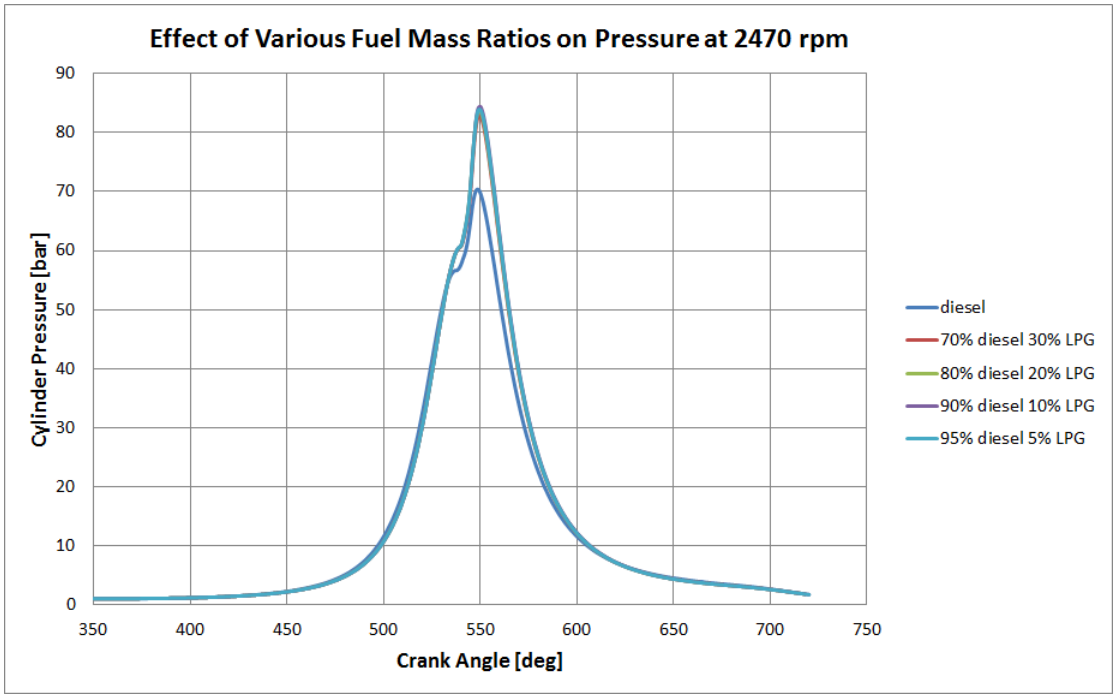

Figure 7.2 Effect of change in fuel mass ratios on cylinder pressure at 2470 rpm

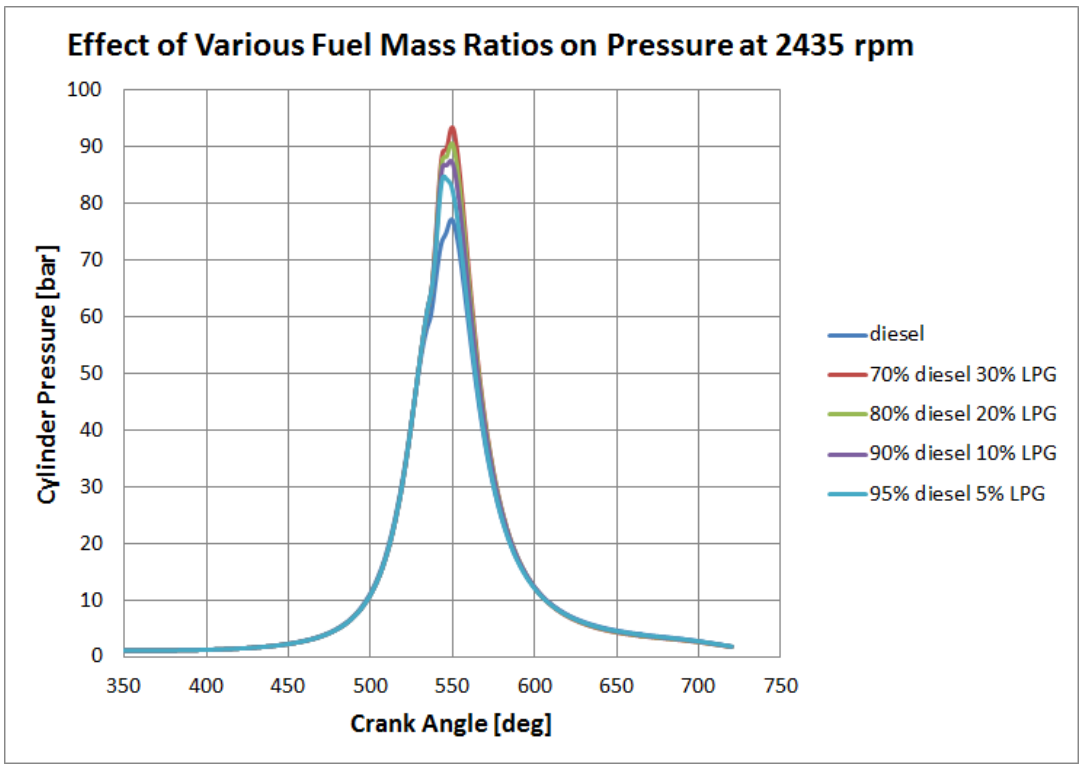

Figure 7.3 Effect of variation in fuel mass ratios on cylinder pressure at 2435 rpm

Broadly speaking, the study found out that for all the cases examined, the increase associated with the maximum in-cylinder pressure did not exceed 100 bars. Therefore, this suggests that, following modification of the diesel engine to operate using diesel and LPG simultaneously, for the various engine operating regimes investigated, the addition of the respective LPG fuel mass ratios looked into would not pose a problem to the engine combustion. For the various LPG fuel mass ratios examined, the values of the peak cylinder pressure were compared against those observed for the pure diesel operation. The comparative analyses revealed the following:

- For the case of 95% diesel and 5% LPG at 3050 rpm, compared to diesel engine operation, the maximum cylinder pressure was shown to increase from 66.32 bar to 74.50 bar representing an increase of 12.3% as illustrated in Figure 7.4.
- For the case of 90% diesel and 10% LPG at 3050 rpm, compared to pure diesel engine operation, the maximum cylinder pressure was shown to increase from 66.32 bar to 75.56 bar representing an increase of 13.9% as illustrated in Figure 7.4

- For the case of 80% diesel and 20% LPG at 3050 rpm, compared to diesel engine operation, the maximum cylinder pressure was shown to increase from 66.32 bar to 77.9 bar representing an increase of 17.6% as illustrated in Figure 7.4.
- For the case of 70% diesel and 30% LPG at 3050 rpm, compared to diesel engine operation, the maximum cylinder pressure was shown to increase from 66.32 bar to 78.9 bar representing an increase of 19% as illustrated in Figure 7.4.

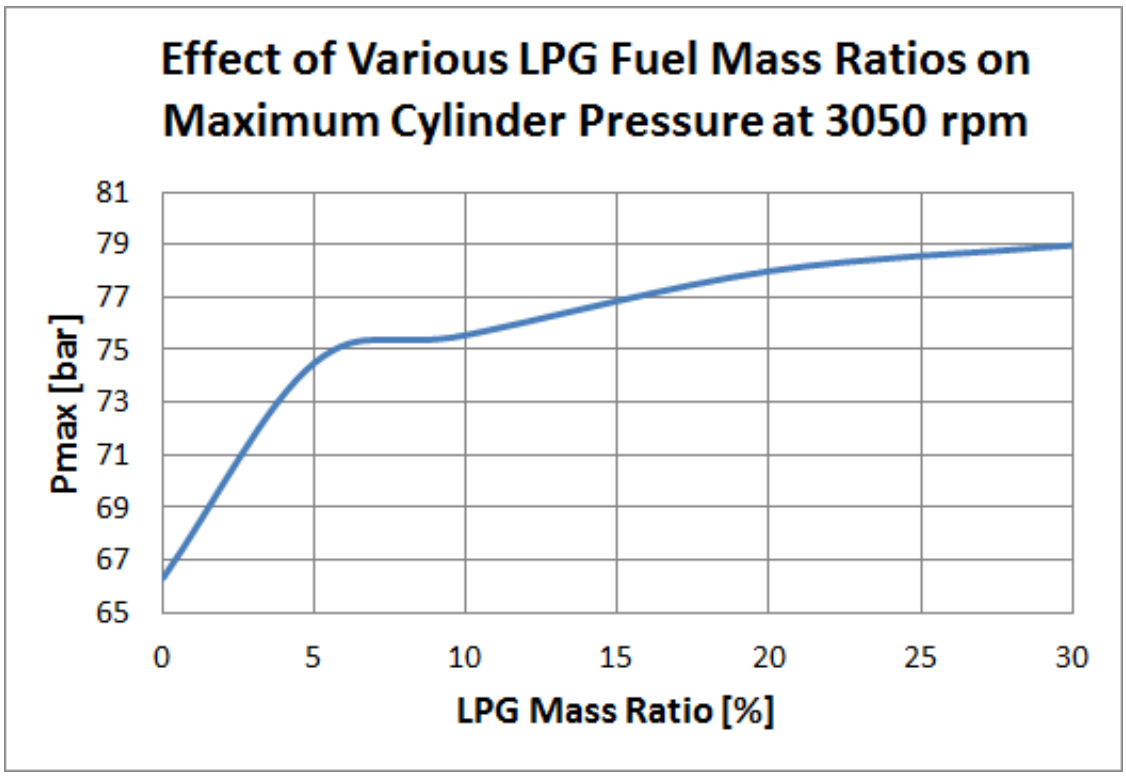

Figure 7.4 Variation of fuel mass ratios with peak cylinder pressure at 3050 rpm

Replication of the above comparative analyses at other engine operating regimes showed a similar pattern (in the sense that the maximum cylinder pressure values for dual fuel scenarios were higher compared to that of the diesel scenario) to that observed during the examination of the 3050 rpm scenario. Consequently, the following are correct according to Figure 7.5

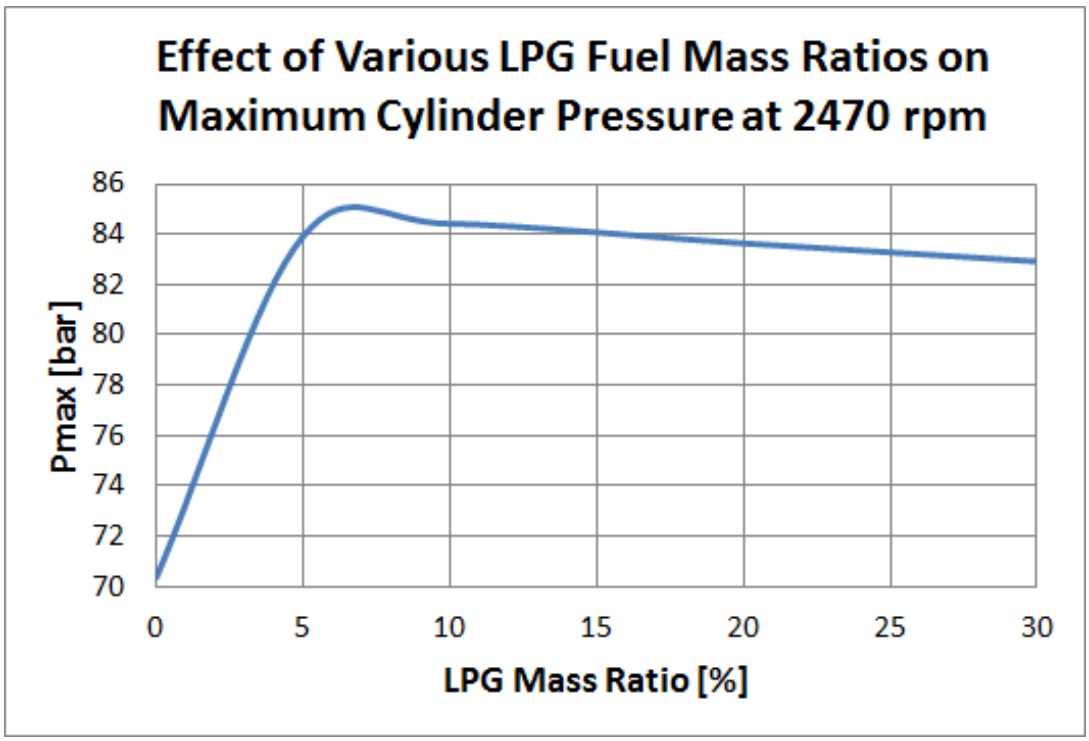

Figure 7.5 Variation of fuel mass ratios with peak cylinder pressure at 2470 rpm

- For the case of 95% diesel and 5% LPG at 2470 rpm, compared to diesel engine operation, the maximum cylinder pressure was shown to increase from 70.36 bar to 83.92 bar representing an increase of 19.27% as illustrated in Figure 7.5.
- For the case of 90% diesel and 10% LPG at 2470 rpm, compared to pure diesel engine operation, the maximum cylinder pressure was shown to increase from 70.36 bar to 84.42 bar representing an increase of 19.98% as illustrated in Figure 7.5
- For the case of 80% diesel and 20% LPG at 2470 rpm, compared to diesel engine operation, the maximum cylinder pressure was shown to increase from 70.36 bar to 83.64 bar representing an increase of 18.87% as illustrated in Figure 7.5.
- For the case of 70% diesel and 30% LPG at 2470 rpm, compared to pure diesel engine operation, the maximum cylinder pressure was shown to increase from 70.36 bar to 82.92 bar representing an increase of 17.85% as illustrated in Figure 7.5.

Turning our attention to the case of 2435 rpm and deploying the similar comparative analyses, Figure 7.6 provides evidence to the fact that the peak cylinder pressures for each respective LPG fuel mass scenario are higher than that of the diesel operation

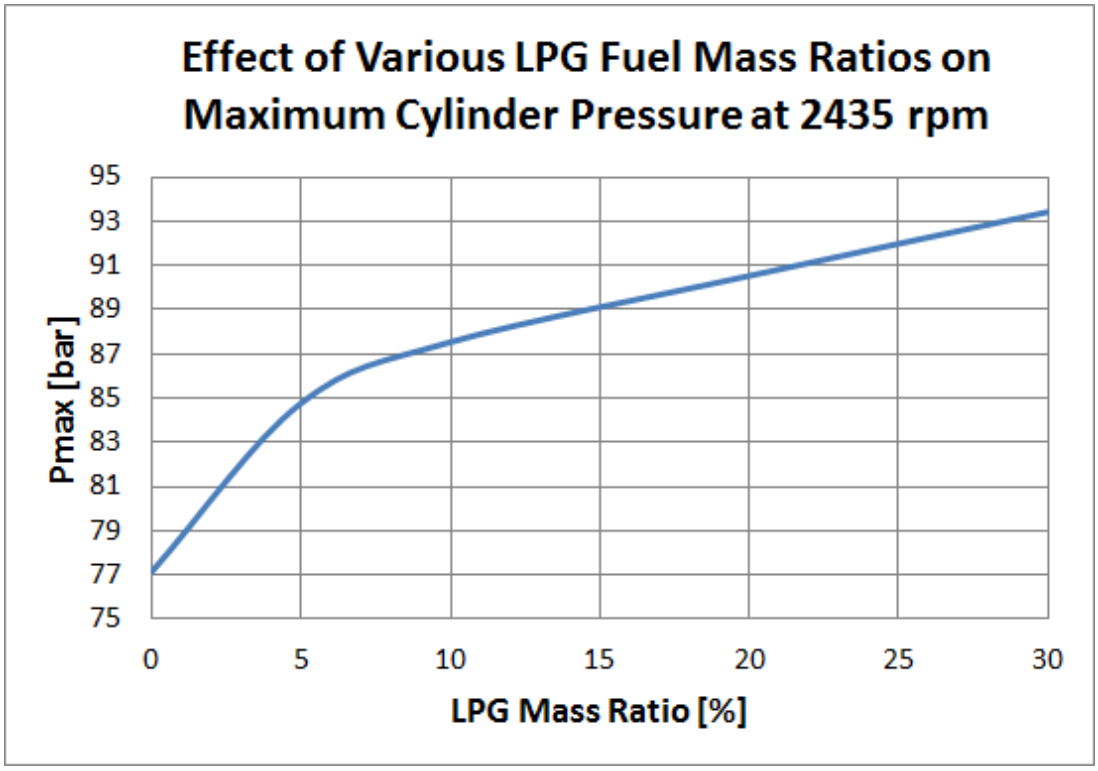

Figure 7.6 Variation of fuel mass ratios with peak cylinder pressure at 2435 rpm

- For the case of 95% diesel and 5% LPG at 2435 rpm, compared to diesel engine operation, the maximum cylinder pressure was shown to increase from 77.16 bar to 84.77 bar representing an increase of 9.87% as illustrated in Figure 7.6.
- For the case of 90% diesel and 10% LPG at 2435 rpm, compared to pure diesel engine operation, the maximum cylinder pressure was shown to increase from 77.16 bar to 87.53 bar representing an increase of 13.45% as illustrated in Figure 7.6
- For the case of 80% diesel and 20% LPG at 2435 rpm, compared to diesel engine operation, the maximum cylinder pressure was shown to increase from 77.16 bar to 90.53 bar representing an increase of 17.33% as illustrated in Figure 7.6.

- For the case of 70% diesel and 30% LPG at 2435 rpm, compared to pure diesel engine operation, the maximum cylinder pressure was shown to increase from 77.16 bar to 93.42 bar representing an increase of 21.07% as illustrated in Figure 7.6

Interestingly, from all the above analyses pertaining to the maximum cylinder pressure, while there was a significant difference between the maximum cylinder pressures when no LPG was used and when 5% LPG was introduced, the differences turned to be much less when higher percentages by mass of LPG were introduced. Summarily, from the above analyses, it is evident that the increase in pressure associated with the introduction of LPG for the various fuel mass ratios examined, will not pose a problem to the engine operation as it falls within the acceptable design limits for the naturally aspirated VW 1.9L diesel engine.

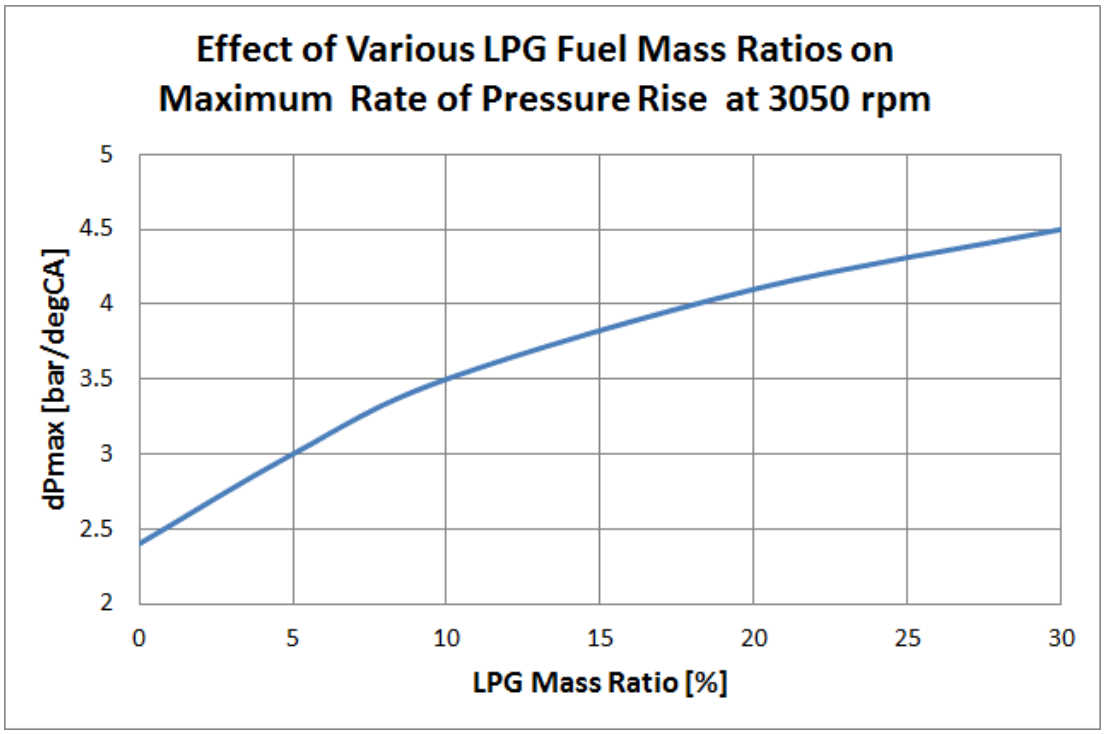

Figure 7.7 Variation of fuel mass ratios with the maximum rate of pressure rise at 3050 rpm

In this study, further analyses relating to the combustion of diesel-LPG focused on the maximum rate of pressure rise combustion characteristic as shown in Figure 7.7, Figure 7.8 and Figure 7.9. The maximum rate of pressure rise is indicative of the

combustion noise of the engine. Remarkably, for every engine operating regime investigated, the maximum rate of pressure rise was shown to increase as the quantity of LPG fuel mass ratio increased.

To ascertain the effect of various LPG fuel mass ratios on the highest engine operating speed studied, the maximum pressure rise values for each dual fuel scenario was compared to that of the diesel scenario. Hence, as can be seen in Figure 7.7, increasing the LPG mass ratio to 5% caused the maximum rate of pressure rise to increase from 2.40 to 3 bar/degCA. Similarly, for the 10%, 20, and 30% LPG mass ratios studied, the maximum rate of pressure rise compared to diesel were 3.5, 4.1 and 4.5 bar/degCA respectively. Evidently, the highest pressure rise in this instance is suggested to occur for the highest mass ratio of LPG fuel used.

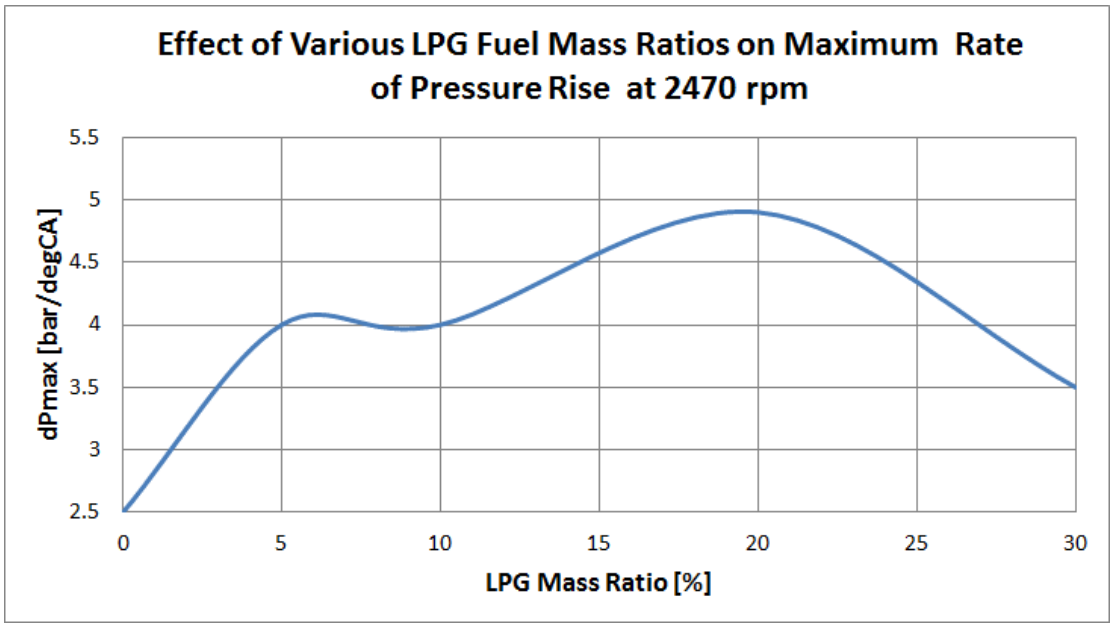

Figure 7.8 Variation of fuel mass ratios with the maximum rate of pressure rise at 2470 rpm

Proceeding in like manner, evaluating the effect of various LPG fuel mass ratios on the maximum rate of pressure rise at 2470 rpm, the following was observed:

- 5% LPG mass fraction caused the maximum rate of pressure rise to increase from 2.5 to 4 bar/degCA
- 10% LPG mass fraction caused the maximum rate of pressure rise to increase from 2.5 to 4 bar/degCA

- 20% LPG mass fraction caused the maximum rate of pressure rise to increase from 2.5 to 4.9 bar/degCA
- 30% LPG mass fraction caused the maximum rate of pressure rise to increase from 2.5 to 3.5 bar/degCA

Curiously, for the 2470 rpm case investigated, it was observed that the maximum rate of pressure rise shown for the 20% LPG was higher than that for the 30% LPG mass fuel ratio scenario. However, this can be explained by carefully examining the respective maximum cylinder pressures. Careful examination of the maximum cylinder pressure values for these two LPG fuel mass scenarios shown in Figure 7.5, indicates a slight drop in maximum cylinder pressure for the higher LPG mass fraction.

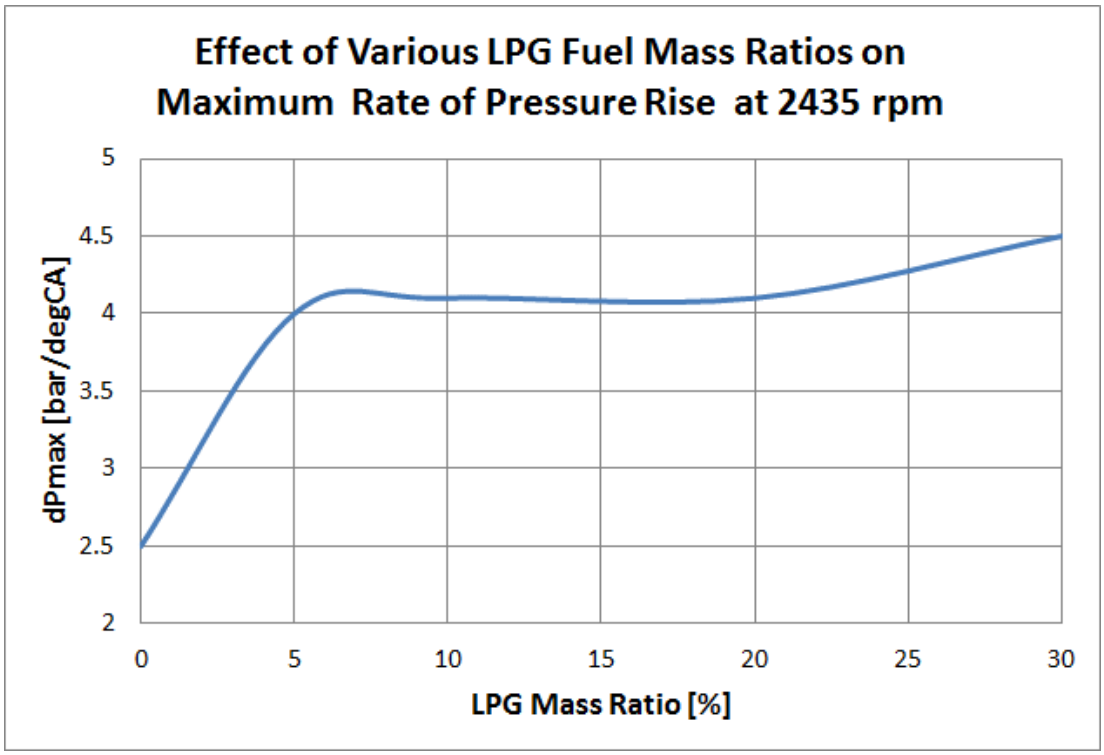

Figure 7.9 Variation of fuel mass ratios with the maximum rate of pressure rise at 2435 rpm

Again, proceeding in like manner to evaluate the effect of various LPG fuel mass ratios on the maximum rate of pressure rise at 2470 rpm, revealed the following:

- 5% LPG mass fraction caused the maximum rate of pressure rise to increase from 2.5 to 4 bar/degCA
- 10% LPG mass fraction caused the maximum rate of pressure rise to increase from 2.5 to 4.1 bar/degCA
- 20% LPG mass fraction caused the maximum rate of pressure rise to increase from 2.5 to 4.1 bar/degCA
- 30% LPG mass fraction caused the maximum rate of pressure rise to increase from 2.5 to 4.5 bar/degCA

7.2.2 Temperature

The temperature within the cylinder is a valuable thermodynamic parameter that is vital in the discussion of combustion characteristics. Moreover, it is one of the factors that have an influence on the formation of oxides of nitrogen pollutants within the combustion space. Owing to its importance, this study examined the effect of various LPG fuel mass ratios on the combustion, and the results are presented in Figure 7.10, Figure 7.11 and Figure 7.12. Generally speaking, the study shows that as the fuel mass ratio of LPG increases, the cylinder temperature also increases. The increases in cylinder temperature can be explained by the associated rise in heat released by the same amount of fuel owing to the higher calorific value of the fuel mixture when LPG is added. The results revealed that, for the respective engine operating regimes, the higher the speed, the higher the temperatures. As seen from the results, the difference between the cylinder temperature of the diesel scenario and the dual fuelling scenario is remarkably visible. However, the study suggests that for each of the various LPG fuel mass ratios examined, while there is a difference in their maximum cylinder temperatures, this difference is not very pronounced.

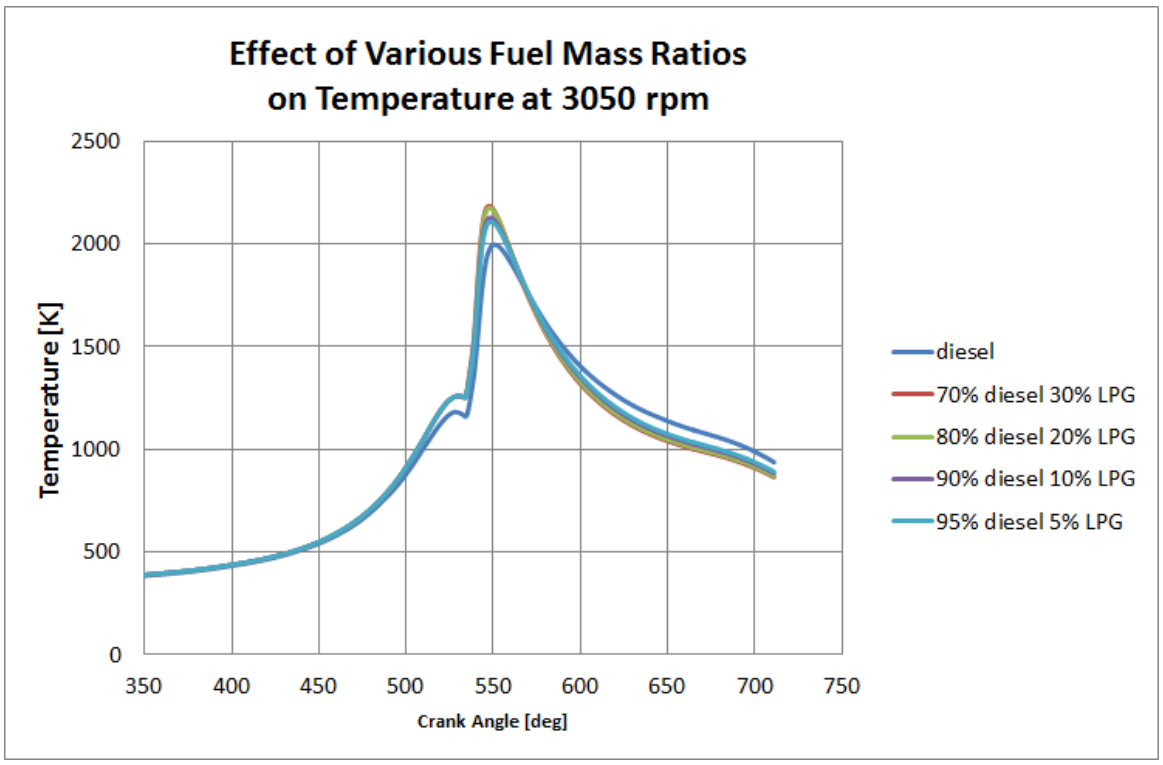

Figure 7.10 Effect of variation in fuel mass ratios on the temperature at 3050 rpm

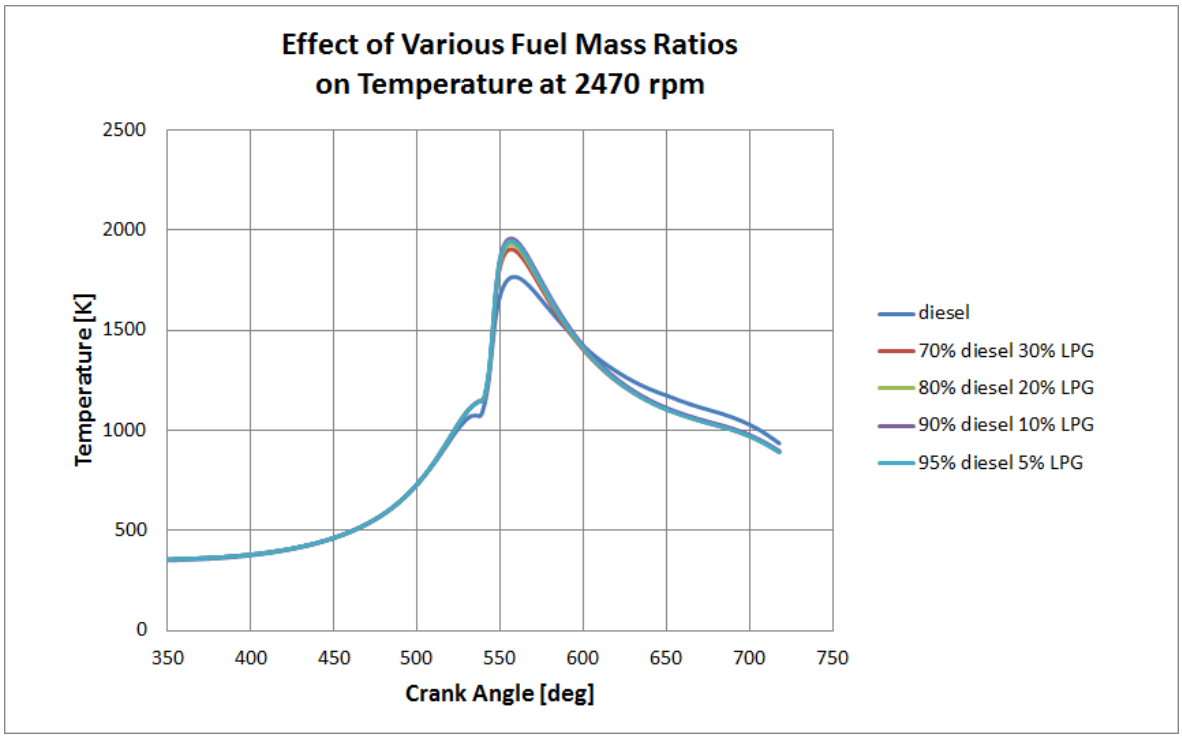

Figure 7.11 Effect of variation in fuel mass ratios on the temperature at 2470 rpm

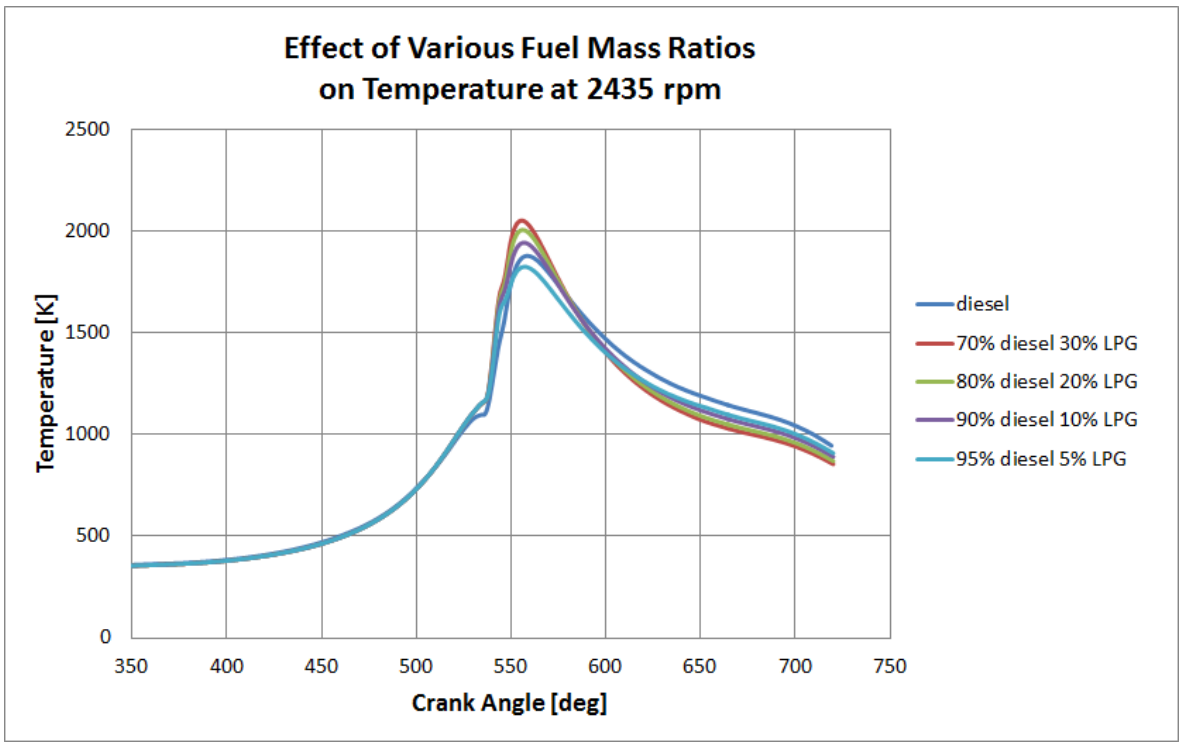

Figure 7.12 Effect of variation in fuel mass ratios on the temperature at 2435 rpm

7.2.3 Rate of Heat Release (ROHR)

A valuable and powerful tool for providing information pertaining to the combustion process and diagnosing engine performance problems is the heat release analysis. In this study, for each scenario examined, the combustion process has been expressed in the heat release rate at each crank angle position as shown in Figure 7.13 - Figure 7.17, Figure 7.19 - Figure 7.23 and Figure 7.25 - Figure 7.29. The rate of heat release (or simply referred to as "heat release") articulates the heat transferred into the system at an incremental crank angle position. Compared to the respective pure diesel engine operations, the ROHR increases for every diesel-LPG scenario examined which supports the explanations advanced for the trends observed pertaining to the cylinder temperature and pressure.

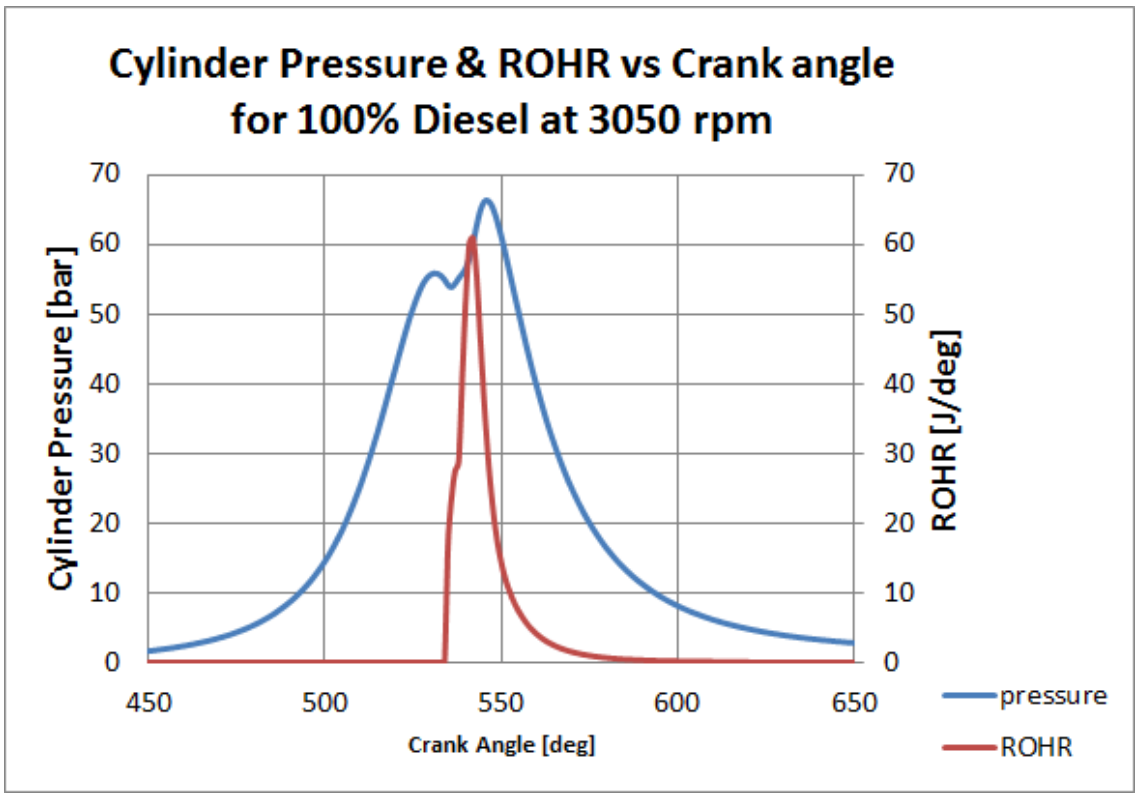

Figure 7.13 Rate of heat release for pure diesel engine operation at 3050 rpm

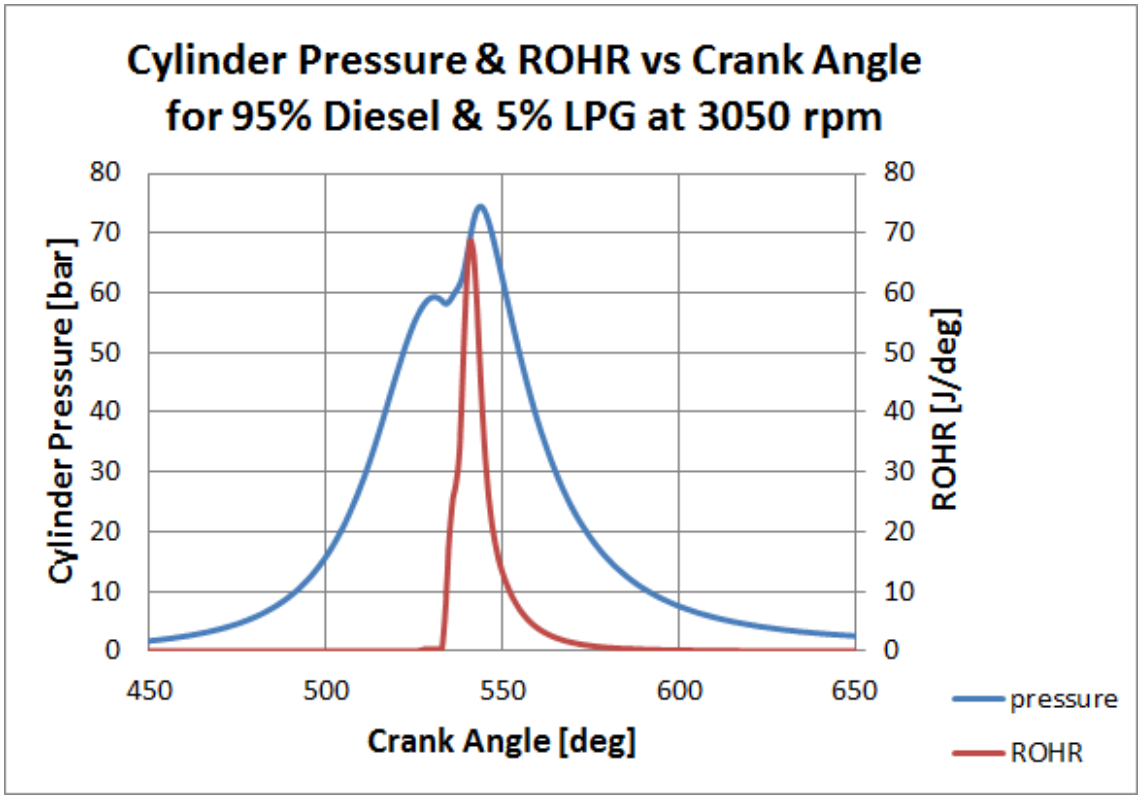

Figure 7.14 Rate of heat release for engine operation with 95% diesel and 5% LPG at 3050 rpm

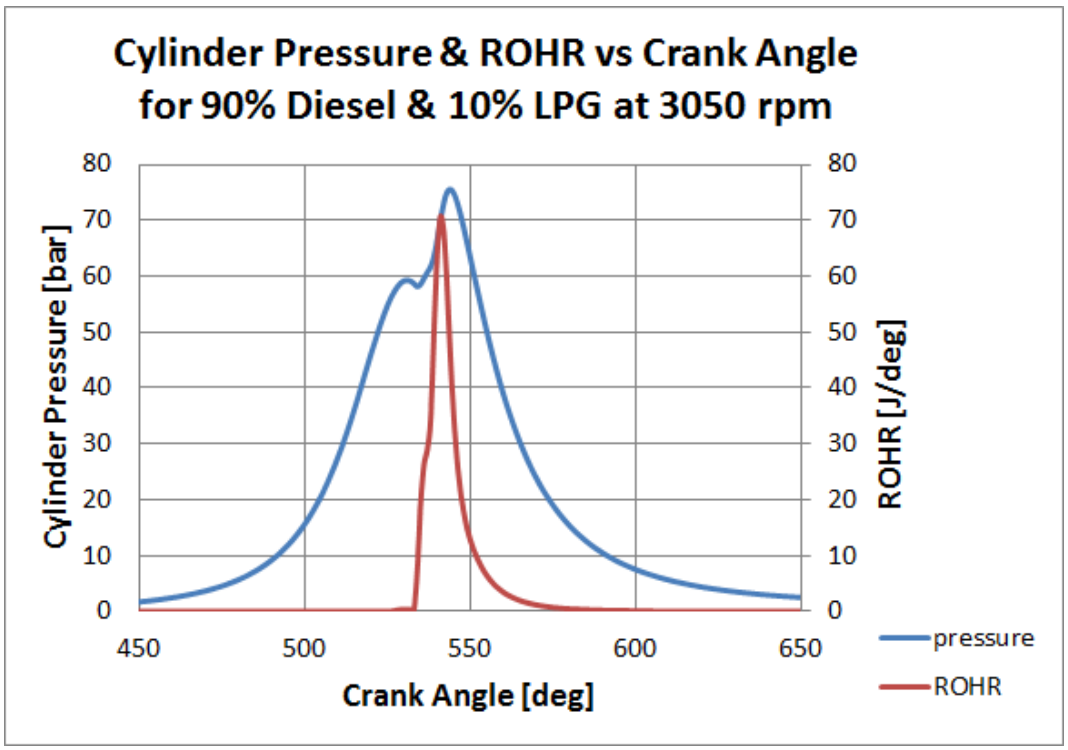

Figure 7.15 Rate of heat release for engine operation with 90% diesel and 10% LPG at 3050 rpm

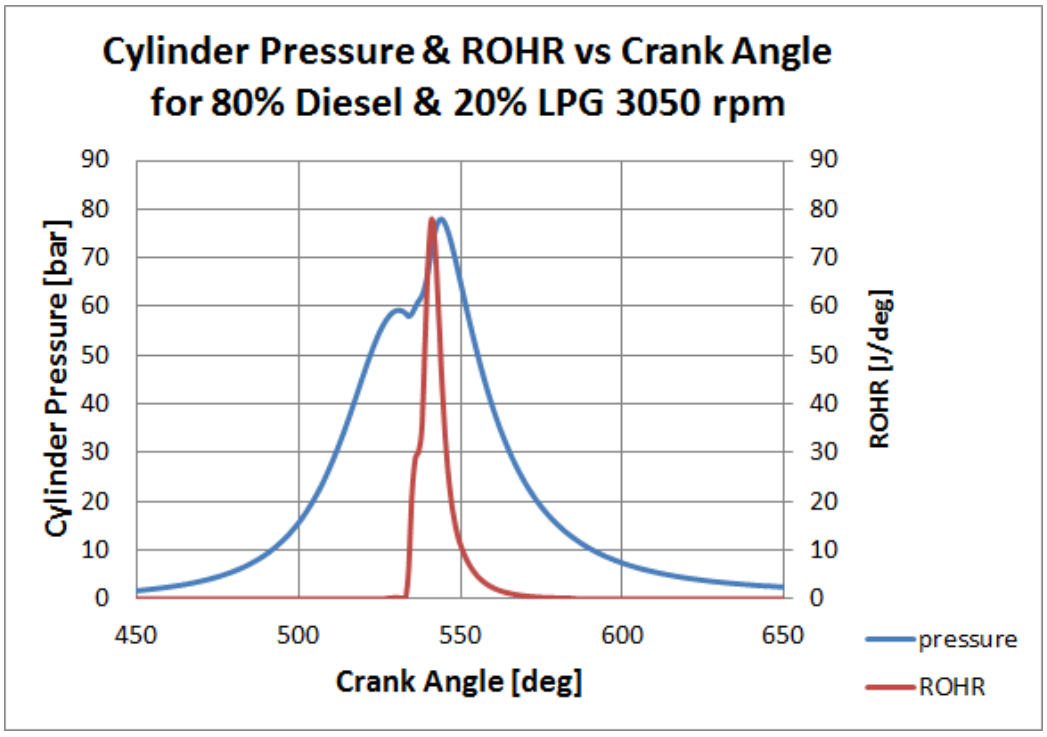

Figure 7.16 Rate of heat release for engine operation with 80% diesel and 20% LPG at 3050 rpm

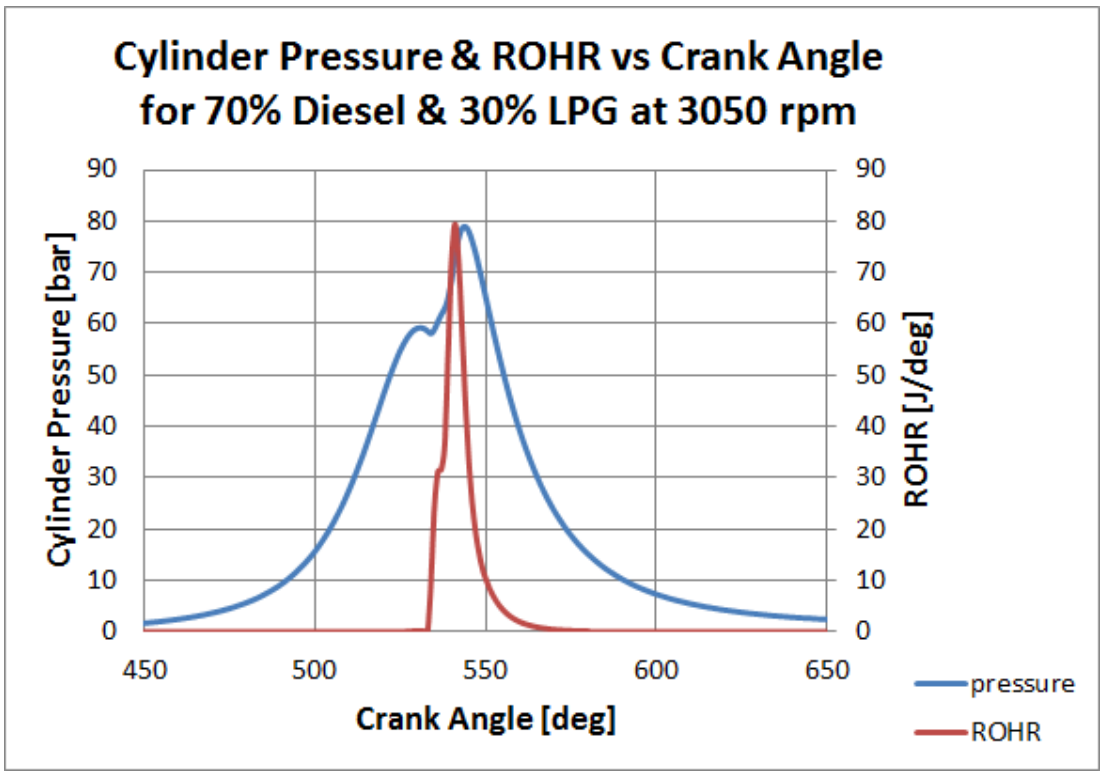

Figure 7.17 Rate of heat release for engine operation with 70% diesel and 30% LPG at 3050 rpm

In Figure 7.13 to Figure 7.17, the study compares the ROHR and cylinder pressure curves obtained for different fuelling scenarios at the same engine operating speed of 3050 rpm. The results highlight that the peak cylinder pressure and the ROHR increase as the LPG mass fraction increases. Consequently, the peak cylinder pressures and rate of heat release are highest for the 30% LPG scenario, followed by the 20%LPG scenarios, then the 10% LPG scenario and lastly the 5% LPG scenario. Each of the LPG scenarios representing dual fuel (diesel-LPG) operation evidently has higher peak cylinder pressures and rate of heat release than the pure diesel operation at the same operating speed. From the results shown, it is permissible to conceive qualitatively that the cycle efficiency of the scenario with the highest LPG fuel mass ratio would be greater than that for the other cases.

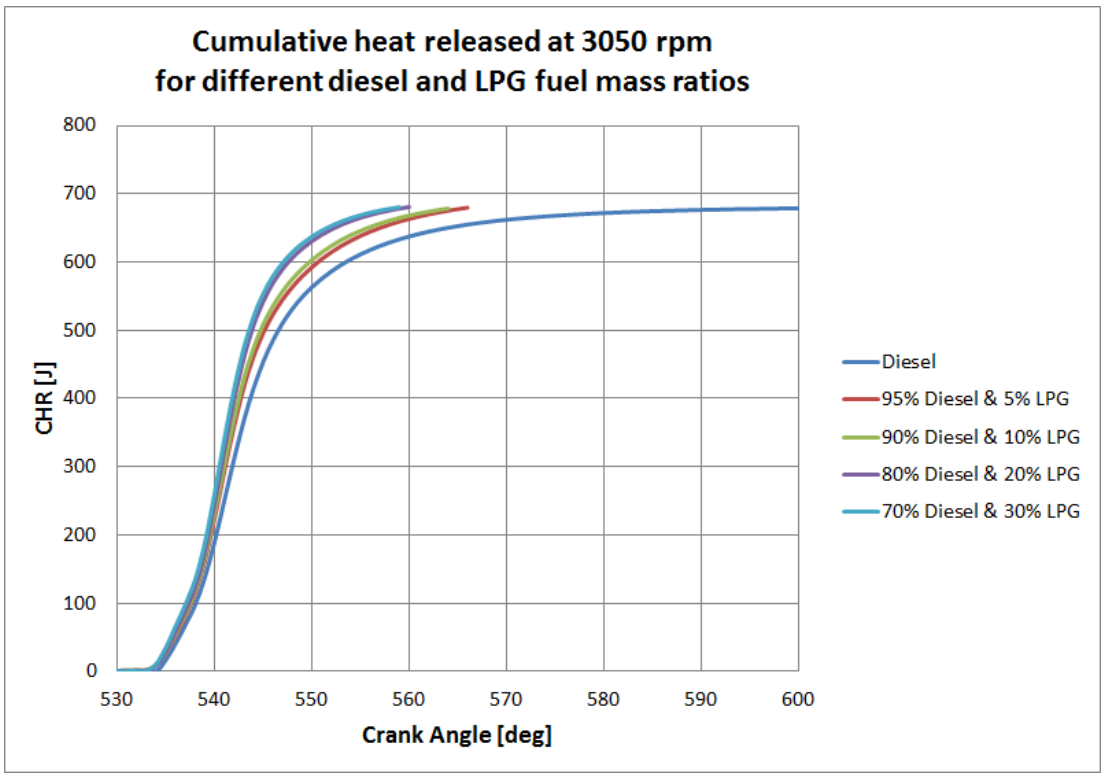

Figure 7.18 Cumulative heat released at 3050 rpm for different diesel and LPG fuel mass ratios

In the course of this study, it was decided to examine the cumulative heat release for the various scenarios simulated at each respective speed. This was chosen on account of the fact that, the individual cumulative heat release curves provide a vivid visual perspective to compare the respective combustion durations as can be seen in Figure 7.18, Figure 7.24 and Figure 7.30. The results as shown in Figure 7.18 illustrate the fact that diesel and LPG combustion start similarly, but then the scenarios involving various amounts of LPG each finish combustion faster than the scenario involving pure diesel fuel. Also, the larger the LPG fuel mass ratio, the shorter it, takes for combustion to complete. This implies that, compared to operating the engine with pure diesel fuel, engine operation using diesel-LPG fuelling leads to a reduction of the combustion duration. At 3050 rpm, the observation of a decrease in combustion duration along with the analyses of pressure and temperature within the cylinder, allow us to perceive that, for the diesel-LPG scenarios, within the cylinder, the increase in pressure and temperature cause the mixture to burn faster thereby shortening the combustion duration.

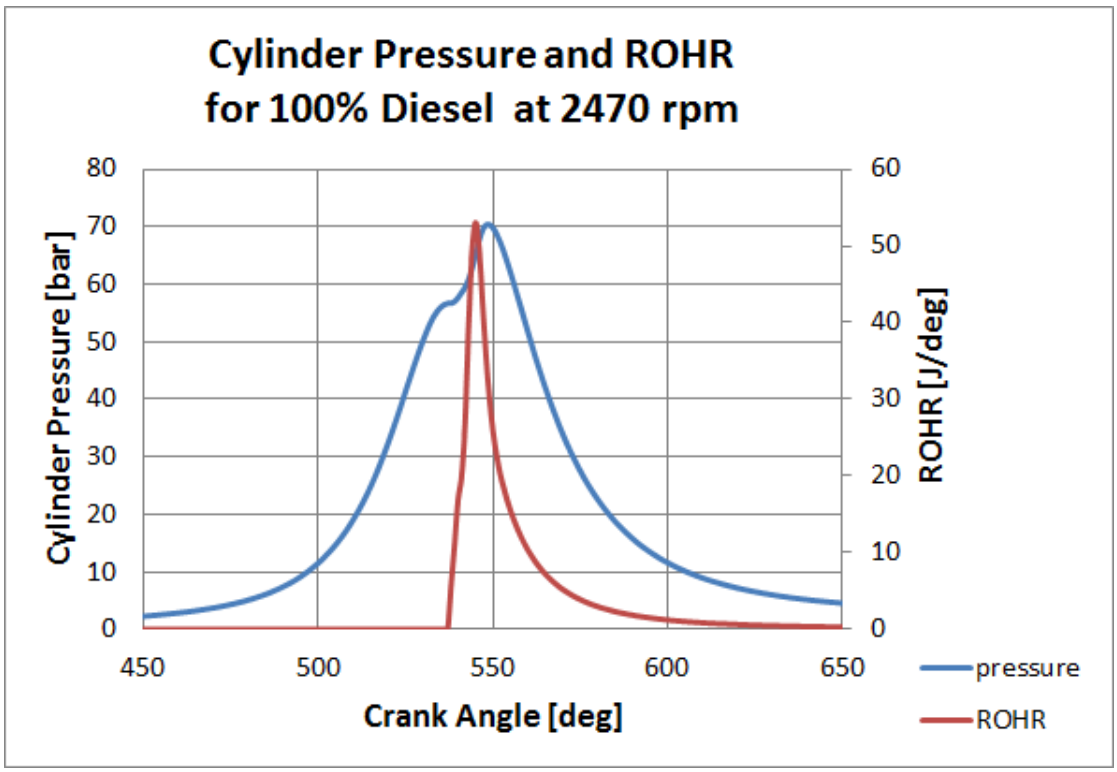

Figure 7.19 Rate of heat release for pure diesel engine operation at 2470 rpm

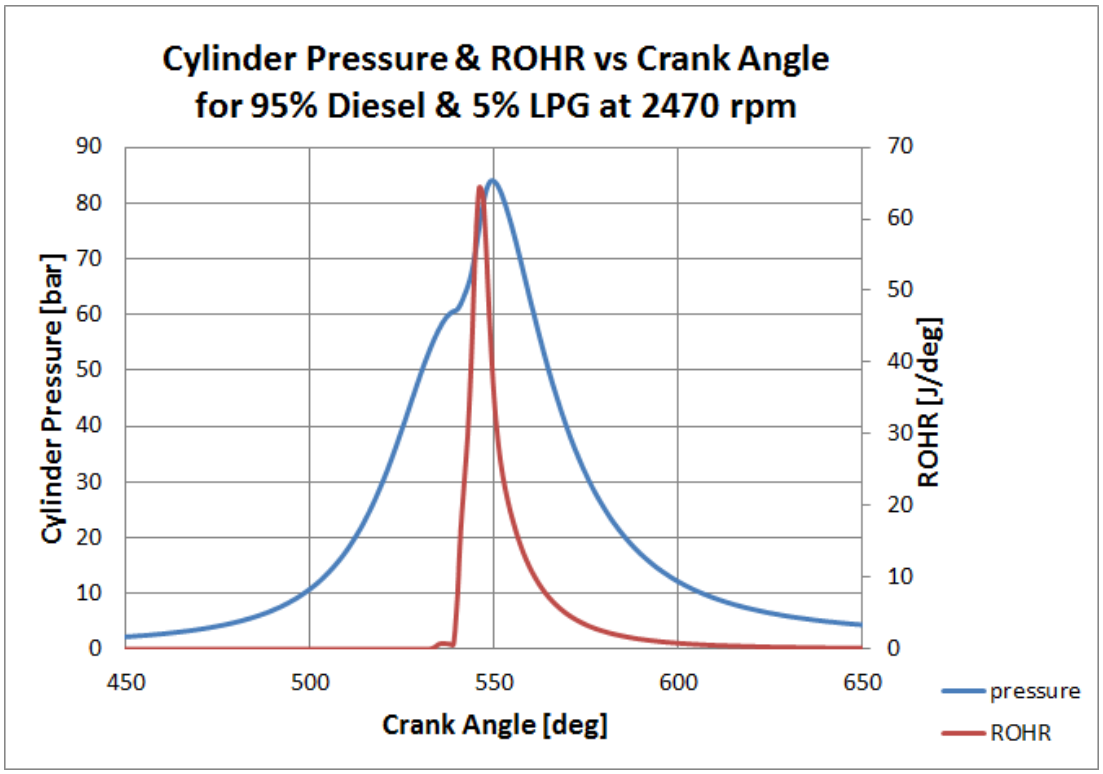

Figure 7.20 Rate of heat release for engine operation with 95% diesel and 5% LPG at 2470 rpm

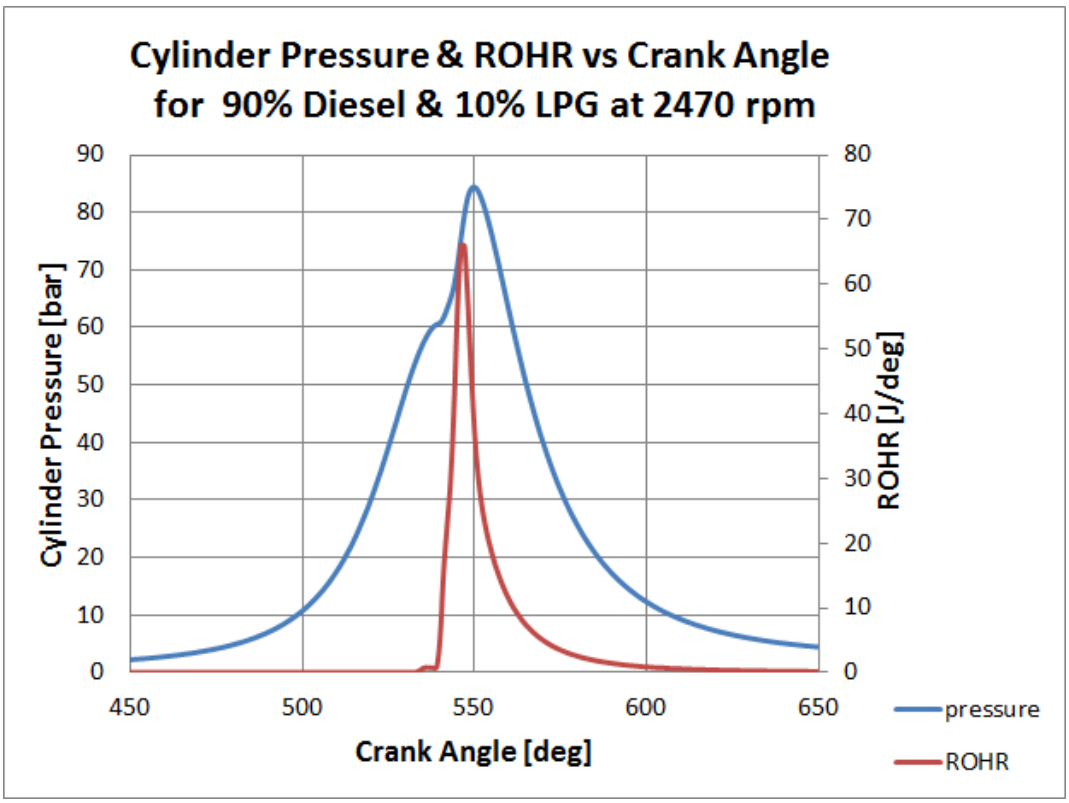

Figure 7.21 Rate of heat release for engine operation with 90% diesel and10% LPG at 2470 rpm

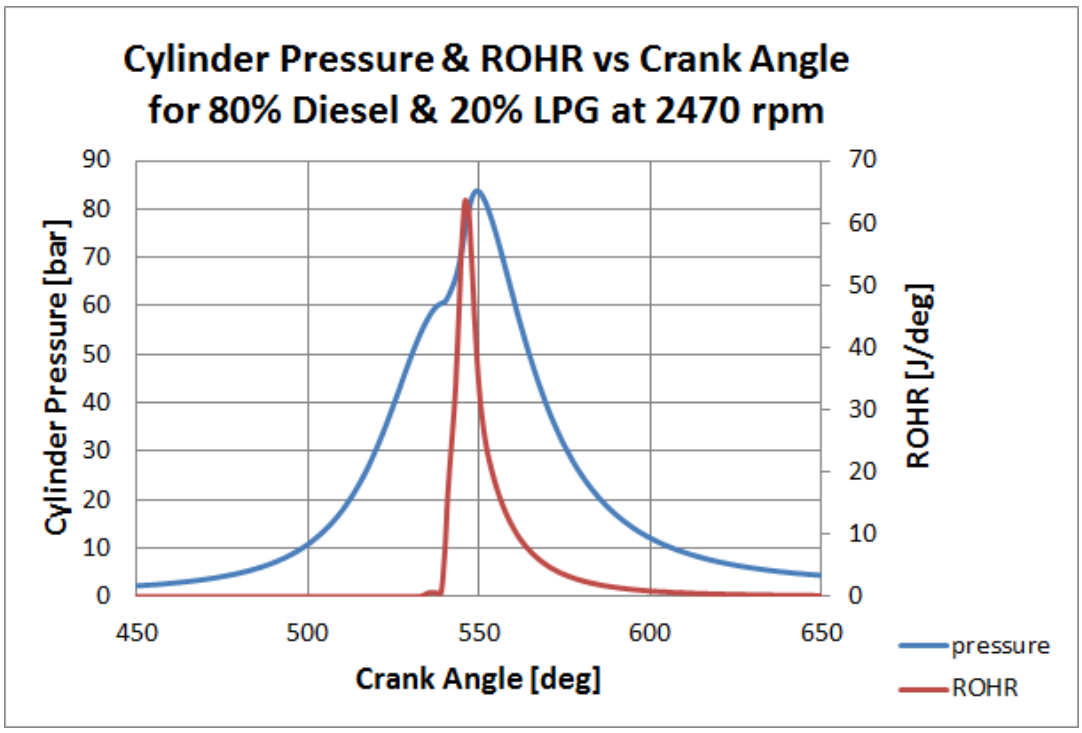

Figure 7.22 Rate of heat release for engine operation with 80% diesel and 20% LPG at 2470 rpm

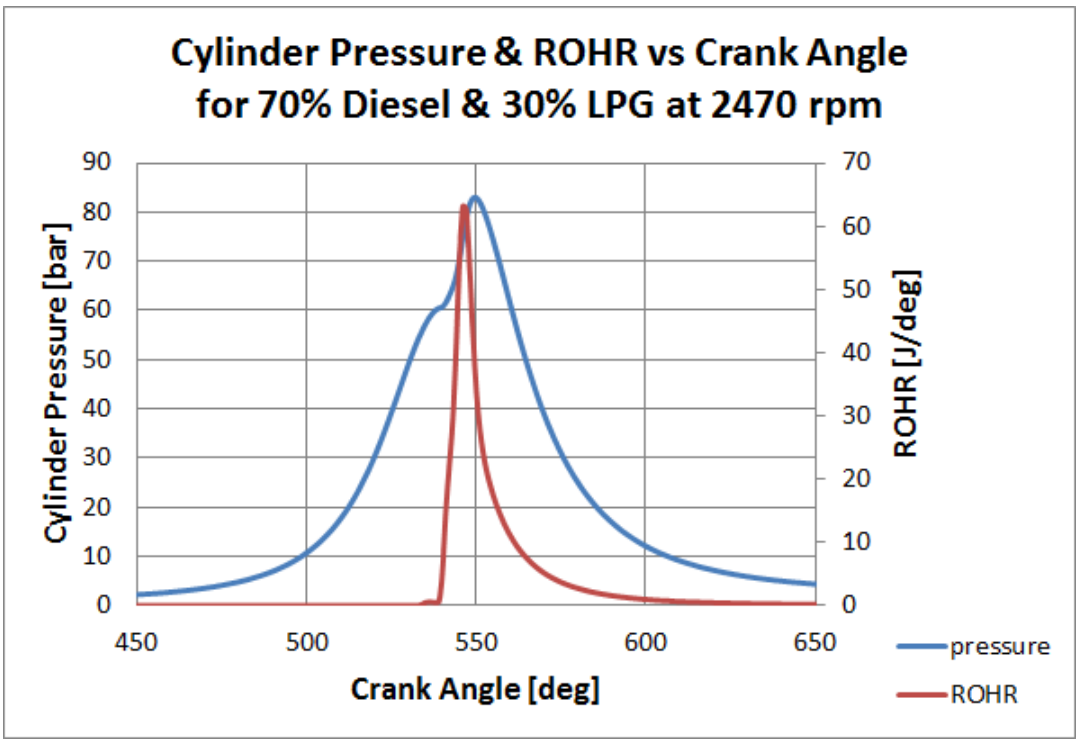

Figure 7.23 Rate of heat release for engine operation with 70% diesel and 30% LPG at 2470 rpm

Similarly, in Figure 7.19 to Figure 7.23, the study compares the heat release and cylinder pressure curves obtained for different fuelling scenarios at the same engine operating speed of 2470 rpm. The results highlight that the peak cylinder pressure and the ROHR increase as the LPG mass fraction increases. Consequently, the peak cylinder pressures and rate of heat release are highest for the 30% LPG scenario, followed by the 20% LPG scenario, then the 10% LPG scenario and lastly the 5% LPG scenario. Each of the LPG scenarios representing dual fuel (diesel-LPG) operation evidently has higher peak cylinder pressures and rate of heat release than the pure diesel operation at the same operating speed. From the results shown, it is permissible to conceive qualitatively that the cycle efficiency of the scenario with the highest LPG fuel mass ratio would be greater than that for the other cases.

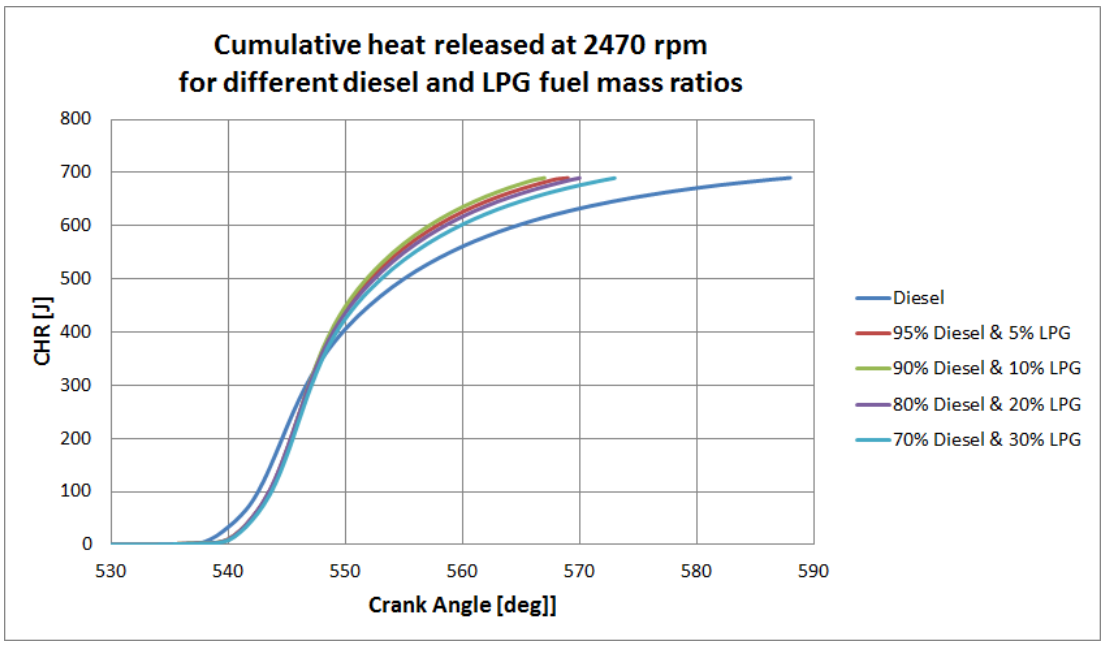

Figure 7.24 Cumulative heat released at 2470 rpm for different diesel and LPG fuel mass ratios

The analysis shown in in Figure 7.24 aims to further compare and illustrate the combustion durations for the each of the respective scenarios computationally investigated. The results in Figure 7.24 show that, for the respective diesel-LPG scenarios examined at 2470 rpm, the combustion period was relatively shorter compared to the combustion period of the pure diesel operation. This finding further corroborates the observations illustrated in Figure 7.18. Broadly speaking, the visual perspective offered by Figure 7.24, suggests that, compared to operating the engine with pure diesel fuel, engine operation using diesel-LPG fuelling leads to a reduction of the combustion duration. However, for this particular scenario examined, it can be perceived that when the 10% LPG mass fraction was added, the combustion was slightly shorter than when 5% LPG mass fraction was introduced.

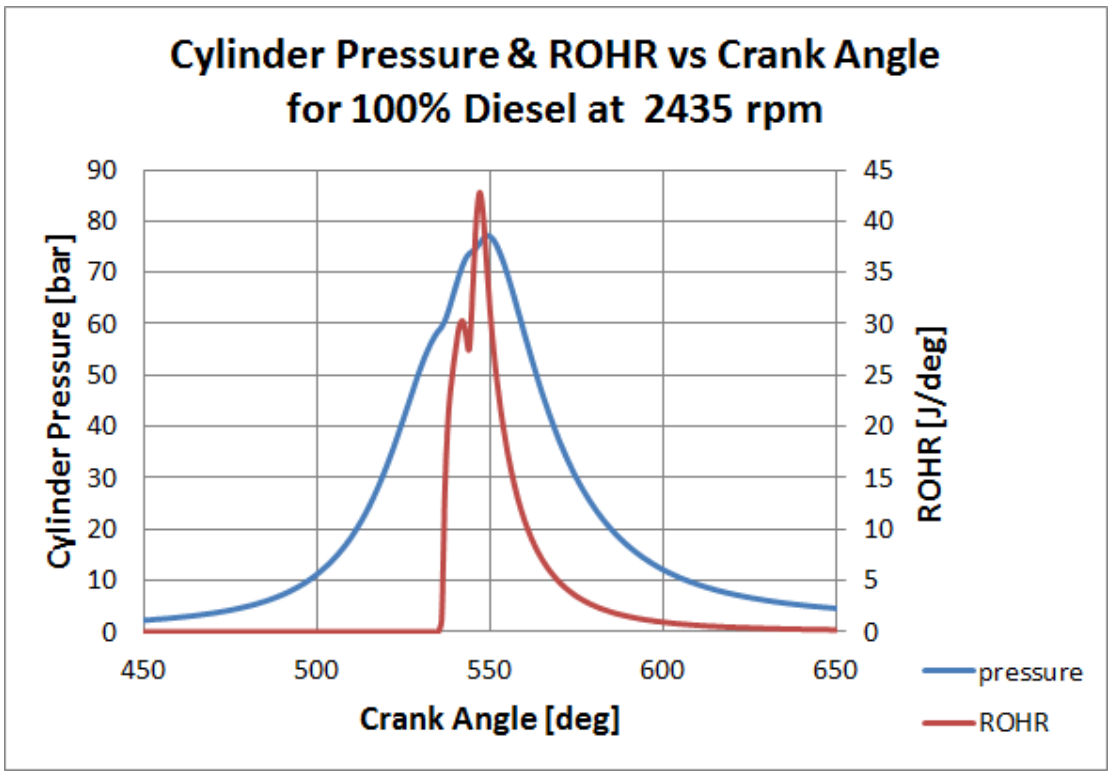

Figure 7.25 Rate of heat release for pure diesel engine operation at 2435 rpm

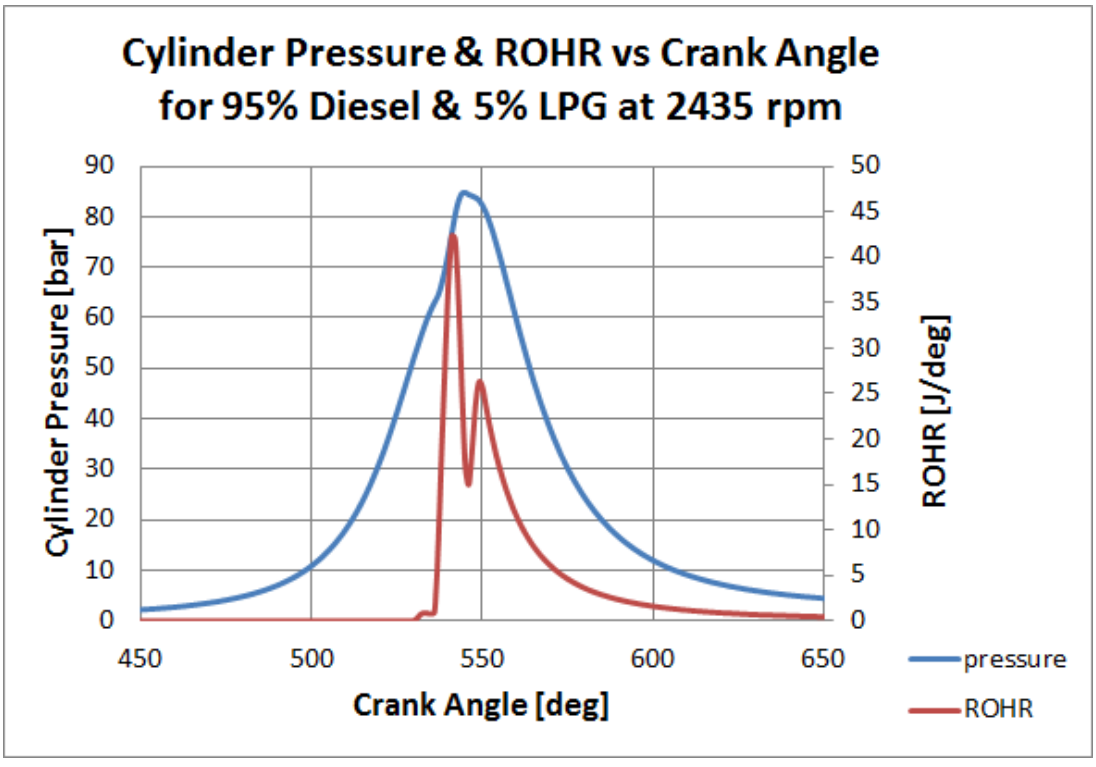

Figure 7.26 Rate of heat release for engine operation with 95% diesel and 5% LPG at 2435 rpm

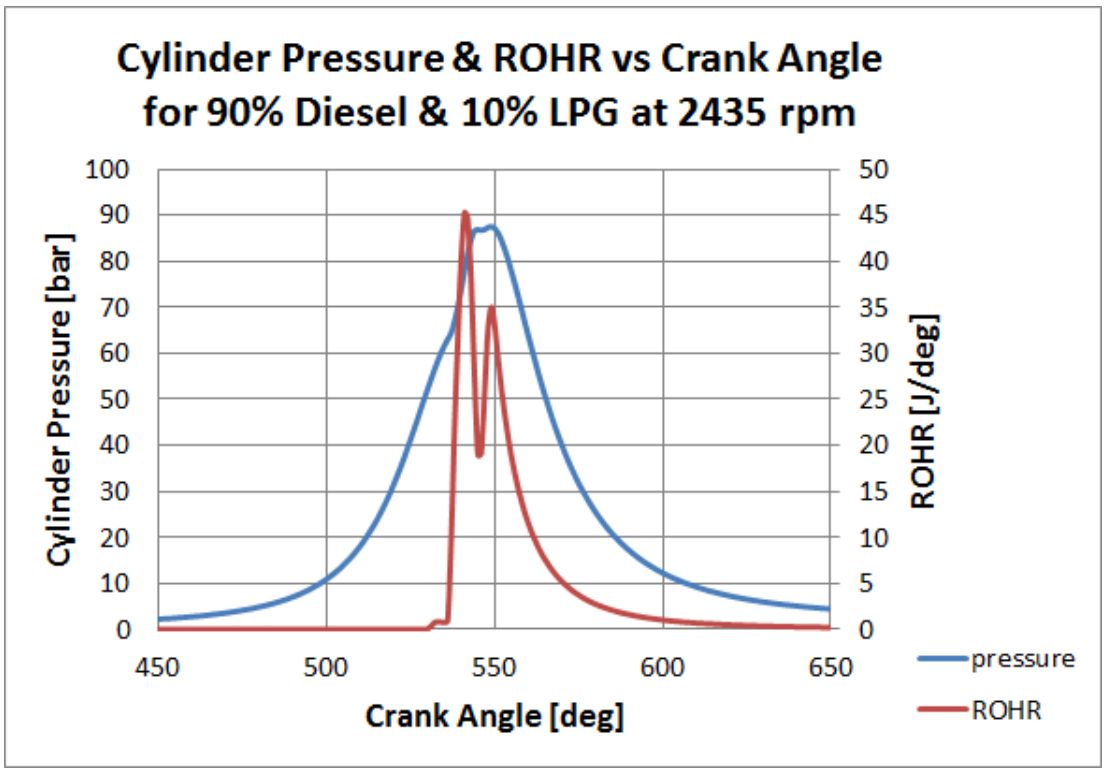

Figure 7.27 Rate of heat release for engine operation with 90% diesel and 10% LPG at 2435 rpm

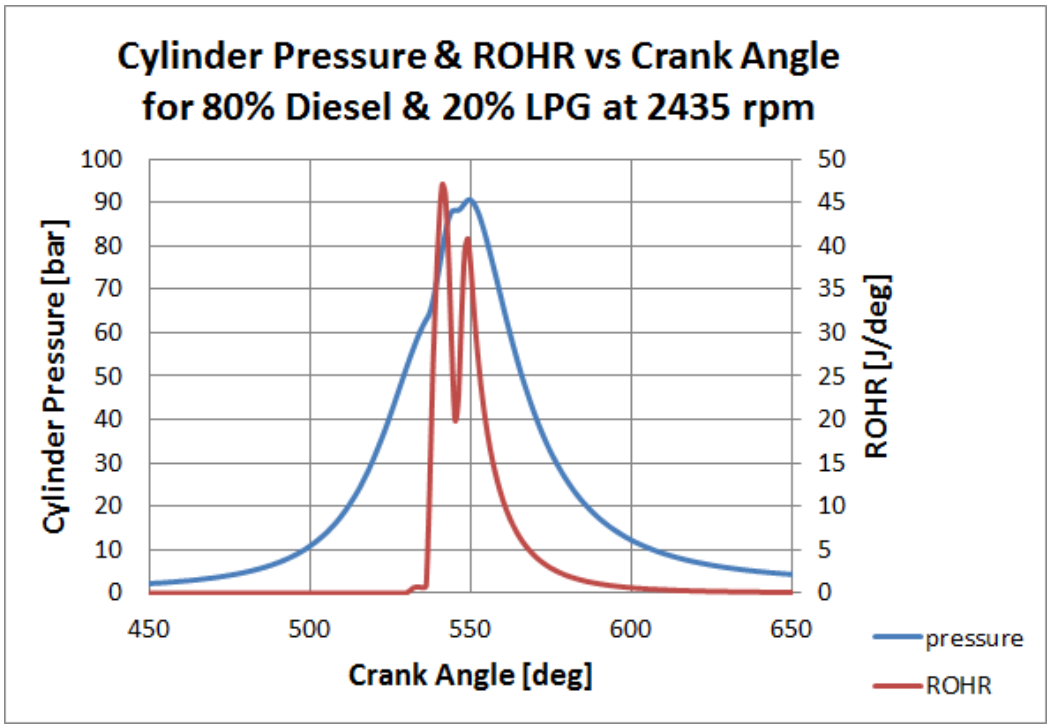

Figure 7.28 Rate of heat release for engine operation with 80% diesel and 20% LPG at 2435 rpm

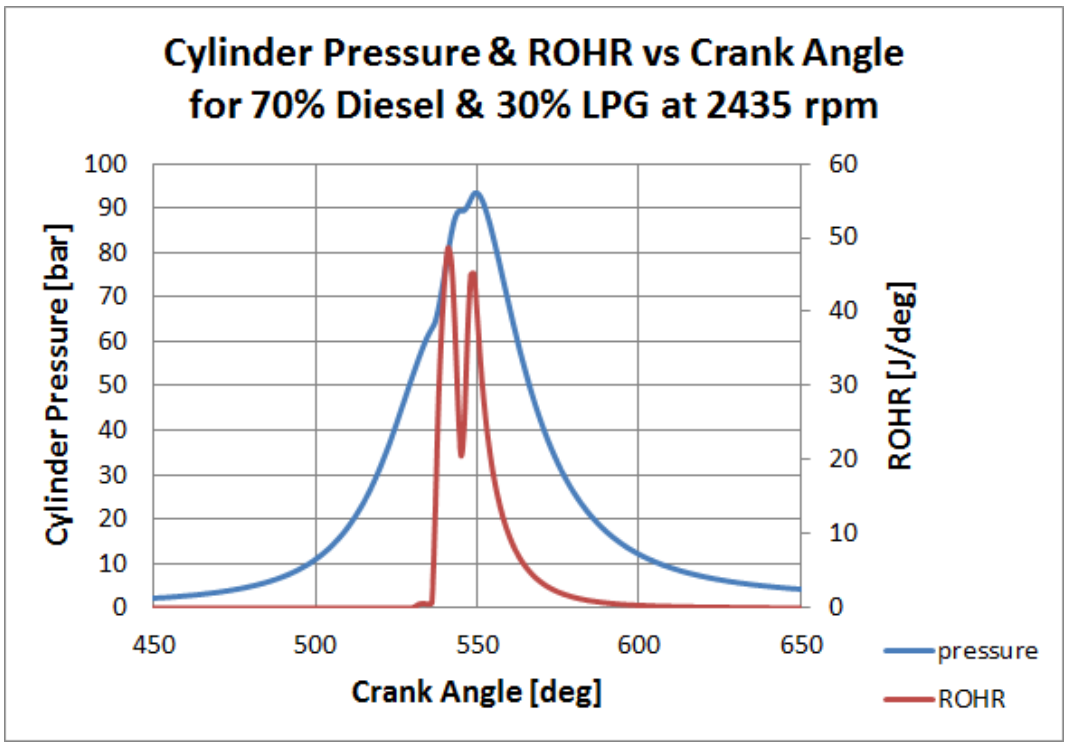

Figure 7.29 Rate of heat release for engine operation with 70% diesel and 30% LPG at 2435 rpm

In like manner, replicative comparative analyses of the results obtained at 2435 rpm were carried out. In Figure 7.25 to Figure 7.29, the study compares the heat release and cylinder pressure curves obtained for different fuelling scenarios at the same engine operating speed of 2470 rpm. Generally, the results highlight that the peak cylinder pressure and the ROHR increase as the LPG mass fraction increases. However, the peak cylinder pressures and rate of heat release are highest for the 20% LPG scenario, followed by the 10%LPG scenario, then the 30% LPG scenario and lastly the 5% LPG scenario. Each of the LPG scenarios representing dual fuel (diesel-LPG) operation evidently has higher peak cylinder pressures and rate of heat release than the pure diesel operation at the same operating speed. From the results shown, it is permissible to conceive qualitatively that the cycle efficiency of the scenario with the highest LPG fuel mass ratio would be greater than that for the other cases.

Interestingly, at 2435 rpm, in all the ROHR cases as shown in red curve, the results indicate that there is an increase in the burning rate of preformed combustion and a decrease in the burning rate of the diffusion combustion

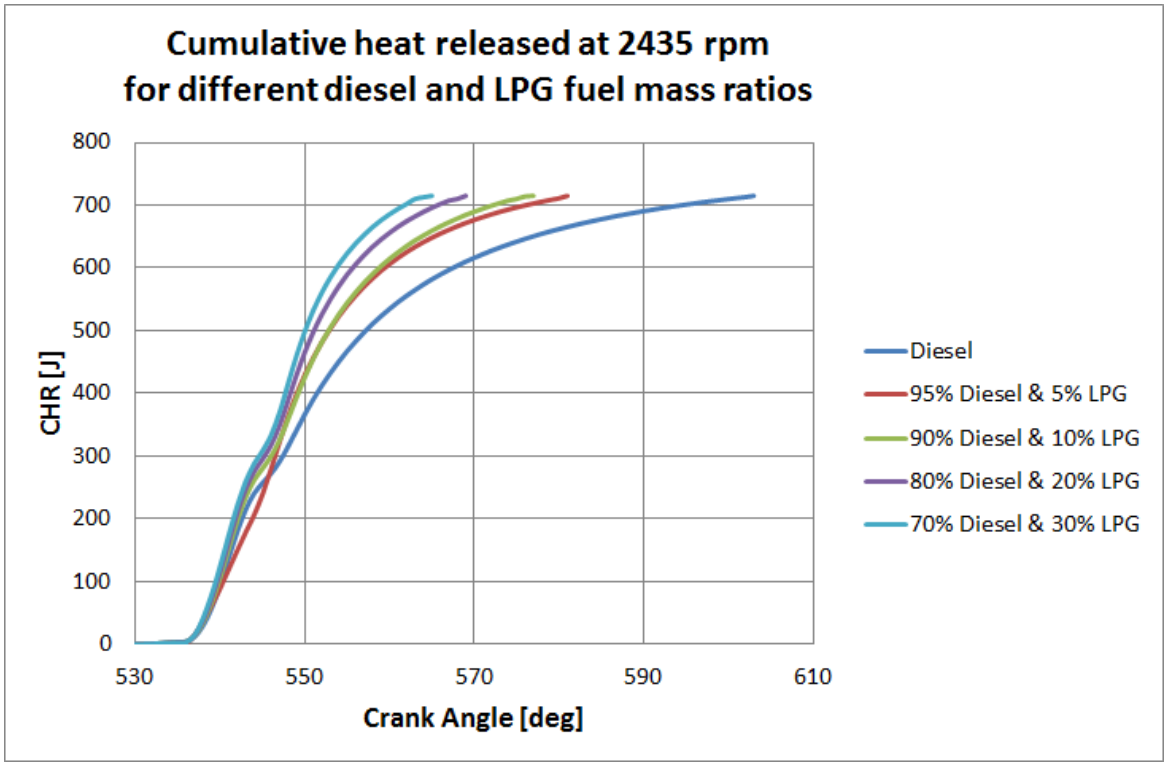

Figure 7.30 Cumulative heat released at 2435 rpm for different diesel and LPG fuel mass ratios

Again, Figure 7.30 illustrates the cumulative heat release for the various fuelling scenarios examined at the said speed. As shown, the results imply that, compared to operating the engine with pure diesel fuel, engine operation using diesel-LPG fuelling leads to a reduction of the combustion duration. Interestingly, in this particular case study, the higher the LPG mass ratio introduced, the shorter the combustion as clearly portrayed in Figure 7.30.

7.3 Diesel-LPG Performance Parameters

Improvement in combustion parameters as explained in the previous section leads to a general improvement in several performance parameters for the diesel-LPG engine operation. This section examines the impact of various LPG fuel mass ratios on performance parameters such as the IMEP, BMEP, Power, Torque, BSEC and BTE.

7.3.1 Indicated Mean Effective Pressure (IMEP)

The IMEP provides information about the average pressure produced within the combustion chamber during the operating cycle. A remarkable thing to note about the IMEP is that it is related to actual pressures that occur within the cylinder and can, therefore, be used as a measure of these pressures. This study provides a comparative analysis of the IMEP at various speeds as seen in Figure 7.31, Figure 7.32 and Figure 7.33.

According to the results shown in Figure 7.31, an increment in the LPG mass fraction causes the IMEP also to increase. This correlates with the observations of the cylinder pressure traces earlier shown in Figure 7.1. It is therefore evident, that the increase in pressure as illustrated will lead to more mechanical work. Following on from this study and the results reported, it is permissible to perceive that, at 3050 rpm, for the highest (30%) LPG mass fraction introduced, the mechanical work will likely be the maximum. Overall the study suggests that the IMEP in each of the diesel-LPG scenarios is higher than that corresponding to the diesel engine scenario.

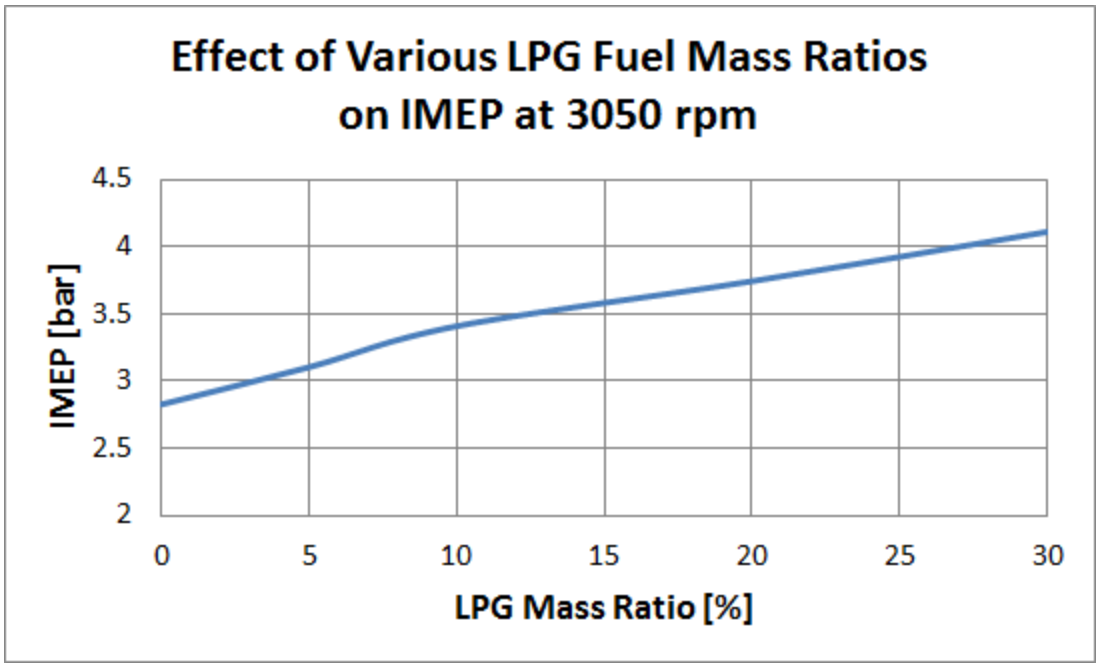

Figure 7.31 Impact of variation in fuel mass ratio on IMEP at 3050 rpm

For the case study at 2470 rpm, the results generally depict that the IMEP for each diesel-LPG scenario is higher than that for the diesel engine operation. However, as the amount of LPG increases from 10% to 30%, the analysis of the results suggest a slight drop in the IMEP as shown in Figure 7.32. The results of the IMEP at this particular operating regime corroborate the pressures occurring within the cylinder as shown in Figure 7.2.

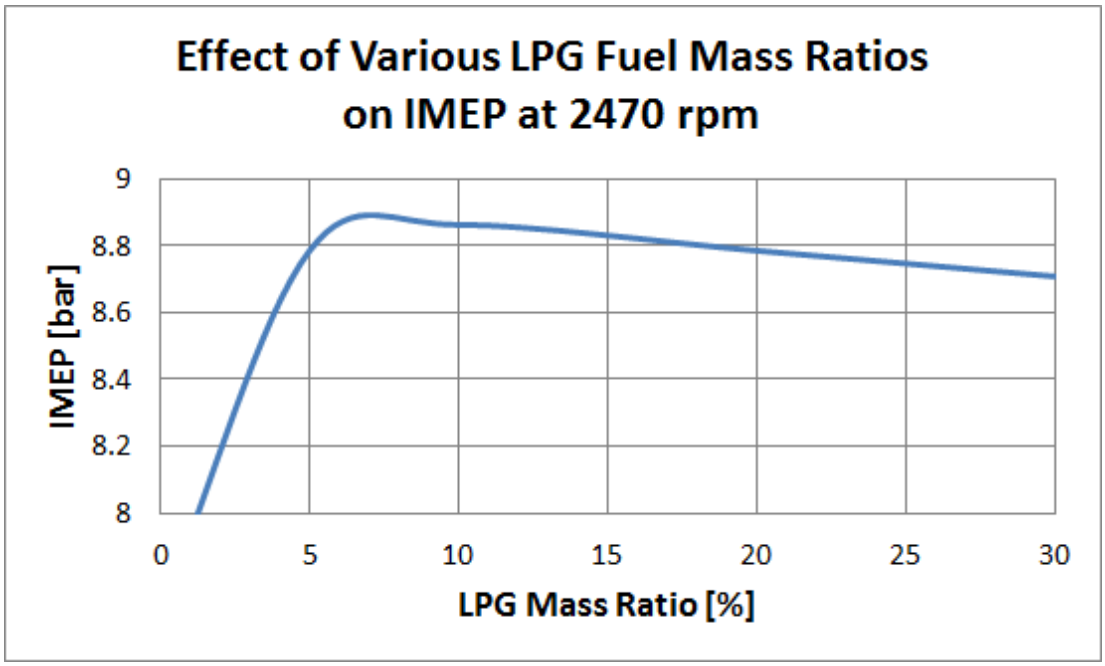

Figure 7.32 Impact of variation in fuel mass ratio on IMEP at 2470 rpm

Replication of the comparative analysis involving the IMEP and LPG fuel mass fractions for a different operating regime provides no significant difference in trend behaviour to that shown in Figure 7.31. Without any exception, the results for the engine operating speed according to Figure 7.33, show that increasing the LPG mass fraction leads to rise in IMEP. Consequently, the IMEP corresponding to the 30% LPG mass fraction is higher than that of the 20% LPG mass fraction which in turn is higher than that of the 10% LPG mass fraction which is also higher than that of the 5% LPG mass fraction.

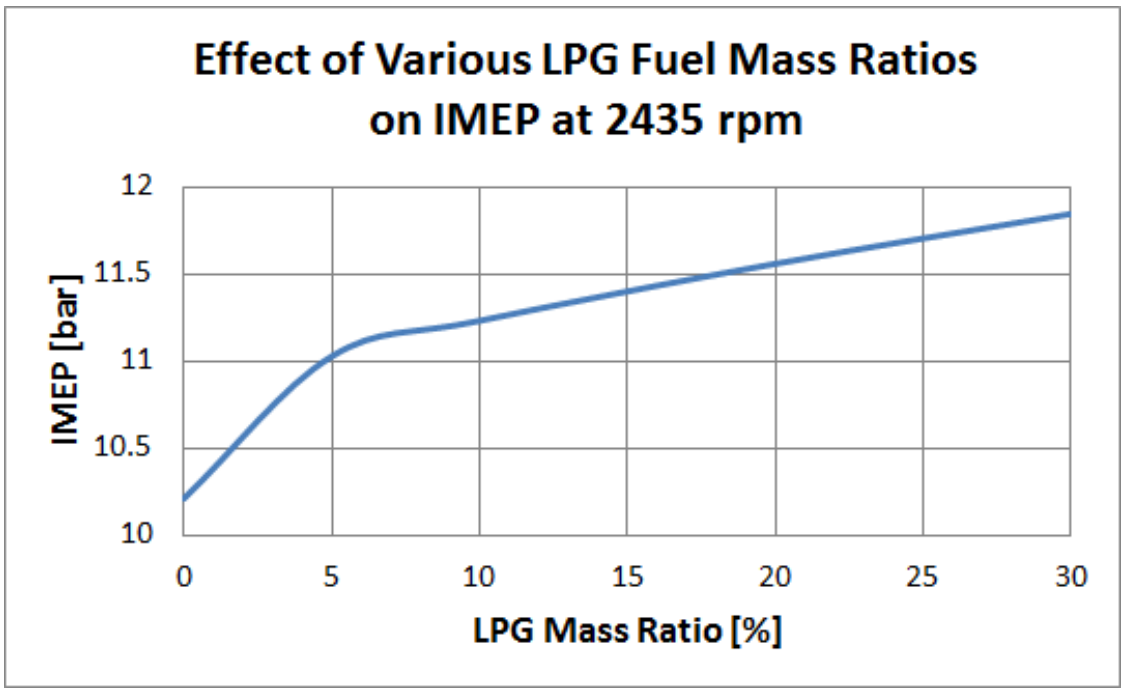

Figure 7.33 Impact of variation in fuel mass ratio on IMEP at 2435 rpm

7.3.2 Brake Mean Effective Pressure (BMEP)

Another very interesting and useful yardstick used in this study to compare engine performance is the BMEP. The BMEP defines the average pressure that if, uniformly imposed on the pistons during each power stroke, would produce the brake power output. While the IMEP has to do with the actual cylinder pressures, the BMEP provides a tool to evaluate the engine efficiency.

This study compares the BMEP at different speeds for the same engine operated using different fuel mass ratios of diesel and LPG. The results of the various comparisons are shown in Figure 7.34, Figure 7.35 and Figure 7.36. Generally, the results show that increasing the LPG fuel mass ratio while decreasing the diesel fuel mass ratio, causes the BMEP to increase and be higher compared to the BMEP of the diesel engine operation. With the exception of the trend shown in Figure 7.35, for all the other case studies, increasing the LPG mass fraction from 10% to 30% leads to a slight increase in the BMEP as can be seen in Figure 7.34 and Figure 7.36.

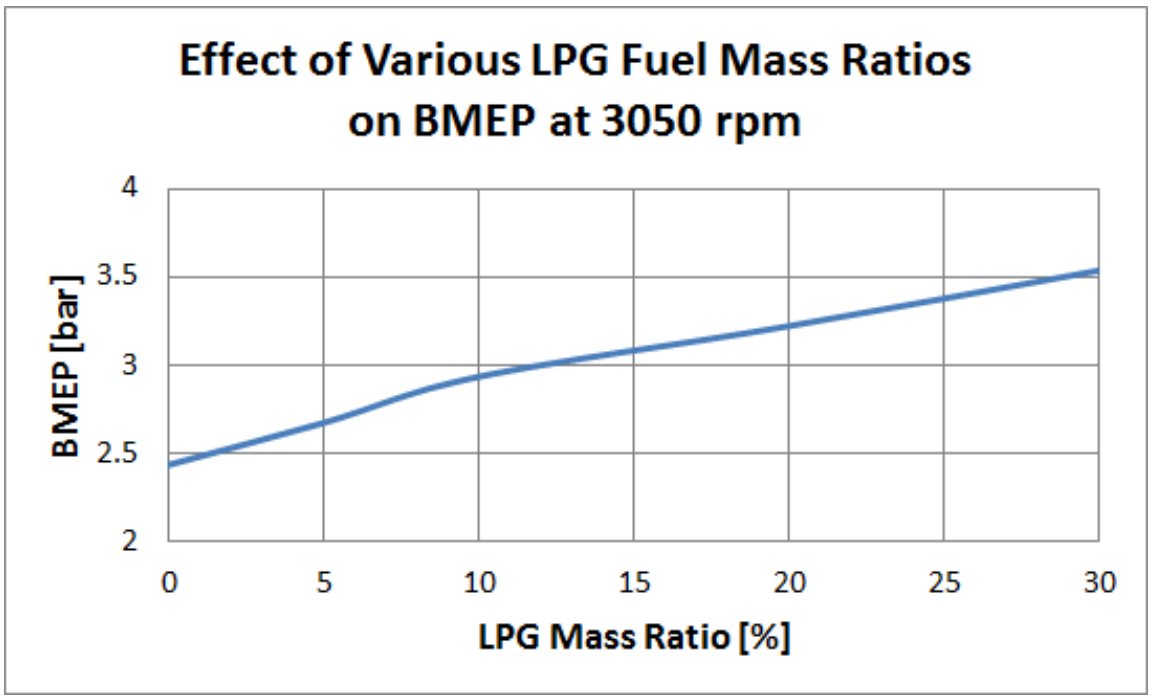

Figure 7.34 Impact of variation in fuel mass ratio on BMEP at 3050 rpm

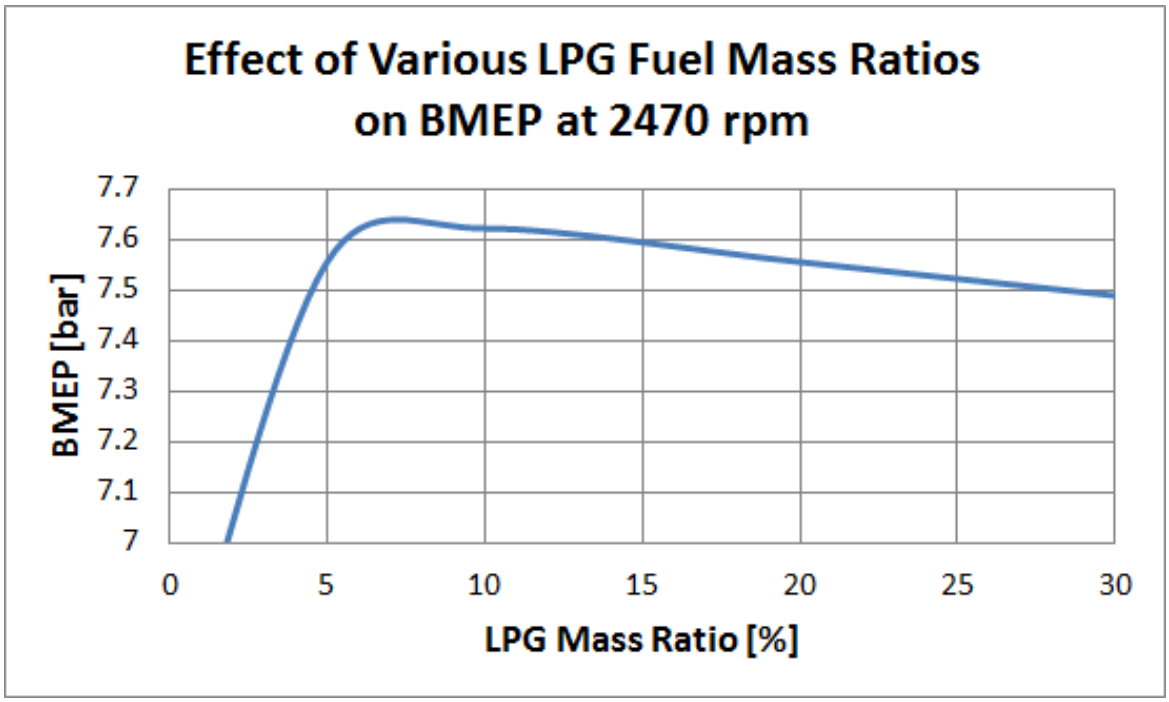

Figure 7.35 Impact of variation in fuel mass ratio on BMEP at 2470 rpm

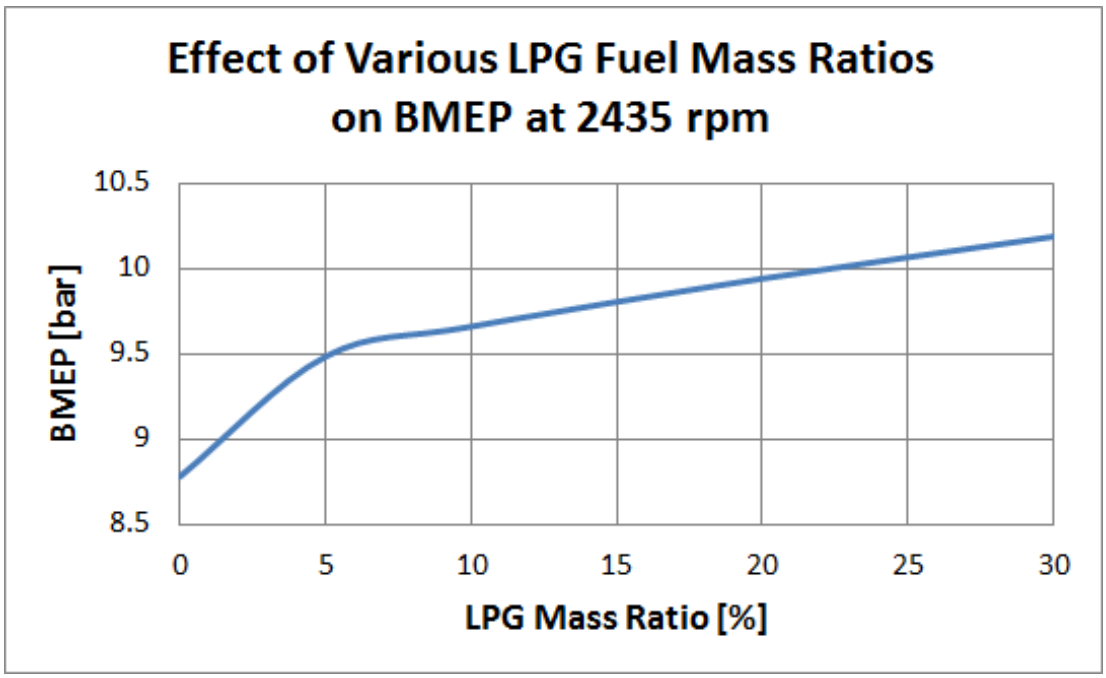

Figure 7.36 Impact of variation in fuel mass ratio on BMEP at 2435 rpm

7.3.3 Torque

The engine torque is a well-known, commonly discussed and widely used parameter, depicting engine performance. The torque is widely referred to as the engine's rotational force, and it typically refers to the amount of work an engine can exert. Torque, therefore, measures the ability of the engine to do work. For all the case studies examined, this study presents the variation of engine torque with different diesel and LPG fuel mass ratios as shown in Figure 7.37, Figure 7.38 and Figure 7.39. As demonstrated in each of these Figures, increasing the LPG mass ratio generally causes the torque to increase. Therefore, compared the pure diesel operation, each of the various diesel-LPG scenarios shows improved torques at the respective speeds computationally investigated.

With the exception of Figure 7.39, the results show no significant difference in the maximum torque between 10% of LPG mass ratio and 30% LPG Mass ratio. For instance, in Figure 7.37, the torque associated with 10% LPG mass fraction is about 40.9 Nm while that associated with the 30% LPG mass ratio is about 42.1 Nm.

Similarly, Figure 7.38 shows the torque obtained for the 10% LPG mass ratio to be about 115 Nm and that obtained for the 30% LPG mass ratio to be about 113 Nm.

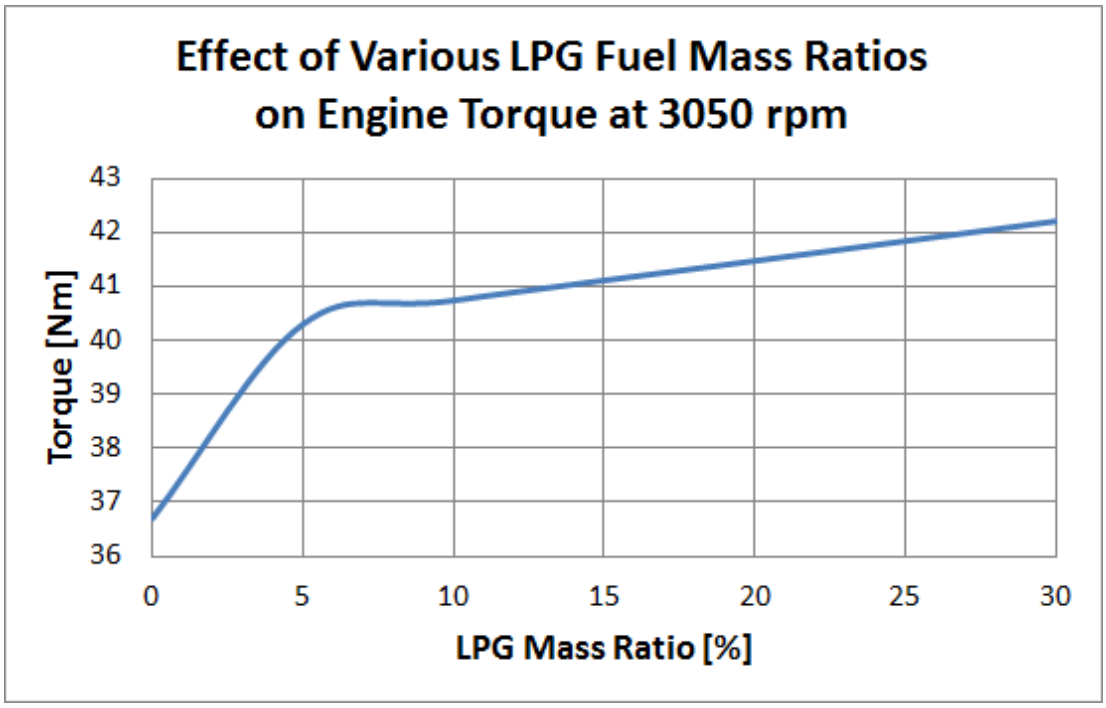

Figure 7.37 Variation of fuel mass ratio with engine torque at 3050 rpm

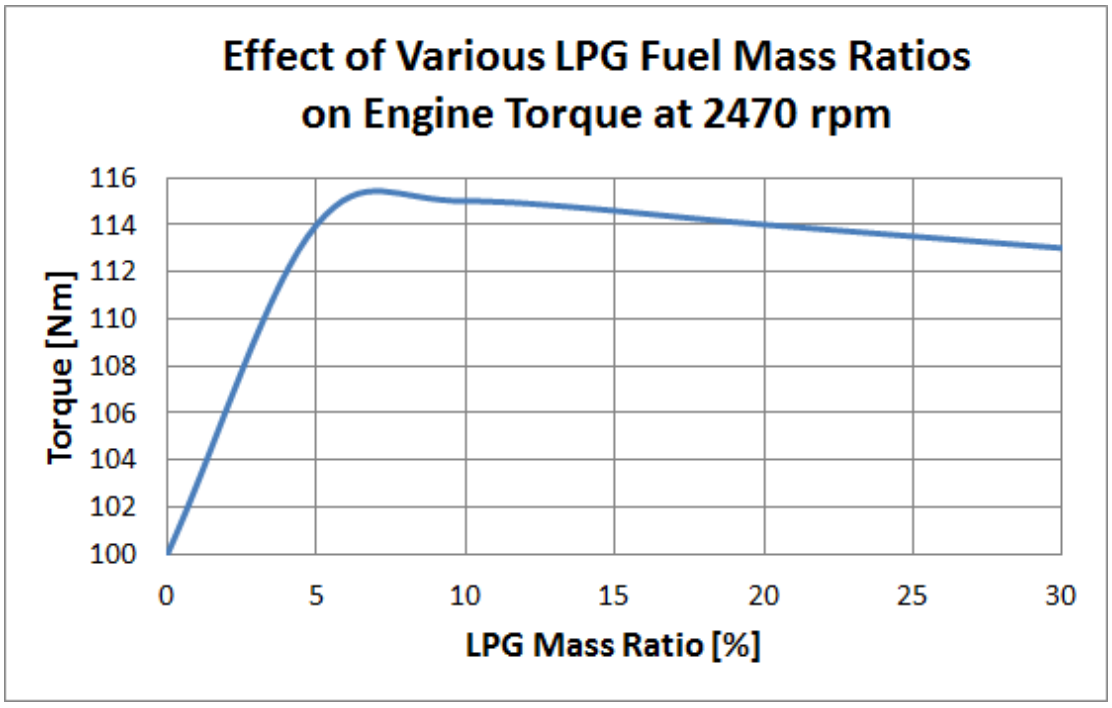

Figure 7.38 Variation of fuel mass ratio with engine torque at 2470 rpm

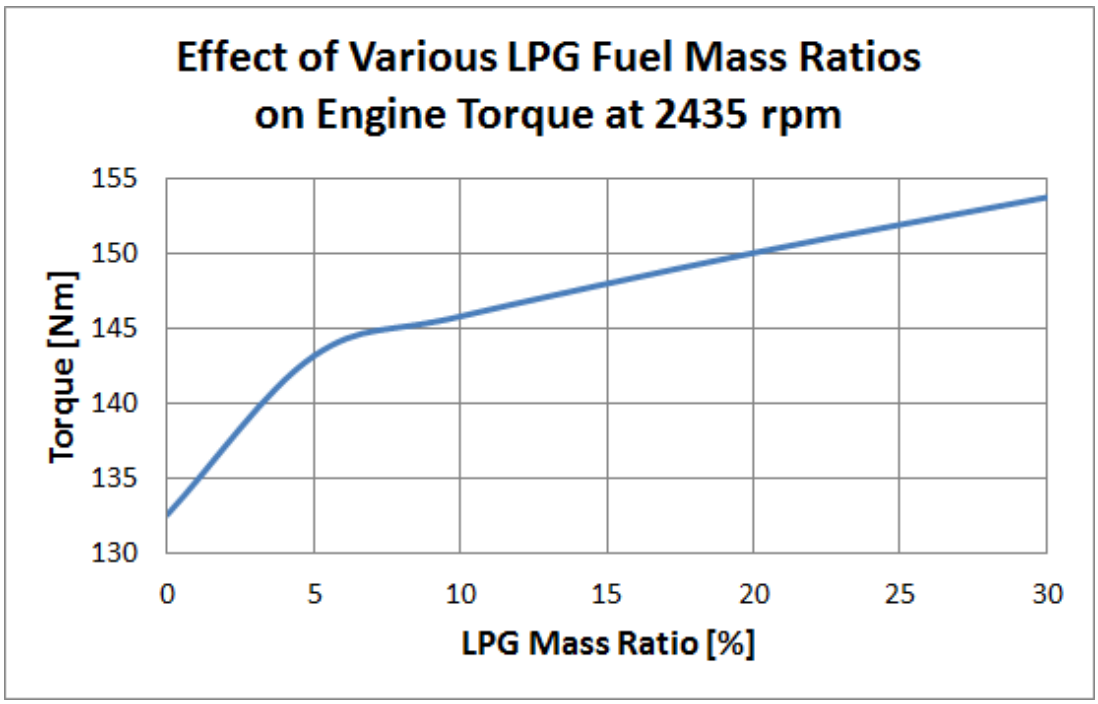

Figure 7.39 Variation of fuel mass ratio with engine torque at 2435 rpm

7.3.4 Power

The engine power is widely considered to be another significant parameter depicting engine performance. While torque is a measure of an engine's ability to do work, power is the rate at which work is done. As far as this fundamental parameter of power is concerned, the results suggest that there was a positive impact when the amount of LPG introduced to the combustion spaces is increased as shown in Figure 7.40, Figure 7.41 and Figure 7.42. On the overall, when compared to the pure diesel engine operation mode, each of the diesel-LPG engine operation modes postulates enhanced performance in terms of power.

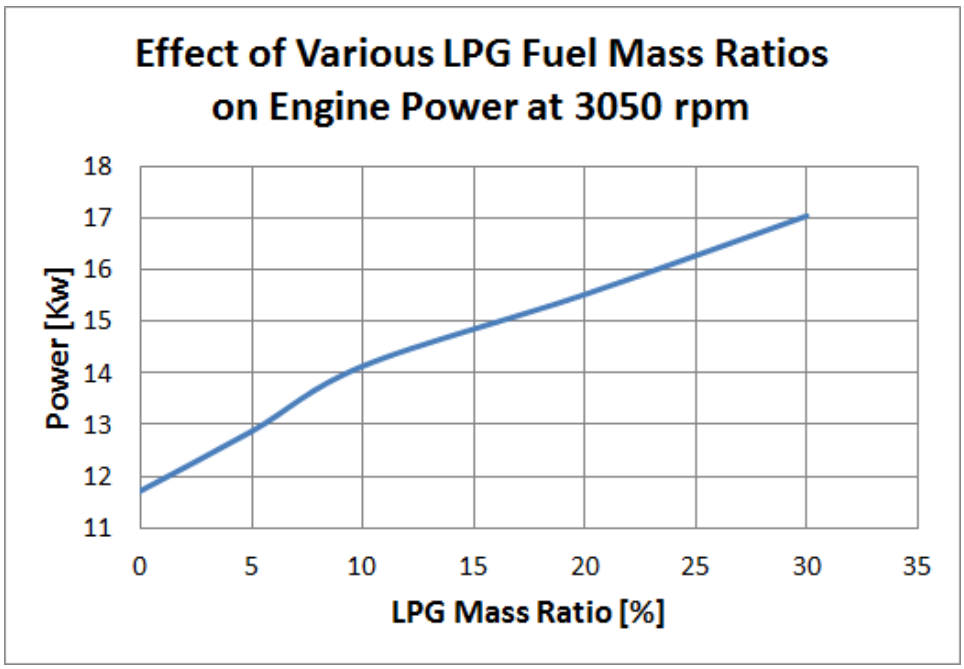

Figure 7.40 Variation of fuel mass ratio with engine power at 3050 rpm

In Figure 7.40, the results show that introducing 5% LPG will cause the power to improve from about 11.9 to 12.9 kW. Interestingly, for higher values of LPG mass ratio, the results highlight the improvement in Power. That is, 30% LPG mass fraction provides slightly more power than the 20% LPG mass fraction which in turn also provides higher power than the 10% LPG mass fraction.

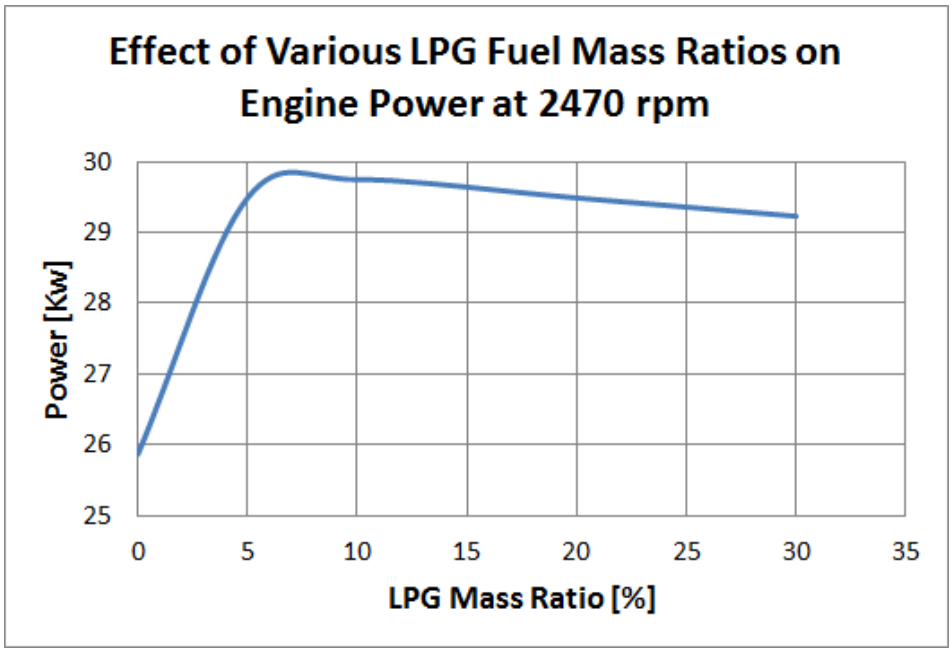

Figure 7.41 Variation of fuel mass ratio with engine power at 2470 rpm

Compared to the power for the diesel engine operation, the results in Figure 7.41 show a significant improvement to the engine power for the 5% LPG mass ratio, and 95% diesel mass ratio scenario examined. However, unlike the other case studies that are shown in Figure 7.40 and Figure 7.42, Figure 7.41 suggests that there is a slight drop in the power when the LPG mass ratio in the diesel-LPG fuel mixture is increased from 10 to 30%.

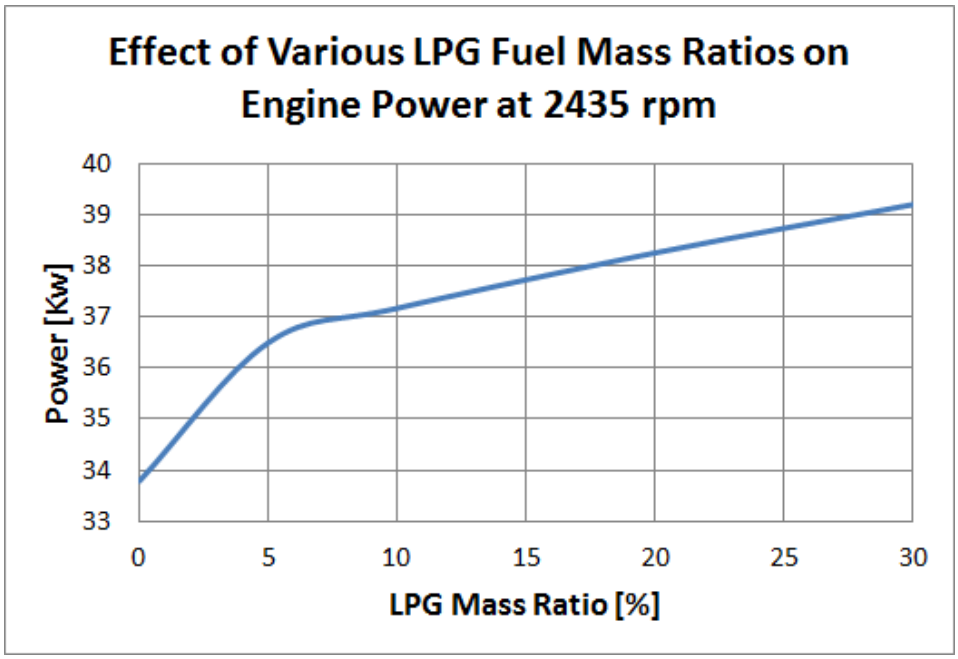

Figure 7.42 Variation of fuel mass ratio with engine power at 2435 rpm

Turning our attention to the case study at 2435 rpm, the results from the study suggest a fairly linear increment in power when LPG mass ratio in the diesel-LPG fuel mixture is increased from 10 to 30% as shown in Figure 7.42. Furthermore, the investigation of the behaviour of the engine power for this engine operating speeds strengthens the findings from the other previous cases wherein the power improves with the introduction of LPG.

7.3.5 Brake Specific Energy Consumption (BSEC)

To investigate the performance of the diesel-LPG engine operation in terms of fuel efficiency, it is more convenient to assess the fuel consumption by evaluating the

BSEC. This is believed to be so, because, in the diesel-LPG engine operation mode, the engine is run using two fuels simultaneously – a liquid fuel and a gaseous fuel. Consequently, regarding the use of different fuels with different heating values to run an engine, the BSEC is generally accepted to be a quite useful parameter as far as studying the engine performance is concerned. Given the above, this study presents comparisons of the BSEC with different mass ratios of LPG and diesel in the diesel-LPG fuel mixture as shown in Figure 7.43, Figure 7.44 and Figure 7.45. In this study, the BSEC is determined as a product of the brake specific fuel consumption and the calorific value taking into consideration the various fuel mass ratios at each instant. The BSEC designates the total amount of fuel energy (LPG and diesel) required to produce a kilowatt of power for an hour. The lower the BSEC, the higher the efficiency. Overall, the findings of the study illustrate that, as the LPG mass ratio increases, the BSEC decreases thereby postulating that the diesel-LPG operation is more fuel efficient for higher values of LPG mass ratio.

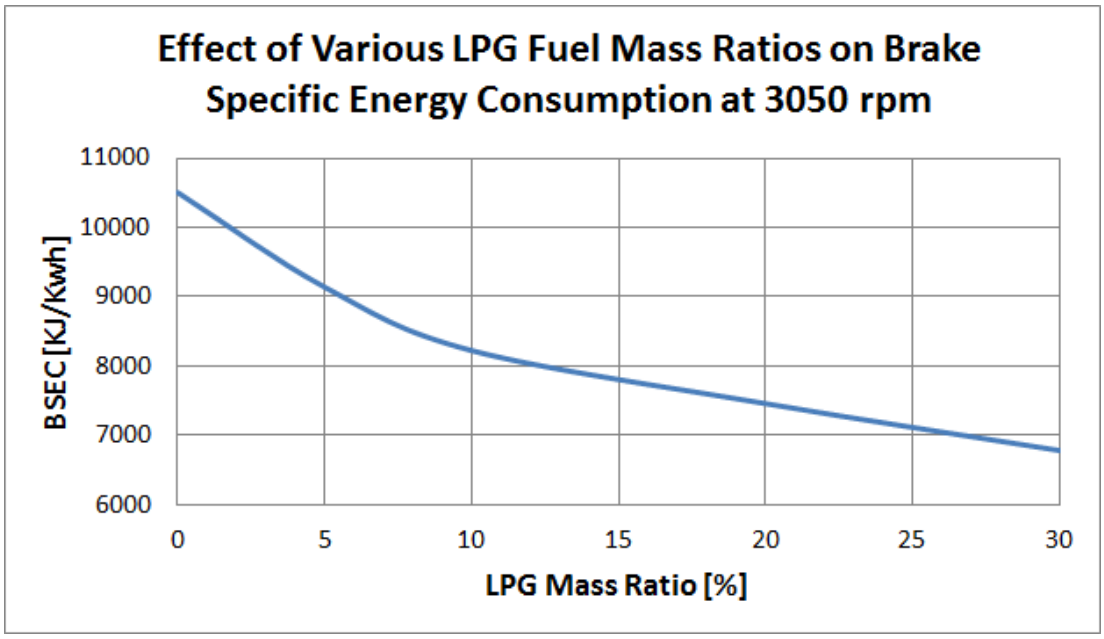

Figure 7.43 Variation of fuel mass ratio with BSEC at 3050 rpm

Figure 7.43 illustrates the variation of the BSEC with various quantities of LPG in the diesel-LPG fuel mixture. From Figure 7.43, it can be observed that, compared to the diesel engine operation, the BSEC is lower when any quantity of LPG is introduced to run the engine. Evidently, the higher the amount of LPG used, the

lower the BSEC. The results demonstrate a significant difference in BSEC values of the pure diesel operation compared to that when 30% LPG and 70% diesel mass ratio is used to run the engine.

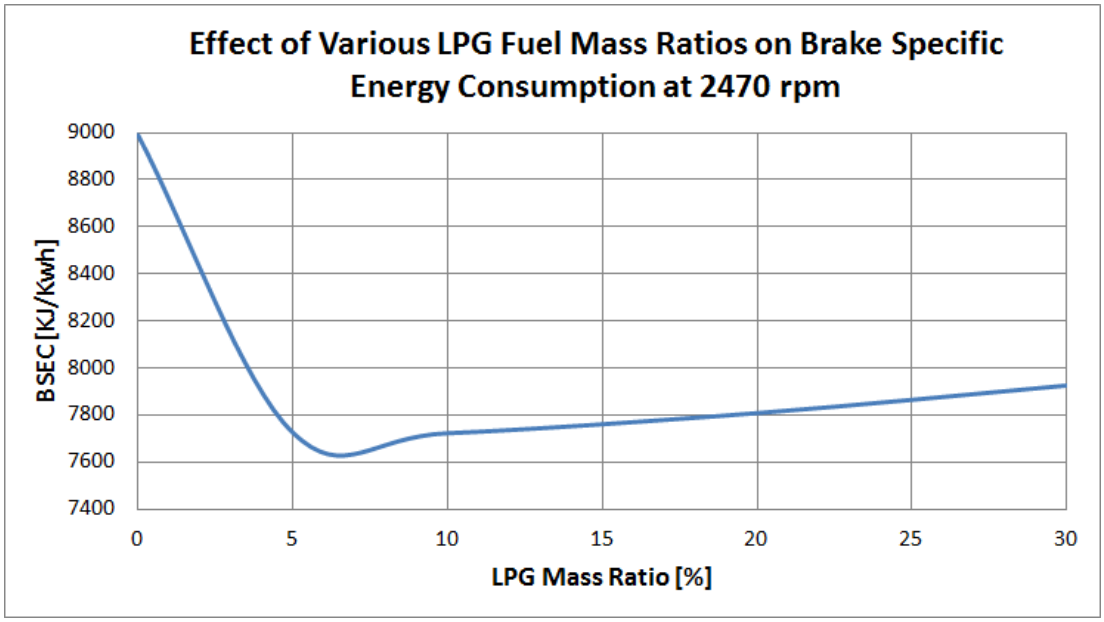

Figure 7.44 Variation of fuel mass ratio with BSEC at 2470 rpm

Further analysis of the BSEC behaviour at other engine speeds was carried out, and again, Figure 7.44 illustrates the variation of the BSEC with various quantities of LPG in the diesel-LPG fuel mixture. Similar to previous analysis at 3050 rpm, from Figure 7.44, it can be observed that, compared to the diesel engine operation, the BSEC is lower when any quantity of LPG is introduced to run the engine. However, for this case study shown in Figure 7.44, the results suggest that the higher the amount of LPG used, the higher the BSEC. As seen from the graph, the difference in the BSEC values for the various LPG fuel mass ratios is not very significant. The results demonstrate a substantial difference in BSEC values of the pure diesel operation compared to that when 30% LPG and 70% diesel mass ratio is used to run the engine.

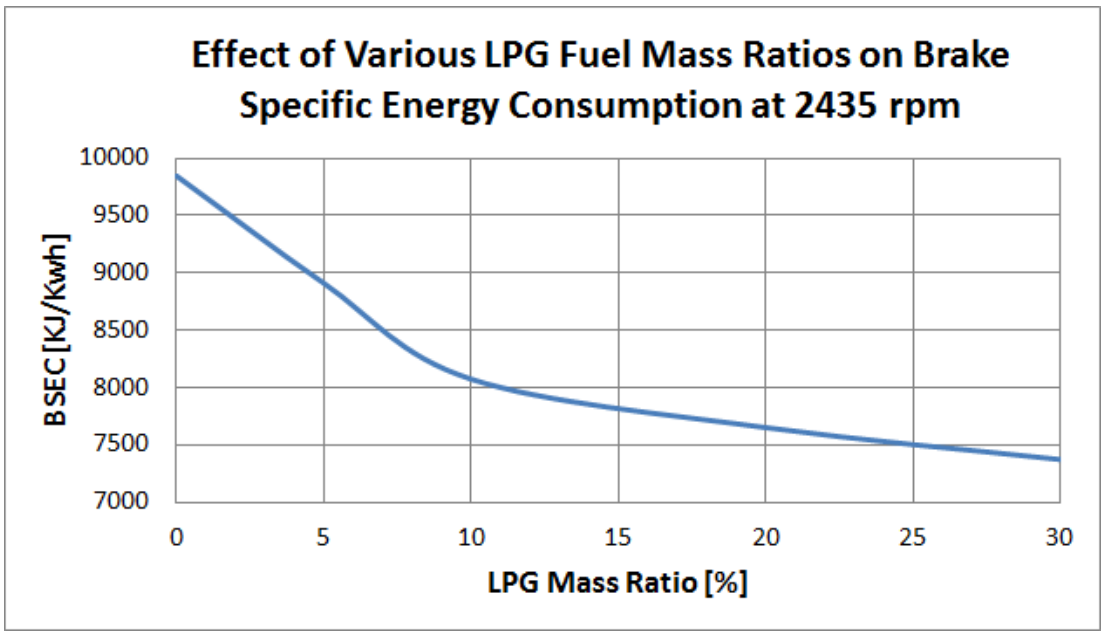

Figure 7.45 Variation of fuel mass ratio with BSEC at 2435 rpm

Comparative analysis involving the BSEC and various fuel mass ratios apportioned to the diesel-LPG fuel mixture was replicated for another engine operating speed. Again, Figure 7.45 illustrates the variation of the BSEC with various quantities of LPG in the diesel-LPG fuel mixture. The findings from this case study examined corroborate those from the 3050 rpm case study. Hence, from Figure 7.45, it can be observed that, compared to the diesel engine operation, the BSEC is lower when any quantity of LPG is introduced to run the engine. Evidently, the higher the amount of LPG used, the lower the BSEC. The results demonstrate a significant difference in BSEC values of the pure diesel operation compared to that when 30% LPG and 70% diesel mass ratio is used to run the engine.

7.3.6 Brake Thermal Efficiency (BTE)

Generally, efficiency (particularly the BTE) is widely considered to be quite a useful parameter in discussions pertaining to engine performance. BTE is the ratio of brake power output to the power input (also referred to as fuel power and depends on the calorific value and mass of fuel supplied). In this study, it was decided to computationally examine the BTE for the various case studies in relation to the

different fuelling scenarios, and the results are highlighted in Figure 7.46, Figure 7.47 and Figure 7.48. The BTE provides a means to assess how well an engine converts heat from the various fuel mixtures to mechanical energy. Overall, for all the engine operating regimes examined, the results show that using diesel-LPG fuel mixtures will provide higher BTE values compared to when the engine is run using pure diesel. In addition, with the exception of the results for the 2470 rpm case study, this study portrays the fact that as the LPG mass ratio in diesel-LPG fuel mixture increases from 5 to 30%, the BTE also increases.

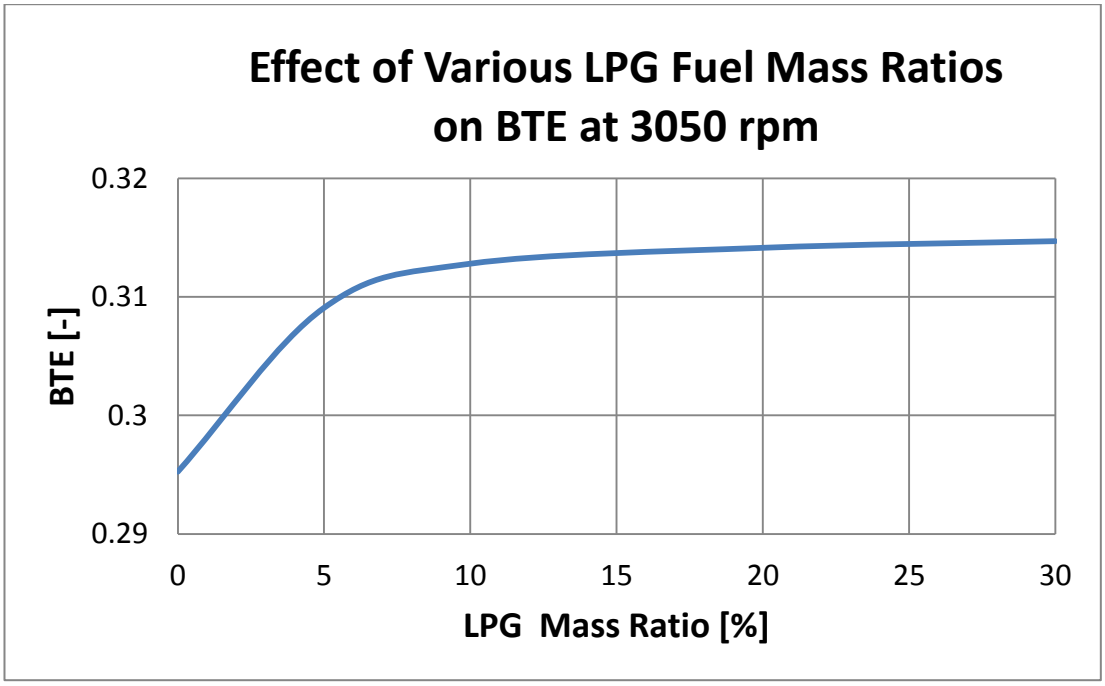

Figure 7.46 Variation of fuel mass ratio with BTE at 3050 rpm

Figure 7.46 demonstrates that there is no significant difference in the BTE values as the LPG fuel mass ratio in the diesel-LPG fuel mixture increases from 5 to 30% at the said engine operating speed. From the examination of this case study, it is remarkable that the highest mass ratio of LPG used in the diesel-LPG fuel mixture produces the highest BTE.

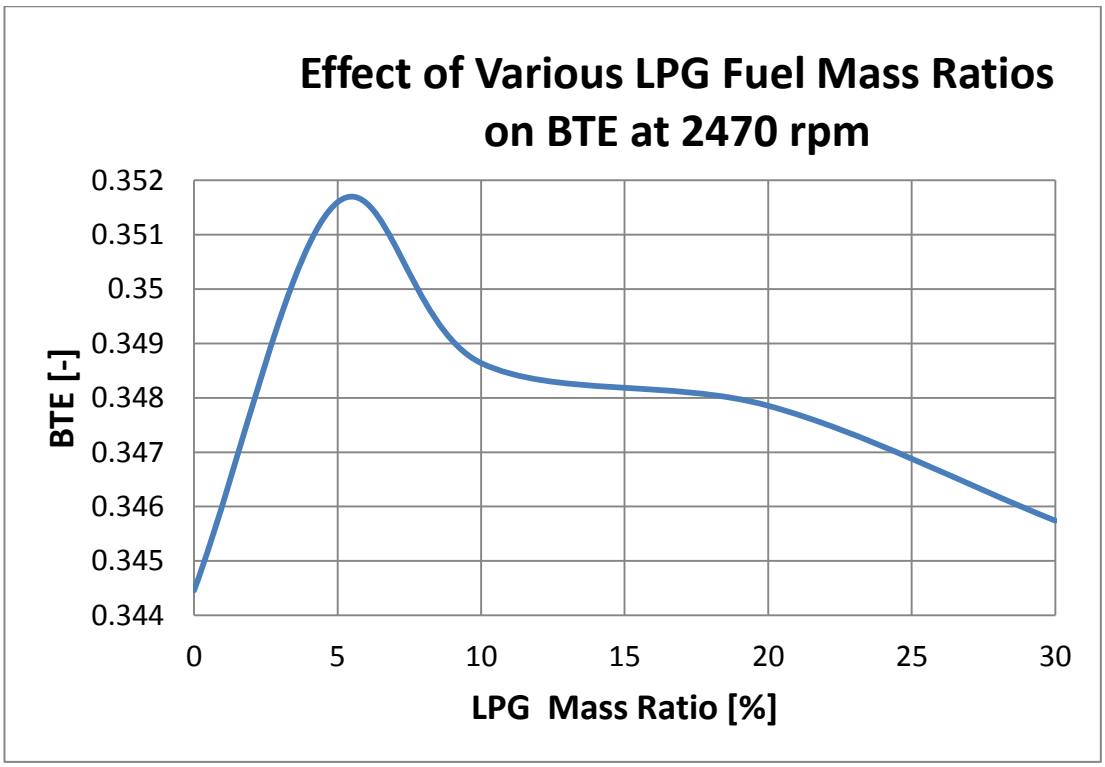

Figure 7.47 Variation of fuel mass ratio with BTE at 2470 rpm

Similar comparative analysis for another engine operating speed is shown in Figure 7.47, and it demonstrates that there is no significant difference in the BTE values as the LPG fuel mass ratio in the diesel-LPG fuel mixture increases from 5 to 30% at the said engine operating speed. However, unlike the results that are shown in the previous case study, Figure 7.47 shows the BTE to decrease slightly as the LPG mass ratio in the diesel-LPG fuel mixture increase. From the examination of this case study, it is remarkable that the highest mass ratio of LPG used in the diesel-LPG fuel mixture produces a BTE much closer to that of the pure diesel operation whereas the smallest amount of LPG quantity used produces the highest BTE.

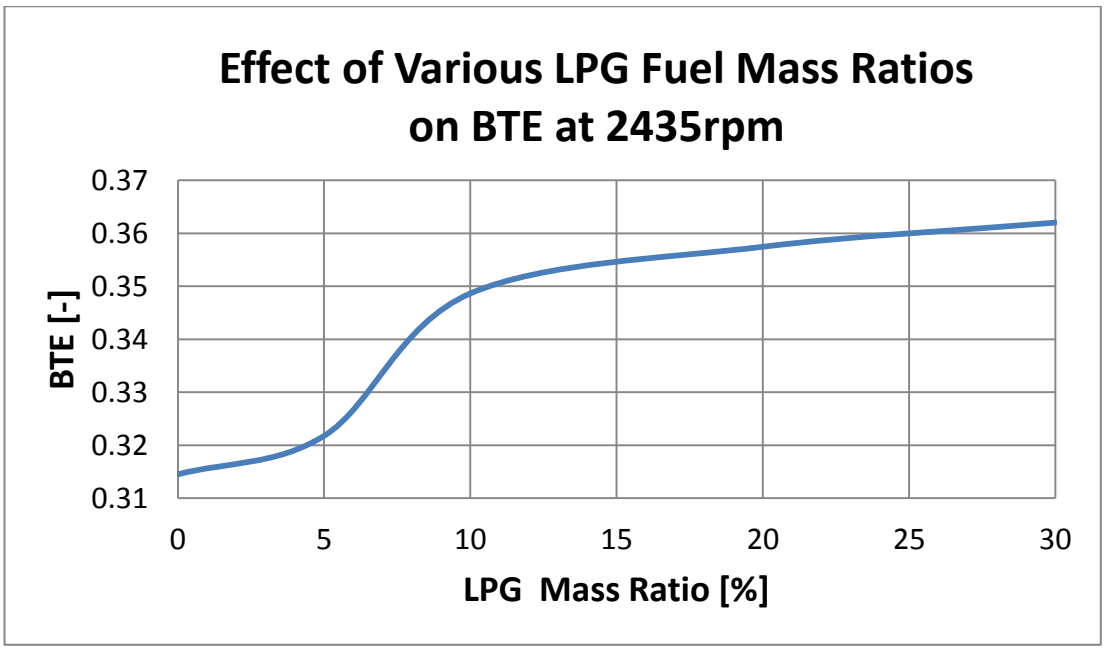

Figure 7.48 Variation of fuel mass ratio with BTE at 2435 rpm

Figure 7.48 further corroborates the findings observed from previous case studies examined in this thesis and demonstrates that there is no significant difference in the BTE values as the LPG fuel mass ratio in the diesel-LPG fuel mixture increases from 5 to 30% at the said engine operating speed. From the examination of this case study, it is remarkable that the highest mass ratio of LPG used in the diesel-LPG fuel mixture produces the highest BTE.

7.4 Volumetric Efficiency of the Diesel-LPG Engine

The BOOST pre-processor allows a plenum or measuring point to be specified as a reference location for the calculation of the air delivery ratio and the volumetric efficiency related to the intake manifold conditions. In the modelling approach used, the injection of LPG into the engine manifold (represented by the plenum shown in Chapter 5, Figure 5.3) replaces some of the space available that would have been filled by a corresponding quantity of air.

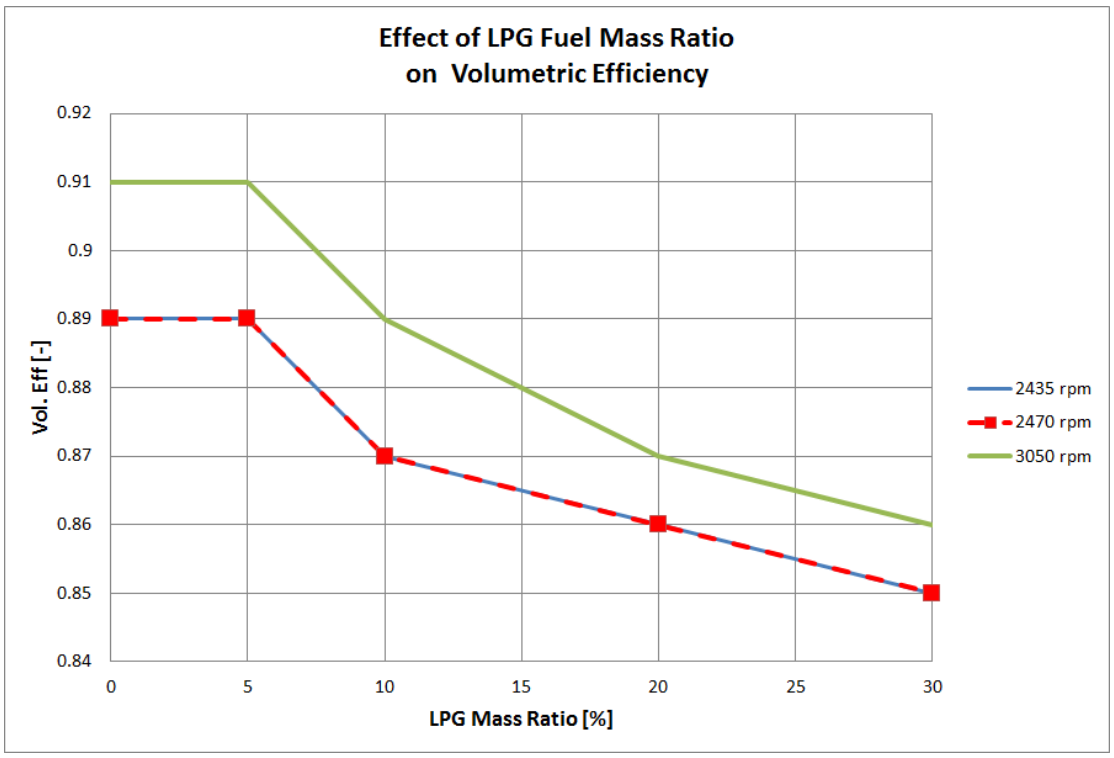

Figure 7.49 Impact of LPG fuel mass ratio on the volumetric efficiency

Consequently, as expected, the volumetric efficiency for the diesel-LPG engine operation is shown in Figure 7.49 to reduce as the quantity of the LPG fuel mass ratio increases regardless of the engine operating regime examined. In addition, for all the different fuel mass ratios used in the diesel-LPG fuel mixture, the results demonstrate that the volumetric efficiency is higher when the speed is higher.

7.5 Diesel-LPG Engine Emissions

In dual-fuel engines, changes in numerous factors affect the essential characteristics and amount of emissions that emanate from the exhaust. The numerous factors are enumerated in (Karim, 2015). Typically, the major constituents of dual-fuel engine exhaust consist of oxides of nitrogen (NO_x), unburned hydrocarbons (HC), particulate emissions and oxides of carbon (CO and CO_2) (Liu et al., 2013, Ma et al., 2013). To investigate the emission characteristics in this study, oxides of nitrogen (NO_x), carbon monoxide (CO) and soot were examined for the various case studies, and the results are shown in Figure 7.50, Figure 7.51 and Figure 7.52. Given that the

experimental facility at the disposal of this author could not measure emissions, the various emission models in this study could not be calibrated nor validated. Hence, the findings from this study are based strictly on computational simulation and the ability of the chosen AVL MCC combustion model to predict these emissions. That said, the various constants and multipliers for the emission models shown in Figure 5.12 were used based on the AVL Software user guidelines for naturally aspirated direct injection engines.

7.5.1 Nitrogen oxide (NO_x) emissions

In dual-fuel engines, air (which is mainly composed of oxygen and nitrogen) and the gaseous fuel are drawn into the combustion space. The air/gaseous fuel mixture is subsequently compressed, and then diesel fuel is later injected into the compressed mixture towards the end of the compression stroke. Ideally, in this process, the nitrogen in the air should not react with the oxygen allowing nitrogen to be emitted out of the engine. Nevertheless, because of the high temperatures associated with the combustion chamber of diesel-LPG engines, nitrogen reacts with the oxygen which leads to the formation of NO_x emissions. On the evidence of the above, it is obvious that temperature and oxygen concentration play a critical role in NO_x formation.

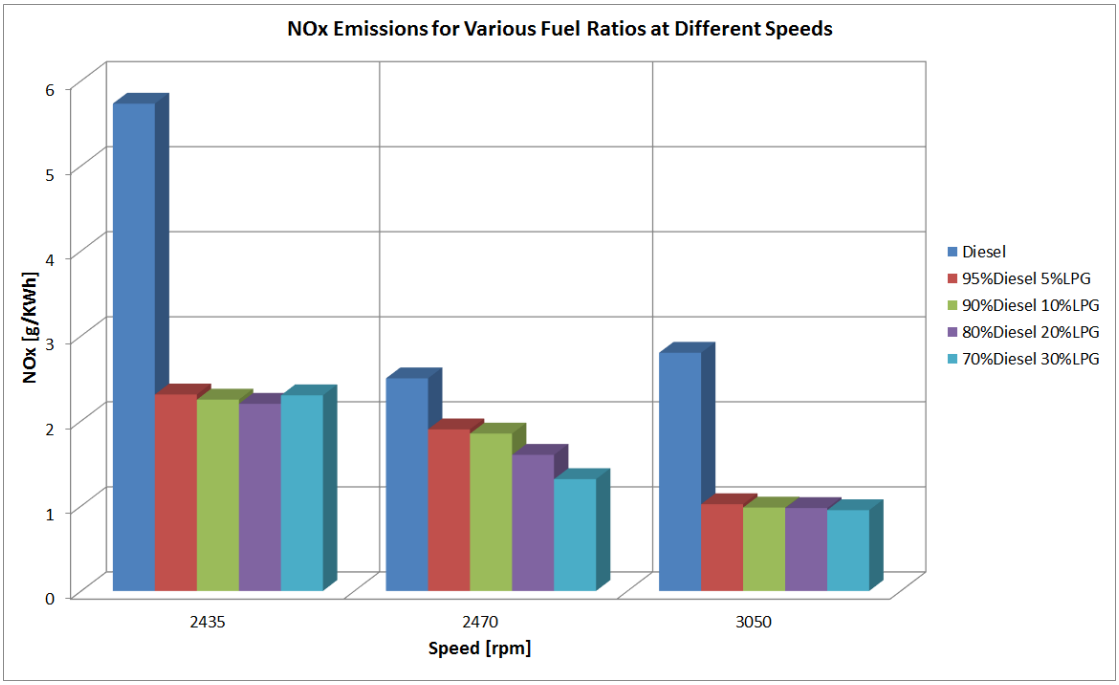

Figure 7.50 Comparison of NOx emissions at different speeds for various fuel mass ratios

Figure 7.50 depicts the results obtained following the comparative analysis of the predicted NO_x emissions for all the case studies examined in this thesis. According to the results, generally, the higher the speed, the lower the amount of NO_x predicted because the formation of NO_x depends on time. Therefore increasing engine speed will reduce the residual time available for NO_x formation. Furthermore, the results reveal that regardless of the speed, increasing the LPG fuel mass ratio in the diesel-LPG fuel mixture will lead to a reduction in the NO_x emissions. This is because the formation of NO_x depends on the oxygen concentration and the presence of LPG, leads to a reduction of the oxygen concentration at the onset of NO_x formation which consequently causes the NO_x emissions to reduce.

For the 3050 rpm case study, the results suggest that there is no significant difference in the NO_x emissions when the LPG fuel mass ratio in the diesel-LPG fuel mixture is increased from 5 to 30%. The same analysis applies to the case study at the engine operating speed of 2435 rpm. Interestingly, from the visual perspective offered by the results of the case study when the engine operating speed is 2470 rpm, it is perceived that the decrease in NO_x emissions when the LPG fuel mass ratio in the diesel-LPG fuel mixture increases, is considerable. The results of this particular case

study have further strengthened my confidence in the hypothesis that as the amount of LPG introduced increases, the amount of NO_x emissions produced, reduces.

Turning attention to a comparison between the NO_x emissions associated with the pure diesel operation and the diesel-LPG operation, there was a significant difference between their respective NO_x values. Evidently, the NO_x emissions produced by the diesel-LPG engine operation were lower than those produced by the corresponding pure diesel operation at each engine operating speed examined.

7.5.2 Carbon monoxide (CO) emissions

Carbon monoxide is a colourless, odourless, poisonous gas that can arise due to incomplete combustion. When there is not enough oxygen to convert all carbon to carbon dioxide, some fuel does not get burned, and some carbon would end up as CO. CO is thought to be an undesirable emission and also signifies lost chemical energy that was not fully used in the engine.

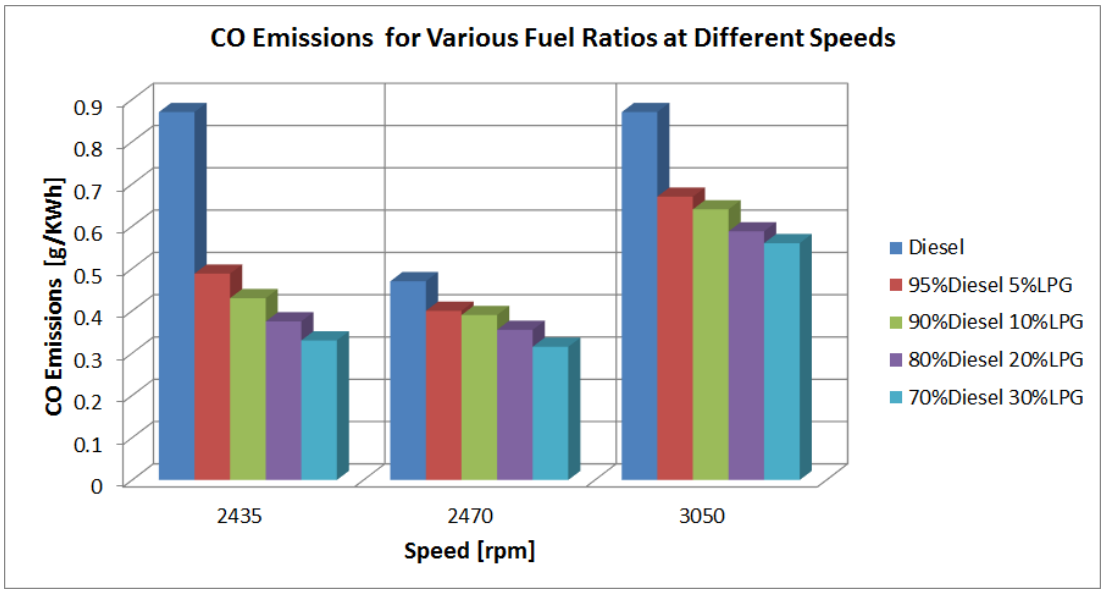

Figure 7.51 Comparison of CO emissions at different speeds for various fuel mass ratios

Figure 7.51 presents a comparative analysis for the CO emissions associated with diesel engine operation as well as the diesel-LPG operation taking into consideration

different LPG and diesel fuel mass ratios. Generally, the results show that, for all the case studies examined, the CO emissions of the pure diesel operation will be higher than those associated with the corresponding diesel-LPG engine operation. Since the local mixtures in the case of diesel-LPG fuelling are richer, this accounts for the purported decrease in CO emissions shown in Figure 7.51.

The results also highlight that as the LPG mass ratio is increased in the diesel-LPG fuel mixture at each operating speed, the CO emissions progressively decrease. Therefore, the highest amount of LPG used is depicted to emit the least amount of CO.

7.5.3 Soot

The exhaust emanating from compression ignition engines contains solid carbon soot particles. Soot comprises mainly of carbon. However, other elements like oxygen and hydrogen are commonly present in minute amounts. Soot is produced during the high-temperature combustion of the fuel.

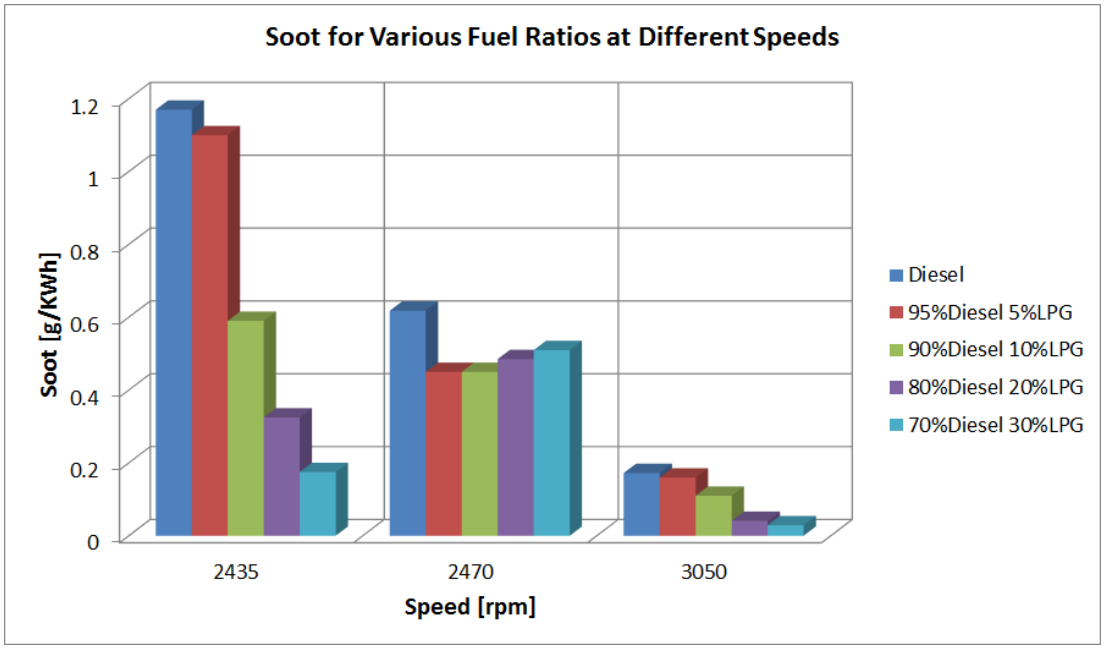

Figure 7.52 Comparison of soot at different speeds for various fuel mass ratios

Figure 7.52 presents the soot emission results obtained for the pure diesel operation and the different diesel-LPG fuel scenarios examined at each respective engine operating speed. It is widely considered that the diffusion combustion plays a critical part and is the major cause of soot formation. Consequently, a reduction in the rate of diffusion combustion (as shown in the various heat release diagrams in section 7.2.3) leads to a decrease of soot as revealed in Figure 7.52

With the exception of the results associated with the case study at 2470 rpm, the study postulates that increasing the LPG mass fraction in the diesel-LPG fuel mixture will lead to a reduction in the soot quantity emitted. For the different LPG mass ratios, the drop in soot quantity is shown to be more significant at 2435 rpm. Another attracting observation from the comparative analysis is the fact that, the soot is predicted to decrease as the speed increases (with the 80% diesel and 20% LPG, 70% diesel and 30% LPG scenario being the exceptions). As revealed in Figure 7.52, note that the soot produced is smallest for the 3050 rpm case study.

7.6 Synopsis of Chapter Seven

In summary, this chapter has presented the results obtained after it reminded the reader of the aim of this study. The results presented and discussed were categorised into four main sections that addressed the diesel-LPG combustion, the diesel-LPG performance, the impact of LPG introduction on the volumetric efficiency, and the diesel-LPG engine operation. Generally, the findings from this study are significant in the sense that, based on the computational methodology adopted, they provide evidence suggesting that increasing the LPG fuel mass ratio in a diesel-LPG fuel mixture used to run an engine will improve the performance and reduce emissions. Consequently, the findings detailed in this chapter might have important implications for helping retrofitted engines to reduce emissions. The next chapter concludes the study and provides recommendations given that the findings of chapter seven might have several implications for future research into diesel-LPG engine operation.

8 Conclusions and Recommendations

Since the main of this study was, as mentioned in Chapter two, to numerically investigate the performance and emission characteristics associated with dual fuel engine operation wherein LPG and diesel fuels are simultaneously used, the work carried out in this research has been written and presented in eight chapters as earlier mentioned.

Chapter one introduced the entire study. It stated the research problem and also provided the rationale and background for the study. Additionally, it provided evidence to support the choice of gaseous fuel usage in internal combustion engines. Chapter one then closed by giving an outline of the thesis and a summary of its contribution.

Chapter two was quite short and concise. It specified the central aim and enumerated some specific objectives of the study.

Chapter three reviewed the literature relevant to the study. Given the nature of the research carried out, this chapter additionally examined information about modelling and simulation of combustion in ICEs. The chapter concluded by presenting some of the author's views in a critical appraisal of the literature.

The overall methodological approach adopted for this research was organised and described across three chapters (four, five and six).

Chapter four began by outlining the experimental study carried out. It illustrated the set-up of the engine within the laboratory. Additionally, it described the process of modifying diesel engines to operate as dual fuel engines.

Then, Chapter five discussed the computation and simulation of the pure diesel and diesel-LPG engine operation, implemented using AVL BOOST. It also discussed and provided a brief overview of the theoretical framework of several sub-models that were used to build the overall one-dimensional engine model.

Chapter six provided insight into the calibration and validation of the various models based on the cylinder pressure data and several performance parameters, notably the maximum cylinder pressure, the timing of peak cylinder pressure, power and torque.

Chapters seven presented and discussed the results obtained. The results presented focused on the combustion, performance, volumetric efficiency and emissions of the diesel-LPG engine operation in relation to the diesel engine operation.
Chapter eight presents the assumptions, limitations and significant contribution while drawing conclusions and providing recommendations for future research.

8.1 Assumptions

In most instances, the nature of research requires that the researcher must assume something(s) to discover something else. In other words, research is fundamentally built upon assumptions. In the same way, the research presented herein is based on several assumptions. All things being considered, it, therefore, seems reasonable to enumerate the assumptions upon which the results presented in this thesis are based upon. Given that the main research methodology used in this study involved computational simulation of the diesel and diesel-LPG engine operations using AVL BOOST, significantly, the following assumptions that were considered when developing the models are worth mentioning. They include:

- The pressure and temperature of the cylinder charge are uniform and vary with crank angle
- The cylinder content is homogenous at each instant
- The cylinder mixture behaves like an ideal gas and hence can be modelled using ideal gas laws
- The study assumes that gas leakage through valves and piston rings is negligible; hence the mass remains constant
- Additionally, the heat transfer from gas to the wall is assumed to be as a result of convection primarily.
- At each instant, thermodynamic equilibrium is assumed
- All the cylinders are considered to behave in like manner. Hence, the four cylinders in the engine have been modelled identically.
- LPG is assumed to consist of Propane and Butane in the ratio 60:40 respectively

8.2 Limitations

It is plausible that a number of limitations could have influenced the results presented in this study. The first is that the diesel-LPG model could not be calibrated and validated. This limitation underlines the difficulty of collecting experimental data related to the diesel-LPG engine operational mode owing to a prolonged break down of the experimental facility. The limitation is further compounded by the lack of relevant published data relating to cylinder pressure measurement for the test engine under consideration in this study when it is being run simultaneously using diesel and LPG. Despite this limitation, the experimental data pertaining to the diesel engine operation that was obtained was efficiently used to calibrate and validate the model used to simulate the pure diesel engine operation

As the focus of this study was on investigating (computationally) the diesel-LPG engine performance and emissions in relation to the pure diesel engine operation while predominantly taking into consideration various diesel and LPG fuel mass ratios, it is not inconceivable that the diesel-LPG model was developed using the performance characteristics of the pure diesel operation as the benchmark. Having said that, it is also not inconceivable that the availability of experimental data pertaining to the cylinder pressures (when diesel and LPG fuels were used to run the engine), would probably have led to similar evaluations if the same focus was kept while investigating the parameters presented in this thesis.

The second limitation is that, unfortunately, it was not possible to obtain experimental measurements for the various emissions as the test facility available was not equipped with such equipment. Despite this limitation, owing to the fact that the AVL mixing controlled combustion model used can predict emissions, from a purely computational investigation perspective the significant relationships of NO_x, CO and Soot vis-à-vis the various LPG and diesel fuel mass ratios could be examined.

Despite these limitations, the methodological approach adopted in this study represents a viable research methodology and has led to the many exciting

observation presented in chapter seven of this study. Despite these exciting findings and bearing in mind the limitations enumerated above, the results from this study should consequently be treated with the utmost caution and applying due diligence whenever and wherever necessary.

8.3 Significant Contribution

This thesis, based on a report of research that reflects sound practice, embodies insight into research focused on the numerical investigation of the performance and emission characteristics associated with dual fuel engine operation wherein LPG and diesel fuels are simultaneously used. The importance and significance of using alternative fuels that are more environmental-friendly along with conventional fuels to run direct injection engines cannot be emphasised too much. Therefore, compared to the diesel engine operation, the findings of this study, which systematically illustrate improved engine performance and reduced emissions of the diesel-LPG engine operation, demonstrate just how valuable the simultaneous use of an environmental-friendly fuel along with diesel is.

- The significant – albeit modest – contribution of this thesis consists of contributing to the discourse about dual-fuel engine operation vis-à-vis the diesel engine operation with a particular focus on examining the impact that, increasing the LPG mass ratio exerts on the engine performance and emissions. Given that research is not done in isolation but is instead a discourse among researchers, each providing evidence and arguments that contribute to knowledge and provide insight, this thesis, on its part has provided evidence to substantiate the findings made while presenting the limitations with which the conclusions were obtained.
- Predominantly, the sort of significant contribution offered by this thesis pertains to re-contextualization of existing theory, techniques or models. This thesis has demonstrated the application of existing theoretical models to a new context – one that involves using them to simulate the diesel-LPG operation of an originally pure direct injection diesel engine operation. As far

as the author is aware, at the time of writing this thesis, this is the first time that the AVL MCC model has been applied to simulate the diesel-LPG engine operation for the VW 1.9L naturally aspirated engine. The AVL MCC technique used in modelling the combustion clearly has an advantage over the vibe or double vibe technique since it can predict while the vibe and double vibe essentially predefine. Furthermore, the methodological framework used embodies a clear and systematic original research work.

- Another sort of contribution from this thesis that is worth mentioning is the drawing together of two ideas and showing that their combination reveals something meaningful and useful as far as diesel-LPG engine operation is concerned. As mentioned in chapter five of this study, the computational methodology involved the combination of the AVL MCC idea/model with the Andree and Pacherneeg ide/model. The amalgamation of these two ideas/models has led to something meaningful and useful as shown by the results throughout chapter seven.
- Turning our attention to the significance of the findings from this study, why should anyone care? Why should they matter? They should because the findings from this study further widen our knowledge about the potential of using an environmental-friendly fuel along with conventional diesel to improve the performance of existing original pure direct injection naturally aspirated diesel engines.
- The results from this study offer evidence to support the hypothesis stipulated in chapter two that usage of a gaseous fuel along with conventional diesel as an alternative internal combustion engine fuelling option is thought to be very promising. Moreover, the study set out to further investigate this thought and the hypothesis that, the higher the amount of gaseous fuel used to substitute diesel, the more environmentally friendly the internal combustion engine (in this case diesel/LPG engine) will be. The findings from this study confirm and validate the usefulness of this hypothesis.
- This study provides additional informative support that can be beneficial to a plethora of stakeholders associated with emission regulations, modification of diesel engines to diesel-LPG engines etc.

The following publications emanated in the course of doing this research. They are:

- Anye Ngang, E. and Ngayihi Abbe, C. (2018). Experimental and numerical analysis of the performance of a diesel engine retrofitted to use LPG as secondary fuel. Applied Thermal Engineering, 136, pp.462-474.
- Anye, E. (2016). Numerical Investigation of a 4-Stroke, 8-Cylinder Diesel Engine Using a 1-D Code. American Scientific Research Journal for Engineering, Technology, and Sciences, [online] 26(4). Available at: http://www.asrjetsjournal.org/index.php/American_Scientific_Journal/article/view/2391
- Anye, E. (2015). Energy Efficiency via Engine Improvements: A review of Dual Fuel Engine Development. In: Low Carbon Shipping - SCC Conference 2015. [Online]. Available at: http://lowcarbonshipping.co.uk/files/Ben_Howett/SCC2015/energy_efficiency_via_engine_improvements_a_review_of_dual_fuel_engine_development.pdf

8.4 Conclusions

Returning to the hypothesis posed in chapter two, section 2.3 and bearing in mind the results presented in chapter seven, it is now possible to state that, with the exception of a few cases, the higher the amount of LPG used to substitute diesel, the lower the NO_x, CO and soot emissions would be produced at various engine operating speeds. Following the computational investigation, this thesis has given an account of the performance and emission characteristics of the diesel-LPG engine operation predominantly taking into account variations if fuel mass ratios of diesel and LPG. The mixing controlled combustion model used in this study is capable of describing the combustion in direct injection diesel engines. It has been used to model diesel-LPG engine performance and demonstrated reasonable results, suggesting that it can be used satisfactorily to describe the effect of different fuel mass ratios on the performance and emission parameters examined. Taken together, the presented results suggest that under similar engine operating regimes, the diesel-LPG engine operation demonstrates enhanced performance compared to the pure diesel operation

for the cases examined in this study. The upshot of this is the possibility that modifying existing direct injection naturally aspirated diesel engines to allow them also function with diesel and LPG can lead to them performing better while exhibiting a reduction in emissions. While providing possible clues for future research, the work carried out within the stipulated limitations, provides a platform for concluding that increasing the LPG fuel mass ratio by up to 30%, can improve the performance while accounting for reduced emissions. Generally, the diesel-LPG engine operation showed better performance than the corresponding pure diesel operation regardless of the fuel mass ratio investigated. The current findings from this study might have important implications for helping to reduce emissions as the diesel-LPG engine operation has shown its potential to contribute to the reduction of specific emissions emanating from naturally aspirated direct injection engines. This could hypothetically lend support to advocacy for the modification of existing conventional naturally aspirated direct injection diesel engines to be modified to permit them to equally operate using both diesel and LPG. Therefore, in my view, this study and its findings constitute a significant initial step towards the above.

8.5 Recommendations

It is hoped that this research will serve as a basis for future studies. From the difficulties associated with experimentally collecting cylinder pressure data for the diesel-LPG engine operation, it is suggested that future studies make that a top priority as this will go a long way to help calibrate and validate the computational models. Additionally, it is recommended that further data collection and experimentation of the diesel-LPG engine operation would be required to quantitatively determine precisely how these different mass ratios actually and realistically affect the various performance and emission parameters computationally investigated in this study.

Lastly, while this study has used a one-dimensional model to obtain meaningful results, it is recommended that more detailed studies utilise three-dimensional computational models as they tend to be more detailed.

BIBLIOGRAPHY

ABD-ALLA, G. H., SOLIMAN, H. A., BADR, O. A. & ABD-RABBO, M. F. 2000. Effect of pilot fuel quantity on the performance of a dual fuel engine. *Energy Conversion & Management* 41**,** 559-572.

ABD-ALLA, G. H., SOLIMAN, H. A., BADR, O. A. & ABD-RABBO, M. F. 2002. Effect of injection timing on the performance of a dual fuel engine. *Energy Conversion and Management,* 43**,** 269-277.

ANANT, J., POONIA, M. & JETHOO, A. 2012. Mathematical Modeling of the Dual Fuel Engine Cycle.

ANDREE, A. & PACHERNEGG, S. J. 1969. Ignition Conditions in Diesel Engines. *SAE Transactions,* 78**,** 1082-1106.

ARGUSMEDIA. 2016. *Statistical Review of Global LPG 2016* [Online]. Available: www.argusmedia.com/~/media/files/pdfs/white-paper/statistical-review-of-global-lpg-2016.pdf?la=en [Accessed 30 May 2017].

ASHOK, B., ASHOK, S. D. & KUMAR, C. R. 2015. LPG diesel dual fuel engine–A critical review. *Alexandria Engineering Journal,* 54**,** 105-126.

ASLAM, M., MASJUKI, H., KALAM, M., ABDESSELAM, H., MAHLIA, T. & AMALINA, M. 2006. An experimental investigation of CNG as an alternative fuel for a retrofitted gasoline vehicle. *Fuel,* 85**,** 717-724.

ASSANIS, D. N., FILIPI, Z. S., FIVELAND, S. B. & SYRIMIS, M. 2003. A predictive ignition delay correlation under steady-state and transient operation of a direct injection diesel engine. *Journal of Engineering for Gas Turbines and Power,* 125**,** 450-457.

AVL 2014. AVL BOOST Theory: Combustion models - pre-defined heat release.

BADR, O., KARIM, G. & LIU, B. 1999. An examination of the flame spread limits in a dual fuel engine. *Applied Thermal Engineering,* 19**,** 1071-1080.

BARBOUR, T., CROUSE, M. & LESTZ, S. 1986. Gaseous fuel utilization in a light-duty diesel engine. SAE Technical Paper.

BARI, S. 1996. Effect of carbon dioxide on the performance of biogas dual fuel engine. *WREC***,** 1-4.

BENSON, R. S. & WHITEHOUSE, N. D. 1979. Internal Combustion Engines. 1st ed.: Pergamon.

BLAZEK, J. 2015. *Computational fluid dynamics: principles and applications*, Butterworth-Heinemann.

BORA, B. J., DEBNATH, B. K., GUPTA, N., SAHOO, N. & SAHA, U. 2013. Investigation on the flow behaviour of a venturi type gas mixer designed for dual fuel diesel engines. *Int. J. Emerging Technol. Adv. Eng,* 3**,** 202-209.

BORG, J. M. & ALKIDAS, A. C. 2008. Investigation of the effects of autoignition on the heat release histories of a knocking SI engine using Wiebe functions. SAE Technical Paper.

CAMERETTI, M., TUCCILLO, R., DE SIMIO, L., IANNACCONE, S. & CIARAVOLA, U. 2016. A numerical and experimental study of dual fuel diesel engine for different injection timings. *Applied Thermal Engineering,* 101**,** 630-638.

CARLUCCI, A. P., DE RISI, A., LAFORGIA, D. & NACCARATO, F. 2008. Experimental investigation and combustion analysis of a direct injection dual-fuel diesel–natural gas engine. *Energy,* 33**,** 256-263.

CAT. 2018. *MAK Dual fuel* [Online]. Available: https://www.cat.com/en_US/by-industry/marine/dual-fuel.html [Accessed 26/09/2018 2018].

CEVIZ, M. A., KALELI, A. & GÜNER, E. 2015. Controlling LPG temperature for SI engine applications. *Applied Thermal Engineering,* 82**,** 298-305.

CHALLEN, B. & BARANESCU, R. 1999. *Diesel engine reference book*, Butterworth-Heinemann Ltd.

CHIODI, M. 2011. Simulation of Internal Combustion Engines. *An Innovative 3D-CFD-Approach towards Virtual Development of Internal Combustion Engines.* Springer.

CHIODI, M. & BARGENDE, M. 2001. Improvement of engine heat-transfer calculation in the three-dimensional simulation using a phenomenological heat-transfer model. SAE Technical Paper.

CHMELA, F., ORTHABER, G. & SCHUSTER, W. 1998. Die Vorausberechnung des Brennverlaufs von Dieselmotoren mit direkter Einspritzung auf der Basis des Einspritzverlaufs. *MTZ-Motortechnische Zeitschrift,* 59**,** 484-492.

CHMELA, F. G. & ORTHABER, G. C. 1999. Rate of Heat Release Prediction for Direct Injection Diesel Engines Based on Purely Mixing Controlled Combustion. SAE International.

CHRISTEN, C. & BRAND, D. 2013. Gas and Dual fuel engines as a clean and efficient solution *International Council on Combustion Engines.* Shanghai.

CLIFT, R., GRACE, J. R. & WEBER, M. E. 2005. *Bubbles, drops, and particles*, Courier Corporation.

CUMMINS. 2018. *Dual fuel engines for drilling* [Online]. Available: https://www.cummins.com/engines/drilling/dual-fuel-engines-drilling [Accessed 26/09/2018 2018].

DEMIR, U., YILMAZ, N., COSKUN, G. & SOYHAN, H. S. 2015. Evaluation of zero dimensional codes in simulating IC engines using primary reference fuel. *Applied Thermal Engineering,* 76**,** 18-24.

DENT, J. C. 1971. A Basis for the Comparison of Various Experimental Methods for Studying Spray Penetration. SAE International.

DHOLE, A., YARASU, R. & LATA, D. 2016. Investigations on the combustion duration and ignition delay period of a dual fuel diesel engine with hydrogen and producer gas as secondary fuels. *Applied Thermal Engineering,* 107**,** 524-532.

DIMITROV, D. & PIRKER, D.-I. G. 2006. Konsistente Methodik zur Vorausrechnung der Verbrennung in Kolbenkraftmaschinen. *MTZ-Motortechnische Zeitschrift,* 67**,** 468-474.

DOS SANTOS, F. & LE MOYNE, L. 2011. Spray atomization models in engine applications, from correlations to direct numerical simulations. *Oil & Gas Science and Technology–Revue d'IFP Energies nouvelles,* 66**,** 801-822.

ELKOTB, M. 1982. Fuel atomization for spray modelling. *Progress in Energy and Combustion Science,* 8**,** 61-91.

EPA, U. S. 2007. Light-Duty Automotive Technology and Fuel Economy Trends: 1975 through 2007.

ERGENÇ, A. T. & KOCA, D. Ö. 2014. PLC controlled single cylinder diesel-LPG engine. *Fuel,* 130**,** 273-278.

ERKUŞ, B., KARAMANGIL, M. I. & SÜRMEN, A. 2015. Enhancing the heavy load performance of a gasoline engine converted for LPG use by modifying the ignition timings. *Applied Thermal Engineering,* 85**,** 188-194.

ESTHER, P. 2016. *LPG: International price trends – An overview* [Online]. Available: www.wlpga.org/wp-content/uploads/2016/05/2.-Esther-Pua-Gold-Coast-2016.pdf [Accessed 30 May 2017].

EUROSTAT. 2017. *Energy price statistics* [Online]. Available: http://ec.europa.eu/eurostat/statistics-explained/index.php/File:Consumer_prices_of_petroleum_products,_EU,_2005%E2%80%9315_(%C2%B9)_(EUR_per_litre)_YB16.png [Accessed 6 June 2017].

FERGUSON, C. R. & KIRKPATRICK, A. T. 2015. *Internal combustion engines: applied thermosciences*, John Wiley & Sons.

FU, Y. & XIAO, B. 2017. A method to precisely control the diesel substitution rate of diesel-natural gas dual fuel engine. *Applied Thermal Engineering*.

FUJIMOTO, H., SATO, G. & TANABE, H. 1980. Illumination delay in diesel spray. *JASE Paper***,** 149.

GALINDO, J., CLIMENT, H., PLÁ, B. & JIMÉNEZ, V. 2011. Correlations for Wiebe function parameters for combustion simulation in two-stroke small engines. *Applied Thermal Engineering,* 31**,** 1190-1199.

GHOMASHI, H. 2015. *Modelling the combustion in a dual fuel HCCI engine. Investigation of knock, compression ratio, equivalence ratio and timing in a Homogeneous Charge Compression Ignition (HCCI) engine with natural gas and diesel fuels using modelling and simulation.* University of Bradford.

GIST, R. L., OTTO, K. W. & WHITLEY, C. S. 2006. Special Report: World LPG production may outpace demand.

GODSAVE, G. A. E. 1953. Studies of the combustion of drops in a fuel spray—the burning of single drops of fuel. *Symposium (International) on Combustion,* 4**,** 818-830.

GOLDSWORTHY, L. 2012. Combustion behaviour of a heavy duty common rail marine Diesel engine fumigated with propane. *Experimental Thermal and Fluid Science,* 42**,** 93-106.

HARDENBERG, H. & HASE, F. 1979. An empirical formula for computing the pressure rise delay of a fuel from its cetane number and from the relevant parameters of direct-injection diesel engines. *SAE Transactions***,** 1823-1834.

HARPER, D. & SELVIN, H. C. 1973. Computer Simulation and the Teaching of Research Methods. *The American Sociologist***,** 64-70.

HENHAM, A. & MAKKAR, M. K. 1998. Combustion of simulated biogas in a dual-fuel dieel engine. *Energy Conversion & Management,* 39**,** 2001-2009.

HEYWOOD, J. 1988. *Internal combustion engines fundamentals*, McGraw-Hill.

HIROYASU, H. & ARAI, M. 1990. Structures of fuel sprays in diesel engines. SAE Technical Paper.

HOHENBERG, G. F. 1979. Advanced Approaches for Heat Transfer Calculations. SAE International.

HOLMES, C. 2008. LPG world supply and demand. *Gaz d'Aujourd'hui***,** 61-65.

HOUNTALAS, D. & PAPAGIANNAKIS, R. 2002. Theoretical and experimental investigation of a direct injection dual fuel diesel-natural gas engine. SAE Technical Paper.

HOUNTALAS, D. T. & PAPAGIANNAKIS, R. G. 2000. Development of a Simulation Model for Direct Injection Dual Fuel Diesel-Natural Gas Engines. SAE International.

HOUNTALAS, D. T. & PAPAGIANNAKIS, R. G. 2001. A Simulation Model for the Combustion Process of Natural Gas Engines with Pilot Diesel Fuel as an Ignition Source. SAE International.

IKURA, S., KADOTA, T. & HIROYASU, H. 1975. Ignition delay of fuel sprays in a constant volume bomb. *Trans. JSME,* 41**,** 1559-1568.

IMABOPPU, S., SHIMONOSONO, H., HIRANO, Y., FUJIGAYA, K. & INOUE, K. 1993. Development of a Method for Predicting Heat Rejection to the Engine Coolant. SAE Technical Paper.

IMO 2014. MARPOL Annex VI, Regulation 13.

JENNINGS, M. J. & MOREL, T. 1991. A computational study of wall temperature effects on engine heat transfer. SAE Technical Paper.

JOHNSON, S., CLARKE, A., FLETCHER, T. & HYLANDS, D. A Phenomenological Approach to Dual Fuel Combustion Modelling. ASME

2012 Internal Combustion Engine Division Fall Technical Conference, 2012. American Society of Mechanical Engineers, 781-791.

JUNG, J., SONG, S. & HUR, K. B. 2017. Numerical study on the effects of intake valve timing on performance of a natural gas-diesel dual-fuel engine and multi-objective Pareto optimization. *Applied Thermal Engineering,* 121**,** 604-616.

KADOTA, T., HIROYASU, H. & OYA, H. 1976. Spontaneous ignition delay of a fuel droplet in high pressure and high temperature gaseous environments. *Bulletin of JSME,* 19**,** 437-445.

KARIM, G., WIERZBA, I. & AL-ALOUSI, Y. 1996. Methane-hydrogen mixtures as fuels. *International Journal of Hydrogen Energy,* 21**,** 625-631.

KARIM, G. A. 1983. The dual fuel engine of the compression ignition type - Prospects, Problems and Solutions - A Review. *SAE Technical Paper 831073.*

KARIM, G. A. 2003a. Combustion in gas fueled compression: ignition engines of the dual fuel type. *TRANSACTIONS-AMERICAN SOCIETY OF MECHANICAL ENGINEERS JOURNAL OF ENGINEERING FOR GAS TURBINES AND POWER,* 125**,** 827-836.

KARIM, G. A. 2003b. Combustion in Gas Fueled Compression: Ignition Engines of the Dual Fuel Type. *Journal of Engineering for Gas Turbines and Power,* 125**,** 827.

KARIM, G. A. 2015. *Dual-fuel diesel engines*, CRC Press.

KRIEGER, R. B. & BORMAN, G. L. 1966. *The computation of apparent heat release for internal combustion engines,* New York, N.Y., ASME.

KRISHNAN, S. R., SRINIVASAN, K. K. & MIDKIFF, K. C. 2007. Phenomenological Modeling of Low-Temperature Advanced Low Pilot-Ignited Natural Gas Combustion. SAE International.

KRISHNAN, S. R., SRINIVASAN, K. K., SINGH, S., BELL, S. R., MIDKIFF, K. C., GONG, W., FIVELAND, S. B. & WILLI, M. 2004. Strategies for Reduced NO[sub x] Emissions in Pilot-Ignited Natural Gas Engines. *Journal of Engineering for Gas Turbines and Power,* 126**,** 665.

KULESHOV, A. S. 2009. Multi-Zone DI Diesel Spray Combustion Model for Thermodynamic Simulation of Engine with PCCI and High EGR Level.

KUSAKA, J., OKAMOTO, T., DAISHO, Y., KIHARA, R. & SAITO, T. 2000. Combustion and exhaust gas emission characteristics of a diesel engine dual-fueled with natural gas. *JSAE Review,* 21**,** 489-496.

LAHIRI, D., MEHTA, P. S., POOLA, R. B. & SEKAR, R. 1997. Utilization of oxygen-enriched air in diesel engines: fundamental considerations. Argonne National Lab., IL (United States).

LAKSHMINARAYANAN, P. & AGHAV, Y. V. 2010. *Modelling diesel combustion*, Springer Science & Business Media.

LATA, D. & MISRA, A. 2010. Theoretical and experimental investigations on the performance of dual fuel diesel engine with hydrogen and LPG as secondary fuels. *International journal of hydrogen energy,* 35**,** 11918-11931.

LE, T. A. 2011. Experimental Study on Performance, Emissions and Combustion Characteristics of a Single Cylinder Dual Fuel LPG/Diesel Engine. SAE Technical Paper.

LEERMAKERS, C., VAN DEN BERGE, B., LUIJTEN, C., DE GOEY, L. & JAASMA, S. 2011. Direct injection of diesel-butane blends in a heavy duty engine. *SAE International Journal of Fuels and Lubricants,* 4**,** 179-187.

LIU, C. & KARIM, G. 3D-CFD Simulation of Diesel and Dual Fuel Engine Combustion. ASME 2007 Internal Combustion Engine Division Fall Technical Conference, 2007. American Society of Mechanical Engineers, 41-50.

LIU, J., YANG, F., WANG, H., OUYANG, M. & HAO, S. 2013. Effects of pilot fuel quantity on the emissions characteristics of a CNG/diesel dual fuel engine with optimized pilot injection timing. *Applied Energy,* 110**,** 201-206.

LIU, Z. & KARIM, G. 1997. Simulation of combustion processes in gas-fuelled diesel engines. *Proceedings of the Institution of Mechanical Engineers, Part A: Journal of Power and Energy,* 211**,** 159-169.

MA, S., ZHENG, Z., LIU, H., ZHANG, Q. & YAO, M. 2013. Experimental investigation of the effects of diesel injection strategy on gasoline/diesel dual-fuel combustion. *Applied energy,* 109**,** 202-212.

MAN, B. W. 2012. *ME-GI dual fuel MAN B&W engines*.

MANSOUR, C., BOUNIF, A., ARIS, A. & GAILLARD, F. 2001. Gas–Diesel (dual-fuel) modeling in diesel engine environment. *International Journal of Thermal Sciences,* 40**,** 409-424.

MATTARELLI, E., RINALDINI, C. A. & GOLOVITCHEV, V. I. 2014. CFD-3D analysis of a light duty Dual Fuel (Diesel/Natural Gas) combustion engine. *Energy Procedia,* 45**,** 929-937.

MATVOZ, M. 2017. *LPG station in United Kingdom* [Online]. Available: https://www.mylpg.eu/stations/united-kingdom [Accessed 31 May 2017].

MATVOZ, M. 2018. *Chart of fuel prices in United Kingdom* [Online]. Available: https://www.mylpg.eu/stations/united-kingdom/prices [Accessed 26 September 2018].

MBARAWA, M. & MILTON, B. E. 2005. An examination of the maximum possible natural gas substitution for diesel fuel in a direct injected diesel engine. *R & D Journal incorporated in the " the SA Mechanical Engineer",* 21**,** 3-9.

MIKULSKI, M. & WIERZBICKI, S. 2016. Numerical investigation of the impact of gas composition on the combustion process in a dual-fuel compression-ignition engine. *Journal of Natural Gas Science and Engineering,* 31**,** 525-537.

MIKULSKI, M., WIERZBICKI, S. & PIĘTAK, A. 2015. Zero-dimensional 2-phase combustion model in a dual-fuel compression ignition engine fed with gaseous fuel and a divided diesel fuel charge. *Eksploatacja i Niezawodność,* 17.

MIYAMOTO, N., CHIKAHISA, T., MURAYAMA, T. & SAWYER, R. 1985. Description and analysis of diesel engine rate of combustion and performance using Wiebe's functions. SAE Technical Paper.

MURTY, K. A. 1975. *Introduction to combustion phenomena,* CRC Press.

NABER, J. D. & SIEBERS, D. L. 1996. Effects of gas density and vaporization on penetration and dispersion of diesel sprays. SAE technical paper.

NEGURESCU, N., PANA, C. & CERNAT, A. Theoretical and experimental investigations on the LPG fuelled diesel engine. Proceedings of the FISITA 2012 World Automotive Congress, 2013. Springer, 37-49.

NORRIS, J. 2009. Light Goods Vehicle-CO2 Emissions Study: Task Report for Task 5-Assessment of the potential for CO2 emissions reductions. *Report to the Department for Transport, AEA, Harwell, Didcot*.

NORRIS, J., STONES, P. & REVERAULT, P. 2010. Light Goods Vehicle CO2 Emissions Study: Final report. *AEA, Oxford Rep. ED05896*.

NWAFOR, O. 2003. Combustion characteristics of dual-fuel diesel engine using pilot injection ignition. *Journal of the Institution of Engineers(India), Part MC, Mechanical Engineering Division,* 84**,** 22-25.

NWAFOR, O. M. I. 2000. Effect of advanced injection timing on the performance of natural gas in diesel engines. *SaÅdhanaÅ,* 25**,** 11-20.

NWAFOR, O. M. I. 2002. Knock characteristics of dual-fuel combustion in diesel engines using natural gas as primary fuel. *Sadhana,* 27**,** 375-382.

NWAFOR, O. M. I. & RICE, G. 1994. Combustion characteristics and performance of natural gas in high speed indirect injection diesel engine. *Renewable Energy,* 5**,** 841-848.

OGAWA, H., MIYAMOTO, N., LI, C., NAKAZAWA, S. & AKAO, K. 2001. Low emission and knock-free combustion with rich and lean biform mixture in a dual-fuel CI engine with induced LPG as the main fuel. SAE Technical Paper.

OGUMA, M., GOTO, S., SUGIYAMA, K., KAJIWARA, M., MORI, M., KONNO, M. & YANO, T. 2003. Spray characteristics of LPG direct injection diesel engine. SAE Technical Paper.

ONORATI, A., FERRARI, G. & D'ERRICO, G. 2001. 1D unsteady flows with chemical reactions in the exhaust duct-system of SI engines: predictions and experiments. SAE Technical Paper.

PAPAGIANNAKIS, R. & HOUNTALAS, D. 2003. Experimental investigation concerning the effect of natural gas percentage on performance and emissions of a DI dual fuel diesel engine. *Applied Thermal Engineering,* 23**,** 353-365.

PAPAGIANNAKIS, R., HOUNTALAS, D. & KOTSIOPOULOS, P. 2005. Experimental and theoretical analysis of the combustion and pollutants formation mechanisms in dual fuel DI diesel engines. SAE Technical Paper.

PAPAGIANNAKIS, R., HOUNTALAS, D. & RAKOPOULOS, C. 2007. Theoretical study of the effects of pilot fuel quantity and its injection timing on the performance and emissions of a dual fuel diesel engine. *Energy Conversion and Management,* 48**,** 2951-2961.

PAPAGIANNAKIS, R., RAKOPOULOS, C., HOUNTALAS, D. & RAKOPOULOS, D. 2010. Emission characteristics of high speed, dual fuel, compression ignition engine operating in a wide range of natural gas/diesel fuel proportions. *Fuel,* 89**,** 1397-1406.

PATTAS, K. & HÄFNER, G. 1973. Stickoxidbildung bei der ottomotorischen Verbrennung. *MOTORTECHN. Z.,* 34.

PAYKANI, A., SARAY, R. K., KOUSHA, A. & TABAR, M. S. 2011. Performance and emission characteristics of dual fuel engines at part loads using simultaneous effect of exhaust gas recirculation and pre-heating of in-let air. *International Journal of Automotive Engineering,* 1**,** 53-67.

PIROUZPANAH, V. & SARAY, R. K. 2006. A predictive model for the combustion process in dual fuel engines at part loads using a quasi dimensional multi zone model and detailed chemical kinetics mechanism. *International Journal of Engineering Transactions B Applications,* 19**,** 83.

PIĘTAK, A. & MIKULSKI, M. 2011. On the modeling of pilot dose ignition delay in a dual-fuel, self ignition engine. *Silniki Spalinowe,* 50.

POONIA, M., RAMESH, A. & GAUR, R. 1998. Effect of intake air temperature and pilot fuel quantity on the combustion characteristics of a LPG diesel dual fuel engine. SAE Technical Paper.

PRADEEP, V., BAKSHI, S. & RAMESH, A. 2015. Direct injection of gaseous LPG in a two-stroke SI engine for improved performance. *Applied Thermal Engineering,* 89**,** 738-747.

PRASHANT, G., LATA, D. & JOSHI, P. 2016. Investigations on the effect of ethanol blend on the combustion parameters of dual fuel diesel engine. *Applied Thermal Engineering,* 96**,** 623-631.

RAINE, R. R. 1990. A performance model of the dual fuel (diesel/natural gas) engine. SAE Technical Paper.

RAKOWSKI, I. S. 2012. Phenomenological Combustion Models. *Combustion Engines Development.* Springer.

RAO, G., RAJU, A., RAJULU, K. G. & RAO, C. M. 2010. Performance evaluation of a dual fuel engine (Diesel+ LPG). *Indian Journal of science and Technology,* 3**,** 235-237.

RASLAVIČIUS, L., KERŠYS, A., MOCKUS, S., KERŠIENĖ, N. & STAREVIČIUS, M. 2014. Liquefied petroleum gas (LPG) as a medium-term option in the transition to sustainable fuels and transport. *Renewable and Sustainable Energy Reviews,* 32**,** 513-525.

RAVI, K. & PORPATHAM, E. 2017. Effect of piston geometry on performance and emission characteristics of an LPG fuelled lean burn SI engine at full throttle condition. *Applied Thermal Engineering,* 110**,** 1051-1060.

RENE, S. L. 2012. *Dual-fuel ME-GI engine performance and the economy* [Online]. Available: http://www.ngva.eu/images/MAN-Rene-Sejer.pdf [Accessed].

REUTER, U. & SCHEIE, E. 1988. Self-ignition of diesel sprays and its dependence on fuel properties and injection parameters. ASME 88-ICE-14.

RICHARDS, R. 1999. DUAL FUEL ENGINES *In:* BERNARD, C. & RODICA, B. (eds.) *Diesel Engine Reference Book.* 2nd ed. Oxford: Butterworth-Heinemann (A division of Reed Educational and professional publishing Ltd).

ROBERT BOSCH GMBH 1996. *Automotive handbook,* Warrendale, Soc.of Automotive Engineers.

SAHOO, B. B., SAHOO, N. & SAHA, U. K. 2009. Effect of engine parameters and type of gaseous fuel on the performance of dual-fuel gas diesel engines—A critical review. *Renewable and Sustainable Energy Reviews,* 13**,** 1151-1184.

SAITO, H., KAWABATA, Y. & SAKURAI, T. 1999. Study on the Lean Burn Gas Engine Ignited by Pilot Fuel Injection (Part 3). *Annual Technical Report Digest.*

SAITO, H., KAWABATA, Y. & SAKURAI, T. 2000. Study on the Lean Burn Gas Engine Ignited by Pilot Fuel Injection (Part 4).

SALEH, H. 2008. Effect of variation in LPG composition on emissions and performance in a dual fuel diesel engine. *Fuel,* 87**,** 3031-3039.

SARAF, R. R., THIPSE, S. S. & SAXENA, P. K. 2009. Lambda Characterization of Diesel-CNG Dual Fuel Engine. 170-174.

SARAVANAN, N. & NAGARAJAN, G. 2009. An insight on hydrogen fuel injection techniques with SCR system for NO x reduction in a hydrogen–diesel dual fuel engine. *international journal of hydrogen energy*, 34**,** 9019-9032.

SCHUBIGER, R. A., BOULOUCHOUS, K. & EBERLE, M. K. 2002. Rußbildung und Oxidation bei der dieselmotorischen Verbrennung. *MTZ-Motortechnische Zeitschrift*, 63**,** 342-353.

SCOT, W. 2011. *Natural gas diesel engines* [Online]. Available: http://www.brighthub.com/environment/renewable-energy/articles/118992.aspx [Accessed 7 June 2017].

SELIM, M. Y. E. 2001. Pressure-Time Characteristics in diesel engine fuelled with natural gas. *Renewable Energy*, 22**,** 473-489.

SELIM, M. Y. E. 2004. Sensitivity of dual fuel engine combustion and knocking limits to gaseous fuel composition. *Energy Conversion and Management*, 45**,** 411-425.

SHI, Y., GE, H.-W. & REITZ, R. D. 2011. Computational optimization of internal combustion engines. Springer Science & Business Media.

SIEBERS, D. L. 1999. Scaling liquid-phase fuel penetration in diesel sprays based on mixing-limited vaporization. SAE technical paper.

SINGH, R. N., SINGH, S. P. & PATHAK, B. S. 2007. Investigations on operation of CI engine using producer gas and rice bran oil in mixed fuel mode. *Renewable Energy*, 32**,** 1565-1580.

SITKEI, G. 1964. *Kraftstoffaufbereitung und Verbrennung bei Dieselmotoren*, Springer Berlin Heidelberg.

SPADACCINI, L. 1977. Autoignition characteristics of hydrocarbon fuels at elevated temperatures and pressures. *J. Eng. Power*, 99**,** 83-87.

SPALDING, D. B. The combustion of liquid fuels. Symposium (international) on combustion, 1953. Elsevier, 847-864.

SPROAT, R., HASSAN, A., WALDIE, A., JAY, G. & HOLLAND, D. 2006. The Risk Posed to Vehicle Occupants and Rescue Personnel by Dual-Fuelled

Vehicles Fitted with Liquid Petroleum Gas (LPG) Tanks. SAE Technical Paper.

STELMASIAK, Z. 2003. *Studium procesu spalania gazu w dwupaliwowym silniku o zapłonie samoczynnym zasilanym gazem ziemnym i olejem napędowym* Ph.D., Wydaw. ATH.

STEWART, J., CLARKE, A. & CHEN, R. 2007. An experimental study of the dual-fuel performance of a small compression ignition diesel engine operating with three gaseous fuels. *Proceedings of the Institution of Mechanical Engineers, Part D: Journal of Automobile Engineering,* 221**,** 943-956.

TIRA, H., HERREROS, J., TSOLAKIS, A. & WYSZYNSKI, M. 2012. Characteristics of LPG-diesel dual fuelled engine operated with rapeseed methyl ester and gas-to-liquid diesel fuels. *Energy,* 47**,** 620-629.

UMA, R., KANDPAL, T. & KISHORE, V. 2004. Emission characteristics of an electricity generation system in diesel alone and dual fuel modes. *Biomass and Bioenergy,* 27**,** 195-203.

VIBE, I. I. 1970. *Brennverlauf und Kreisprozess von Verbrennungsmotoren,* Berlin, VEB Verlag Technik.

VIOLA, V. 2018. An overview of the global LPG market and its impact in Latin America.

WANG, X., LI, K. & SU, W. 2012. Experimental and numerical investigations on internal flow characteristics of diesel nozzle under real fuel injection conditions. *Experimental Thermal and Fluid Science,* 42**,** 204-211.

WANG, Z., ZHAO, Z., WANG, D., TAN, M., HAN, Y., LIU, Z. & DOU, H. 2016. Impact of pilot diesel ignition mode on combustion and emissions characteristics of a diesel/natural gas dual fuel heavy-duty engine. *Fuel,* 167**,** 248-256.

WATSON, N., PILLEY, A. & MARZOUK, M. 1980. A combustion correlation for diesel engine simulation. SAE Technical Paper.

WEAVER, C. S. & TURNER, S. H. 1994. Dual fuel natural gas/diesel engines: Technology, performance, and emissions. *SAE Technical Paper 940548.*

WILCOX, D. C. 1998. *Turbulence modeling for CFD,* DCW industries La Canada, CA.

WIMMER, A., PIVEC, R. & SAMS, T. 2000. Heat transfer to the combustion chamber and port walls of IC engines-measurement and prediction. SAE Technical Paper.

WOLFER, H. 1959. Ignition Lag in Diesel Engines. *VDI-Forschungsheft,* 392.

WOLFER, H. H. 1938. Ignition lag in diesel engines. *VDI-Forschungsheft,* 392**,** 621-436.047.

WOSCHNI, G. 1967. A universally applicable equation for the instantaneous heat transfer coefficient in the internal combustion engine. SAE Technical paper.

WU, J. S., HSU, K. H., KUO, P. M. & SHEEN, H. J. 2003. Evaporation model of a single hydrocarbon fuel droplet due to ambient turbulence at intermediate Reynolds numbers. *International journal of heat and mass transfer,* 46**,** 4741-4745.

WÄRTSILÄ 2013. Improving engine fuel and operational efficiency.

WÄRTSILÄ. 2014. *Taking dual-fuel marine engines to the next level* [Online]. Available: https://www.wartsila.com/twentyfour7/energy/taking-dual-fuel-marine-engines-to-the-next-level [Accessed 26/09/2018 2018].

WÄRTSILÄ 2015. Wärtsilä low-speed dual-fuel solution. *In:* ENGINES, W. (ed.).

WÄRTSILÄ. 2018. *Dual fuel engines* [Online]. Available: https://www.wartsila.com/products/marine-oil-gas/engines-generating-sets/dual-fuel-engines [Accessed 26/09/2018 2018].

YANG, B., WANG, L., NING, L. & ZENG, K. 2016. Effects of pilot injection timing on the combustion noise and particle emissions of a diesel/natural gas dual-fuel engine at low load. *Applied Thermal Engineering,* 102**,** 822-828.

YASAR, H., SOYHAN, H., WALMSLEY, H., HEAD, B. & SORUSBAY, C. 2008. Double-Wiebe function: An approach for single-zone HCCI engine modeling. *Applied Thermal Engineering,* 28**,** 1284-1290.

ZENG, P. & ASSANIS, D. N. 2004. Cylinder pressure reconstruction and its application to heat transfer analysis. SAE Technical Paper.

ÇINAR, C., ŞAHIN, F., CAN, Ö. & UYUMAZ, A. 2016. A comparison of performance and exhaust emissions with different valve lift profiles between gasoline and LPG fuels in a SI engine. *Applied Thermal Engineering,* 107**,** 1261-1268.

APPENDICES

Appendix 1 – Data of Diesel Engine Mode of Operation

Table A.1 Experimentally-Measured Performance of Diesel Engine operation

Sample No	Brake Setting (%)	Water flow (l/min)	Air inlet pressure (kPa)	Air inlet Temp (deg C)	Coolant inlet Temp	Coolant Outlet Temp	Exhaust Temp (degC)	Engine speed (rpm)	Torque (Nm)	Calc Power (kW)	Air Density (kg/m^3)	Air Volume Flow rate (m^3/s)	Volumetric Efficiency (%)
1	52	12.2	-1.71	35.4	14.1	44.7	651	3598	115.0	43.33	1.14	0.045	78.48
2	53	12.2	-1.52	37.5	14.5	46.1	656	3419	117.0	41.90	1.14	0.042	78.15
3	54	11.9	-1.33	36.1	14.5	47.1	662	3237	120.2	40.74	1.14	0.039	77.06
4	55	12.1	-1.17	35.9	14.5	46.9	664	3029	122.6	38.91	1.14	0.037	77.11
5	55	12.1	-1.04	37.5	14.6	46.5	662	2789	124.9	36.48	1.14	0.035	79.14
6	56	12.1	-0.98	38.7	14.6	45.5	660	2607	126.7	34.59	1.13	0.034	82.38
7	57	12.2	-0.85	40.6	14.8	44.7	657	2429	128.3	32.62	1.13	0.032	82.90
8	56	12.4	-0.72	40.8	14.5	43.9	649	2218	126.0	29.27	1.13	0.029	83.22
9	56	12.1	-0.63	40.6	14.6	42.8	650	2010	126.5	26.62	1.13	0.027	86.21
10	56	11.9	-0.62	41.2	14.8	41.0	640	1770	124.7	23.10	1.12	0.027	96.73

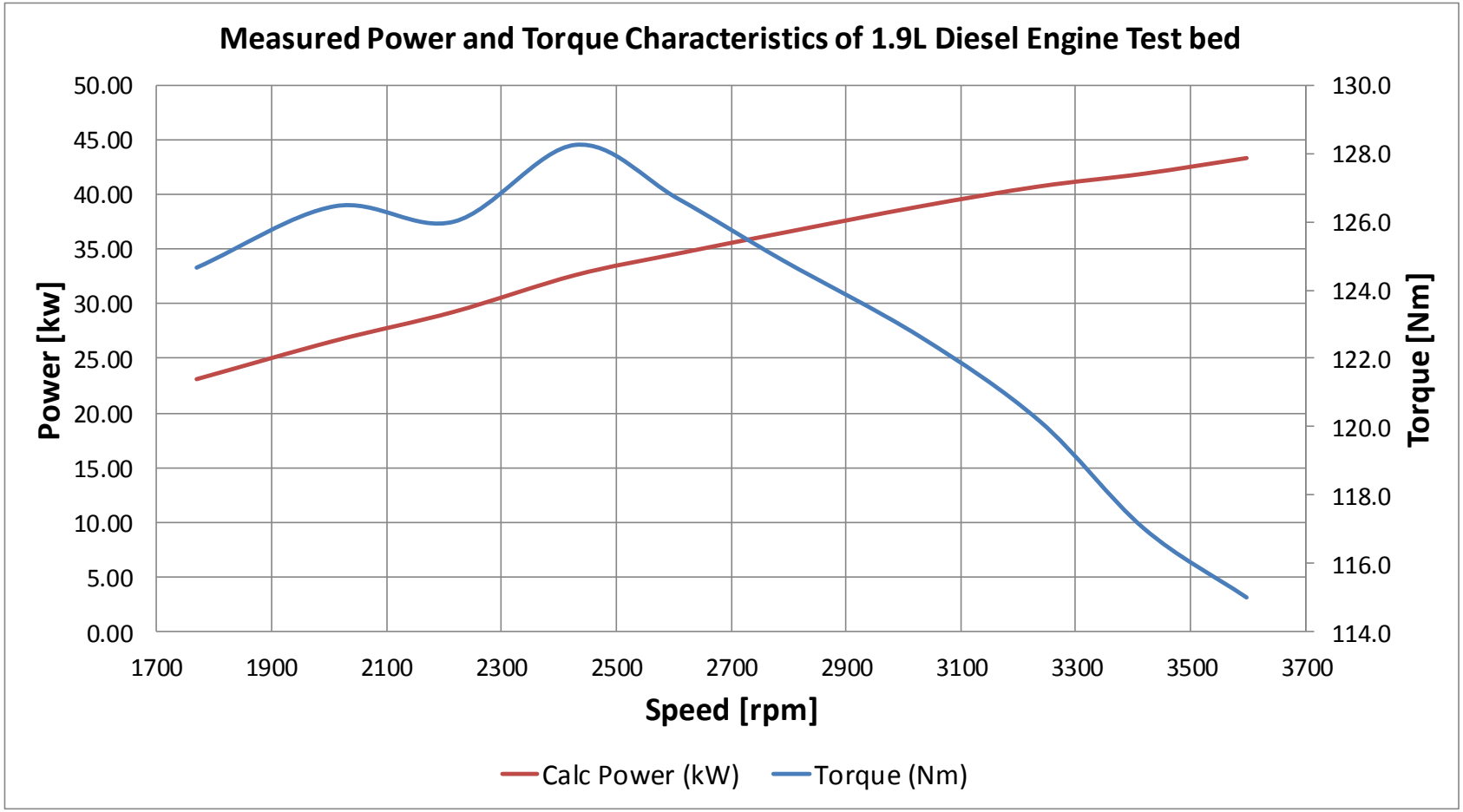

Figure A.1 Experimentally-determined power-torque characteristics with respect to the engine speed of the diesel engine test rig

Appendix 2 – Torque, Power and Valve Geometry of Engine

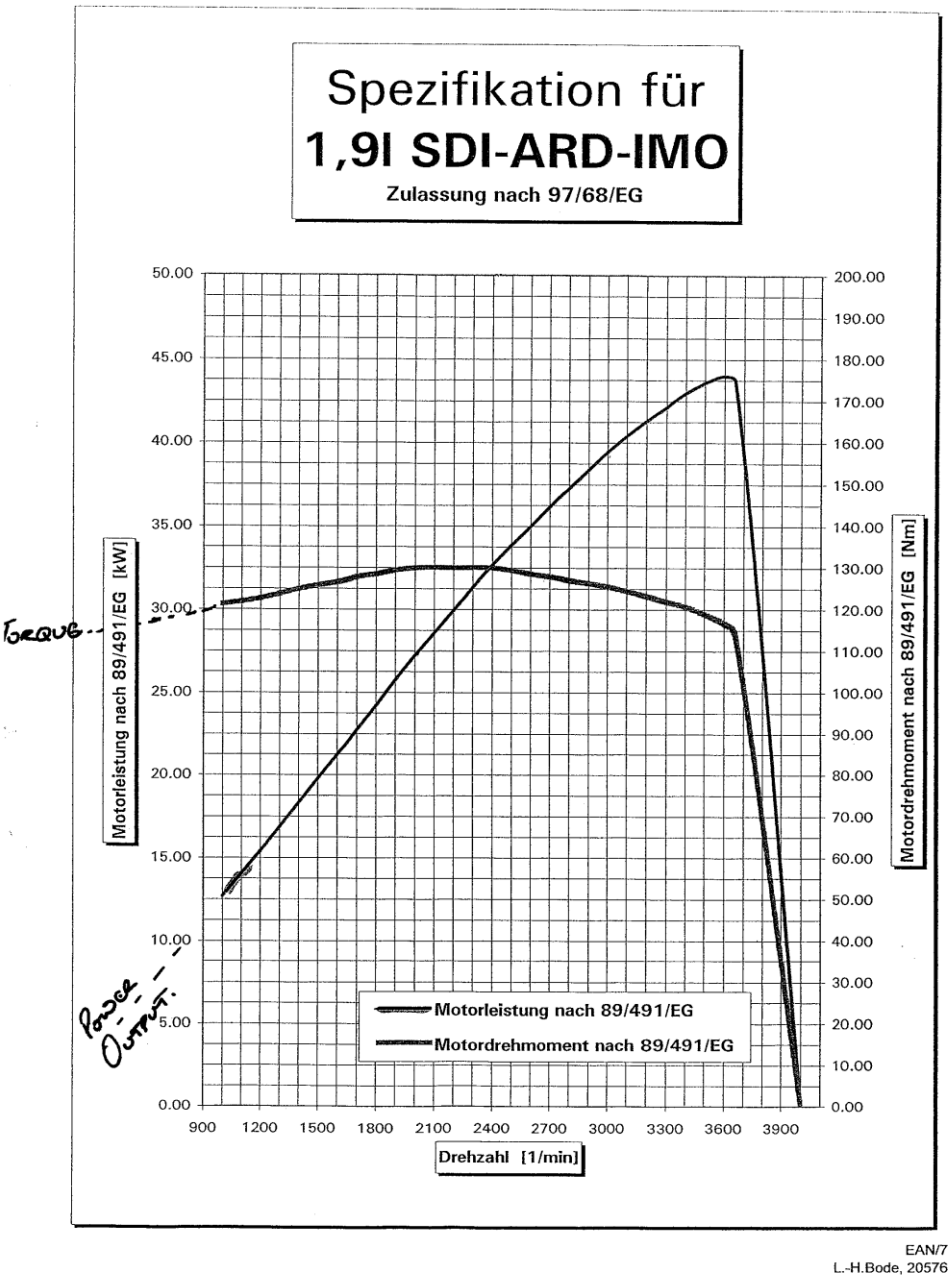

Figure A.2 Power-Torque characteristics of the engine test rig

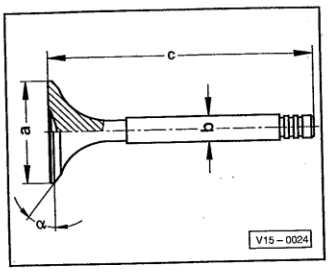

◄ **Fig. 3 Valve dimensions**

Note:
Valves must not be reworked. Only lapping-in is permitted.

Engine code AVM

Dimension		Inlet valve	Exhaust valve
Ø a	mm	35.95	31.45
Ø b	mm	6.963	6.943
c	mm	96.85	96.85
α	∠°	45	45

Engine codes ARD and BEQ

Dimension		Inlet valve	Exhaust valve
Ø a	mm	35.95	31.45
Ø b	mm	6.963	6.943
c	mm	96.55	96.35
α	∠°	45	45

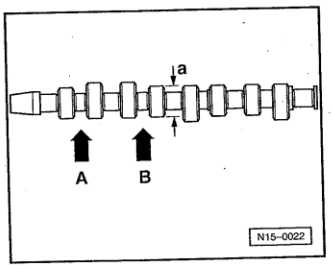

◄ **Fig. 4 Camshaft identification, valve timing**

Identification

- Cam base diameter: a = 38 mm Ø
- Identification by stamped numbers and letters between inle haust cams:

Engine codes	AVM	ARD, BEQ
No. 1 cylinder -arrow A-	38 A	38 E
No. 2 cylinder -arrow B-	DE	DE

Valve timing at 1 mm valve lift

Engine codes	AVM	ARD, BEQ
Inlet opens after TDC	16 °	11 °
Inlet closes after BDC	25 °	25 °
Outlet opens before BDC	28 °	40 °
Outlet closes before TDC	19 °	10 °

Figure A.3 Valve data of the engine test rig

Appendix 3 – Specification of Various Sensors used on the Engine Test Rig

Table A.2 List of the sensors used in the study and their specifications

Sensor	Manufacturer	Model/Type	Range	Accuracy
Flow meter (diesel supply)	BIOTECH	VZS-003-ALU	0.001 - 0.3 L/min	+/- 1%
Flow meter (diesel return)	BIOTECH	VZS-003-ALU	0.005 - 1.5 L/min	+/- 1%
Load cell	APP. MEAS.	DBBSM-50kg-003-000	0 - 50 kg	<+/- 0.03
In-cylinder pressure	KISTLER	6055BP	0 - 250 bar	<+/- 0.4
Brake setting	N/A	N/A	N/A	N/A
Intake Manifold Air Pressure	Honeywell	26PC	0.5 - 250 psi	+/- 0.2
Intake Manifold Air Temperature	Armfield	'K' type thermocouple		
Exhaust Manifold Temperature	Armfield	'K' type thermocouple		
Engine speed	RS	Magnetic pick-up		
Torque	SMD[2]	S200		
Eddy Current Dynamometer	Zelu/Klam	K-40 PAU	≤ 145 Nm	

[2] Strain Measurement Devices

Appendix 4 – Summary of Simulation Input Data

Table A.3 Summary of Simulation Input Data

			3050 rpm					2470 rpm					2435 rpm				
			Diesel-LPG (D-L) [%]					Diesel-LPG (D-L) [%]					Diesel-LPG (D-L) [%]				
Element	Parameter	Units	100D-0L	95D-5L	90D-10L	80D-20L	70D-30L	100D-0L	95D-5L	90D-10L	80D-20L	70D-30L	100D-0L	95D-5L	90D-10L	80D-20L	70D-30L
Intake System Boundary (SB1)	Pressure	bar	1	1	1	1	1	1	1	1	1	1	1	1	1	1	1
	Gas Temperature	degC	298	298	298	298	298	298	298	298	298	298	298	298	298	298	298
Pipe	Pressure	bar	1	1	1	1	1	1	1	1	1	1	1	1	1	1	1
	Gas Temperature	degC	300	300	300	300	300	300	300	300	300	300	300	300	300	300	300
Intake Plenum (PL1)	Pressure	bar	1	1	1	1	1	1	1	1	1	1	1	1	1	1	1
	Temperature	degC	330	330	330	330	330	330	330	330	330	330	330	330	330	330	330
Cylinder	Bore	mm	79.5	79.5	79.5	79.5	79.5	79.5	79.5	79.5	79.5	79.5	79.5	79.5	79.5	79.5	79.5
	Stroke	mm	95.5	95.5	95.5	95.5	95.5	95.5	95.5	95.5	95.5	95.5	95.5	95.5	95.5	95.5	95.5
	Compression Ratio	[-]	19	19	19	19	19	19	19	19	19	19	19	19	19	19	19
	Con-Rod Length	mm	144	144	144	144	144	144	144	144	144	144	144	144	144	144	144
	Piston Pin Offset	mm	0	0	0	0	0	0	0	0	0	0	0	0	0	0	0
	Effective Blow-By Gap	mm	0.0008	0.0008	0.0008	0.0008	0.0008	0.0008	0.0008	0.0008	0.0008	0.0008	0.0008	0.0008	0.0008	0.0008	0.0008
	Mean Crankcase Pressure	bar	1	1	1	1	1	1	1	1	1	1	1	1	1	1	1
	Pressure at EO	bar	4.7	4.7	4.7	4.7	4.7	4.7	4.7	4.7	4.7	4.7	4.7	4.7	4.7	4.7	4.7
	Temperature at EO	degC	900	900	900	900	900	900	900	900	900	900	900	900	900	900	900
	Excess Air Ratio	[-]	1.6	1.6	1.6	1.6	1.6	1.6	1.6	1.6	1.6	1.6	1.6	1.6	1.6	1.6	1.6
	Heat Release		AVL MCC	AVL MCC	AVL MCC	AVL MCC	AVL MCC	AVL MCC	AVL MCC	AVL MCC	AVL MCC	AVL MCC	AVL MCC	AVL MCC	AVL MCC	AVL MCC	AVL MCC
Exhauust Plenum (PL2)	Pressure	bar	2.5	2.5	2.5	2.5	2.5	2.5	2.5	2.5	2.5	2.5	2.5	2.5	2.5	2.5	2.5
	Temperature	deC	500	500	500	500	500	500	500	500	500	500	500	500	500	500	500
Exhaust System Boundary (SB2)	Pressure	bar	1	1	1	1	1	1	1	1	1	1	1	1	1	1	1
	Gas Temperature	degC	400	400	400	400	400	400	400	400	400	400	400	400	400	400	400
	Excess Air Ratio Value	[-]	1.2	1.2	1.2	1.2	1.2	1.2	1.2	1.2	1.2	1.2	1.2	1.2	1.2	1.2	1.2
Engine	Cycle Type		4-Stroke	4-Stroke	4-Stroke	4-Stroke	4-Stroke	4-Stroke	4-Stroke	4-Stroke	4-Stroke	4-Stroke	4-Stroke	4-Stroke	4-Stroke	4-Stroke	4-Stroke
Monitor	Sensor channel		IMEP	IMEP	IMEP	IMEP	IMEP	IMEP	IMEP	IMEP	IMEP	IMEP	IMEP	IMEP	IMEP	IMEP	IMEP
Fuel	Species		Classic	General	General	General	General	Classic	General	General	General	General	Classic	General	General	General	General
	Property Dependencies		(P,T, Mixture)	(P,T, Mixture)	(P,T, Mixture)	(P,T, Mixture)	(P,T, Mixture)	(P,T, Mixture)	(P,T, Mixture)	(P,T, Mixture)	(P,T, Mixture)	(P,T, Mixture)	(P,T, Mixture)	(P,T, Mixture)	(P,T, Mixture)	(P,T, Mixture)	(P,T, Mixture)
	Reference Pressure	bar	1	1	1	1	1	1	1	1	1	1	1	1	1	1	1
	Refrence Temperature	degC	24.85	24.85	24.85	24.85	24.85	24.85	24.85	24.85	24.85	24.85	24.85	24.85	24.85	24.85	24.85
	Components		Diesel	D, 60%P,40%B	D, 60%P,40%B	D, 60%P,40%B	D, 60%P,40%B	Diesel	D, 60%P,40%B	D, 60%P,40%B	D, 60%P,40%B	D, 60%P,40%B	Diesel	D, 60%P,40%B	D, 60%P,40%B	D, 60%P,40%B	D, 60%P,40%B
	Lower Heating Value	KJ/Kg	42800	42954	43100	43416	43724	42800	42954	43100	43416	43724	42800	42954	43100	43416	43724
Simulation Control	End of Simulation	cycles	10	10	10	10	10	10	10	10	10	10	10	10	10	10	10
	Average Cell size	mm	10	10	10	10	10	10	10	10	10	10	10	10	10	10	10